624

CRUSTAL DEFORMATION STUDIES AND PREDICTION OF ERUPTIONS OF MOUNT ETNA, SICILY

A thesis

submitted by

IAN MICHAEL PHILLIPS, B.Sc. A.R.C.S

for the degree of

Doctor of Philosophy

of

The University of London

The Department of Geophysics

Imperial College of Science and Technology

London.

January, 1979

We shall not cease from exploration
And the end of all our exploring
Will be to arrive where we started
And know the place for the first time.

T.S. Eliot

To

My Parents

ABSTRACT

Tiltmeters were installed at two sites on Mount Etna, and these recorded tilt during the period between September 1973 and May 1977. The resultant data were examined for a) short-period, tidal signals and b) long-period, secular changes.

Spectral analysis did not produce any clear information regarding the nature of tidal signals on the volcano, and no firm conclusions could be drawn as to whether the eruptive or quiescent phases of Etna affected or were affected by the tides.

The long-period tilts showed some correlation with volcanic activity, but overall there was insufficient data to enable no more than speculative predictions of eruptions or inferrences as to the internal mechanisms of the volcano to be made.

Statistical analysis of the periods between eruptions lends considerable support to the theory that summit and flank eruptions are fed by separate but inter-connected magma conduits.

A detailed analysis of nearly four hundred years of eruptions fails to give any support for theories proposing the triggering of eruptions by mechanisms such as earth tides or sunspots.

ACKNOWLEDGEMENTS

In the course of this work the author has received much help and advice from many people, and he would like to extend his thanks to them. Principal amongst those has been Professor R.G. Mason, who has supervised this study, and given much advice on the preparation of this thesis.

The author was assisted in some of the field work by Paul Davis and Dave Young of the Geodesy and Geophysics Department, Cambridge University and also by Ibrahim Mohamed who, in addition, provided valuable advice on aspects of computer usage. Valuable discussions have been held with John Murray of University College, London and Nigel Henbest of Leicester University.

The sunspot number data was kindly provided by the Solar Department of the Royal Greenwich Observatory, and the Natural Environment Research Council provided both the author's research studentship and field grants for the work.

Finally many thanks must go to Brenda for the difficult task of typing the thesis, and the even more difficult task of reading my writing.

CONTENTS

Abstract			3
Acknowledgements			4
Contents			5
Chapter 1		Introduction	7
Chapter 2		Mount Etna - Its background and locale	
	2.1	Introduction	14
	2.2	Geological aspects of Sicily	19
	2.3	Geology of Mount Etna	22
	2.4	Geomorphology and the summit region	29
	2.5	Tectonic setting of Sicily	33
	2.6	Tectonic control of Mount Etna	39
Chapter 3		Earth Tides	
	3.1	Introduction	41
	3.2	Theory	46
	3.3	Astronomical development	53
	3.4	Love numbers	63
	3.5	World-wide observations	70
Chapter 4		Volcano tilt measurements and the Etnean tiltmeters	
	4.1	Tilt measurements on volcanoes	77
	4.2	Field instruments - description	85
	4.3	Laboratory and field assessment of the tiltmeters	96
	4.4	Installation of the tiltmeters on Etna	98

Chapter 5 Tiltmeter results

5.1 Introduction 111

5.2 Data processing 113

5.3 Spectral analysis 117

5.4 Etnean tidal power spectra 133

5.5 Etnean activity 1973 - 1977 145

5.6 Long term tilt activity 150

Chapter 6 Prediction of eruptions

6.1 Introduction 168

6.2 Eruptive mechanisms of Mount Etna 169

6.3 Repose period statistics for Mount Etna 174

6.4 Tidal control of eruptions 197

6.5 Sunspot triggering of eruptions 234

Chapter 7 Conclusions 238

References 245

Appendices 270

CHAPTER I

INTRODUCTION

Volcanoes have fascinated man since he first set eyes upon them and these most spectacular of all natural phenomena have often been regarded as gods or homes of gods. Not merely did they strike awe into mens hearts but they also possessed an almost overwhelming attraction, that of providing the surrounding land with a rich, fertile soil often in an otherwise barren landscape. This attraction was often to prove fatal and over the centuries volcanoes have exacted a terrible toll on those unfortunate enough to have to depend upon them for their livelihood. In A.D. 79 Vesuvius, in the most famous of all eruptions, killed around 2,000 people in the towns of Pompeii and Herculaneum. Krakatoa in Indonesia, in one of the most violent eruptions of all time killed over 36,000 people and in 1902 Mt. Pelee in the Caribbean Island of Martinique destroyed 30,000 lives in a matter of seconds. It is because of disasters such as these that a need for predicting volcanic eruptions arises. The problem is not just one of predicting an eruption to within a few days but also predicting the ferocity and overall danger to life; in all the eruptions just mentioned there was considerable evidence beforehand to warn the inhabitants, without the need for sophisticated scientific observations, but misunderstandings of the situation, underestimating the danger, and bureaucratic maladministration combined to ensure such an enormous death toll. One of the main problems facing those trying to predict eruptions was highlighted in 1976 when the French government,

fearing a repeat of the 1902 Mt. Pelee disaster, evacuated a large area of nearby Guadeloupe anticipating an eruption of Soufriere. This action was taken against the advice of Haroun Tazieff, the leading volcanologist on the site and the resultant non-eruption created a good deal of recrimination all round as well as financial problems for the Guadeloupe government. The prime considerations then are accuracy in terms of time of eruption and the danger to life.

Fortunately for those living in the shadow of Etna the danger to life is not great. Etna's eruptions are not violently explosive in the manner of Vesuvius or Krakatoa, although such eruptions have occurred in historical times notably in 1669, but are characterized by large volumes of extruded lava. This lava moves at a slow enough rate to allow people and livestock to be evacuated at the last moment; vineyards and orchards are not so lucky and much fertile land was destroyed in the large 1971 eruption. Even though there is no direct threat to life, a fore-knowledge of an eruption would be of undoubted help to any administration in providing it with valuable planning time.

Volcano prediction is still very much in its infancy. Decker (1973) considers the term 'prediction' to be too precise and deterministic and prefers to use the term 'forecasting', and while advances are always being made there is still a long way to go before confident predictions can be made.

The principle methods used to determine the state of a volcano area the monitoring of:-

1) Seismic and microseismic activity.
2) Crustal Deformation (Tilt).
3) Changes of the geothermal temperature.
4) Variations in the geomagnetic, gravity and geoelectric fields.
5) Various geochemical parameters such as the temperature, volume or composition of fumarole gases.

The two most popular approaches are via seismic activity and crustal deformation. References to the other approaches can be found in Minakami (1974), Decker (1973) and Yokoyama (1972). The monitoring of seismic activity is a well advanced field of research pioneered in Japan (Minakami, 1974; Kubotera and Yoshikawa, 1963; and many others) but also in the USSR (Tokarev, 1971; Gorshkov, 1960) and on Hawaii (Jaggar, 1920). A reconnaissance survey of Etnean seismicity and microseismicity has recently been completed (M. Muniruzaman, 1977) and the results indicate that further, more extensive, coverage may prove fruitful.

The monitoring of crustal deformation, as with the seismic monitoring, is a well established approach, and here the Hawaiian volcanoes have been extensively studied (Jaggar, 1920; Jaggar and Finch, 1929; Jones A.E, 1937 and others) as have many Japanese volcanoes (Hagiwara 1947; Hagiwara et al., 1948, 1949a, 1949b, 1951; Hagiwara and Kasahara 1951 and others) and more recently tilt stations have been

established on other volcanoes around the world (Fiske et al., 1977; Fedotov et al 1977). All the early measurements of crustal deformation were based on precise levelling surveys and it was not until the development of the portable water-table tiltmeter (Eaton, 1959) that continuous monitoring was possible.

The geophysical techniques listed above have not only found use in eruption prediction but have also been applied to the examination of of the internal mechanism of the volcano (Eaton and Lipman, 1977; Wadge, 1974, 1976) and in the future the two approaches will probably go hand-in-hand, the one supplying information about the other.

On the whole, Etna has been a neglected volcano; geological observations were begun by Lyell in the early nineteenth century but it took the eruption of 1971 to stimulate any real interest in the use of geophysical methods, and then it was British volcanologists, who took the initiative. There had been some previous geophysical measurements, including a gravity survey (Klerkx, 1970) and some seismic profiling across and down through Sicily, which yielded little information on Etna.

Measurements of crustal deformation have since been carried out by two separate approaches a) A series of biannual precise levelling surveys by a team from University College, London under J. Guest and b) Continuous tilt monitoring by Imperial College, London under R.G. Mason and G. Walker.

The initial aim of the research described in this thesis was to extend the continuous tilt monitoring programme begun in 1973 (Wadge, 1974) with the intention of gathering more information with regard to volcano prediction and the internal mechanisms of Etna. (Mason, 1975). However, a precise gravity survey in 1974 (Mason et al., 1974) revealed unexpected differences between the tidal gravimetric factor (ratio of observed:predicted tidal amplitudes) at the various sites on the volcano, and as a result it was decided to make a more thorough investigation of this phenomena and a detailed gravity study has been recently completed (Mohamed, 1978). The aim of this research then extended from one of crustal deformation monitoring to an examination of tidal signals during eruptive and quiescent phases of the volcano (Phillips, 1978). The predictive aspect was also extended from one based simply on geophysical techniques (in this case crustal deformation only) to include a statistical approach similar to that of Decker (1973) and an investigation of the possibilities of eruption triggering by other phenomena such as Earth tides and sunspots, both of which have attracted increasing attention in recent years. Here again an assessment of the influence of tides or sunspots can provide valuable information on the internal mechanism of Etna.

The layout of the remainder of this thesis is as follows:-

In Chapter 2 the background geology of Mount Etna and the neighbouring region is briefly described, as is the complicated plate tectonic setting of Sicily.

The relevance of Earth tides was referred to above, and Chapter 3 deals with the basic theory, and then proceeds to a discussion of previous Earth tide measurements, and some of the difficulties and perturbing forces associated with such measurements, in particular their relevance to the work on Etna.

Thus Chapters 2 and 3 provide a broad background to the problems considered in this thesis, and the investigation of these problems is analysed in the rest of the thesis continuing with Chapter 4 where the two tiltmeters used in this research are described, and their installation and operational history on Etna is also detailed.

Chapter 5 is concerned with the results obtained from the two tiltmeters and analyses the results with reference to both tidal and longer period signals, attempting correlations with known volcanic activity.

Volcano forecasting and eruption triggering is dealt with in Chapter 6 and an assessment of the internal structure of Etna is attempted.

The final Chapter, 7, summarises the results of the previous chapters and makes suggestions for further research.

During the course of this research the computer has been of paramount importance in the analysis of results and the prediction of tides. Three programs have been extensively used, (1) TIDE, (2) SPECANL, and (3) TIDECOM. The first two are modified versions of programs

written by J.C. Harrison, while the third, TIDECOM, was specially written for this research. Descriptions of these programs have been included in an appendix.

CHAPTER 2

MOUNT ETNA - ITS BACKGROUND AND LOCALE

2.1 INTRODUCTION

Mount Etna, standing as it does in the centre of the Mediterranean(Fig. 2.1) has been close to one major civilization or another for well over 5,000 years and its influence on them must have been quite considerable. The Greeks were certainly well acquainted with Etna and their literature contains numerous references to it. Both Hephaestus (The Greek 'Smith' god) and Vulcan, his Roman equivalent, were supposed to house their forges deep within her bowels and a later Greek philosopher, Empedocles, lived throughout the year on Etna and is reputed to have leapt into the crater as a rather grandiose act of defiance to the gods. In due course the Torre del Filosofo on the upper Southern flank of the volcano was named in his honour and he may well have regarded that as due recompense.

Although eruptions on the volcano have been recorded as far back as 1500 B.C. (Imbo 1965) scientific research, as generally where the geological sciences were concerned, was late in coming. Maps and drawings of the volcano were produced in the late eighteenth century (q.v. Wadge 1974 for references) but it was not until the mid-nineteenth century that the first major geological work was reported (Wadge 1974). Geophysical research was even later in its

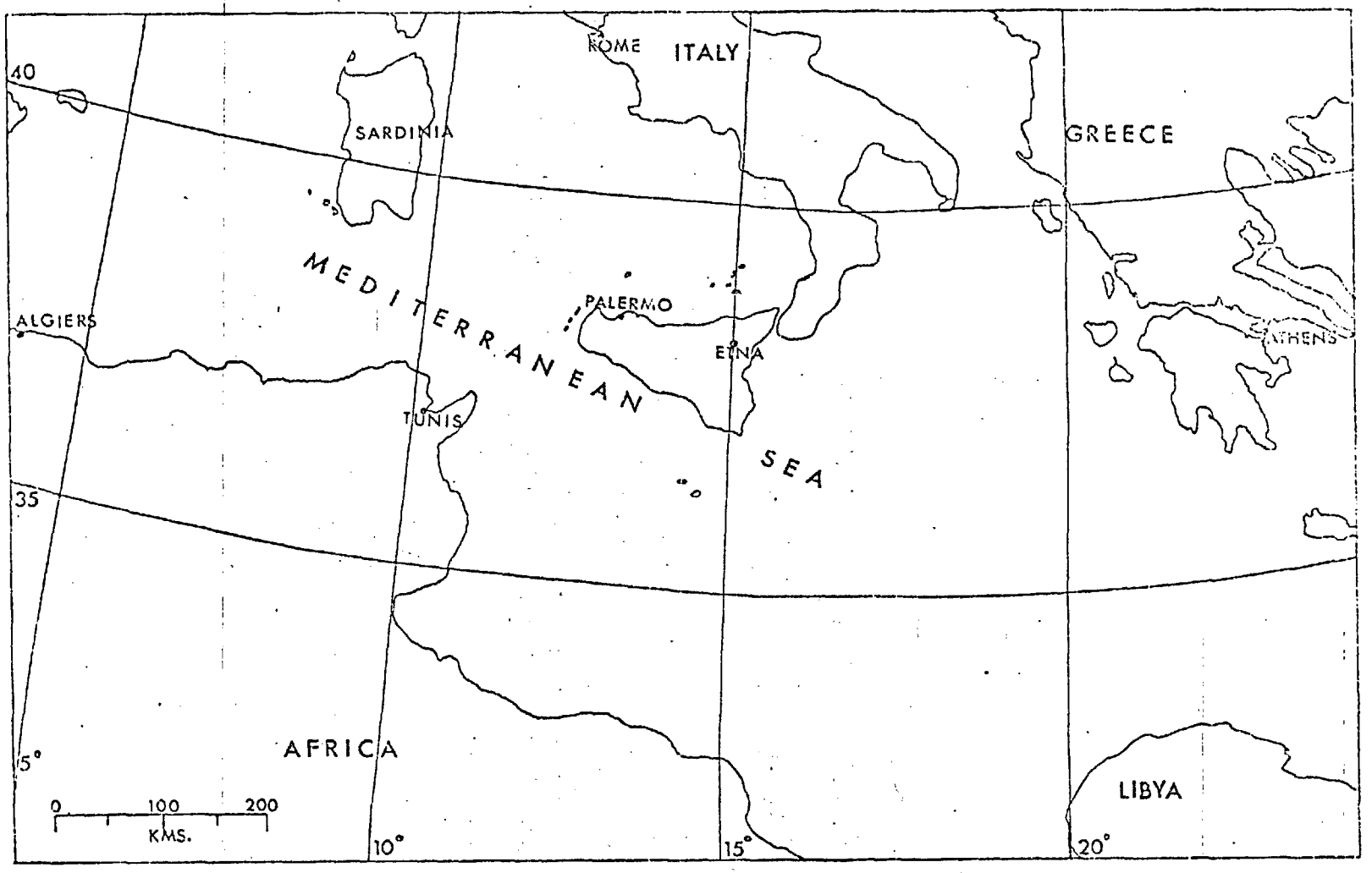


FIG. 2.1

MT ETNA AND ITS MEDITTERANEAN SETTING

inception and almost all the significant work has been carried out in the 1960's and 1970's.

Etna's historical notoriety resides not only in its prominent location but also, and primarily, because it is Europe's largest and most active volcano. The summit reaches over 3,000 metres in height and has geographical co-ordinates of $37^{\circ}45'$N and $15^{\circ}01'$E. The whole volcano spreads over 1300 kms^2. At its base it is approximately elliptical having a north-south axis of fifty kilometres and an east-west axis of forty kilometres. Its size and activity contribute to make Etna rank second only to Vesuvius as Europe's, if not the World's, most famous volcano.

Considering the enormous number of recorded eruption, more than on any other volcano except Stromboli, and its prominent location in one of the most populous of regions historically speaking, it is perhaps surprising how little is known of the workings of Etna. Partly, this is due to the late involvement of science, but also to the manifest complexity of the volcano. There are over two hundred adventive cones (secondary cones, formed on the flank of an existing volcano) covering its surface (Fig.2.2), many of them from recent eruptions, and their comparative abundance would alone indicate a complicated system of channels or widespread fragmentation within the volcano, facilitating the transference of magma.

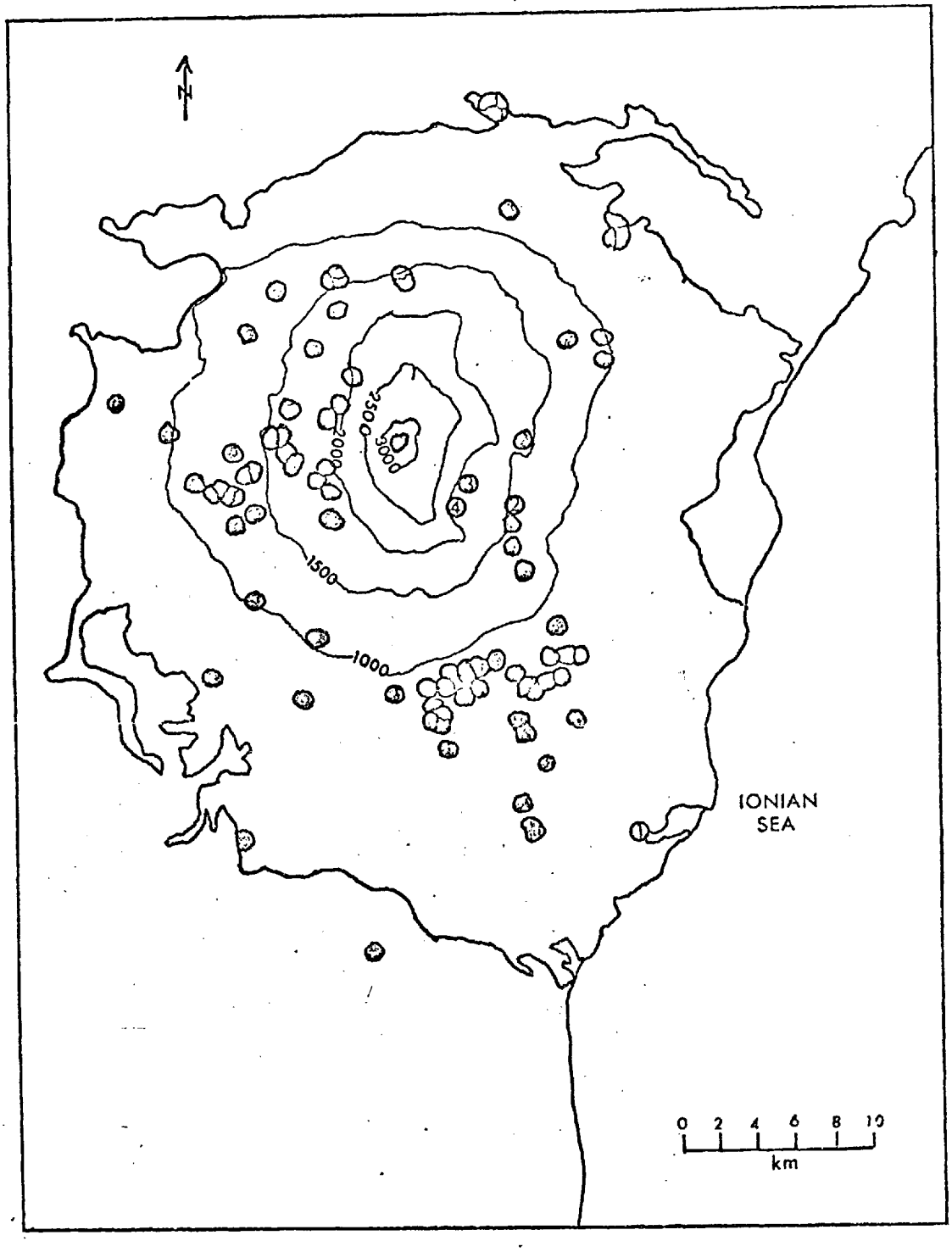


FIG. 2.2

Adventive Cones and Major Ancient Eruptives Centres
(after Rittmann, 1963)

1 - Submarine Fissure Eruption
2 - Val del Calanna Eruption
3 & 4 - Trifoglietto I & II Volcanoes within the present Valle del Bove

A discussion of the eruptive features of Etna is reserved for Chapter 6. In the rest of this chapter the relevant geology of Etna and Sicily and their tectonic setting will be considered.

2.2 GEOLOGICAL FEATURES OF SICILY

A brief consideration of the geology of Sicily is helpful in providing a greater understanding of the setting of Etna and its own major geological features.

Sicily can be divided geologically into four separate structural blocks (Caire 1970), (Fig. 2.3), (1) The Ragusa - Iblei Carbonate Platform, (2) The Neogene Sedimentary Basins, (3) The Flysch Nappes, (4) The Peloritani Massif.

1. Ragusa - Iblei Carbonate Platform.

The Ragusa Plateau in Sicily's south-east is an external palaeogeographic unit and has not been affected by the tangential Alpine tectonism and may be considered as an extension of the Sahara Desert beyond the Sicilian - Tunisian basin. It is striated by a series of normal faults striking SSW and SSE and is separated from the Caltanisetta Basin (q.v.) by a system of faults and flexures extending NNE into the Iblean mountains, which represent the passage of basaltic extrusions during the early Miocene, including those underlying the Quaternary volcano of Mount Etna.

2. Neogene Sedimentary Basins.

This region comprises almost all of Western Sicily reaching Catania in the east and lying between the Ragusa Plateau to the south

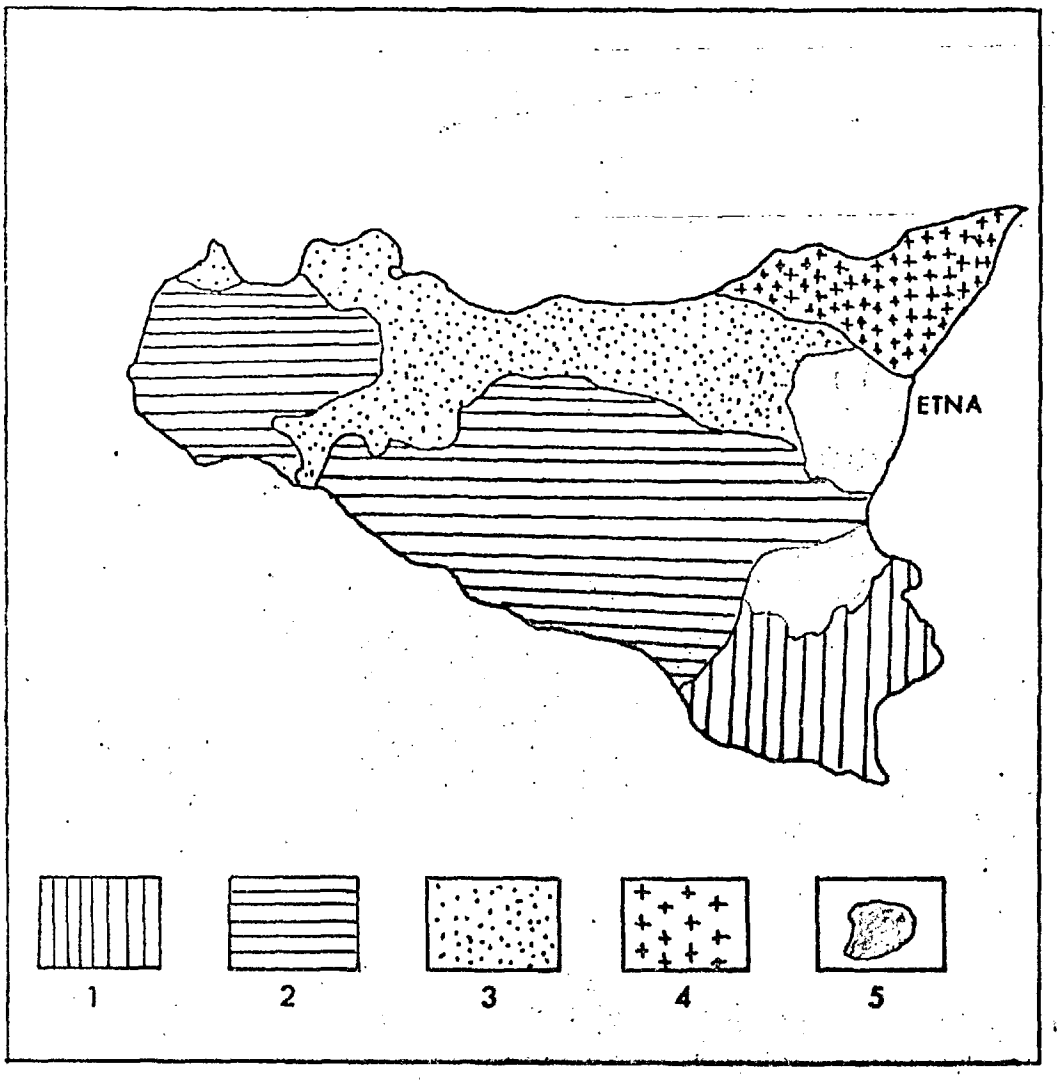


FIG. 2.3

Major Geological Features of Sicily (after Barberi et al.,1974)

1 - Ragusa-Iblei Carbonate Platform

2 - Neogene Sedimentary Basins

3 - Flysch Nappes

4 - Peloritani Massif

5 - Recent Volcanics

and the Nebrodi and the Peloritani Massifs to the north. The most important of these basins is the Central Sicilian (Caltanisetta) Basin. The tectonic uplift of Sicily during the lower Pliocene has resulted in upper Pliocene and lower Quaternary deposits being found in this basin at heights of several hundred metres.

3. The Flysch Nappes.

The central northern region of Sicily is composed of a series of flysch nappes dating from the Cretaceous to the Miocene. These nappes are similar to their corresponding equivalents in North Africa. The most internal nappes show, in plan view, curving boundaries, concave to the northwest and also overthrusts which have moved from the inside to the outside of these arcs. The Monte Soro Nappe, which forms the main element of the Nebrodi Mountains, extends south of the Peloritani Mountains (q.v.) and underneath Mount Etna.

4. The Peloritani Massif.

The Peloritani Massif, lying to the northeast, is the Sicilian continuation of the Calabrian arc. It comprises a metamorphic basement with granitic intrusions affected by reversal and overthrusting towards the south.

This brief description of the salient aspects of the geology of Sicily provides an appropriate introduction to a description of the geology of Mount Etna itself.

2.3 GEOLOGY OF MOUNT ETNA.

Submarine basaltic volcanism has been traced back to the Middle Triassic period for the south eastern region of Sicily (Cristofolini, 1973) giving rise to pillow lavas and hyaloclasites through fissures in a carbonate platform. The Iblean mountains, further north, are the site of volcanic rocks dating from the Miocene, Pliocene and Pleistocene ages. During the Middle Quaternary, submarine fissure eruptions of basaltic magma occurred in a shallow, Sicilian clay gulf in the area presently occupied by Mount Etna. The tectonic uplift of Sicily resulted in these submarine eruptions becoming sub-aerial and in due course gave rise to the complex volcanic system comprising Mount Etna. This northward trend in volcanism is illustrated in Fig. 2.4.

Mount Etna itself sits upon a sedimentary basin composed of flysch type deposits of Cretaceous to Miocene age in the north, Miocene sandstones in the west and Pleistocene alluvial deposits in the Plain of Catania to the south.

The most impressive structural feature and one of the most important geological aspects of the volcano is the enormous depression, east of the summit, called the Valle del Bove (Fig. 2.5). Its provision of a cross-section of the volcano complex is foremost amongst the reasons for its geological importance. Klerkx (1968) determines at least four stages in the development of Etna from an examination of

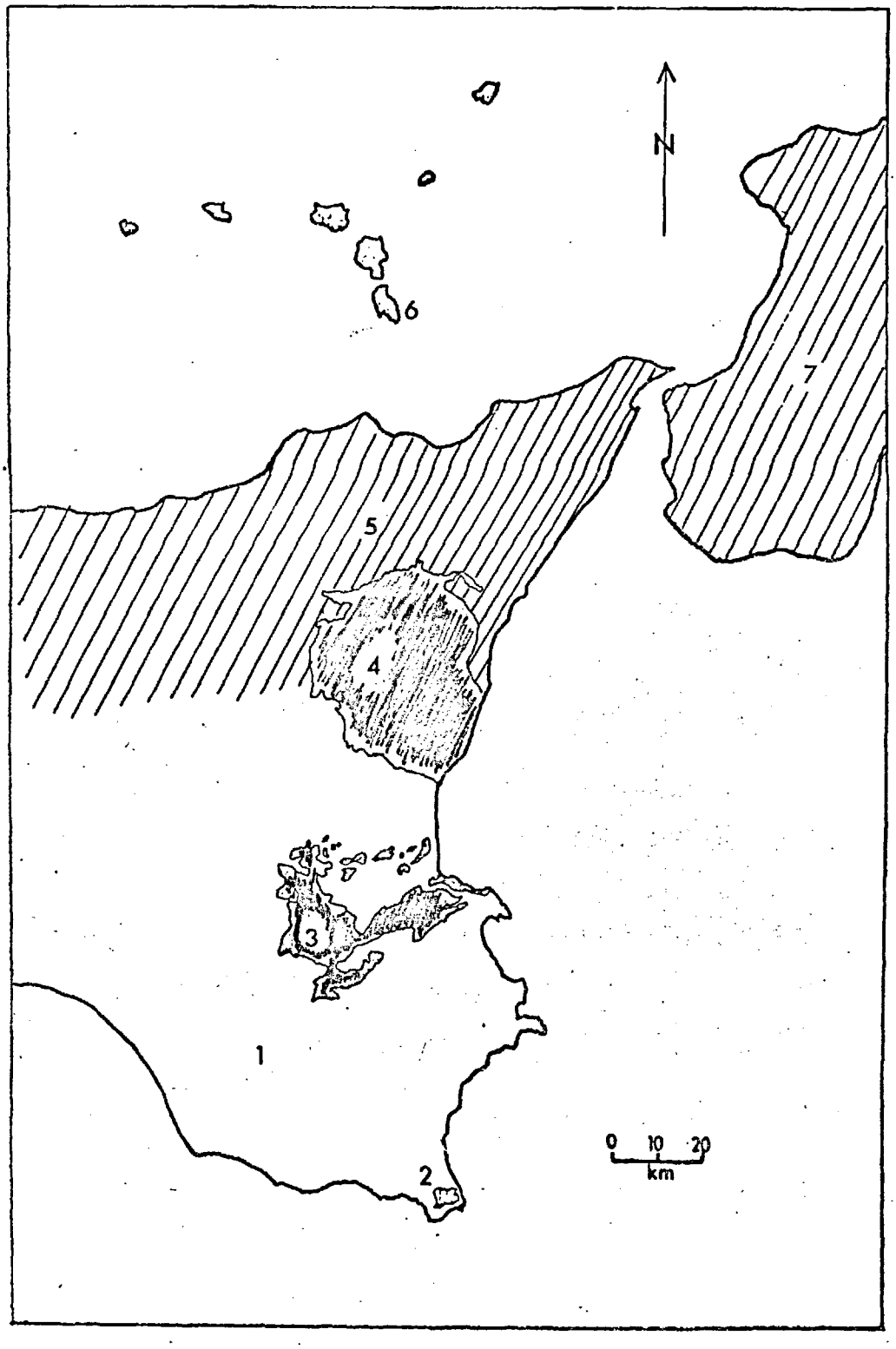


FIG.2.4

Northward Trend of Volcanism (Rittmann, 1973)

1 - Ragusa oil field (Triassic & Jurassic); 2- Pachino & Capo Passero (Cretaceous); 3 - Iblean Mountains (Neogene to Lower Pleistocene) 4 - Mt. Etna (Lower Quaternary to Recent); 5 - Peloritani Mountains 6 - Eolian Islands (Quaternary); 7 - Calabrian Mountains

MT. ETNA

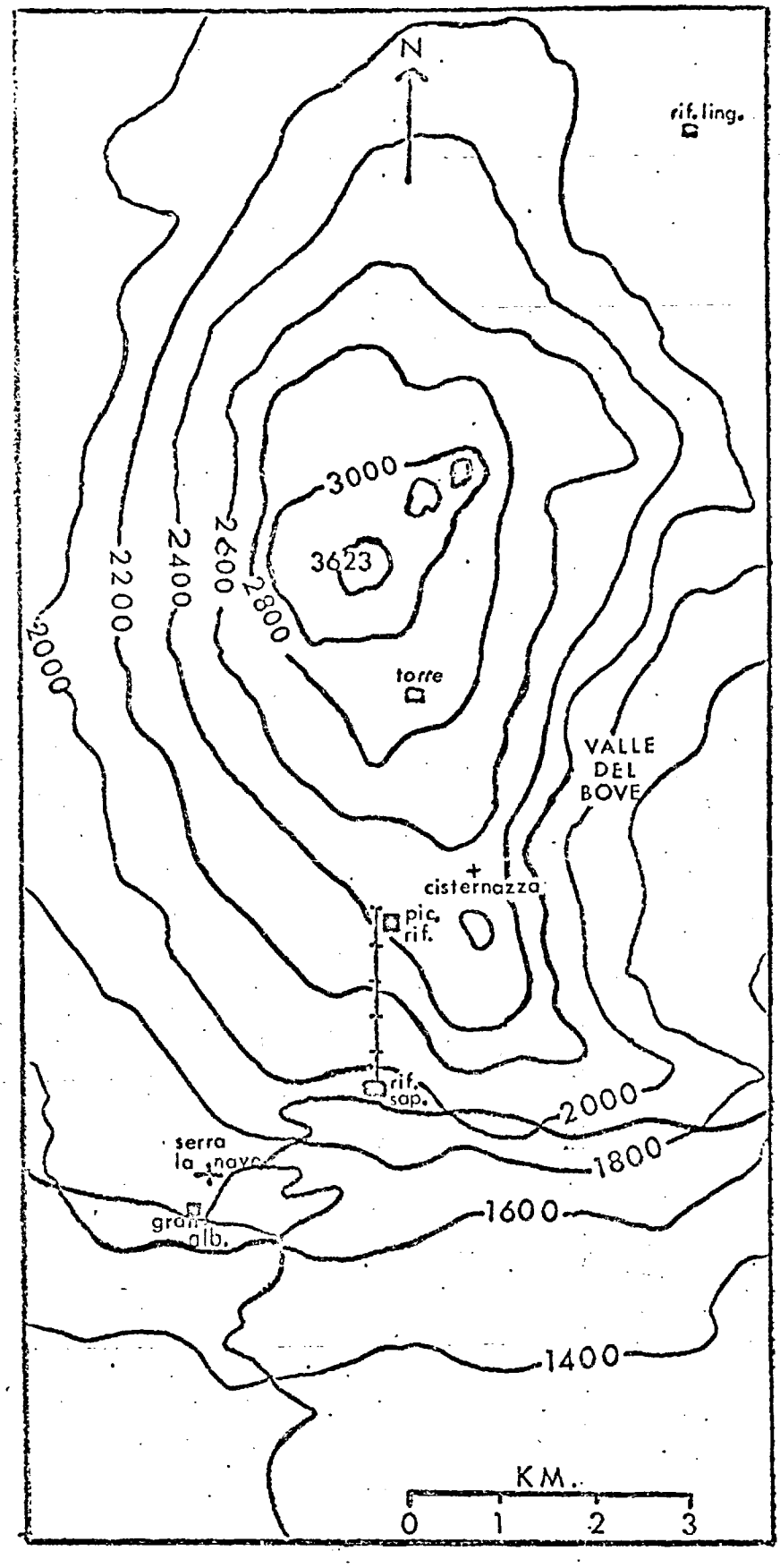


FIG. 2.5

Mt. Etna, showing Valle del Bove and the tiltmeter sites; Cisternazza and Serra la Nave

the Valle del Bove. The four stages reveal a westwards trending volcanism starting from a site at the Valle del Calanna and developing via Trifoglietto I and II in the Valle del Bove itself up to the present volcanic centre of Mongibello. These stages are depicted in Fig. 2.6.

The most widely accepted explanation of the origin of the Valle del Bove is due to Kieffer (1969), who postulates its formation in a violent pumiceous explosion resulting in the destruction of Trifoglietto II. In view of the radio-carbon dates of 5000 ±130 years B.P. obtained for the widespread ash deposits of the eastern and south-eastern slopes of the Valle del Bove (Sturiale, 1967) he assumed this to be the probable date of the cataclysm. Although Klerkx (1968, 1970) indicates that the latite - andesites of Trifoglietto II are much older than 5000 years this does not rule out Kieffer's proposed solution.

As a result of a gravity survey of Etna (Klerkx and Evrard, 1970) considerable doubt must now be cast on the pumice - explosion theory, however. The gravimetric map produced as a result of this theory clearly indicates a positive anomaly (27 mgals) situated in the Valle del Bove over the area proposed by Klerkx (1970) as the centre of Trifoglietto II. According to Yokoyama (1963), however, pumiceous calderas should give rise to negative and not positive gravity anomalies.

Rittman (1973) also suggests an explosive genesis for the Valle del Bove, similar to that forming the Bandai San Caldera in 1883. This

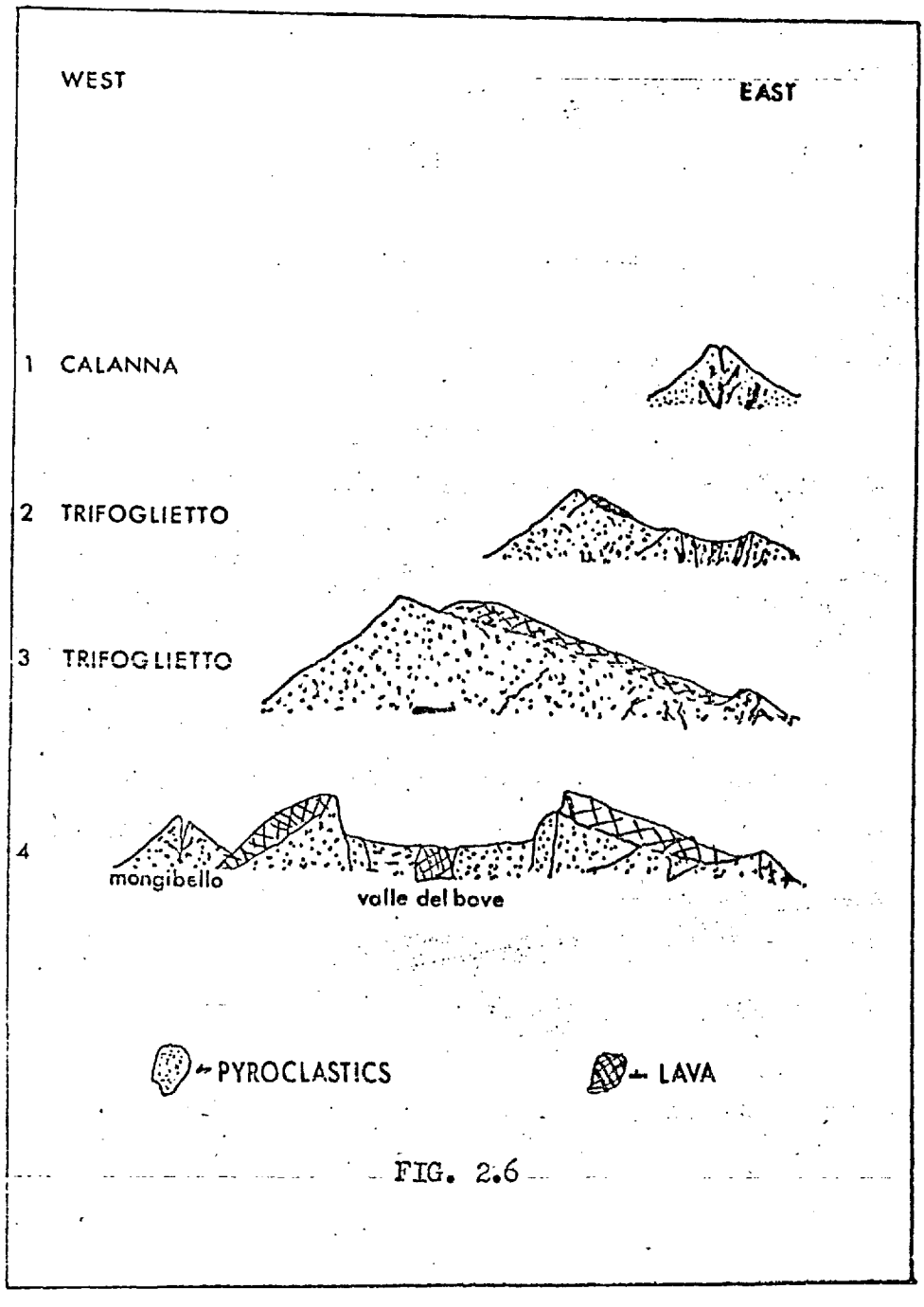


FIG. 2.6

Hypothetical profiles at four stages in the evolution of the volcanoes that occupied the Valle del Bove. Stage 4 represents the Trifoglietto volcano before the formation of the post-Trifoglietto cones. (after Kleriax, 1970)

hypothesis still seems to run into the same problems as the previous one and, as Rittmann himself states 'none of these attempts offers a satisfactory explanation'.

A further problem as yet unsolved, has been the question of a central magma chamber. Whilst most authors favour the non-existence of such a chamber research into the transportation of magma within the volcano shows the problem to be extremely complicated. In passing it might be added that this is not particularly surprising, given the eruptive history of Etna. It is instructive to consider the degree of variance between authors on the matter of a magma chamber. Rittmann (1973), during an assessment of various chemical analyses of Etnean lavas states "..... These facts confirm the non-existence of a single great magma reservoir beneath Mt. Etna." and he continues by saying that the variance in lava composition can be easily explained by assuming that the magma rises along a series of abyssal fissures from a deep source. Contrariwise Cristofolini (1973) commenting on the petrography of Etnean lava flows, says "..... the above stated conditions can be fulfilled only if the magma undergoing differentiation is stored in relatively large batches .....". These two statements may not, however, be at quite such odds as they initially appear since Rittmann only commits himself specifically against a "single great magma reservoir" and Cristofolini does not propose a single chamber so much as a series of distinct magma storage locations. This is a view supported by Carter and Bell (1975) who find that the

chemical data oppose the idea of a large magma chamber, which would involve considerable crystal fractionation but is in accordance with the sub-volcanic dyke-sill plexus of Wadge (1974).

Although geophysical evidence relating to this seminal problem will be discussed later it is pertinent to note that Machado (1965) deduces not only the existence of a magma chamber but also its magnitude and location. Based on a comparison of the observed and theoretical seismic intensities from the 1908 Messina earthquake he estimates a chamber forty kilometres wide by one hundred kilometres in length at a depth of five kilometres. Since this result is based on a study of intensities and not magnitudes and also for an earthquake occurring some sixty years before the publication of this paper it must be regarded with a good deal of caution. Further research along these lines was begun by a group from Cambridge University in 1977 but as yet no results are available.

From geodetic evidence Wadge (1976) considers that the Chasm can act as a magma reservoir for flank eruptions. This would appear to be a very reasonable conclusion considering the divergence of opinion based on purely geological grounds.

2.4 GEOMORPHOLOGY AND THE SUMMIT REGION

The morphology of a volcano is generally determined by the products of any eruption and their manner of effusion; it will thus parallel the history of the activity of the volcano.

Rittmann (1962) regards Etna as a basaltic shield volcano overlain by a strato-volcano, the basal part of which is dominated by lavas. There are three distinct morphological units. The highest of these is the summit cone rising some 300 metres above the summit plateau (Piano del Cratere). This Piano del Cratere is almost certainly the latest of several infilled calderas and forms the second morphological unit. The third unit is represented by the flanks of the volcano, which generally become steeper at higher altitudes. There is, however, an abrupt change of slope at 1800 metres and this 1800 metre level is also important when considering the location of flank eruptions (q.v. Chapter 6).

The three units can be seen in the volcano profiles of Fig.2.7.

Summit Region

The summit region comprises the main central crater and a slightly smaller, though more active, secondary crater known as the Northeast Crater. The central crater contains within it two cratered cones, the '1964' crater and the Chasm (La Voragine) and a collapse

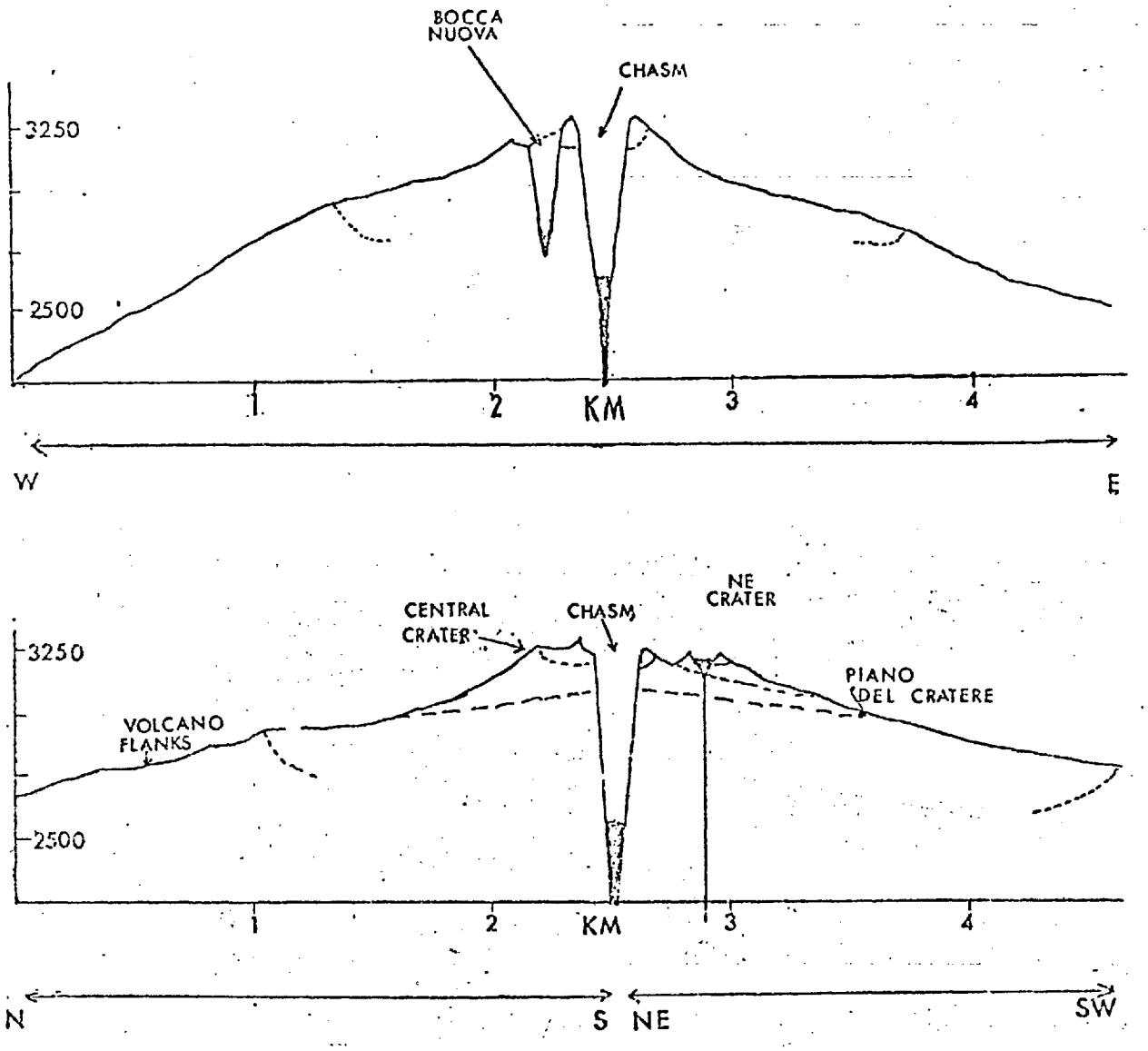


FIG. 2.7

Volcano profiles intersecting the Summit region (after Guest, 1973)

crater, the Bocca Nuova. Guest (1973) has described the geology of the summit region and a map of the region is shown in Fig. 2.8. Changes were recorded by Murray (1977) mainly around the Northeast Crater. The Chasm is less than twenty years old while the central crater as a whole dates back over three hundred years. Spallanzare (1798) reported by Wadge (1974) gives a review of several descriptions of the summit region, indicating the ephemeral nature of the craters and cones within the central crater.

The Calderas.

There are two calderas lying just below the summit. The Cratere del Piano lies at an altitude of 2900 - 2950 metres and to the north, at a slightly lower level, is the Cratere Ellittico so named because of its elliptical outline. The exact temporal relationships between the calderas is not known but both indicate that caldera collapse has been an important factor in determining the structure of the summit region over the past few thousand years.

The Flanks.

Etna's flanks are characterised by the number of adventive cones and craters distributed over their surface. Wadge (1974) estimates that they represent some 2700 years of flank activity assuming a constant rate of production, which seems a reasonable assumption.

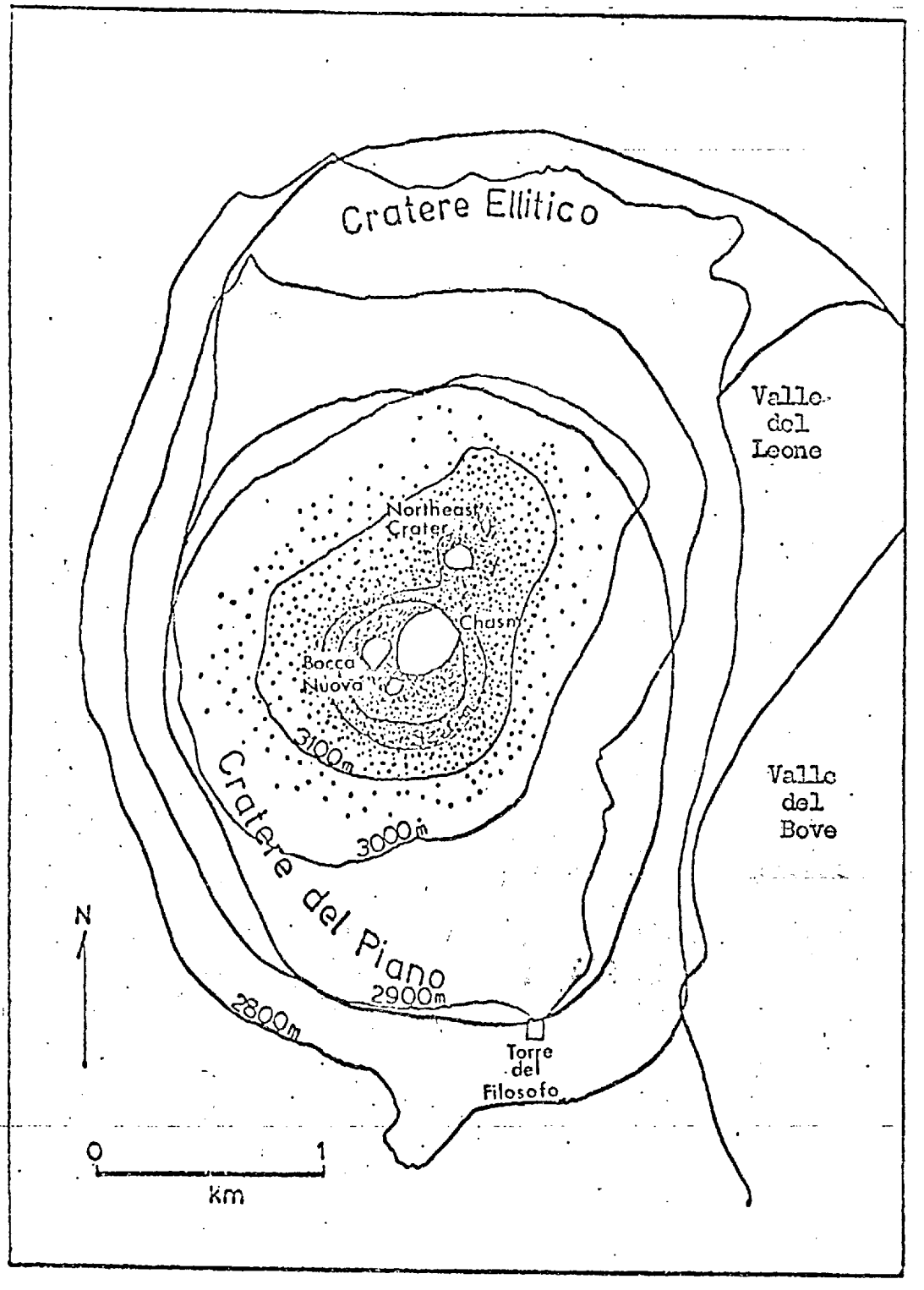


FIG. 2.8
Probable outlines of the summit calderas (after Wadge, 1974)

2.5 TECTONIC SETTING OF SICILY

The tectonics of the Mediterranean has been the subject of much discussion in recent years, and for the region around Sicily and Southern Italy in particular a considerable amount of research has been conducted and yet has still resulted in rather vague solutions which immediately prompt the question; "why does Etna appear to be on the wrong side of the Europe-Africa plate boundary?"

Palaeomagnetic data from volcanic rocks in the Ragusan platform shows that Sicily has been fixed with respect to the African plate from the Upper Cretaceous but until the Plio-Pleistocene was palaeomagnetically distinct from the European plate (Barberi et al., 1974(a)). From this, it can be reasonably inferred (Grindley, 1973) that the African plate, carrying Sicily along with it, collided with the European plate towards the end of the Oligocene, resulting in the formation of the Aeolian arc volcanoes. In the Lower Miocene, the thrusting nappes and metamorphic belt of the Peloritani Mountains to the north of Etna were formed.

A definitive placing of the plate boundary in this region is hampered by the lack of seismic data from the region (McKenzie, 1970). The available seismic data indicates that the African plate is under-thrusting the Euro-Asiatic plate with a slope of approximately 58° in the Lipari region and 35° in the Aegean region (Caputo et al., 1970)

(Fig. 2.9) a conclusion which is supported by the available gravity, volcanic and heat flow data (Caputo et al., 1970). The plate boundary determined by McKenzie (1970) is vague in the region of Sicily for the reason indicated above, but an analysis of geochemical data (Barberi et al., 1974 (a)(b)) confirms the position of the plate boundary north of Etna (Fig. 2.10), whilst still being tentative regarding its definitive lineation. The dextral motion of Calabria with respect to Sicily shown by Barberi et al. (1974 (a)(b)) and indicated in Fig. 2.10 should be detectable by the current electromagnetic distance measuring equipment now available. The only attempt to measure this (Caputo et al., 1974) gives results that are far from being conclusive, primarily because only four points were chosen, two on either side of the Straits of Messina, the purported plate boundary and also, for reasons the authors themselves indicate, the short time interval between the first and last measurements and the comparatively small variations in line length.

Seismic investigations in northern Sicily (Giese et al., 1973) suggest a crustal thickness of 38 kms. in the region of Etna, and Barberi et al. (1974 (a)) say that the crustal thickness increases from the Sicily Channel in the south to the north coast of Sicily and that it may reach 40 kms. under Etna although they point out that the crust/mantle interface is indistinct in the north. Belderson et al. (1974) deduce the existence of a poorly developed ridge in the Ionian Sea concentric with the Calabrian arc. The existence of this Calabrian ridge implies crustal shortening related to the compression concomitant with the Benioff zone beneath the Calabrian arc. This compression is probably due to the south-easterly motion of the Tyrrhenian region.

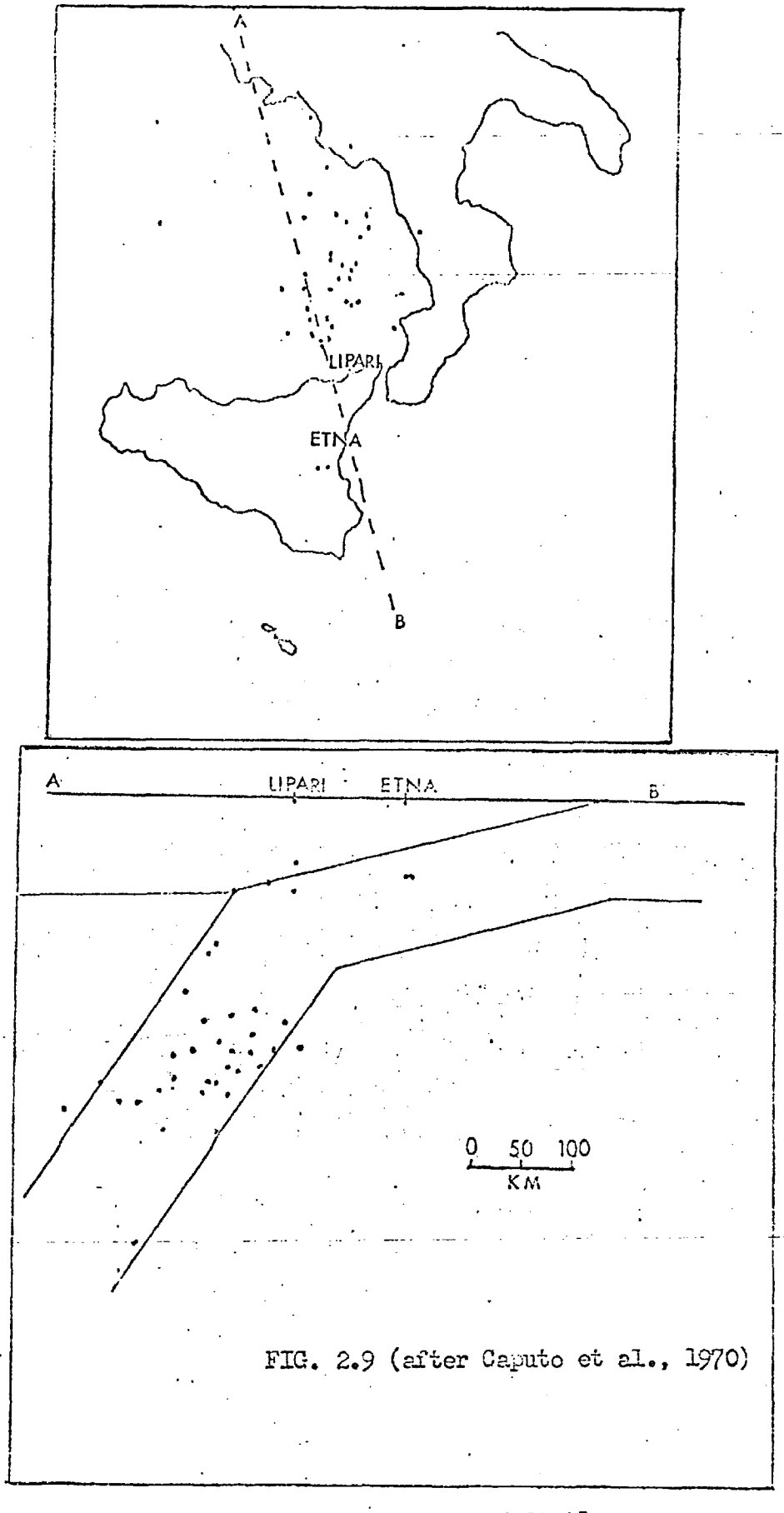


FIG. 2.9 (after Caputo et al., 1970)

Seismic data for southern Italy and Sicily.
Dots are earthquake epicentres. Vertical section is along the dotted line.

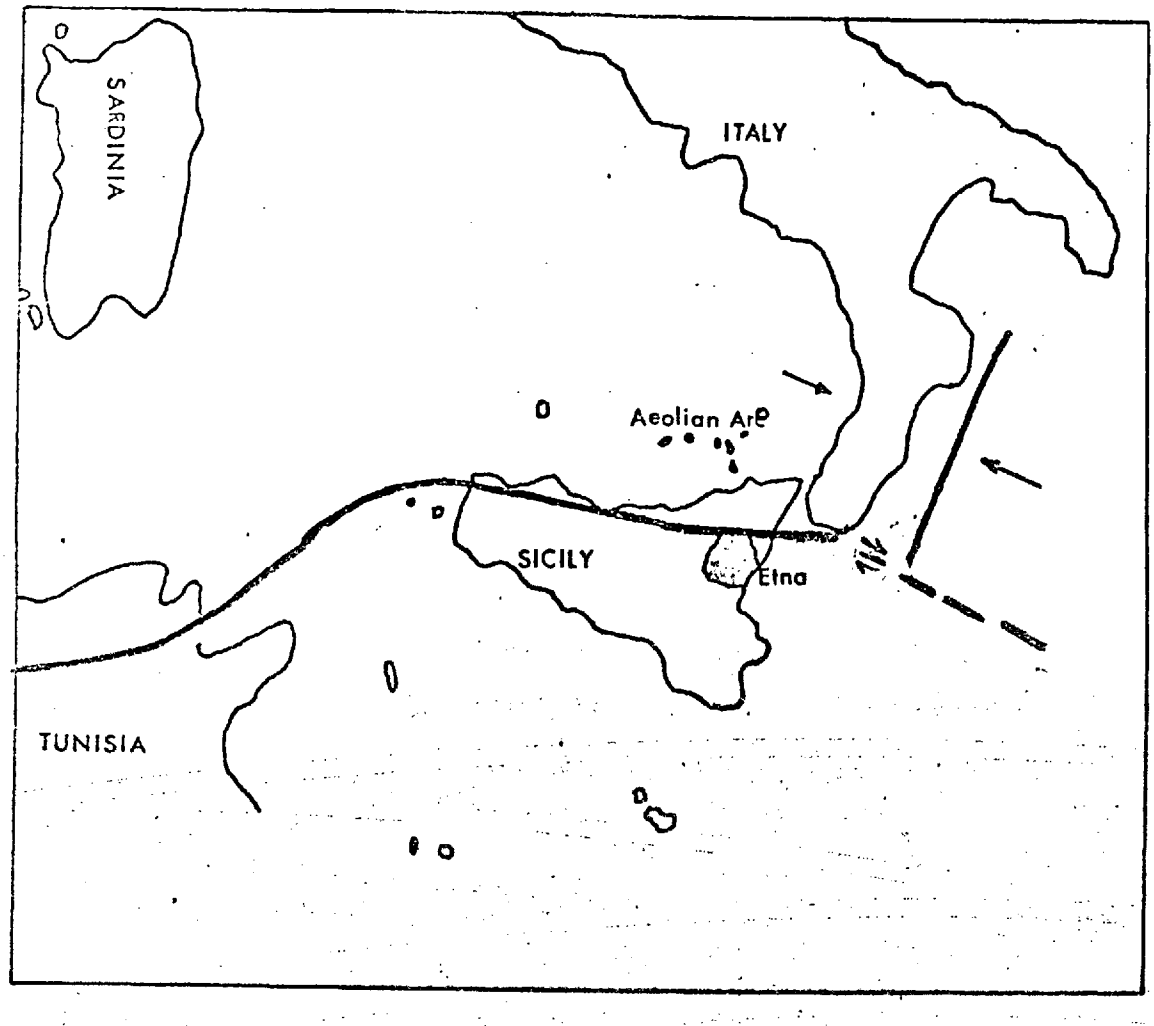


FIG. 2.10

Probable location of the Euro-African plate boundary in the vicinity of Sicily. (after Barberi et al., 1974b)

Arrows indicate the direction of motion

Geochemical studies of the Aeolian arc to the north of Sicily reveal it to be in a senile evolutionary state (Barberi et al., 1974(b)) and additionally a comparison of the $^{87}Sr/^{86}Sr$ ratio for Etnean and Aeolian lavas reveals a difference (.7033 to .7045) which shows a dissimilar provenance for the two systems, contrariwise the volcanic rocks from the Sicily Channel give the same $^{87}Sr/^{86}Sr$ ratio, indicating a similarity in the tectonic setting for the two regions, a finding which is supported by morphological considerations (Wadge, 1974). The $^{87}Sr/^{86}Sr$ ratio has also been used to support arguments showing that Etna's source magma has not been affected by crustal assimilation.

There have been many attempts to explain Etna's unusual position vis-a-vis the plate boundary. Barberi et al. (1974 (a)) relate the geochemistry of the volcanic products of Eastern Sicily to the various compressional and distentional tectonics of the area, and to probable changes in the Afro-European plate boundary since the Triassic. Eastern Sicily has, however, been on the border between the colliding continental plates since the Upper Miocene, giving rise to local distensive tectonic features related to the stress field directed normally to the motion of the oceanic uthosphere. There is no attempt by Barberi et al. (1974(b)) to explain how distensive tectonics could exist above a subducting plate. To solve this Grindley (1973) proposes a high rate of arc migration and claims that '..... rates of arc migration are sufficiently rapid to allow crustal dilatation normal to the Calabrian arc at the present day.....'. The overriding

impression must be, however, that this is an intractable problem requiring a great deal more investigation which, it is satisfying to note, is being carried out.

2.6 TECTONIC CONTROL OF MOUNT ETNA

The fault system controlling Mount Etna is shown in Fig.2.11. There are three major series of faults (Rittmann, 1973); one trending NNE - SSW along the coast of Sicily, a second is directed ENE - WSW and a third ESE - WNW. The ascent of magma is facilitated by faults and the distribution of eruptive centres reflects the tectonics of the basement (Fig.2.2). The ENE strike-slip faults south of the centre of Etna have considerable influence on the basement of Etna (Ritsema, 1969). The most important fault is, nevertheless, the NNE trending 'Messina Fault'. This is an extremely active fault responsible for the major earthquakes of 1783 and 1908 as well as many minor quakes. There is also evidence that Etna is rising isostatically. The sedimentary basement has risen as indicated by outcrops of Sicilian ~~Plaisancian~~ (Quaternary) at a height of 800m. on the eastern slope and 1050m. on the western slope (Rittmann, 1973). Grindley (1973) calculated this rate of uplift to be about 1mm/yr. Francavigalia (1959) and Ogniben (1963) consider the uplifted basement to be a WNW-ESE trending anticline whilst Rittmann (1963) prefers a horst-like feature controlled by a N-S trending normal fault parallel to the Ionian graben.

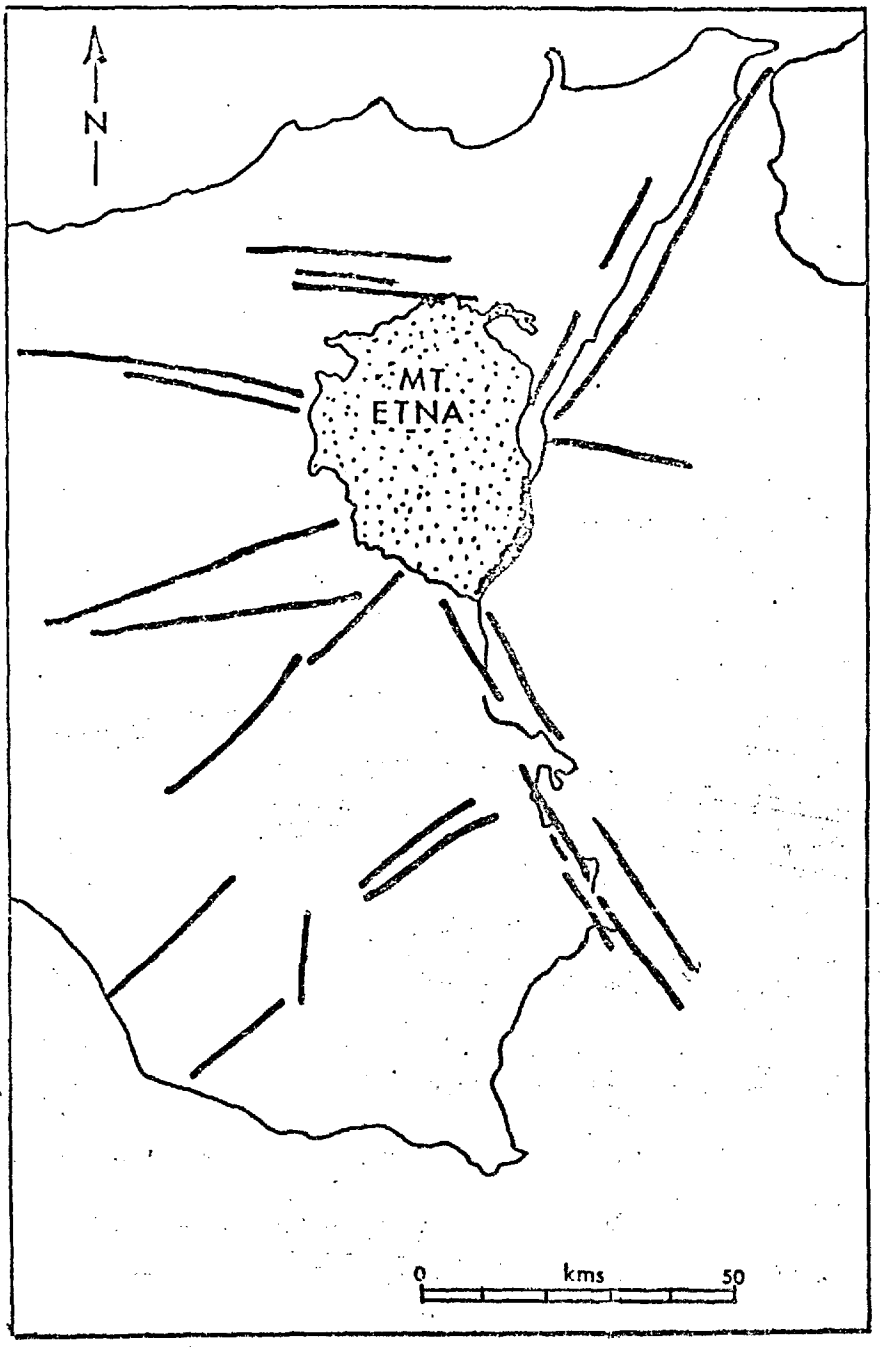


FIG. 2.11

The major fault system around Mt.Etna (after Rittmann, 1963)

CHAPTER 3

EARTH TIDES

3.1 INTRODUCTION

Tides on the earth, both solid earth and ocean, arise because of the differential gravitational attraction of the sun and the moon on different parts of the earth coupled with the relative motion of those perturbing bodies.

The tides can be grouped into three separate categories dependent upon the periodicities of their components, these are long-period, diurnal and semi-diurnal. The long-period tides include all tides with periods in excess of one day and arise because of the motion of moon around the earth (month) and the earth around the sun (year). The diumal tides arise because of the earths axial rotation. Tides occur with periods of a half of the fundamental periods, that is, semi-annual, fortnightly and semi-diurnal The reason for this can be simply explained with reference to Fig.3.1. A perturbing body M acting on the Earth E exerts a greater gravitational attraction at A than at O and a lesser at B.

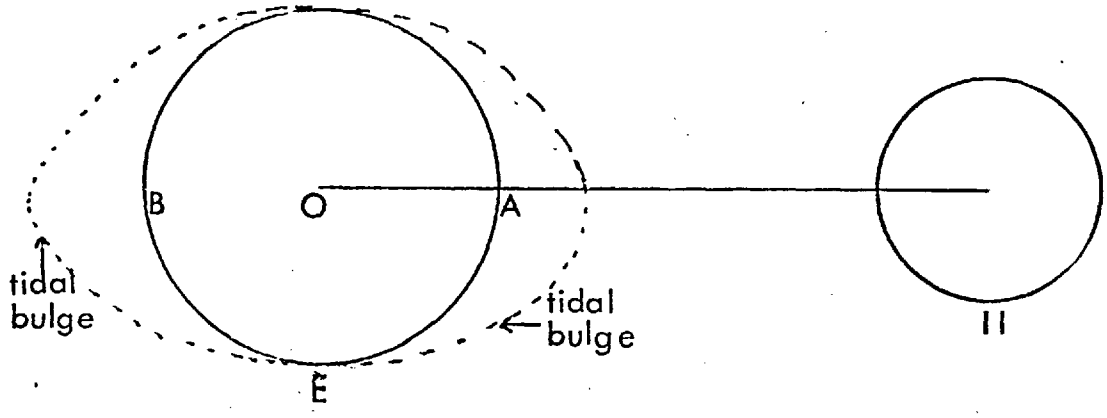


Fig. 3.1

Tidal bulge formed by the Earth's surface relative to the Earth's mass centre

This results in a tidal bulge, relative to the earth's mass centre. In practice this tidal bulge lags three degrees behind the line of centres OM because of friction due to the rotation of the Earth. Since the rotational period of the Earth is less than that of the moon round the earth, the lagging tides are carried ahead of the moon. Perturbational effects give rise to many tidal components with periods adjacent to the ones referred to here, a detailed development of which is given in section 3.

One of the effects of Earth tides and also one of the earliest observed is to cause fluctuations in the water level in wells and this has lead to considerations of the effects of the tides on volcanoes due to fluctuations in magma column levels. This phenomenon and other related topics are considered in Chapter 6 where tidal triggering of Etnean eruptions is analysed.

The elacticity of the earth, the liquid core and its structure and rheology in general all act to modify the Earth tides and one of the major uses of tidal observations is as an experimental test of the various Earth models. Tidal measurements have also been used in the examination of more esoteric theories such as gravitational shielding during a total eclipse but in this study we shall only be concerned with the tides as indicators of particular tectonic features (Tomaschek, 1957).

The nomenclature for the various tidal components introduced by Darwin (1882) involves the letters M or S, depending upon whether the originator of the component is the Moon or the Sun, and a subscript numeral indicating the period, 2 for semi-diurnal and 1 for diurnal. This is a useful notation for the principal terms but is inadequate when one has to deal with the hundreds of components obtained from a complete tidal analysis (Cartwright and Taylor, 1971).

As will be shown in the following section, the period of any tidal component can be expressed as follows:-

$$\text{Period} = a\tau + bs + ch + dp + eN' + fp_s$$

where τ, s, h etc., are certain fundamental astronomical periods, τ, for example, being the mean lunar day, s the tropic month, h the tropic year, etc., and a-f are integer coefficients appropriate to the particular component. This expression is commonly referred to as the argument of the tidal component. Doodson (1922) devised a scheme whereby each component is specified by a six-digit argument number made up as follows:-

$$a,\ (b+5),\ (c+5),\ .\ (d+5),\ (e+5),\ (f+5)$$

The reason for adding 5 to each of the coefficients except a is that it was initially thought these coefficients can have values ranging from -4 to +4, and so by adding 5 to each of them the possibility of some of the digits being negative is avoided. In fact, very occasionally, some of the coefficients do exceed this range (Cartwright & Taylor, 1971).

Thus, for example,

M2 has period	2τ	and argument number 255.555
O1 "	" $\tau-2s+p$	and " " 135.655

The first three digits are grouped together and are known as the constituent number. It is possible, from an inspection of the argument number to determine the length of data required to separate any two components, for example, components differing in the first digit require only one days data, a months data is required for components differing only in the second digit and a years data for those differing in the third digit. Components having similar constituent numbers require several years data and the importance of this is illustrated in Chapter 5.

3.2 THEORY

The theory regarding the forces exerted on the Earth by the Sun and Moon was developed in detail by Bartels (1957) originally in connection with ocean tides. There were many earlier theories notably those of Darwin (1882, 1907), Love (1909, 1911) and Doodson (1922) but Bartels was the first to use an accurate lunar theory. The following discussion is derived and adapted from Bartels.

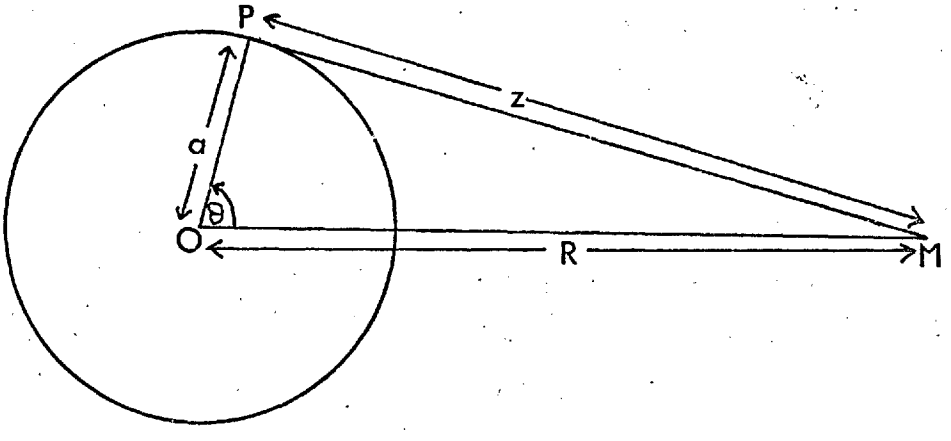


Fig. 3.2.

Diagram illustrating the notation of the expression of the tidal attraction of the moon.

Consider a point P on the surface of a sperical Earth, radius a, centre O and the Moon, centre M at distances Z and R from P and O respectively (Fig. 3.2). Then the gravitational potential at P due to M is:-

$$V = GM/Z \qquad 3.1$$

$$\text{and } Z^2 = a^2 + R^2 - 2aR\cos\theta \qquad 3.2$$

$$\text{Thus} \quad V = \frac{GM}{R}\left[1 + \left(\frac{a}{R}\right)^2 - \frac{2a}{R}\cos\theta\right]^{-\frac{1}{2}} \qquad 3.3$$

$$\text{and since } a \ll R \quad V = \frac{GM}{R}\left[1 + \frac{a}{R}\cos\theta + \left(\frac{a}{R}\right)^2\left(3\cos^2\theta - \frac{1}{2}\right) + \ldots\ldots\right] \qquad 3.4$$

The first term, GM/R, is simply the familiar Newtonian gravitational potential and since it is independent of θ it does not give rise to any tidal forces.

The second term, $GMa\cos\theta/R^2$, is the centripetal potential and this also does not produce any tidal forces.

This leaves the expression, $GMa^2(3\cos^2\theta - \frac{1}{2})/R^3$, and higher terms. In general since $a/R \simeq 1/60$ only the above term is normally considered. It may be noted, in passing, that the terms of this expansion are Legendre polynomials in $\cos\theta$.

Thus the tidal potential due to the moon can be written.

$$V = \frac{3}{4} GM \frac{c^2}{d^3} \left[\left(\frac{d}{c}\right)^3 \left(\cos 2\theta + \frac{1}{3}\right) \right] \qquad 3.5$$

Where c is the mean Earth - Moon distance, and d is the mean radius of a spheroidal earth, and is equal to $\sqrt[3]{a^2 b}$ where a and b are the semi-major and semi-minor axis lengths of the earth.

A similar expression can be derived for the tidal potential on the Earth due to the Sun. The term $(d/c)^3$ and its solar equivalent varies with the Earth - Moon distance and thus has a monthly periodicity. Since, however, the orbit is approximately circular we can take, as a first approximation:

$$\left(\frac{d}{c}\right)^3 \simeq 1$$

and a similar approximation can be made for the solar term.

The expression, $3GM\, c^2/4d^3$, is commonly known as Doodson's constant, D. It is convenient to write the expression in the form:

$$D = \frac{3}{4} \frac{M}{E} g\, d^4 \frac{(\sin^3 \pi)}{a^3} \qquad 3.6$$

where M and E are the masses of the Moon and Earth respectively, g is the mean gravity, d is the mean Earth radius, a is the equatorial

radius of the Earth, and $\sin \pi = a/R$ is the sine of the lunar parallax (Explanatory Supplement to the Astronomical Ephemeris, 1976) Currently accepted values of these parameters are given in Table 3.1 (Melchior, 1978)

PARAMETER	VALUE
M/E	1/81.3
d	6,371,023.6 m
g	9.82024
a	6,378,160.0 m
$\sin \pi$	0.01659251

Table 3.1

Parameters of the Lunar Orbit

In the tidal equation, 3.5, the term $(\cos 2\theta + 1/3)$ varies between $+ 4/3$ and $- 1/3$. This is the same for both the Moon and the Sun. The value of D is related to the amplitude of the tidal potential. The value of Ds,(D for the Sun) can be obtained from D in the following way:-

$$Ds = D.\frac{S}{M} \qquad 3.7$$

where S is the mass of the Sun.

Using the values given in Table 3.1 in equation 3.6 we obtain:

$$D = 2.627723 \ M^2S^{-2}$$

and from equation 3.7

$$Ds = 0.45990 \ D$$

Thus the effect of the Sun on tidal phenomena is approximately half that of the Moon. This is quite different from the normal gravitational attraction and arises because the tides are a differential effect giving a term proportional to the inverse cube of the Earth-Sun or Earth Moon distance. The tidal effect falls off very rapidly with distance and the tidal effects due to other planets even when considered at maximum perturbation are negligible, being less than 10^{-4} times that due to the Moon.

The tidal force, F, at a point on the Earth's surface is given by:

$$\underline{F} = - \text{grad } V$$

and then, from Fig. 3.3

$$\underline{Z} = -\frac{\partial V}{r} \quad ; \quad \text{vertical component} \tag{3.8a}$$

$$\underline{X} = -\frac{\partial V}{r\partial\theta} \quad ; \text{ N-S horizontal component} \tag{3.8b}$$

$$\underline{Y} = -\frac{\partial V}{r \sin\theta \partial\lambda} \quad ; \quad \text{E-W horizontal component} \tag{3.8c}$$

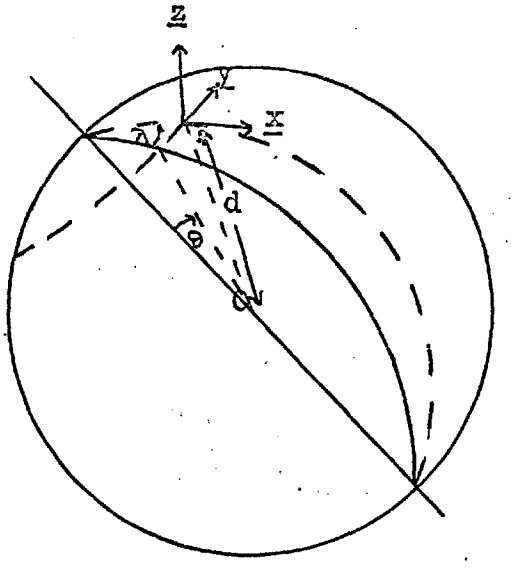


Fig. 3.3

Directions of tidal forces on the Earth's surface

$\underline{Z}$ is the variation in the acceleration of gravity Δg, therefore, at the surface of the Earth:

$$\Delta g = -\left(\frac{\partial V}{\partial r}\right)_{r = d} = -\frac{2V}{d}$$

and its numerical value is; .08249 mgal

Thus the Moon produces a tidal range of 0.165 mgal and the Sun, .0759 mgal.

The deviation of the vertical, or tilt, is derived from equations 3.8 a-c and is given by:

$$n_1 \simeq \tan n_1 = \frac{1}{dg}\frac{\partial V}{\partial \theta} \qquad \text{N-S tilt} \qquad 3.9a$$

$$n_2 \simeq \tan n_2 = \frac{1}{dg \sin\theta}\frac{\partial V}{\partial \lambda} \qquad \text{E-W tilt} \qquad 3.9b$$

The total tilt, n, is given by:

$$n = \frac{2D}{gd} \sin 2Z \qquad 3.10$$

where Z is the polar angle. This yields a numerical coefficient $8.399.10^{-8}$ rad. for the Moon, and $3.862.10^{-8}$ rad for the Sun, giving a total possible tilt range of 245.31 nrads.

3.3 ASTRONOMICAL DEVELOPMENT

The expression 3.6 for the tidal potential V is inconvenient when it comes to evaluating V because of the need to know θ, the local co-ordinate of the perturbing body. The expression can be simplified by introducing certain astronomical terms (Fig. 3.4). From a consideration of spherical trigonometry:

$$\cos\theta = \sin\phi \sin\delta - \cos\phi \cos\delta \cos H \qquad 3.11$$

It may be noted that eqn. 3.11 differs from the equivalent expression given by Melchior (1966) in its use of - cosH for cosH, this is a matter of convention and does not affect the further development of the theory.

Substituting from 3.11 into 3.6 gives:

$$V = D.(d/c)^3\left[(\cos^2\phi\cos^2\delta\cos 2H - \sin 2\phi \sin 2\delta \cos H + 3(\sin^2\phi - 1/3)(\sin^2\delta - 1/3)\right] \qquad 3.12$$

The equation thus provides three terms in spherical harmonics (Fig. 3.5) described in greater detail by Melchior (1978). Essentially the three terms are dependent upon the declination of the perturbing body δ, the latitude of the observation site ϕ and, in two of the terms, the hour angle H.

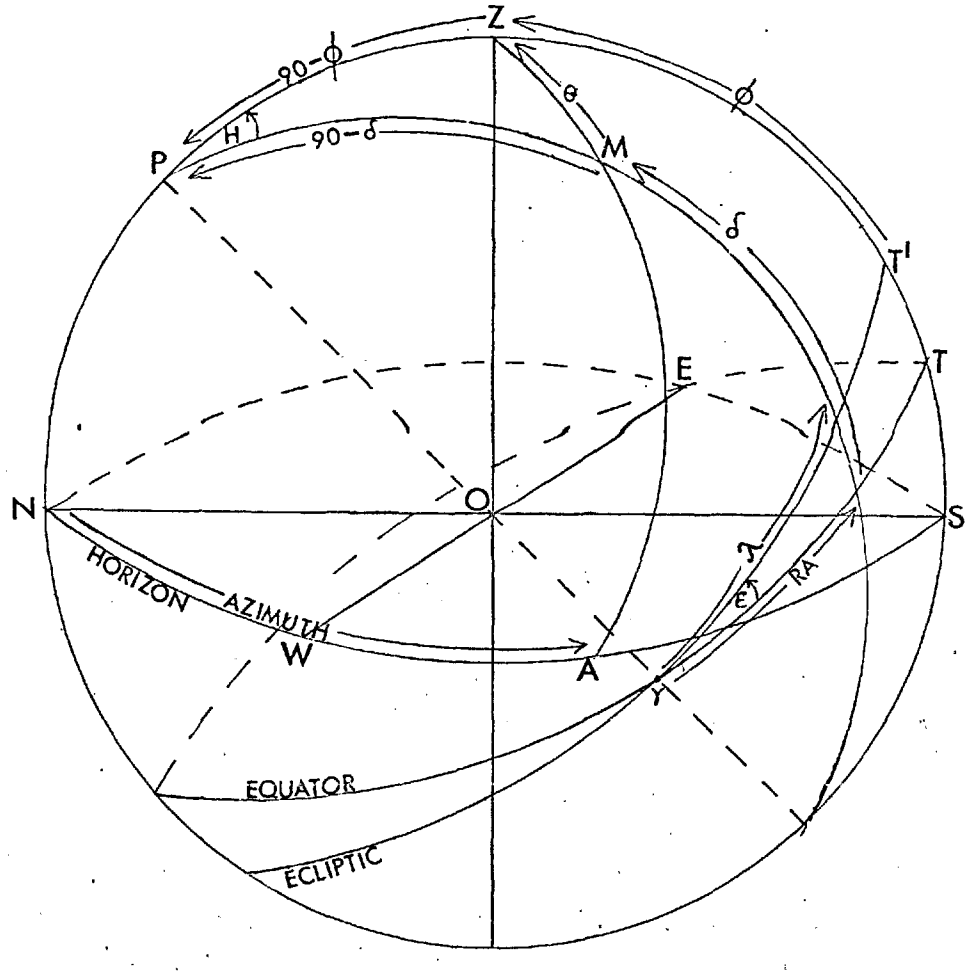


FIG. 3.4

Celestial Sphere and Astronomical Co-ordinates illustrating the terms used in the text.

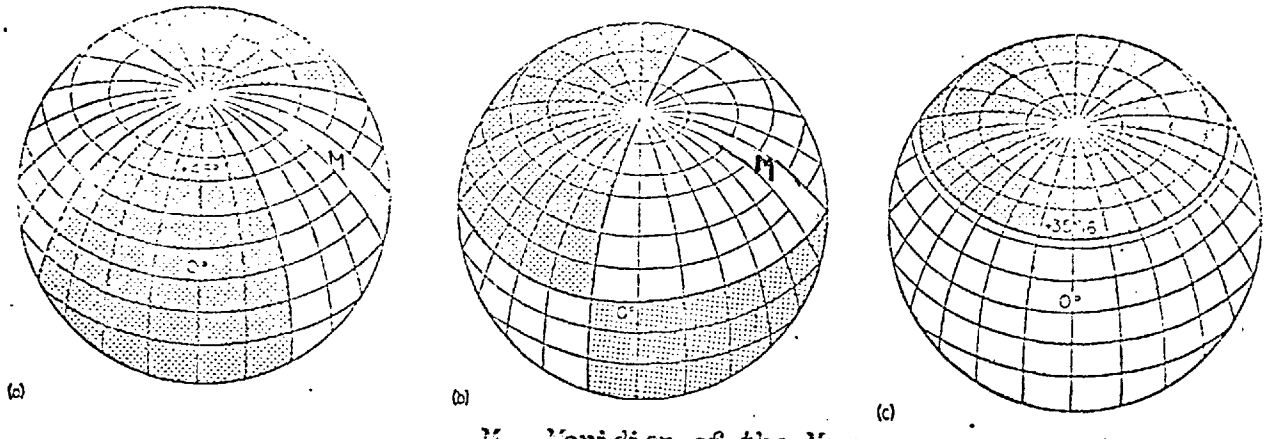
O - Observer Z - Zenith P- Pole M - Moon

ϕ - Latitude, λ - Longitude } along the ecliptic

RA - Right Ascension, δ - Declination } along the equator

γ - Vernal equinox; H - Hour angle; $T\gamma$ - Local Apparent Sidereal Time

ZM - Local co-ordinate of the perturbing body (θ)



M - Meridian of the Moon

FIG. 3.5

The semi-diurnal, diurnal and long-period tides represented as three types of second order spherical harmonics.

a) Semi-diurnal tides (Sectorial function)

b) Diurnal tides (Tesseral function)

c) Long-period tides (Zonal function)

The shaded and unshaded areas show the regions, on the Earth's surface, where the tide is negative and positive respectively. (after Melchior, 1966)

In the following discussion certain astronomical terms are used and these are listed in Table 3.2.

τ	mean lunar time
t	mean solar time
s	mean longitude of the Moon
h	mean longitude of the Sun
p	longitude of the lunar perigee
$N' = -N$	longitude of the lunar ascending node (N is retrograde)
ps	mean longitude of the perihelion

Table 3.2

Orbital Parameters

Sidereal time $t' = \tau + s = t + h$ (Fig. 3.4)

Thus $t = \tau + s - h$

The variables s, h, p, N, and ps are all time-dependent and values are listed in the Astronomical Ephemeris.

Certain of the terms in equation 3.12, δ and d/c, are time-dependent. The equations used to evaluate them are complicated and need not be given here. They can be found in Melchior (1978).

As referred to above, equation 3.12 gives three terms. Because of the time dependency of δ and d/c each of the terms is comprised of a series of time-dependent components.

Long-period waves derive from the term: $3\,(\sin^2\varphi - 1/3).\,(\sin^2\delta - 1/3).\,D.\,(d/c)^3$. They are called long period since they are dependent on the orbital periods of the Sun and Moon around the Earth only and not on the axial period of rotation of the Earth.

The most important long-period terms are; aconstant term Mo resulting in a permanent flattening of the Earth; a fortnightly term Mf of argument 2s and period 13.66 days and a monthly term Mm of argument s-p and period 27.55 days.

A similar expression can be derived for the Sun and gives rise to the following major components:

So - a constant term similar to Mo

A semi-annual wave SSA of argument 2h and period 182.62 days and an annual wave Sa of argument h-ps and period 365.259 days.

Diurnal terms derive from the expression:- $\sin 2\varphi \sin 2\delta \cos H.D.(d/c)^3$

and as with the long-period waves this expression can be expanded to give a series of lunar diurnal terms of which the most important are:

O1 of argument $\tau - s$ and period 1.035 mean solar days

Klm of argument $\tau + S$ and period 0.997 m.s.d.

the solar expression generates the following waves:

P2 of argument t-h and period 1.000 m.s.d.

and Kls of argument t + h and period 0.997 m.s.d.

since $t + h = \tau + S$ the Sun and Moon both give rise to waves of the same frequency.

Similarly for semi-diurnal waves the general term is:

$$\cos^2 \delta \cos^2 \varphi \cos 2H.\ D.\ (d/c)^3$$

and this leads to the following lunar terms:

M2 of argument 2τ and period 12 hrs. 54 mins.

and K2m of argument $2(\tau + s)$ and period 11 hrs. 58 mins.

and corresponding solar terms:

S2 of argument $2\tau + 2s - 2h$ and period 12 hrs.

and K2s of argument 2 (t + h) and period 11 hrs. 58 mins.
As with the diurnal terms the arguments of K2s and K2m are the same.

A full analysis yields many hundreds of different waves (Cartwright and Taylor, 1971).

The above analysis considers only the vertical potential. Tilt terms can be computed from eqn. 3.9 a and b and components for all three terms are listed in Table 3.3.

Period	Vertical	N-S	E-W
Long	$3(\sin^2\varphi - 1/3)(\sin^2\delta - 1/3)$	$-3\sin 2\varphi(\sin^2\delta - 1/3)$	-
Diurnal	$-\sin 2\varphi \sin 2\delta \cos H$	$2\cos 2\varphi \sin 2\delta \cos H$	$2\sin\varphi \sin 2\delta \sin H$
Semi-Diurnal	$\cos^2\varphi \cos^2\delta \cos 2H$	$\sin 2\varphi \cos^2\delta \cos 2H$	$\cos\varphi \cos^2\delta \sin 2H$

Table 3.3

Coefficients of Tidal Tilt.

An inspection of Table 3.3 shows that the same waves will be found in tidal tilt as in tidal gravity. The latitude variation is different however. Figs. 3.6, 3.7a and 3.7b give the amplitude variation of the principal waves as a function of latitude and Fig. 3.8 shows the curves described by the direction of the vertical at different latitudes.

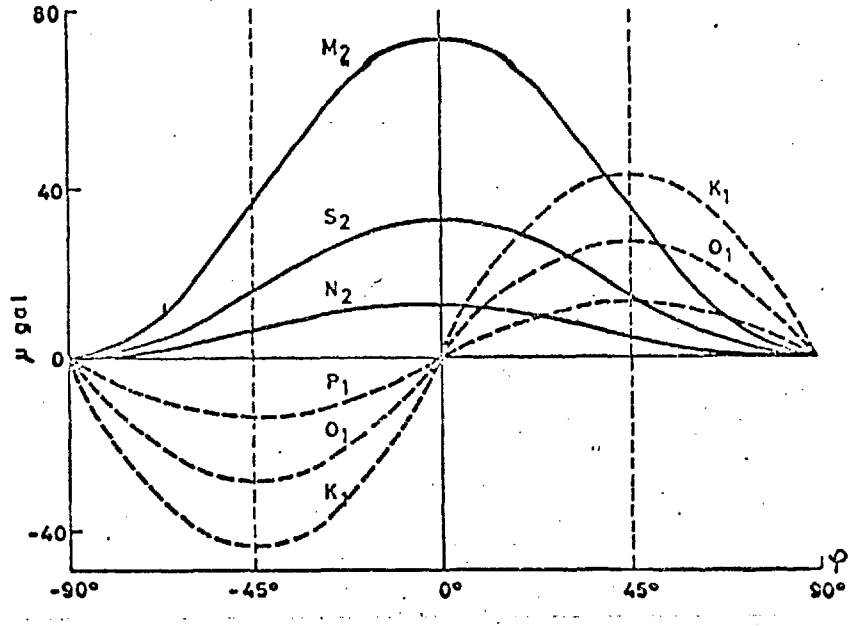


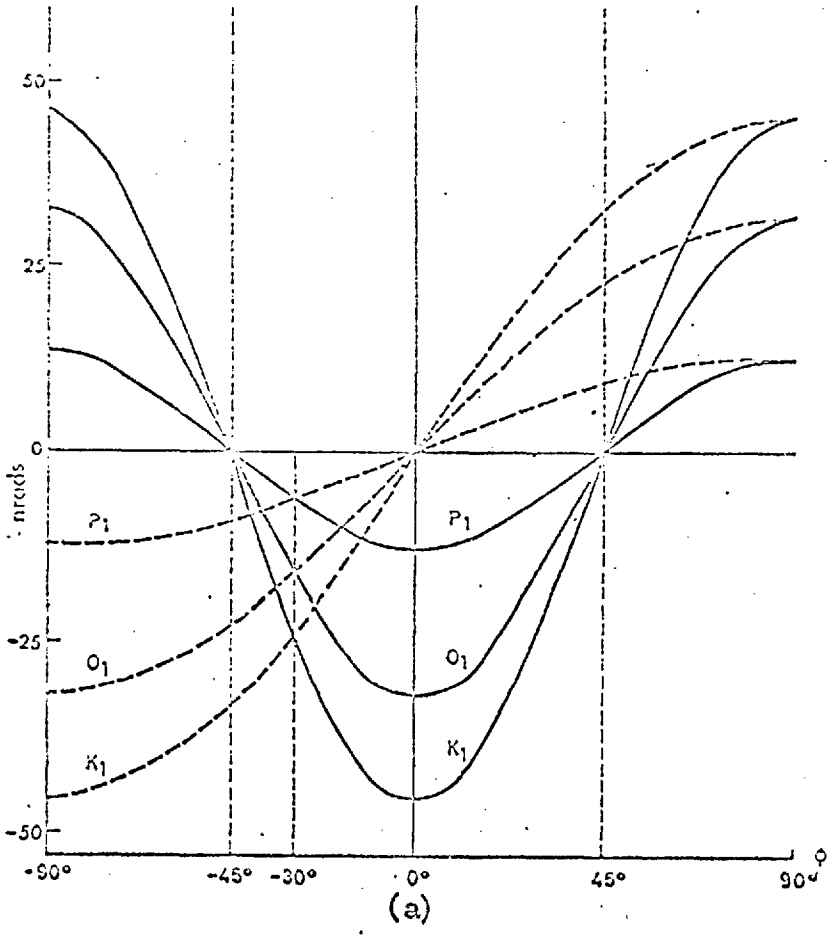
FIG. 3.6

Amplitude variation of the principal waves as a function of latitude for the vertical component of the tidal force.

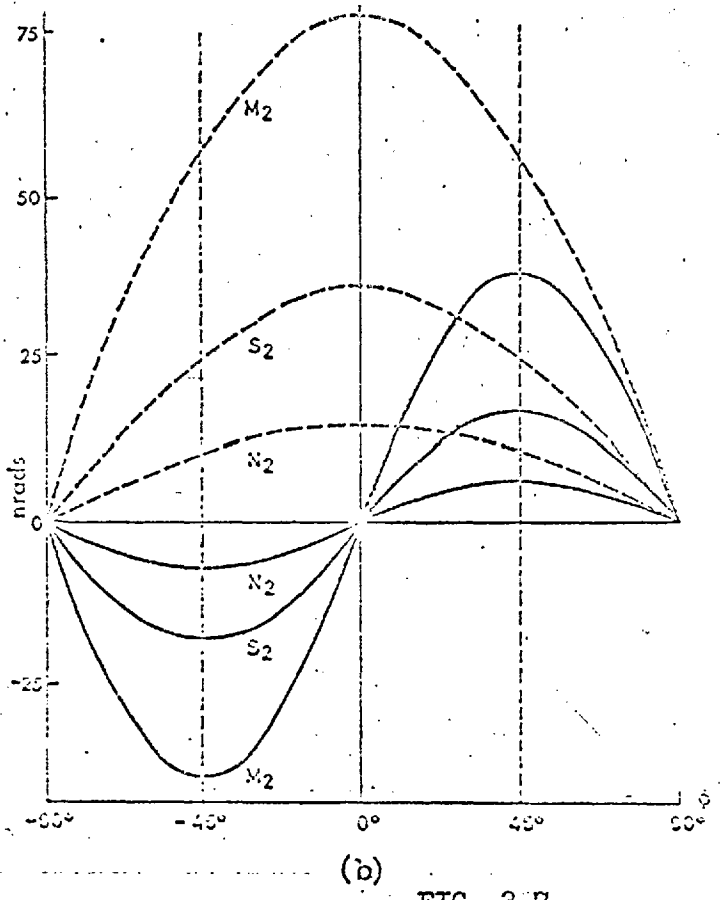
K_1, O_1, P_1: Diurnal waves

M_2, S_2, N_2: Semi-diurnal waves

(after Melchior, 1978)



(a)



(b)

FIG. 3.7

Amplitude variation of the: (a) Principal diurnal waves, and (b) Principal semi-diurnal waves, for the components of tilt

Solid line: North-South component. Dashed line: East-West component

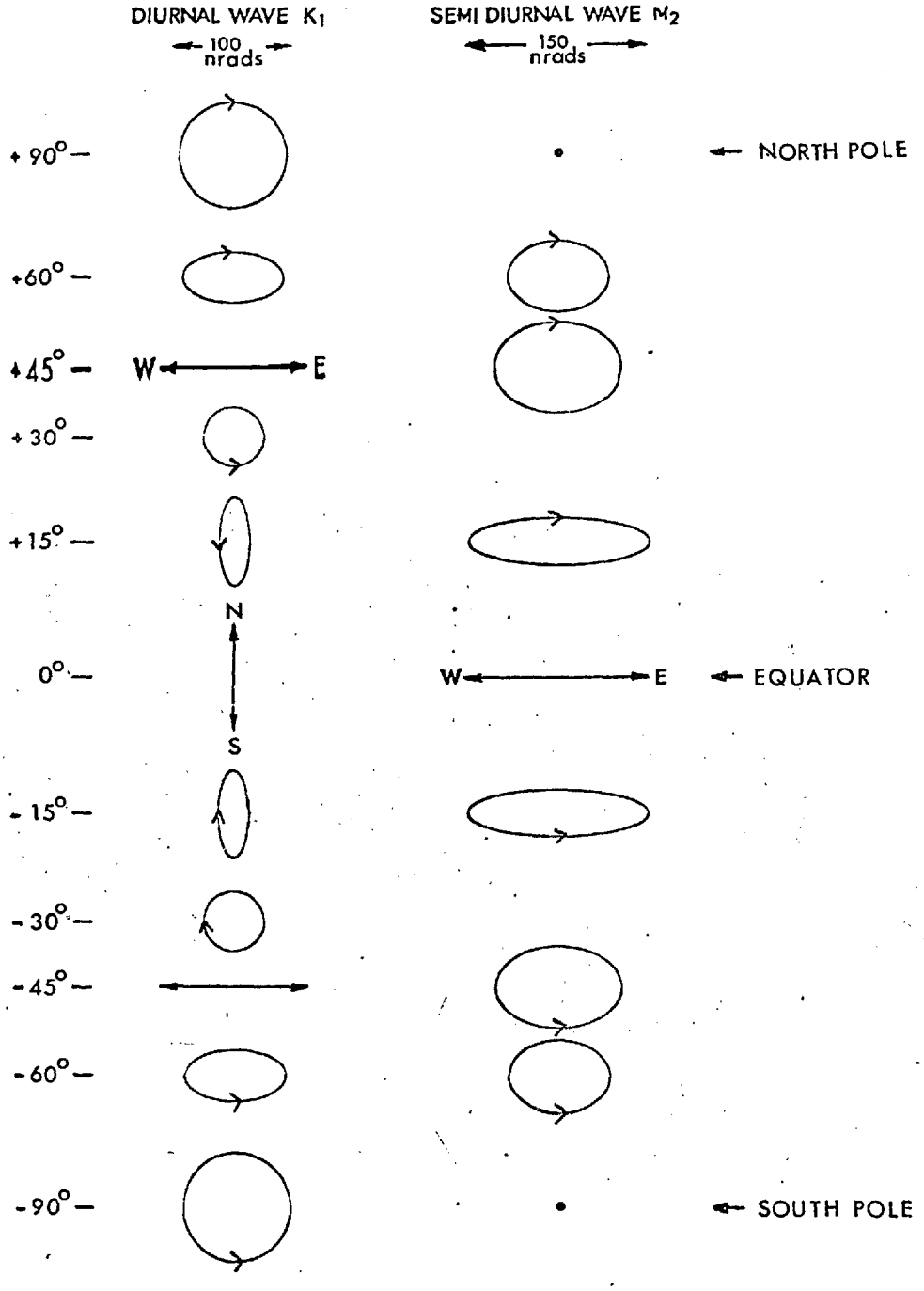


FIG. 3.8

Curves described by the direction of the vertical at different latitudes. (after Melchior, 1978)

3.4 LOVE NUMBERS

So far the Earth-tide theory has only considered the potential on a rigid Earth. In practice the earth is not rigid; it yields elastically to the tidal forces. This has two consequences, (1) the surface rises and falls tidally, the sense being such as to increase the amplitude of the tidal changes of gravity, and (2) the mass distribution of the earth is modified in such a way as to decrease the tidal amplitude. In an effort to characterize the tidal potential to account for these effects, Love (1911) introduced two dimensionless quantities which bear his name, later Shida (1912) introduced a third quantity to provide a complete description of the phenomena.

The displacements at the Earth's surface due to tidal forces can be written (Melchior, 1966):

$$Z = hV/g \qquad \text{radial} \tag{3.13a}$$

$$x = \frac{\ell}{g}\frac{\partial V}{\partial \theta} \qquad \text{N-S} \tag{3.13b}$$

$$y = \frac{\ell}{g \sin\theta}\frac{\partial V}{\partial \lambda} \qquad \text{E-W} \tag{3.13c}$$

where h is the first Love number and ℓ is Shida's number.

The redistribution of material in the Earth results in a modification of the potential which can be expressed as follows:

$$V' = kV$$

Where V' is the potential due to the deformation and k is the second Love number. The total tidal potential becomes (1 + k) V.

Thus h represents the ratio of the height of the Earth tide to the height of the corresponding static ocean tide at the surface, assuming the oceans to be incompressible: k represents the ratio of the additional potential produced by this deformation to the deforming potential and ℓ represents the ratio between the horizontal displacement of the crust and that of the corresponding static ocean tide.

From these definitions, parameters can be derived which reflect the relationship between the predicted tide for a rigid Earth and observations made on the real Earth.

1. Variations of the Intensity of Gravity

The total gravitational potential acting on the Earth can be written (Melchior, 1966).

$$V_o' = V + V' + Z \frac{\partial V_o}{\partial r} + V_o$$

where $-\frac{\partial V_o}{\partial r} = g_o$

and the variation in g is given by:

$$\Delta g = \left(\frac{\partial V}{\partial r} + \frac{\partial V'}{\partial r} + z \frac{\partial^2 V_o}{\partial r^2} \right)$$

and, as derived earlier, $\frac{\partial V}{\partial r} = \frac{2V}{r}$

$$\frac{\partial^2 V_o}{\partial r^2} = -\frac{\partial g}{\partial r} = \frac{2g}{r}$$

and $\frac{\partial V'}{\partial r} = -\frac{3V'}{r}$

since $\partial V'/\partial r$ is the attraction of a mass coating, and on the Earth's surface $V' = kV$

and using Clairaut's Theorem: $V = \frac{3}{4}\frac{k^2}{r^3}(A-C)(\cos 2\theta + 1/3)$

where C is the moment of intertia of the layer about the axis of rotation and A is the value of the other two principal moments of interia:

$$\therefore \quad \Delta g = \frac{2V}{r}(1 + h - 3/2k)$$

$$= -(1 + h - 3/2k)\,\partial V/\partial r$$

Comparing this with equation 3.8a, it is seen that the ratio of the tidal potential for an elastic earth to that for a rigid earth is given by: $\delta = \underline{1 + h - 3/2k}$

where δ is the ratio of the tidal potential for an elastic earth to that for a rigid earth. δ, is known as the Tidal Gravitational Constant .

2. Deviations of the Vertical with respect to the crust

As mentioned earlier, if the earth were completely rigid there would be no deformation of its surface. On the other hand if the earth possessed no rigidity at all, that is, it were a perfect liquid then its surface would constantly deform so as remain an equipotential of the resultant field. Thus the surface of the earth would always be normal to the vertical and there would be no deviation of the vertical. In practice, therefore, yielding of the earth reduces the amplitude of tilt from that expected for a rigid earth.

From equation 3.9a the N-S tilt, n_1, measured on the surface is given by:-

$$n_1 = \frac{1}{dg} \frac{\partial V}{\partial \theta}$$

In the case of deformation the potential, V, becomes $(1 + k)V$ as mentioned previously. Thus the deviation of the vertical is given by:- $$\frac{(1+k)}{dg} \frac{\partial V}{\partial \theta}$$

However, the surface of the earth also deforms, and in such a way as to reduce the tilt. The tilt due to this deformation is given by: $$-\frac{h}{dg} \frac{\partial V}{\partial \theta}$$ (Melchior, 1978)

Thus the tilt measured at the surface, i , in a N-S direction is given by:

$$i = \frac{(1+k-h)}{dg} \quad \frac{\partial V}{\partial \theta}$$

Similarly it can be shown that the E-W tilt, j , is given by:

$$j = \frac{(1+k-h)}{dg} \quad \frac{\partial V}{\sin\theta \partial \lambda}$$

Then comparing these equations with 3.8b and 3.8c respectively, it is seen that the ratio of the deviation of the vertical for an elastic earth to that for a rigid earth is given by:

$$\gamma = 1+k-h$$

The tidal deformation is accompanied by cubic expansions of the earth. An analysis, similar to those given above, yields a coefficient, f, where:

$$f = 4h - 6\ell$$

It must be stressed at this point that Love numbers are parameters relating to the whole Earth and not to localised regions on it. The first attempt to determine theoretical values for these numbers used Kelvin's assumption of a homogeneous and incompressible

Earth. Takeuchi (1950) in a pioneering paper evaluated Love's number for a series of Earth models based on Bullen's work on density distributions within the Earth and assuming different values for μ, the rigidity of the Earth's core. His results are summarised in Table 3.4, from

μ	0	10^7	10^9	10^{11}	10^{13}
h	.606	.601	.600	.530	.109
k	.281	.275	.275	.243	.055
ℓ	.082	.081	.081	.083	.092
δ	1.184	1.188	1.187	1.165	1.026
γ	0.675	0.674	.675	0.713	0.946

Table 3.4

Values of Love Numbers etc. for different Earth rigidities, μ in cgs units

which it can be seen that for an increase in rigidity up to 10^{11} cgs units δ changes by less than 2%. The position is complicated by the fact that h, k, and ℓ are frequency dependent and different values hold for each of the components listed in Table 3.4. Melchior (1978) lists values of different components for different Earth models and these are summarised in Table 3.5.

	Molodensky Model I	Molodensky Model II	Jeffreys and Vicente Central Particle Model	Jeffreys and Vicente Roche Model
P_1	1.153	1.158	1.209	1.172
K_1	1.137	1.143	1.183	1.185
O_1	1.160	1.164	1.221	1.211

	Gutenberg - Bullen ($\mu=10^{11}$)	Gutenburg - Bullen A
12 hr	1.154	1.150

	Jeffreys - Bullen A	Jeffreys - Bullen B
12 hr	1.151	1.152

TABLE 3.5

Computed values of the gravimetric factor at various tidal frequencies according to different models of the Earth. (adapted from various sources)

3.5 WORLD-WIDE OBSERVATIONS

Observations of tidal tilt and gravity have been carried out over many years and had the original objective of determining δ and γ and thus to improve the knowledge regarding the rheology of the Earth. Unfortunately, matters have been less simple than was originally anticipated and "..... the output is confusing and disappointing" (Lennon and Baker, 1973). The theoretical predictions mentioned earlier where manifestly different Earth models result in Love numbers with a range of only 2-3% indicates the accuracy of observational data required. So far this has not been forthcoming. Lennon and Baker (1973) and Baker and Lennon (1973a) citing evidence from around the world show anomalies of $\pm$ 40% in North-South tilt, $\pm$ 15% in East-West tilt and $\pm$ 8% in gravity variations for the M2 component, usually the easiest to measure. Table 3.6 gives experimentally determined values of δ for different tidal components and a comparison with Table 3.5 illustrates their divergence from each other and from theory. It can also be seen, from Table 3.6, that the gravitational constant for tidal components of similar frequency, for example, M2 and S_2, may differ from each other by up to 8% at the same site. In part this may be explained by an inadequate amount of data (q.v. Chapter 5), but this does not seem to explain all the differences, and there is no satisfactory explanation of these differences.

STATION	DAYS OF OBSERVATION	$\delta(M_2)$	$\delta(S_2)$	$\delta(K_1)$	$\delta(O_1)$
Hyderabad	132	1.1562	1.156	1.1076	1.1409
Hong Kong	110	1.2025	1.212	1.1491	1.1993
Alice Springs	266	1.1673	1.164	1.1371	1.1644
Port Moresby	146	1.2264	1.268	0.9421	1.0640
Cairo	60	1.1840	1.143	1.1462	1.1591
Brusells	2302	1.1946	1.225	1.1493	1.1610
Trieste	104	1.2119	1.221	1.1584	1.1769
Cambridge	60	1.1961	1.119	1.1183	1.1191

TABLE 3.6

Gravimetric factors measured at various stations throughout the world (adapted from Melchior et al., 1976; Ducarme and Melchior, 1978)

STATION	INSTRUMENT	Tilt per 1mb change of pressure
Oura	E-W Tilt	-28.13 nrads
	N-S Tilt	-72.75 nrads
Akibasan	E-W Tilt	-26.18 nrads
		Tilt per 1°C change of temperature
Akibasan	E-W Tilt	-18.91 nrads
	N-S Tilt	-1.41 nrads

TABLE 3.7

Effects of pressure and temperature on tilt measured at certain Japanese sites. (after Tanaka, 1969)

Instrumental inadequacies do not seem responsible for these anomalous results (Lennon and Baker, 1973) although the siting of instruments may be an important factor, particularly with respect to instruments installed in tunnels (King and Bilham, 1973) via the strain-tilt coupling effect, and those sited near faults (King, 1971; Tomaschek, 1957). These effects can be compensated for, however, by careful siting of the instruments. Harrison (1976a), utilising finite element techniques to investigate theoretically varied topographies, has shown that very large tilts can be induced on comparatively gentle slopes and that these perturbations extend to considerable depths so that it becomes impracticable to use deep enough holes to alleviate this problem. Additionally, geological inhomogeneities can also modify surface tilts. In general, all these problems are exacerbated by the use of short base-line tiltmeters.

One effect which cannot be compensated for, though, is that due to the oceans, generally known as the ocean loading effect (Melchior, 1978). Ocean tides vary considerably over the Earth, and the problem of calculating the loading is extremely complex. Fortunately for this study the Mediterranean is comparatively tide free and the loading is small. Zadro and Chiarutini (1975) have calculated it to be 0.2 μgal. for the vertical change in gravity and about 15 n rads for the M2 component of tilt.

A problem often neglected in Earth tide studies, though of particular importance in this study is the additional ground deformation arising from meteorological influences. Solar heating of the ground can considerably disturb tilt measurements, and diurnal amplitudes of 500nrads. have been observed at depths of 3 metres (Tomaschek, 1957). This is larger than the total tilt tide, which is of the order of 300 nrads. Tomaschek derives an expression for the tilt angle:-

$$Ws = m[\sin 25 \cos(t-M) + n \cos^2\delta \cos(2t-N)]\ Wo$$

where $m \cos M = -\cos 2\theta$, $n \cos N = \sin\theta \cos\theta$, $m \sin M = \sin\theta$

$n \sin N = \cos\theta$, δ is the Sun's declination, θ is the pole distance of the station (q.v. Fig. 3.4) and Wo is proportional to the maximum vertical deformation.

Ws consists mainly of a semi diurnal term, with a smaller diurnal term. This unfortunately does not correspond with observation, where the diurnal term predominates, and this implies that the perturbation is strongly dependent upon local topography.

Berger (1975) considered the problem of an infinite homogeneous half-space and the effects upon it of a temperature variation considered as a travelling wave. His conclusion was that at most

these tilts would amount to 2 n rads. per ^{o}C and that there was little advantage to be gained from burial of the instrument except at great depths. Harrison and Herbst (1978), however, object to Berger's conclusions on the grounds that the real world is not an infinite half-space ~~which and~~ is, in this case, not a particularly enlightening approximation. Using finite element modelling techniques they conclude that the tilt changes can be quite considerable, depending upon the surface topography. For a temperature change of 10^{o}C they calculate that the tilt in the vicinity of a 60^{o} slope would reach 86 μrad. They add, however, that these effects can be mitigated by burying the instrument. A further important point they raise is that any meteorological source of stress in the near surface layers, such as frost or changes in volume associated with changes in moisture content, can be expected to give similar effects. Their conclusions are supported by the studies of Shirokov and Anokhina (1973) who combine the theoretical studies of Jobert (1960) and Popov (1960) with their own experimental studies. Their general conclusions are that temperature tilts can differ considerably between closely related points but that burial of an instrument even as little as two metres can reduce the magnitude of the tilts by a factor of a 100 although the temperature variation may be reduced 500-800 times, indicating that the uppermost surface layers are responsible for the

formation of local diurnaltemperature tilts. Considering the effect on purely tidal measurement, they found deviations of up to 94% from the mean in calculations of γ during different months analysis. Homma (1950) calculated the effect of different installations on the tilt.

Since the Sun is the cause of these additional deformations their periods are mainly 12 and 24 hrs., with long term components. This means that those components most likely to be contaminated by this effect are S2 and P1.

It has been observed (Tomaschek, 1957) that the total maximum of thermal tilt occurs at 6.00 a.m. and this agrees well with observations on Etna.

The general conclusions derived from the preceding discussion of thermal tilt are that it is strongly dependent upon topography, it may be reduced by burial of the tiltmeter, and it can give rise to very large tilts compared with the average tidal tilts.

The other problems affecting tidal measurements are atmospheric tides and atmospheric pressure variations. The effect of atmospheric tides on Earth tide measurements is comparatively small and is principally on the S2 component and it has been ignored for the purposes of this research. The effect due to atmospheric pressure

variations is not inconsiderable and was first demonstrated by Darwin (1907). For a pressure change of 33 m bars. and an assumed modulus of rigidity for the Earth of 6.10^{11} dyn.cm^2, then the influence on a gravity meter due to the elasticity of the ground will be 7 μgal. which is far from negligible. The effect on tilt will be of the order of 25 μrad. which is comparable to 10% of the total signal and represents an important source of noise. Tanaka (1969) considers the effects of various meteorological influences and tidal measurements in Japan some of whose results are reproduced in Table 3.7.

Generally, pressure variations follow a diumal period or have long term effects. The same problems of analysis apply to them as to thermal effects, and the problems of data processing and the analysis of tides are reserved until Chapter 5.

CHAPTER 4

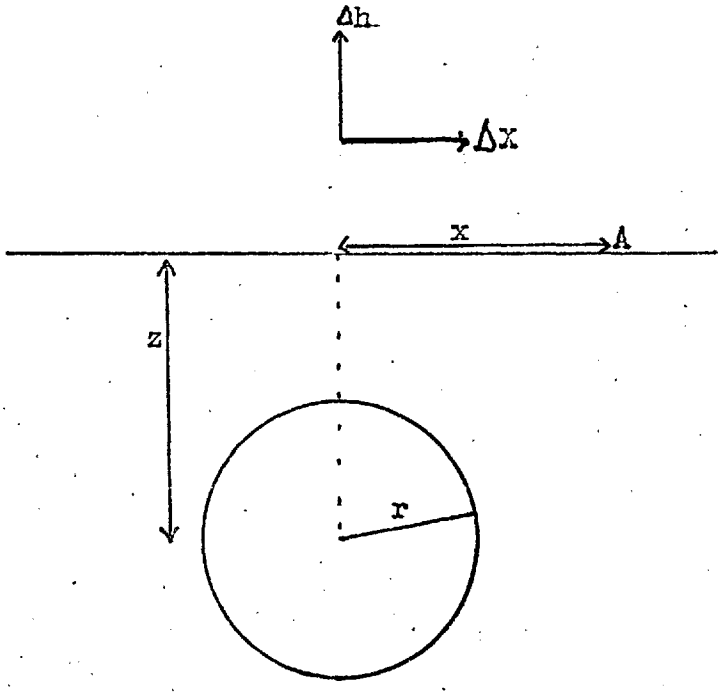
VOLCANO TILT MEASUREMENTS AND THE ETNEAN TILTMETERS

4.1 TILT MEASUREMENTS ON VOLCANOES

There is hardly any need to justify the measurement of tilt on volcanoes. The earliest detailed tilt observations date back to Omori (1911) and much of the early research was carried out in Japan or Hawaii. The pioneering work of Jaggar on the Hawaiian volcanoes is particularly interesting. In an early paper (1920) he comments upon a marked correlation between the measured tilt and the ambient temperature and also between tilt and rainfall. From a volcanological point of view, however, the most important correlation he observed was that between tilt and eruptive activity, manifesting itself in the inflation of the volcano prior to eruption accompanied by deflation during an eruption. Jaggar's paper was followed by a number of papers on the same subject, notably Jaggar and Finch (1929), Wilson (1935) and Jones (1937) on Hawaii, and Minakami (1942, 1947 and 1950) working in Japan.

Two major advances occurred in the late 1950's, the development of the theory of an expanding sperical magma chamber in an ideal, semi-infinite medium (Mogi, 1958) and the introduction of the water-tube

tiltmeter (Eaton, 1959). The theory was initially developed by Yamakawa (1955), in Japanese, and in an English version by Machado (1974).



The deformationsat a point within the crust are extremely complicated, but simplify for a point A, on the earth's surface to give:

$$\Delta x = \frac{3r^3 P}{4\mu} \cdot \frac{x}{(x^2+z^2)^{3/2}} \qquad 5.1a$$

$$\Delta h = \frac{3r^3 P}{4\mu} \cdot \frac{z}{(x^2+z^2)^{3/2}} \qquad 5.1b$$

where Δx is the radial displacement and

Δh " " vertical " at a point (x, 0)

due to a sphere, radius r, at a depth z , under a hydrostatic pressure difference P, where, in the particular case, which is approximately true for many rocks, Poisson's ratio $\sigma = \frac{1}{4}$, i.e. where λ (Lame's constant) $= \mu$ (the modulus of rigidity).

The tilting of the surface can be evaluated from the equation:

$$\tau = \frac{\partial \Delta z}{\Delta x}$$

which gives $$\tau = \frac{9 r^3 P}{4 \mu z^3} \cdot \frac{x/z}{(1+x^2/z^2)^{5/2}} \qquad 5.2$$

The maximum tilt, τ_m, occurs when $x = z/2$

and $$\tau_m = \frac{-9r^3 P}{4\mu z^3} \cdot \frac{\frac{1}{2}}{(1.25)^{5/2}}$$

then $$\tau / \tau_m = 2\,(1.25)^{5/2} \cdot \frac{x/z}{(1+x^2/z^2)^{5/2}}$$

$$\simeq 3.49 \frac{x/z}{(1+x^2/z^2)^{5/2}} \qquad 5.3$$

(It may be noted that some authors give a different numerical coefficient for equation 5.3. This appears to be a mistake, propagated through several papers, due to an initial misprint).

Δh has its maximum value Δho at $x = 0$

$$\text{and } \Delta ho = \frac{3r^3 P}{4\mu z^2}$$

$$= -\frac{1}{3} .3.49. \tau_m$$

$$\simeq -1.16\ z\ .\tau_m \qquad 5.4$$

The Mogi model has been found to apply successfully to some volcanoes, notably Kilauea (Eaton, 1962 and Fiske and Kinoshita, 1969) but it does not appear to be justifiable for the summit region of Etna (Wadge, 1974) or its flanks (Henbest et al., 1978). In spite of interpretational difficulties and the somewhat naive nature of its assumptions the Mogi model continues to be used as the basis of other, more sophisticated models (for example, Yokoyama, 1971, 1974).

A completely different approach to the problem was attempted by Dietrich and Decker (1975) who used finite element techniques to evaluate different magma chamber models. They argued against the use of Mogi's model on the grounds that it assumes a point source of

dilatation and is only accurate if the chamber is small in comparison to its depth which is unlikely considering evidence from extinct volcanoes. One interesting conclusion that can be drawn from the results of Dietrich and Decker is that completely different models give results similar enough to indicate that it would be difficult to distinguish between different models on the basis of real data. The general conclusion is that in order to determine an appropriate model data must be gathered from as wide an area of the volcano as possible and over as long a period of time as possible.

Soon after Mogi published his paper the second major development in volcanic tilt measurement occurred with the construction, in Hawaii of a portable water-tube tiltmeter by Eaton (1959). It had been shown by Hagiwara (1947) that a tiltmeter operating on the principle of the self-levelling of a liquid surface could overcome the difficulties caused by the local effects of the short baseline of pendulum tiltmeters. Eaton improved on this instrument and installed both permanent and portable units around Kilauea. The great advantage of these tiltmeters is their long base line (25-50 metres) which alleviates spurious local tilts. The problem associated with the installation of the correct type of tiltmeter is a fundamental one. In addition to the usual

problem of cost versus accuracy/sensitivity there is the additional problem of portability against accuracy. Eaton's tiltmeter, though nominally a portable system nonetheless requires a base line of 25-50 metres.

The most commonly used instrument in the measurement of tidal tilts is the horizontal pendulum, which, since it requires very stable operating environments, is generally unsuitable for volcanological research. For the latter purpose, borehole tiltmeters are more useful, since they are less prone to the problems of cavitation (King and Bilham, 1973) discussed later in this chapter. Results from a borehole tiltmeter employing a 50cm. vertical pendulum compared favourably with simultaneous measurements from a 5 metre baseline liquid-level tiltmeter (Allen, 1972). One of the problems associated with a borehole instrument is in the recovery of data. This is a particular problem on volcanoes where the tiltmeter would generally be installed some distance from any sort of buildings, including any volcanological observatory, since buildings and trees induce ground tilts in response to atmospheric conditions or human movement. A common approach to the problem is to telemeter the data to an instrument house but on volcanoes telemeter links are prone to damage by lightning, and to ensure a continuous record it is common practice to install a recorder, usually

an analogue instrument, either in or alongside the borehole, to act as a back-up system. In this study the instruments were designed to operate unattended for about a year and it was arranged to collect the data once or twice a year when new power supplies could be installed. Visits could only be made during the summer months since during the winter the whole site is heavily inundated with snow to a depth of at least 10 feet.

Recently there has been a novel and most enterprising approach to the recovery of data and this has been to use an Earth Resources Technology Satellite (ERTS) to monitor tiltmeters over a wide area (Endo et al, 1974). Using the ERTS, volcanoes throughout North and Central America and in Iceland can be monitored, but at present other volcanoes, including Etna, are not within the range of the satellite. However, if the system is successful then there may be further developments along this line. The project described by Endo et al. was established in 1972 and as well as monitoring tiltmeters on volcanoes, seismic event counters were also monitored, principally in California and Washington State but also in Central America. The tiltmeters used were of the same design as that used on Etna and from the results of Endo et al. increased confidence may be placed in the instrument. Summarizing their results, simultaneous measurement made with a mercury-

tube tiltmeter, a water-tube-tiltmeter and the level-bubble borehole tiltmeter on Hawaii agree to within a few microradians; the tilt was not noticeably affected on Kilanea when 50 cm. of rain fell in one month. On the other hand the tiltmeters were damaged several times by lightning, which seems to induce high electric currents in the cables. As well as putting the instruments out of action, at least two of the meters exhibited excessive long term drift even after they had been repaired. The authors also came to the conclusion, in agreement with King (1971) that the shallow installation of tiltmeters in volcanic ash or sand is better than in solid rock. Their general conclusions are favourable to the Autonetics tiltmeter, which is of the type used in the study of tilt on Mt. Etna and whose performance is discussed in the following section. They were not, however, concerned with its performance at Earth tide sensitivity.

4.2 FIELD INSTRUMENTS - DESCRIPTION

Two tiltmeters were used in the course of this research. The first, a borehole instrument, was originally installed in 1973 (Wadge, 1974) whilst the second, a block-mounted instrument, intended for observatory use was installed in 1976. Both these instruments are Autonetics* Biaxial Tiltmeters model numbers SE541B1 (Borehole Instrument) and SE541A1. The tilt sensor is the same for both instruments only its mounting differing, so that a single description will suffice.

The tiltmeter sensor case (Fig.4.1) comprises a glass cap and base, the cap being cylindrical with a concave inner surface having a spherical radius of 12 inches. Four equally spaced platinum electrodes are mounted on the underside of the cap, and a single platinum electrode centrally on the base. The sensor is filled with a conducting fluid leaving enough space for an air bubble which, when the sensor is levelled, covers an equal area of each of the cap electrodes.

*Autonetics is a trade name of the North American Rockwell Corporation. Manufacture of these instruments has now been transferred to Kinemetrics Inc.

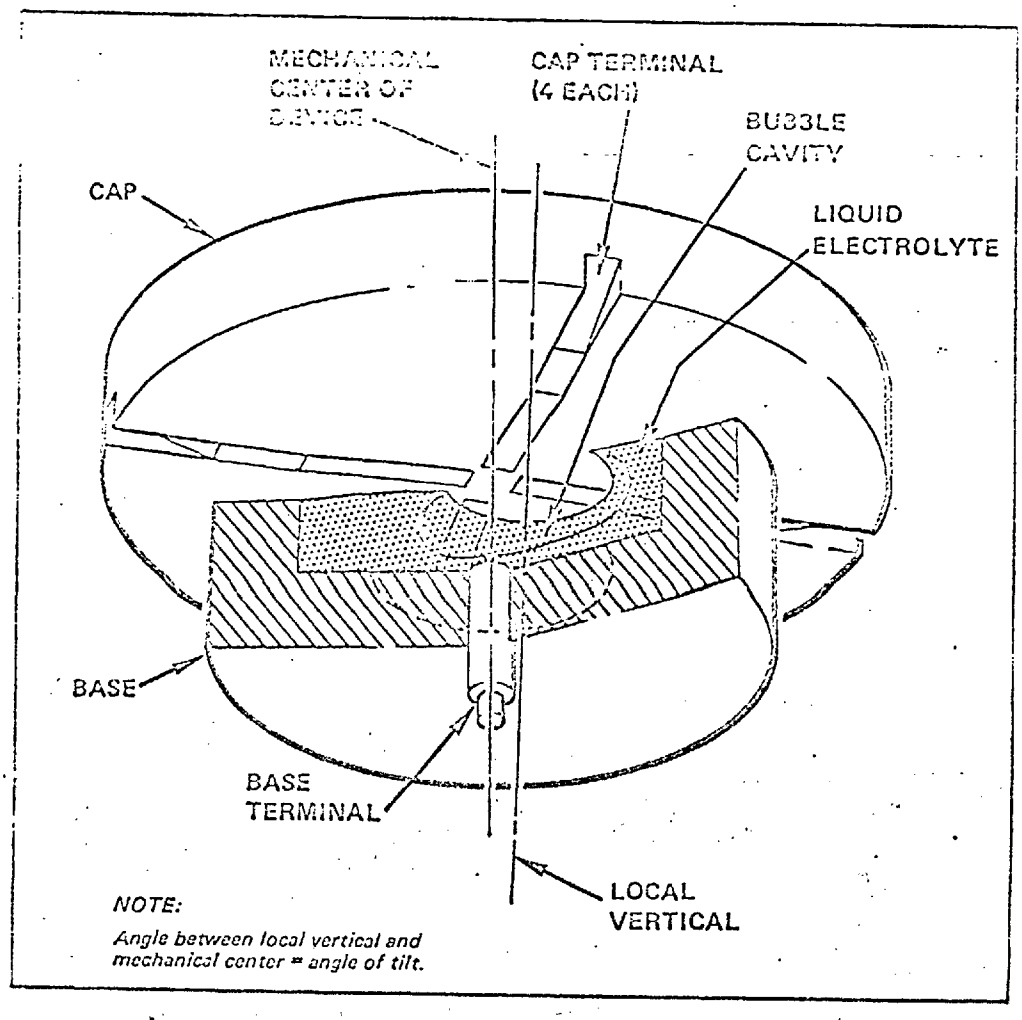


FIG 4.1

Tiltmeter Sensor Assembly

When the sensor is tilted, the areas covered by the bubble change, and this causes a corresponding change in the electrical resistances between the four electrodes and the central electrode, which thus provides a measure of the amount of tilt. These resistances are measured by two A.C. bridge circuits (Fig 4.2). Each A.C. bridge incorporates opposite pairs of electrodes enabling the tilt of two orthogonal axes to be measured simultaneously. The total range of the 12 inch radius tiltmeter sensor is 7m rads. but the output range of the tiltmeter is controlled by the dynamic voltage range and the scale factor gain for the particular instrument. It is typically about 200 μrads.

The electronics of the two tiltmeters are again substantially identical,the only differences being in component specifications to effect different scale factor gains. The electronics module performs the functions of impedance matching, amplifying, demodulating and filtering both axes of the level detector outputs to provide analogue signals. The electronic circuit consists of two identical resistance bridges, each containing two precision resistors, a null adjustment trimmer and a quadrature nulling trimmer capacitor connected to the output of the bubble level electrodes. The output of the bridge when excited with a 5.0 Hz . square wave can be adjusted to null when the tiltmeter sensor is aligned to the gravity vector. A synchronous full-wave demodulator converts this amplified A.C. voltage to a D.C. output voltage for recording. The demodulator output provides a means for

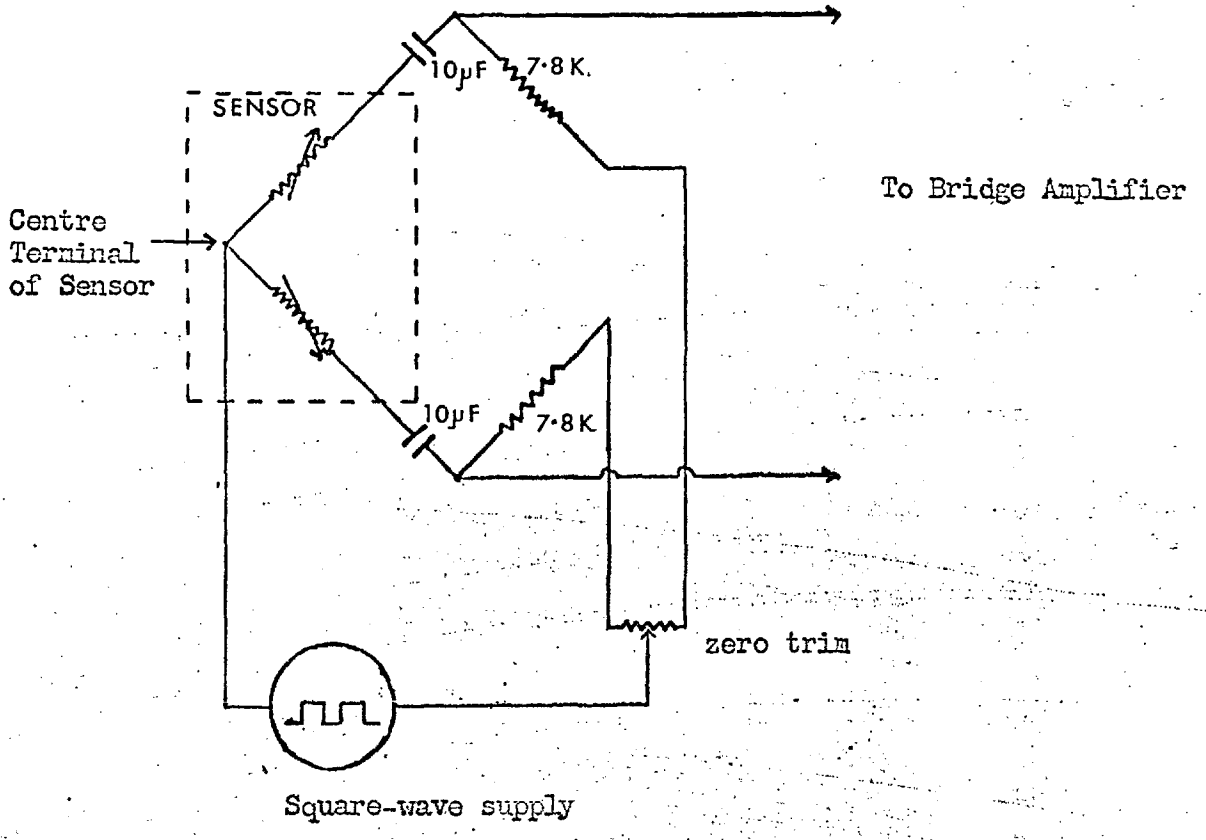


FIG. 4.2

Equivalent bridge circuit for one axis of the tiltmeter. The variable resistors are one pair of cap electrodes. The 10 μF capacitors act as D.C filters, and the 7.8 K resistors are high precision, standard resistors used to complete the bridge circuit.

detecting wide bandwidth signals in the range 1-10 Hz. The unit provides a stage for each channel to allow the gain to be adjusted and an active integrator having a selected time constant of 0.2 to 20 seconds. The unit also has circuitry that provides its own centre tapped regulated excitation signal to the bridge circuits with adjustable amplitude control. The electronics are mounted on a single printed circuit board and installed in a watertight box approximately $4\frac{1}{2}$ x $8\frac{1}{4}$ x $11\frac{1}{2}$ inches in size. An input and output terminal strip are mounted adjacent to the circuit board within the box. Connections are provided between the circuit board and these terminal strips. Two switches are also installed within the box, one of which switches in an integrating circuit, creating a time delayed output signal, while the other is used for calibration. A block diagram of the tiltmeter is shown in Fig. 4.3.

Aspects specific to each tiltmeter will now be described.

Block-Mounted Tiltmeter

This tiltmeter is designed for use on a stable flat surface such as would be provided by a concrete block in a seismic vault. The sensor unit is located in a metal mount/tilt table (Fig. 4.4). The metal container attenuates thermal gradients and provides a stable mechanical attachment to the surface being monited. Data relating to this instrument is given in Table 4.1.

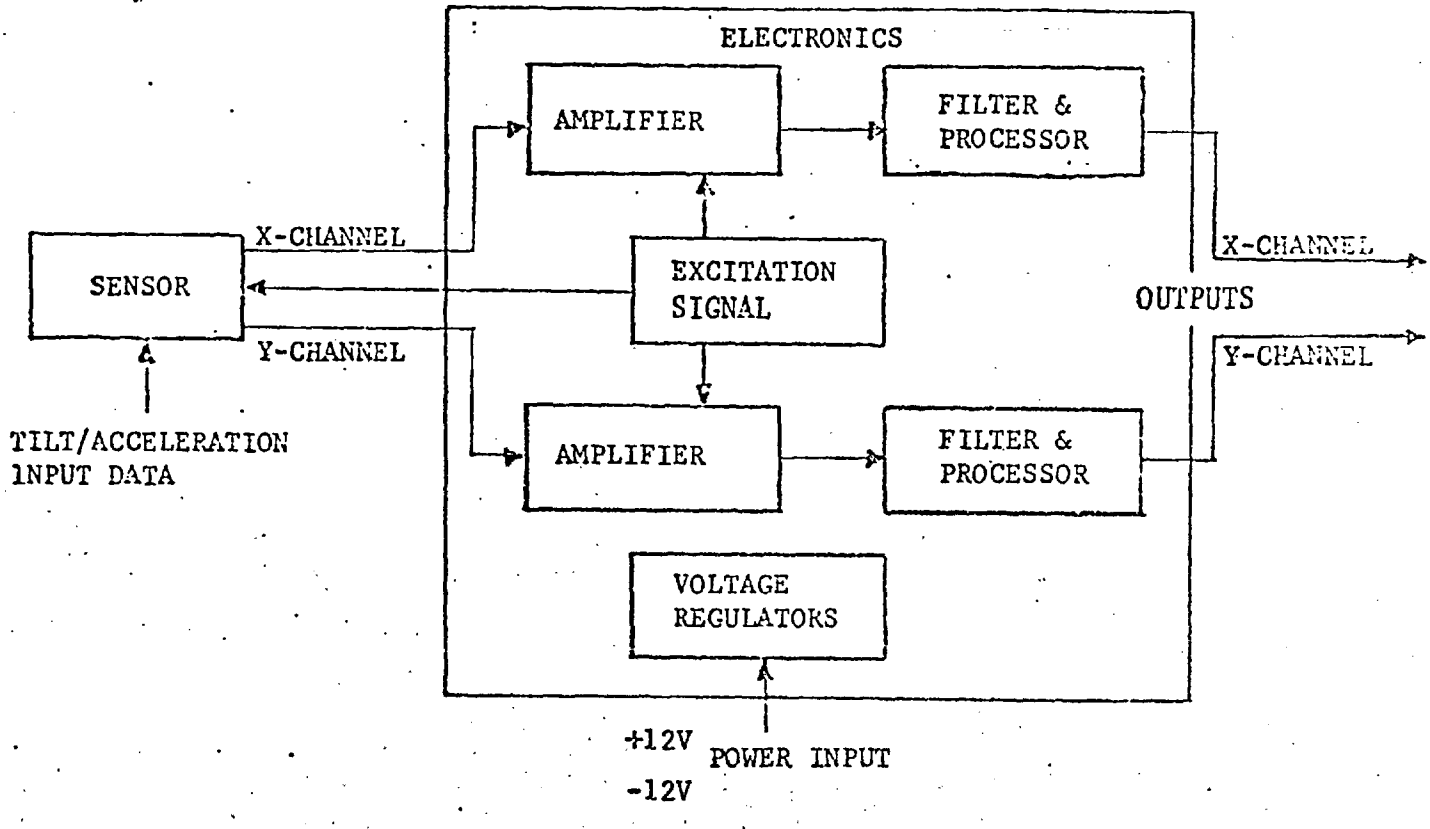


FIG. 4.3

Block diagram, illustrating the various units of the tiltmeter and their operation.

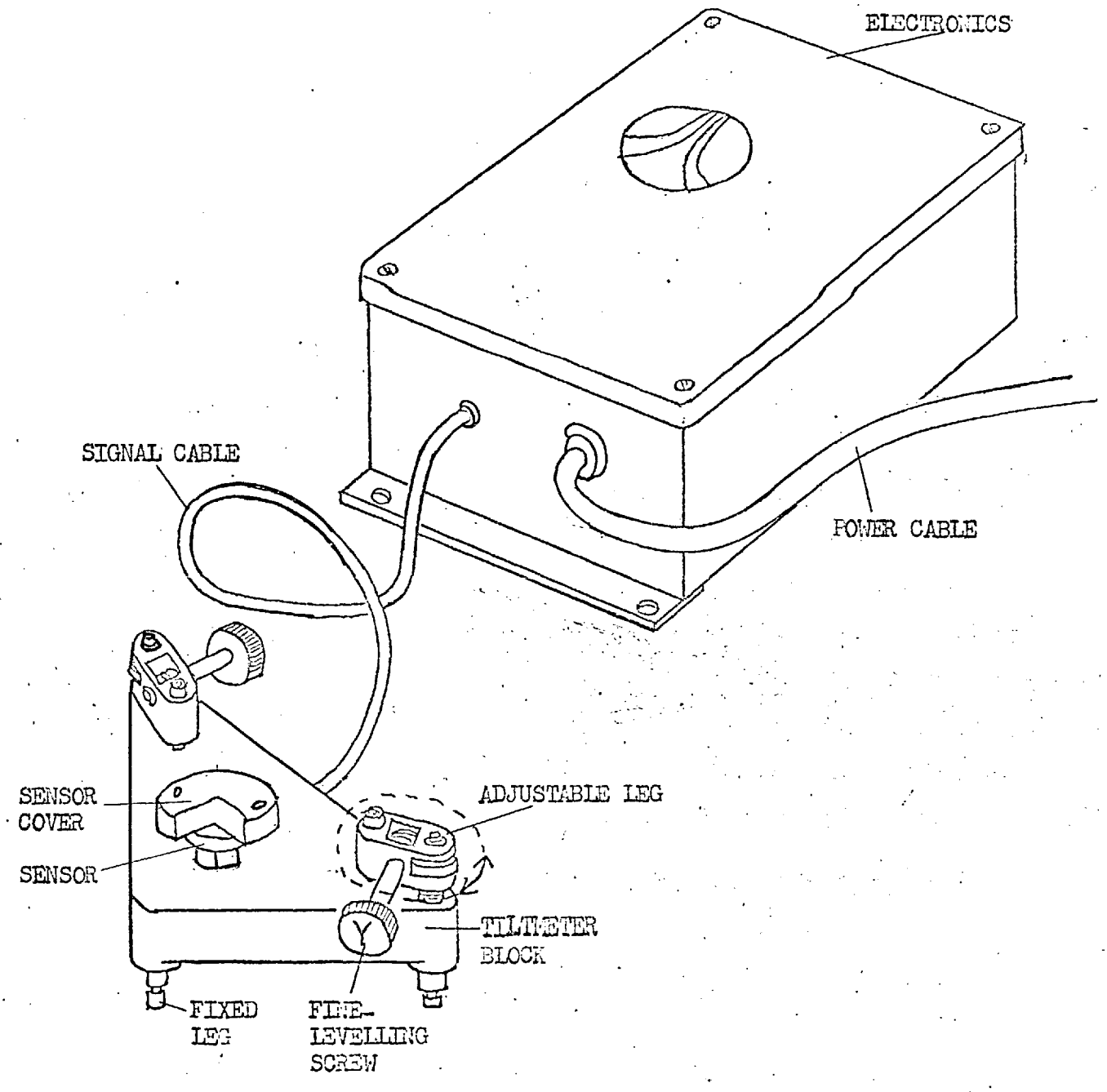


FIG. 4.4

The Block-mounted (Observatory) tiltmeter, and its associated electronics box.

Borehole Tiltmeter

This instrument is designed for use in boreholes at depths typically around 2-3 metres. The sensor is located in a metal mounting container 2 inches in diameter and 2 inches long. As with the block-mounted instrument this metal container attenuates thermal gradients and also seals against moisture. A cylindrical shaft of 2 inches diameter and $3\frac{1}{2}$ feet long is attached to the container. Electrical connections are made between the sensor and a small terminal board located within the cylindrical shaft (Fig.4.5). In order to avoid the possibility of resistance changes in the leads connecting the borehole unit and the electronics unit affecting the accuracy of the measurement, the standard resistances forming the other arms of the bridges are mounted on the terminal board, as also are fixed capacitors which are connected in series with the sensor resistors in the other two arms. A cable, approximately 12 feet long, is connected to the opposite end of the terminal board and extends out of the shaft and connects to the input terminal strip in the electronics module. Waterproof connections are made at the shaft end and the opening to the electronics box. The data sheet for this instrument is contained in Table 4.2.

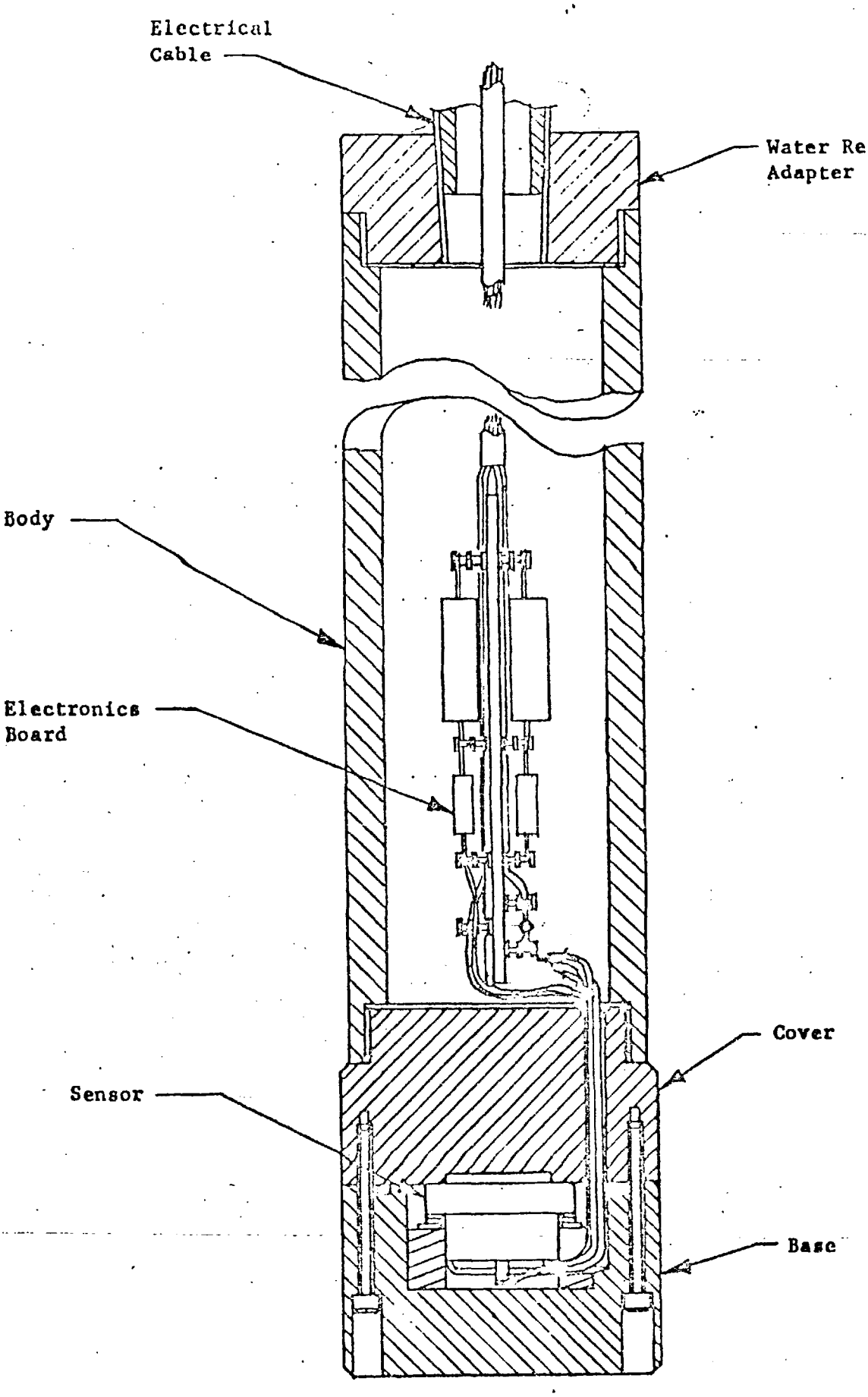


FIG. 4.5

Borehole tiltmeter sensor assembly

DATA SHEET BLOCK MOUNTED TILTMETER SE 541 AI

Functional Characteristics

Linear Sensor Range:	$\pm$ 7 m rads.
Output Range:	$\pm$ 375 μrads.
Output Impedance:	$<100\ \Omega$
Scale Factor:	20 mV /μrad.
RMS Resolution Limit:	8×10^{-9} rads. at 1 Hz bandwidth
Stability:	Driftrate $<$ 0.4 μrad. peak in 20 days
Frequency Response (at 70°F):	Flat within 3 db from DC to 1 Hz; - 40 db per decade from 1 to 10 Hz

Thermal Characteristics

Operating Range:	- 30°C to 60°C
Storage Range:	- 50°C to 70°C
Temperature Gradient Sensitivity:	Drift $\simeq$ 90 μrad / °C where T appears directly across sensor block sides.
Absolute Temperature Sensitivity:	.011 μrad. change / μ rad offset / °C

Power

Power Consumption:	650 m. watts.
Current Drain:	0.027 amps @ 12.6 V
Voltage:	$\pm$12 V Minimum to $\pm$ 15 V Maximum

Table 4.1.

DATA SHEET BOREHOLE TILTMETER SE 541 B1

Functional Characteristics

Linear Sensor Range:	$\pm$ 7 m rads.
Output Range:	$\pm$ 175 μrads.
Output Impedance:	$<$ 100 Ω
Scale Factor:	40 mV/ μrad
RMS Resolution Limit:	8×10^{-9} rads. at 1 Hz bandwidth
Stability:	Drift rate $<$0.4 μrad. peak in 20 days
Frequency Response (at 70°F):	Flat within 3db from D.C. to 1 Hz;
	- 40 dB per decade from 1-10 Hz

Thermal Characteristics

Operating Range:	- 30°C to 60°C
Storage Range:	- 50°C to 70°C
Temperature Gradient Sensitivity:	Drift $\simeq$ 90 μrad./ °C where T appears directly across sensor block sides
Absolute Temperature Sensitivity:	.011 μrad. change/μrad. offset / °C

Power

Power Consumption:	650 mwatts
Current Drain:	0.027 amps @ 12.6 V
Voltage:	$\pm$ 12 V DC Minimum to $\pm$ 15 V Maximum

Table 4.2.

4.3 LABORATORY AND FIELD ASSESSMENT OF THE TILTMETERS

The details of the laboratory tests used to evaluate the data of Tables 4.1 and 4.2 are given by Cooper (1970), together with the mathematical theory of the sensor response.

Some of the performance data, claimed by the manufacturers are questioned by Morrissey (1976) in a USGS technical report specifically evaluating the Kinemetrics TM-1 tiltmeter (This model is identical to those used on Etna). Morrissey is particularly critical of the instrument's temperature stability and found that the output voltage was especially sensitive to changes in the thermal environment of the electronics. Autonetics themselves do not specify whether their 'absolute temperature sensitivity value' is related to the instrument as a whole or just the sensor. Morrissey's findings indicate that a 10^{o}C change can affect the output by up to 1 μrad., this is a value approximately 10 times larger than that given by the manufacturers. So far as the stability of the instrument is concerned the results are more promising. A test apparatus comprising a pendulum suspension was arranged, enabling the sensor to be suspended so that the bubble axis always aligns with the local gravity vector. The resolution of the system is of tidal amplitude (0.1 μrad) and tides are not evident, but secular errors ($>$ 2 days) are longer than 1 μrad. The only checks carried out on the particular instruments used on Etna were to measure the scale factors, and so reservations must be placed on

the stability, thermal or otherwise, of the tiltmeters. The problem is not as important as it would seem, fortunately, since the major source of error arises due to temperature changes in the environment of the tiltmeter sensor or electronics, and the temperature monitored at the different tiltmeter installations showed changes much less than $5^{\circ}C$ per annum, and considerably less over the course of a day, even though the air temperature might vary by $40^{\circ}C$ or more during the same period.

4.4 INSTALLATION OF TILTMETERS ON ETNA

(a) Borehole Tiltmeter

The borehole tiltmeter was originally installed in September 1973 (Wadge, 1974) at an altitude of 2580 metres within a levelling site which had previously been selected for the purpose of installing a tiltmeter. The location of the tiltmeter site, on the southern flanks of the volcano, is shown in Fig. 4.6. The tiltmeter was installed in a 1·5 metre deep borehole which was lined with an aluminium alloy tube. The electronics module along with the recorders and additional electronics was sealed in a waterproof container and buried in a separate hole about 0.5 metre deep which, to prevent unnecessary disturbance to the tiltmeter sensor by the electronics and power supplies, was located about 1.5 metres from the borehole.

Initially, the tiltmeter operated continuously between September 28th, 1973 and August 8th, 1974. During this period the temperature at the sensor was also recorded. Between August 1974 and August 1975 the system did not operate successfully and no useful data was recovered.

One weakness of the original installation was that no provision was made for putting time marks on the record; as the main objective was to study long term changes, an absolute accuracy of only a few hours was thought necessary, and for this, reliance was placed on the uniformity of the chart speed. In August 1975 the system was slightly

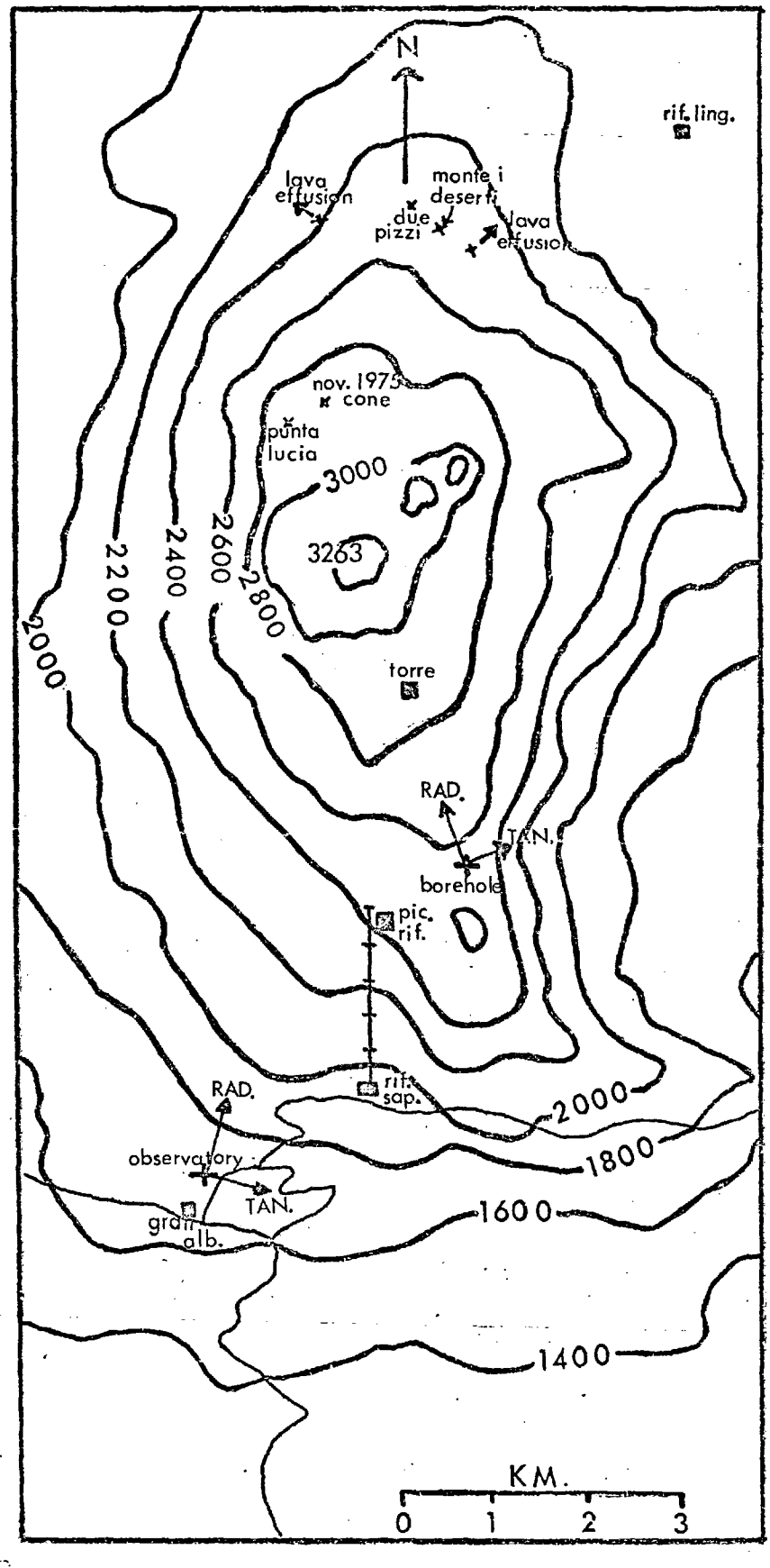


FIG. 4.6

Mt. Etna, showing the location of the tiltmeters and the alignment of the tilt axes, and the major eruptive centres 1973-1977.

modified, the main modification being the provision of a 24 hourly timemark on the record. This substantially increased the timing accuracy at the data processing stage. A modification was also made to the arrangement of the recorders. Instead of recording the separate input channels on separate Rustrak chart recorders both channels were now recorded on the same recorder again at an hourly sampling rate with one tiltmeter axis recorded as a series of short dots and the other axis by a series of dashes. The two recorders were connected in series so that both would record the same signal and thus provide a back-up system should one recorder fail. In the event this proved a necessary precaution.

Another change that was made was that the thermister arrangement monitoring temperature at the sensor was removed, since the variation in temperature over the recording period, which covered both winter and summer, had been negligible ($<3^{\circ}C$).

The site was visited in October 1975 to recover the previous record and install a new one. No modifications or adjustments were made to the system but it was noticed that the waterproof box containing the electronics and recording system had in fact allowed moisture to enter but it was only a small amount and did not appear to have adversely affected the system. In October 1976 the site was once more visited. From the recovered record it was evident that the system had failed at the beginning of March 1976. An examination of the electronics indicated the probable cause of failure to be a lightning strike at or near to the tiltmeter site. Lightning poses a constant threat to

installations of this sort on volcanoes and has caused the failure of many such systems throughout the world. Extensive alterations had to be made both to the tiltmeter electronics and also to the ancilliary electronics controlling the timing and recorders. One of the Rustrak recorders had seized up, a problem which this type of recorder is prone to, and was removed from the system. None of these alterations effected any change in the logic of the system or in the resultant record. When the system was re-installed it was found that one axis was off scale, necessitating a re-alignment of the tiltmeter and this was performed in the manner described by Wadge (1974) and Allen et al. (1973). A final visit to the site was made in November 1977 with the intention of renewing the chart record. When the waterproof box was opened it was found to be several inches deep in water and that all the electronics in the box were severly damaged. It was evident that the extensive repairs required could only be carried out under proper laboratory conditions in London. The tiltmeter sensor and shaft were also recovered as it was decided that the site was not entirely suitable for studies, principally because of its proximity to the Valle del Bove. As was seen in the preceding chapter the siting of tiltmeters is a fundamental consideration when trying to alleviate spurious signals, so that siting an instrument within a few metres of an almost sheer 900 metre high precipice is inviting disaster. An additional problem was due to the slope of the surrounding ground directing surface and sub-surface water towards the tiltmeter, possibly inducing spurious tilts.

A better location would require an area of flat terrain to avoid these problems.

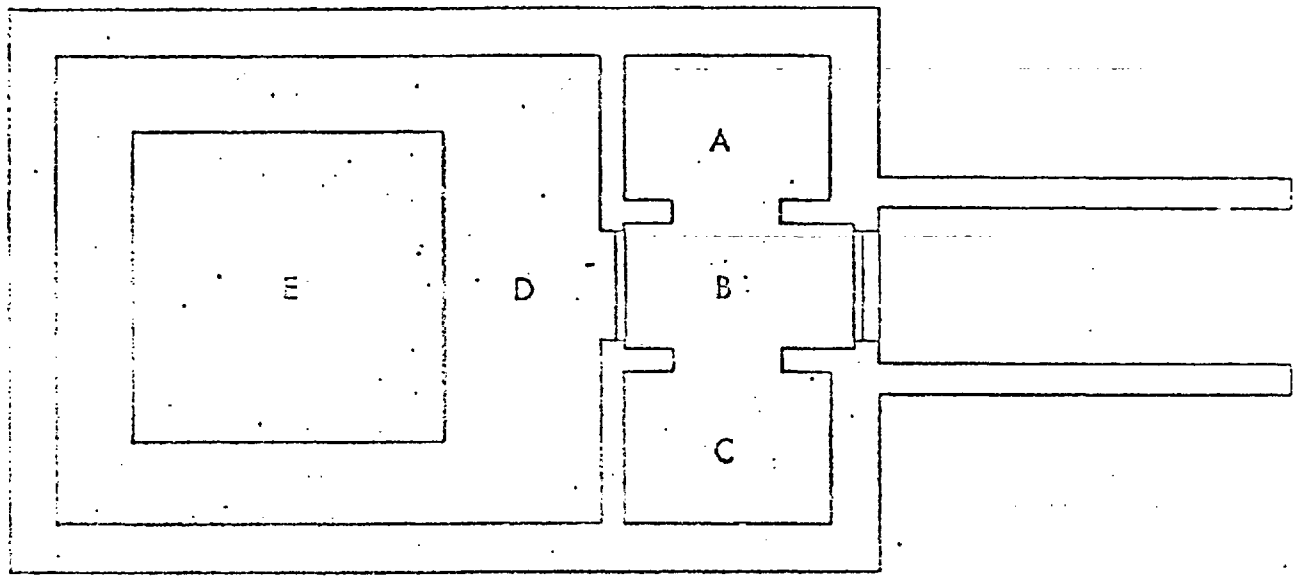
(b) Block-Mounted Tiltmeter

We were fortunately able to obtain use of the seismic vault at the Astrophysical Observatory at Serra La Nave (Fig. 4.5) to install this instrument. It is well placed to observe Etna and within easy access of Catania and the main centres of accommodation offered on Mt. Etna.

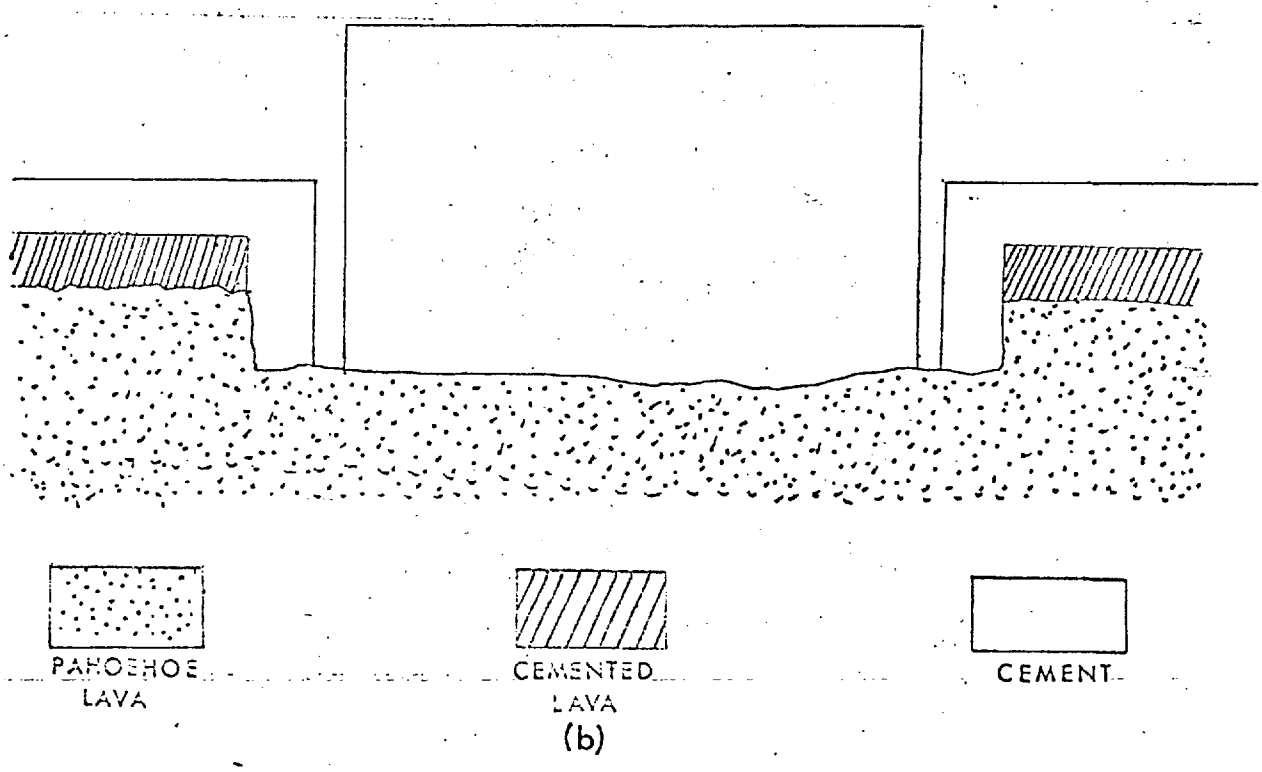
The vault and its construction are described by Bottari and Riuscetti (1967). Their co-ordinates for the station are in error, however, and have been re-calculated by the author to be:-

$37^{o}41'40"$ N; $14^{o}58'26"$ E and 1725m. height.

A plan view of the vault is shown in Fig. 4.7.a and a cross-section of the concrete block is shown in Fig. 4.7b. The vault was sited after careful consideration of the local geology. The main block is installed on a large pahoehoe lava flow at least seven metres deep. Other nearby lava flows were avoided because of their lack of extent, and as an additional precaution six boreholes were sunk in and around the area of the vault to ensure the absence of large cavities. The vault is covered by sand and slag to secure thermal insulation and intermittent measurements over the course of a year have confirmed that the temperature within the vault is around



(a)



(b)

FIG. 4.7
Serra la Nave Observatory. Plan and section views.
A & C - Storage areas; B - Entrance; D - Vault room
E - Insulated concrete block

$14^{o}C$ - $15^{o}C$ (N. Henbest, personal communication). According to Bottari and Riuscetti microseismic disturbances from waves, wind and urban activity is kept within acceptable limits. Additionally the vault is provided with a 220 V A.C. electrical supply.

The system was installed in the vault on August 12th, 1976, with the Y-axis aligned towards the summit (radial) and the X-axis tangential. The initial arrangement is shown in the block diagram Fig.4.8. The tiltmeter electronics require a 12V D.C. supply and to achieve the greatest accuracy should be operated continuously. In an effort to ensure this a $\pm$ 12V D.C. stabilized supply was used to float charge two 12V batteries (Nos. 1 and 3) using the available 220V supply. The signal was fed via a timer-biplexer to an Esterline Angus 'Speed Servo II' chart recorder. The timer-biplexer allowed the signals from the two axes to be displayed in alternate half-hour periods. The Esterline Angus chart recorder is a 220V A.C. operated recorder with a 12 inch wide chart and having a range of input voltage options from 0.5mV to 100V full scale deflection and a range of chart drive speeds from 25 m.m./ hour to 25 mm./sec., it also possesses an input impedance of 20 megohms for millivoltage inputs or 1 megohm for voltage inputs. Because of its A.C. operation the recorder was powered by the mains supply available in the vault, however, since the local supply is unreliable

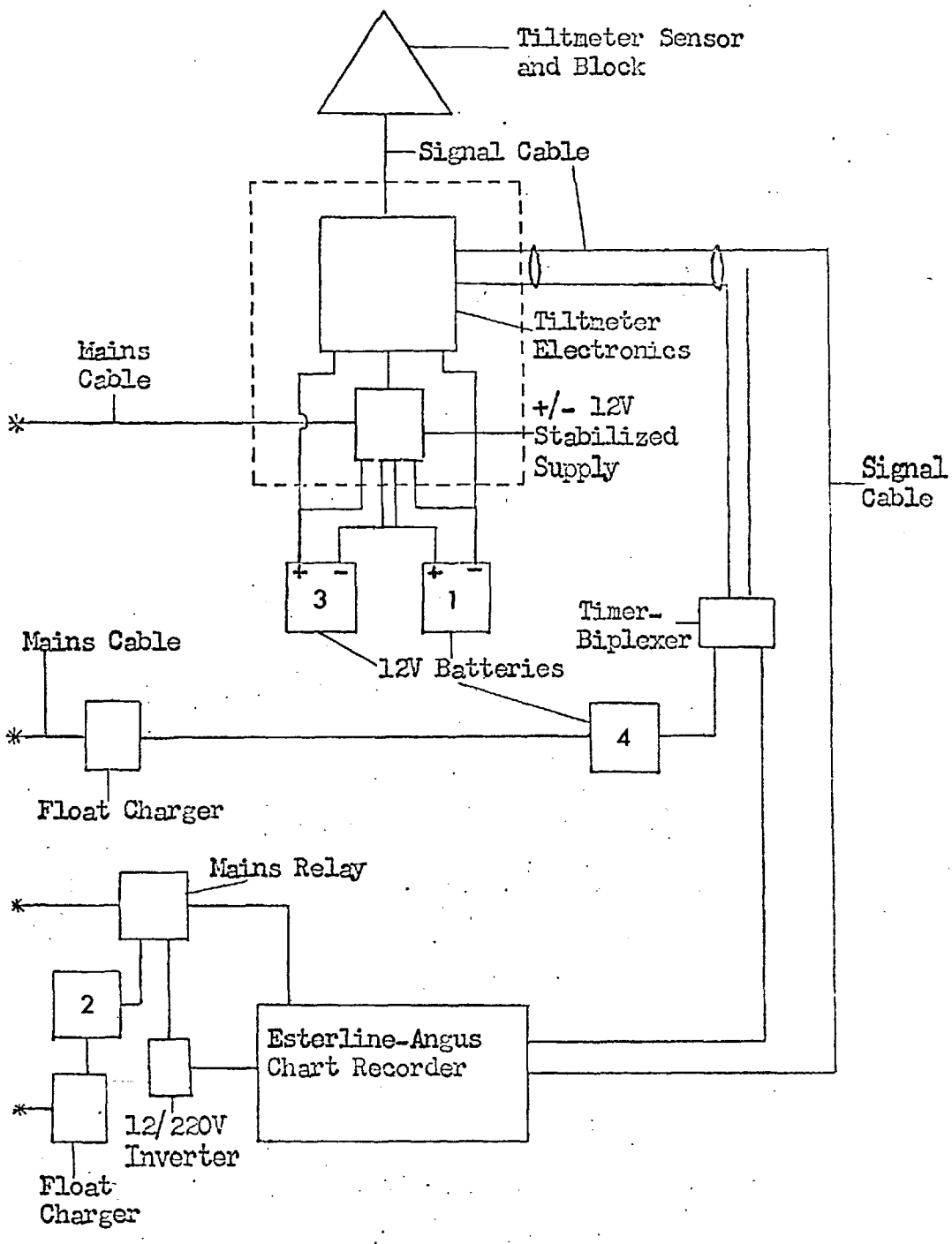


FIG. 4.8

Observatory tiltmeter operating system

12/8/76 - 27/8/76

an emergency A.C. power supply was arranged, using a 12V D.C. to 220V A.C. inverter, the 12V D.C. being provided by a second set of batteries, also float charged off the mains and the system arranged to come into action upon failure of the mains by the provision of a mains relay. The recorder was run at 25 m.m./hour and the recorder sensitivity set at 10V F.S.D. (this corresponds to 500 μrad Full Scale Deflection). This is a comparatively low sensitivity, considered that tidal effects are less than 0.5 μrad, and was set to allow for the excessive drift which was anticipated immediately following installation. No perceptible drift was observed during the first twenty-four hours and the sensitivity was then increased to o.5V (25 μrad). Again, over the next twenty-four hours driftwas minimal and the sensitivity once more increased, this time to 100mV (5 μrad). At this sensitivity the Y-axis (radial) drifted off-scale whereas the X-axis remained well on-scale.

In practice, the inverter system was found to be unreliable, and in view of the fact that the Observatory had its own emergency generator, power cuts being a common occurrence, it was decided to re-design the system to operate without this back-up support. This proved successful and on the few occasions when power was not available to the vault the nature of the recorder enabled the time loss to be calculated. Another modification to the system was the inclusion of a Cambridge CS5 Chart Stopper, allowing an additional $\pm$ 8 chart

widths. This second arrangement is shown in Fig. 4.9. When the chart-stepper was initially interfaced the sensitivity was increased to 30mV (1.5 μrad.) but the resultant record was too noisy and the sensitivity was consequently reduced to 100mV (5 μrad). The system was then left to run during the 1976/77 winter months. The vault was visited in January, 1977 (by a team from Leicester University) and the chart record changed. The vault was visited a second time in May, 1977 and further modifications were made to the system. The chart-stepper was removed and the sensitivity reduced to 5V (250 μrad). The inclusion of the chart-stepper had been intended to facilitate the recording of Earth tides. It now appeared, however, to be affecting the re-zeroing of the tiltmeter axes and it was decided that an adequate length of record had been recovered to permit a preliminary study of tilt tides to be undertaken. The third and final system configuration is shown in Fig. 4.10.

When the vault was visited for a third time, in November 1977, the tiltmeter electronics were discovered to have failed and when due consideration was taken of the plight of the borehole tiltmeter the decision was made to return the instrument to England.

The persistent breakdown of the instrument or one particular axis of an instrument was the main reason for their return. Although the borehole instrument was normally in operation at all times when the observatory tiltmeter was running, only ten days of data were recorded simultaneously on both instruments. The observatory instrument

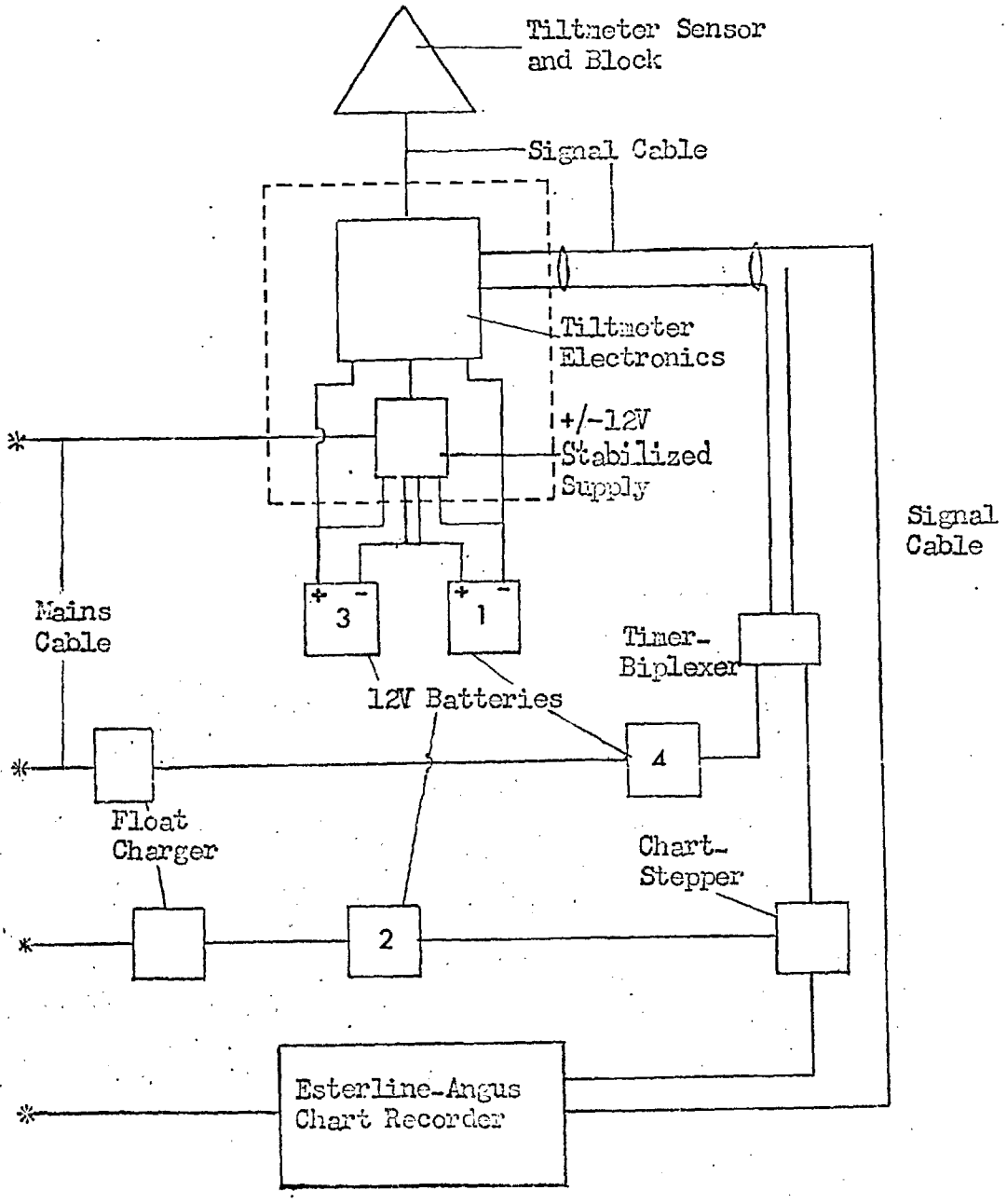


FIG. 4.9

Observatory tiltmeter operating system

27/8/76 - 7/5/77

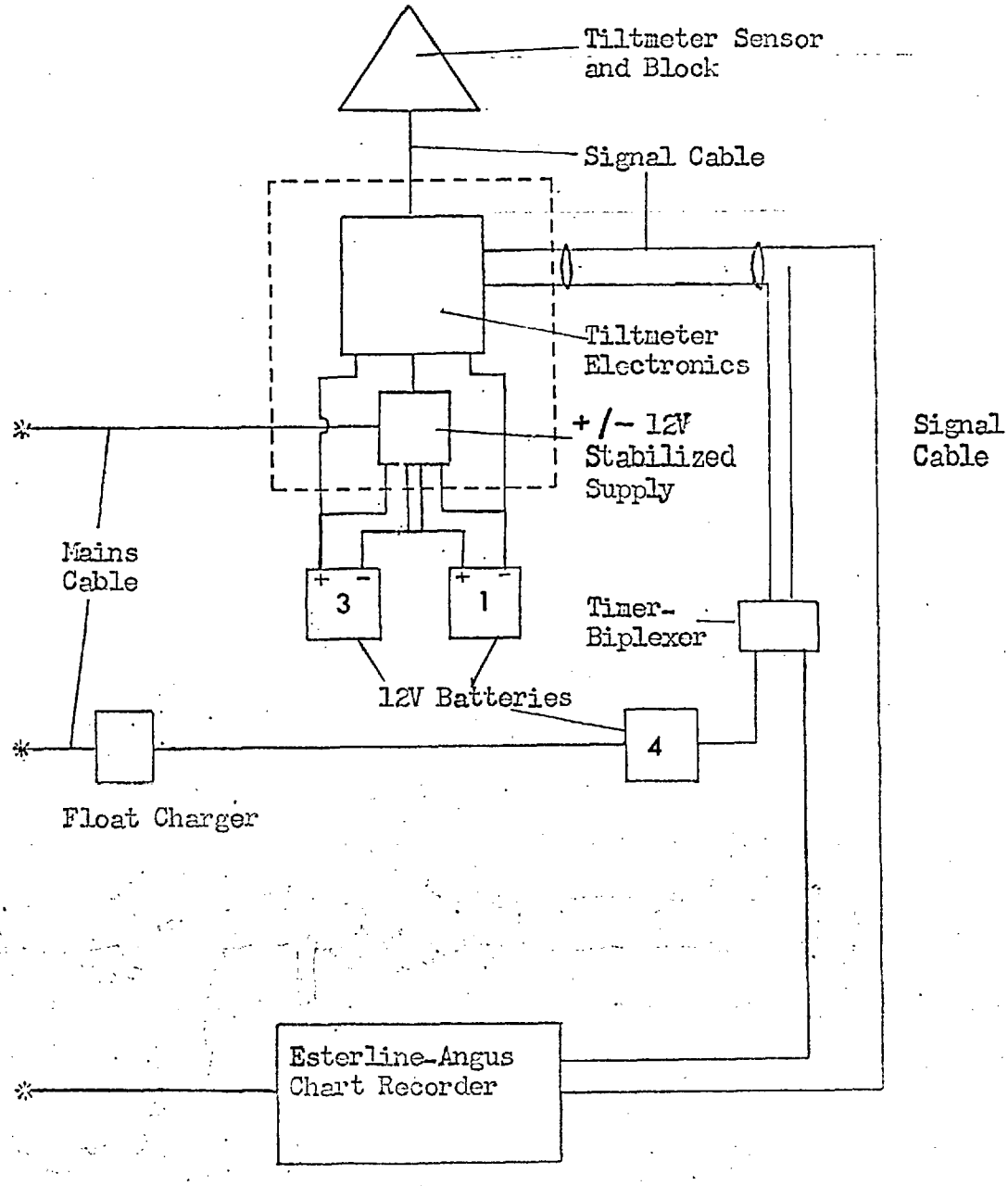


FIG. 4.10

Observatory tiltmeter operating system

7/5/77 - 18/5/77

provided the greater length of record because its faults could be more readily detected and repaired. When the borehole instrument was operating, however, it was capable of running for several months but of course any breakdown would go unnoticed until the site was subsequently visited, which might be several months later. The periods of operation for each instrument are given in Table 4.3.

Borehole		Observatory	
Radial	Tangential	Radial	Tangential
1/12/73-19/2/74	1/12/73-19/2/74		
	15/10/75-1/2/76		
		28/8/76-16/9/76	28/8/76-16/9/76
28/9/76-7/10/76		21/9/76-24/10/76	21/9/76-24/10/76
		24/10/76-19/11/76	
		18/12/76-10/1/77	
		24/1/77-16/2/77	
		7/5/77-18/5/77	7/5/77-18/5/77

TABLE 4.3

DATES OF OPERATION OF THE TILTMETERS

CHAPTER 5

THE TILTMETER RESULTS AND THEIR PROCESSING.

5.1 INTRODUCTION

The preceding chapters have discussed both the historical and the theoretical background to this research. The remainder of this thesis deals with the results, their processing, and the conclusions drawn therefrom.

The present chapter is concerned with the data obtained with the two tiltmeters that were installed on Etna. For reasons discussed in Chapter 1 of this thesis, the tilt data were considered to be made up of two, separable, constituents. The first of these was a short-period constituent, that is, one composed of tilts with a period of less a day, and the second, a long-period constituent.

The short-period tilts, then, the major tidal periods, and their analysis has thus been principally directed to an assessment of the effects of tidal tilt on Etna.

The long-period tilts, on the other hand, can be reasonably assumed to include the majority of the volcano induced tilts, that is,

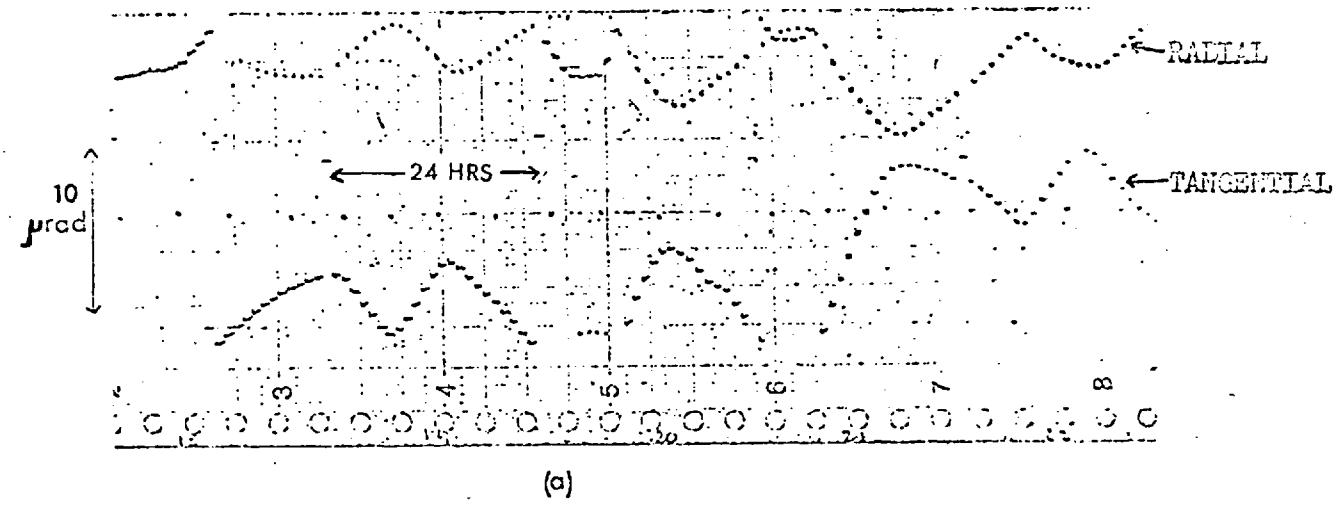
tilts due to internal movements of magma. Whilst it is possible that certain localized movements may have a short periodicity, the evidence available from other volcanoes, as well as general theoretical considerations, indicates that these magmatic movements are a long-term phenomenon.

5.2 DATA PROCESSING

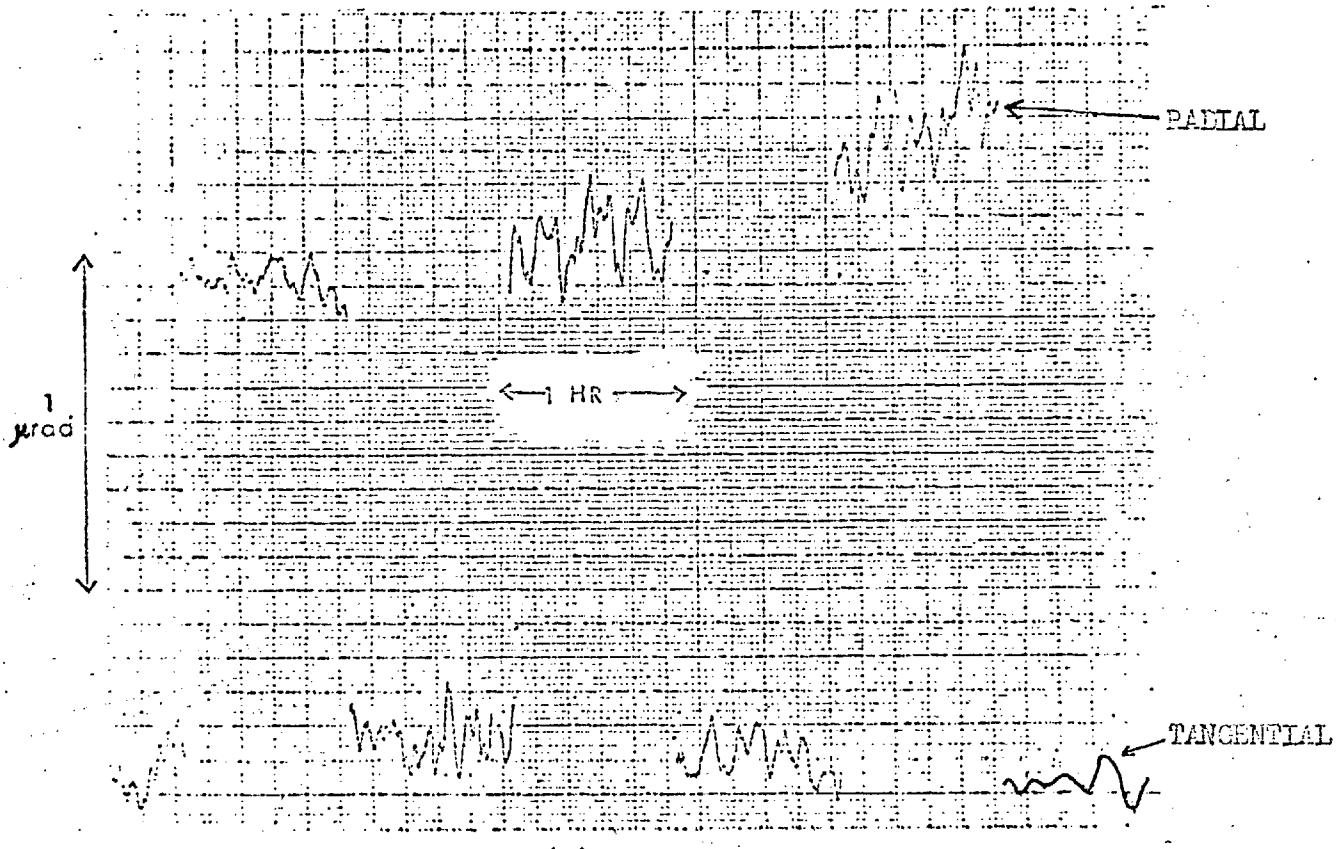
The data from the two tiltmeters was recorded on chart recorders as described in Chapter 4. The Rustrak chart recorders used with the borehole meter have a 6cm. chart width and record onto pressure sensitive paper. The Esterline-Angus recorder uses 12 inch wide heat sensitive paper. Samples of the output are shown in Figs. 5.1a and 1b.

Both tiltmeters were used in the integrating mode, thus effectively filtering out any signal below a 20 second period. This is essential, since the meter responds to microseismic noise, which has a predominant periodicity of 5-10 seconds and an amplitude similar to the Earth tide signal.

The two types of record presented different problems at both the data processing and the analysis stage. The borehole recorders were assumed to have run smoothly without any stoppages for the lifetime of the power supplies. The 1974 record did not have any time-marks, and the time scale of the record was derived by dividing the length of the record by the total time elapsed (Wadge, 1974). Doubt was cast on the accuracy of the time-keeping of the system, however, (J. Horsfall, Private Communication). The most likely cause of any variation lies in the Rustrak recorder rather than in the timing circuit. Ideally the recorders should be free of dust and operate in a dry atmosphere.



(a)



(b)

FIG. 5.1.

Samples of data recorded on the borehole tiltmeter (a) and the observatory tiltmeter (b).

Tilt at the borehole site is sampled hourly, with each axis being recorded for three minutes. The radial axis is indicated by a series of dots, and the tangential axis by a series of dashes.

The observatory tiltmeter operates continuously, recording each axis alternately for an hour.

Whilst this can be achieved in a laboratory environment it is considerably more difficult in the field, and for the borehole site it was more or less impossible. The same problems were not evident in the Observatory, where the instruments were well shielded from the elements. Here the vicissitudes of the electrical mains supply were the main problem. After the standby power system broke down no further attempt was made to deal with the problem and reliance had to be placed in the mains supply. It was possible to detect short stoppages (< 12 hours), or excessive reductions in voltage, at the data processing stage by making use of the periodic diurnal tilt. In agreement with Tomaschek (1957), it was observed that there was a thermally induced diurnal signal having peaks at about 6.00 a.m. and 6.00 p.m. This provided a means for discriminating between discontinuities in the record arising from power failures and those arising from discontinuities in real tilt. In fact there were very few occasions on which this was a problem, the longest stoppage amounting to only six hours. The tilt signal was interpolated over the stoppages by simple linear interpolation. The observed correlation between tilt events and eruptive activity, detailed in section 5.6, permits a reasonable degree of confidence in the timing of both tiltmeters. The reduced sensitivity of the borehole instrument in comparison with that of the Observatory prevented a diurnal signal being easily observed and so a similar check could not be carried out.

The records from both instruments were digitised on a semi-automatic digitiser (Oscar-J*) which provided a hardcopy output via a typewriter, the results then being punched onto computer data cards for further processing. The digitiser is arranged to output a number between 0 and 999 depending upon the position of a cursor. This number is converted into microradians by a conversion factor applied in the computer program immediately prior to data analysis. This conversion factor is dependant upon the width of the chart paper and the recording sensitivity of the recorder as well as on the sensitivity of the tiltmeter.

* Oscar-J is a trade name of the Benson-Lehner Company Ltd.

5.3 SPECTRAL ANALYSIS

After digitization all the data was processed in the same way using the computer program SPECANL. The details of this program are included in the Appendix but the salient aspects of spectral analysis will be described here.

A signal can be considered to be composed of three parts; a random component, a linear trend and periodic components. Limiting the discussion to a consideration of the type of signal encountered in this study, the random component is of two forms; instrument induced noise caused by the tiltmeter and recording system and environmental noise predominantly due to microseismic activity but with a major contribution from the wind. All the noise is at a much higher frequency than the periodic elements of interest. This means that they can be filtered out without adversely affecting the signal. There are two stages to this filtering; in the first place the input signal to the tiltmeter is passed through the integrating circuit referred to previously. The second stage of filtering employs a special tidal filter known as a Doodson filter. The selectivity of this filter is illustrated in Fig. 5.2. This filter is specifically designed to filter out all non-tidal signals. As can be seen from Fig. 5.2 periods in excess of seventy-two hours are 70% filtered, while for 12 and 24 hourly periods there is zero filtering.

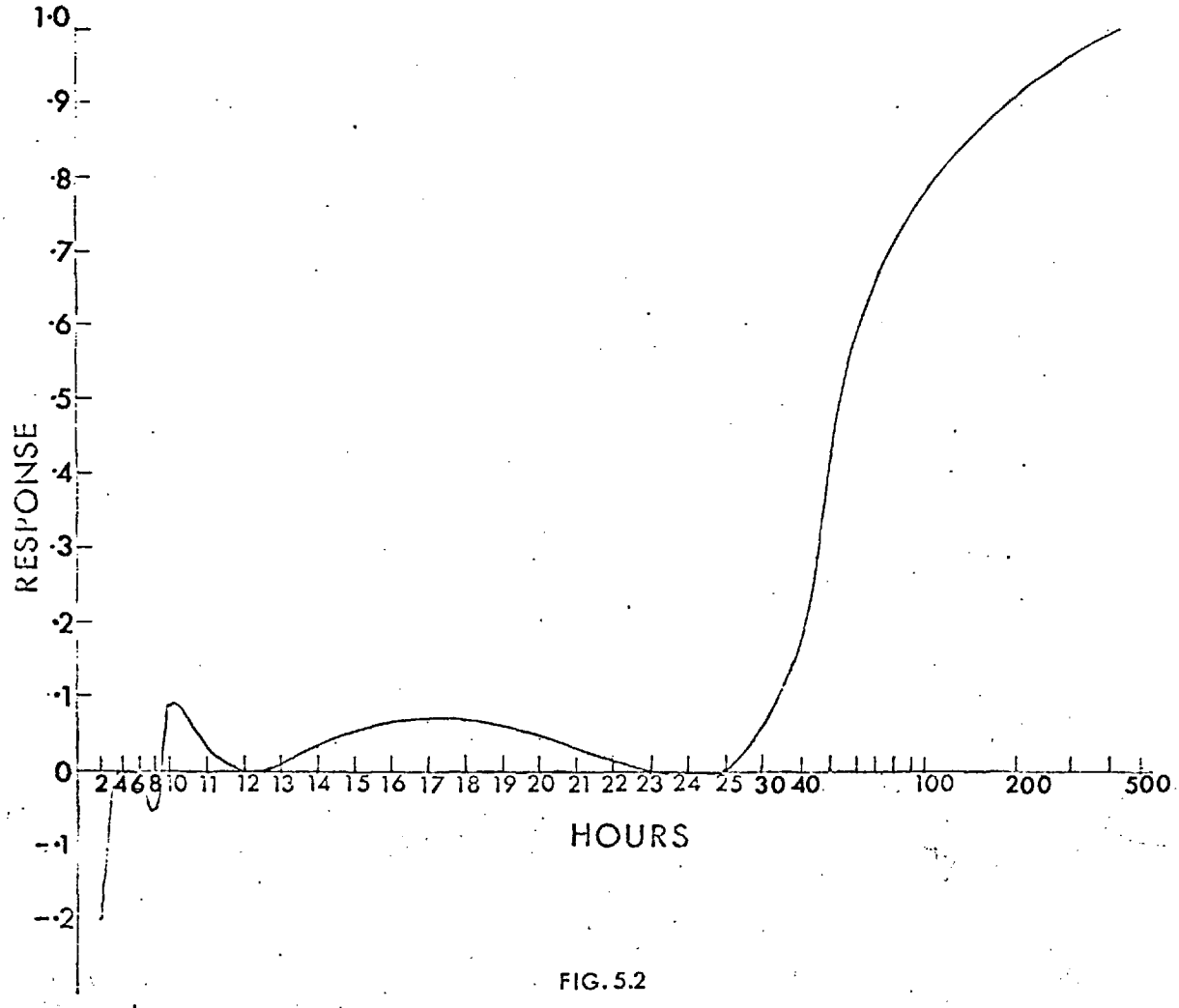


FIG. 5.2

Response characteristics of the Doodson filter.

For explanation see text.

Where the response curve becomes negative(at 2 and 8 hours respectively) the signals at these periods are enhanced. They are, however, not periods close to the tidal periods considered here, and thus cause no problem. The long-period signal removed by the Doodson Filter is composed of long period tidal components, mainly the fortnightly tide, instrumental drift and long period ground movements recorded by the tiltmeter. It is recovered by subtracting the filtered data from the original data and as discussed in section 5.1 is important volcanologically. It is considered in detail in Section 5.6.

The filtered data is then spectrally analysed by Fourier analysis. Spectral analysis techniques are widely described in the literature notably by Jenkins and Watts (1969) and Bath (1975).

According to the principles of Fourier analysis any curve, f(t), can, subject to certain restrictions, be represented by a series of sine and cosine terms

$$f(t) = a_0 + \sum_{n=1}^{\infty} \left(a_n \cos \frac{2\pi nt}{T} + b_n \sin \frac{2\pi nt}{T} \right) \qquad 5.1$$

and the constants are given by:-

$$a_0 = \frac{1}{2T} \int_{-T/2}^{T/2} f(t)\, dt \qquad 5.2a$$

$$a_n = \frac{1}{T} \int_{-T/2}^{T/2} f(t) \cos 2\frac{\pi nt}{T} \, dt \qquad 5.2b$$

$$b_n = \frac{1}{T}\int_{-T/2}^{T/2} f(t) \sin\frac{2\pi nt}{T}\, dt \qquad 5.2c$$

The coefficients a_n and b_n are the Fourier coefficients and it is these that are calculated in harmonic analysis. In practice, of course, all data is processed after some form of digitisation. This leads to the development of a discrete Fourier series given by:-

$$f(v) = a_o + \sum_{n=1}^{N/2} a_n \cos\frac{2\pi n v}{N} + \sum_{n=1}^{N/2} b_n \sin\frac{2n\pi v}{N} \qquad 5.3$$

for a series of N + 1 discrete, equally spaced, intervals with v = 1, 2, --, N and then:-

$$a_o = \frac{1}{N}\sum_{v=1}^{N} f(v) \qquad 5.4a$$

$$a_n = \frac{2}{N}\sum_{v=1}^{N} f(v) \cos\frac{2n\pi v}{N} \qquad 5.4b$$

$$b_n = \frac{2}{N}\sum_{v=1}^{N} f(v) \sin\frac{2n\pi v}{N} \qquad 5.4c$$

and for a given harmonic term

$A_n = (a_n^2 + b_n^2)^{\frac{1}{2}}$ is the amplitude

and $\phi = \tan^{-1}(b_n/a_n)$ " " phase

Two problems arise when dealing with digitised, finite length records. The first of these is known as aliasing and arises

from the digitization of the record. Digitisation implies a sampling interval, and as can be seen from Fig. 5.3, if a simple sine function is sampled at intervals Δt then it is not possible to distinguish between frequencies $f + \frac{n}{2\Delta t}$ for $n = 0, \pm 1, \pm 2$ etc. Thus high frequencies appear, or are 'aliased', at low frequencies. This means that estimates of the amplitude of the low frequencies will be invalid because of the contamination due to aliasing. The corollary of this is that the highest frequency that can be measured is given by $\frac{1}{2\Delta t}$ where Δt is the sampling interval. $1/2\Delta t$ is known as the Nyquist frequency. To avoid this the data is initally filtered to reduce the magnitude of the high frequency signals and then digitised at a frequency high enough to avoid aliasing onto tidal signals. In the course of this research all the data has been digitised at either hourly intervals or, in a few cases, three hourly intervals, which is standard practice in tidal analysis.

The problem arising from the finite length of the signal is more serious. It can be shown (Bath, 1975; Jenkins and Watts, 1969) that for a record of length T the minimum spectral separation is given by:-

$$\Delta f \geqslant \frac{1}{T}$$

that is, signals which differ in frequency by less than Δf cannot be

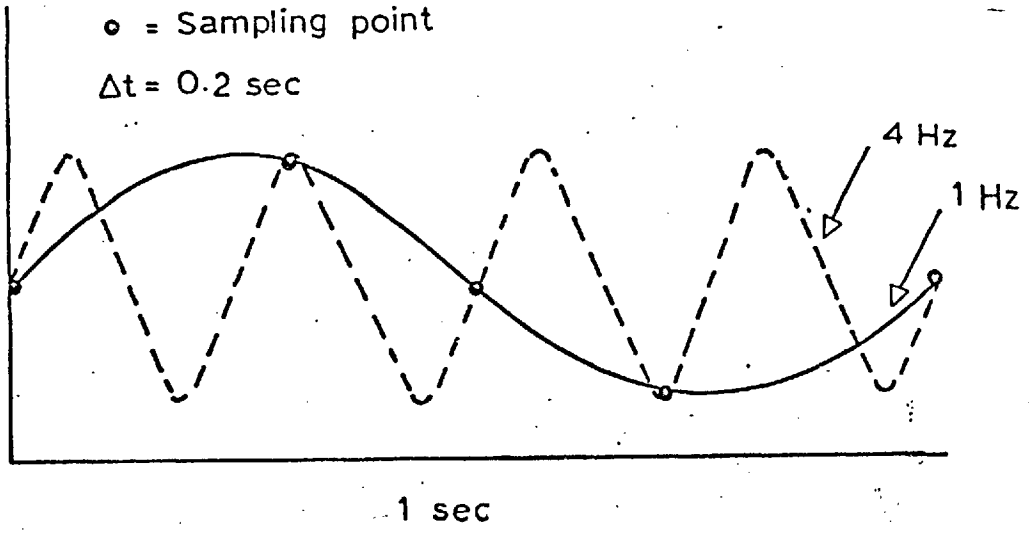


FIG. 5.3

Two aliased sine waves displaying identical sample points. The 1 Hz signal is resolved but the 4 Hz is not.

(after Muniruzzaman, 1977)

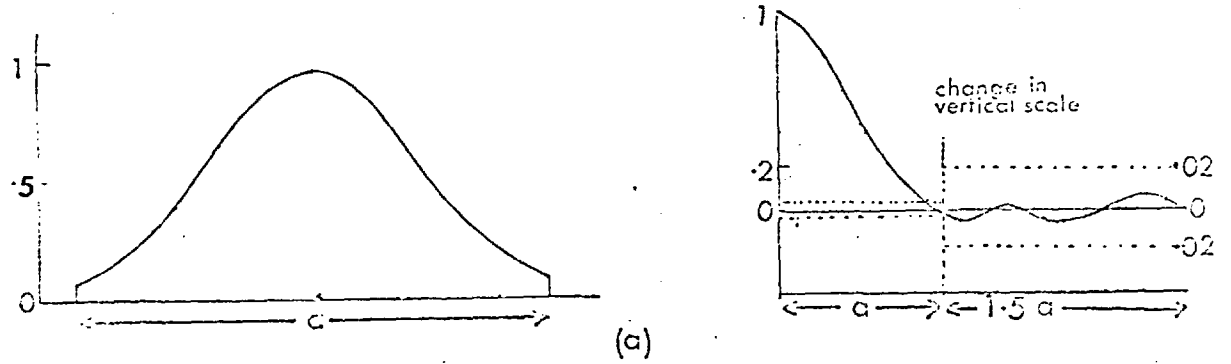
uniquely determined but will contaminate each other. This is equivalent to the Rayleigh resolution criterion in optics. This is of crucial importance in tidal analysis and Fig. 5.4 gives the length of data, in days, required to separate particular components. Many of the components are separable with a months data but some, notably S2 and K2 and P1 and K1 require six months. The longest continuous record obtained in this study is three months and so where values for S2 and K2 and P1 and K1 are shown separately they must be understood to represent not two uniquely determined values but two closely related signals.

Another problem due to the finite length of the record arises because spectral analysis is a transformation from a time-domain representation to a frequency domain representation. A finite length of data can be considered to be an infinite length of data convolved with a 'boxcar' window (Fig. 5.5a). The frequency domain representation is then given by the Fourier transform of the data multiplied by the Fourier transform of the window (Fig. 5.5a). This means that the resultant amplitude will be spread and have sidelobes, both leading to inaccurate results. This problem cannot be entirely eliminated but can be reduced by the use of different spectral windows. A great deal of attention has been paid to windowing techniques, particularly in the works cited, in order to determine the best window for a particular problem. On the whole, differences between them are not

PERIOD / FREQ.	WAVE / WAVE	K_2	S_2	L_2	M_2	N_2	J_1	K_1	P_1	O_1	Q_1
11.967 / .083562	K_2	—	181.95	27.09	13.66	9.13	1	1	1	1	1
12.000 / .083333	S_2	181.95	—	31.83	14.76	9.61	1	1	1	1	1
12.192 / .082024	L_2	27.09	31.83	—	27.54	13.77	1	1	1	1	1
12.421 / .080511	M_2	13.66	14.76	27.54	—	27.56	1	1	1	1	1
12.658 / .078999	N_2	9.13	9.61	13.77	27.56	—	1	1	1	1	1
23.098 / .043293	J_1	1	1	1	1	1	—	27.56	23.94	9.13	6.86
23.934 / .041781	K_1	1	1	1	1	1	27.56	—	182.74	13.66	9.13
24.066 / .041553	P_1	1	1	1	1	1	23.94	182.74	—	14.76	9.61
25.819 / .038731	O_1	1	1	1	1	1	9.13	13.66	14.76	—	27.56
26.868 / .037219	Q_1	1	1	1	1	1	6.86	9.13	9.61	27.56	—

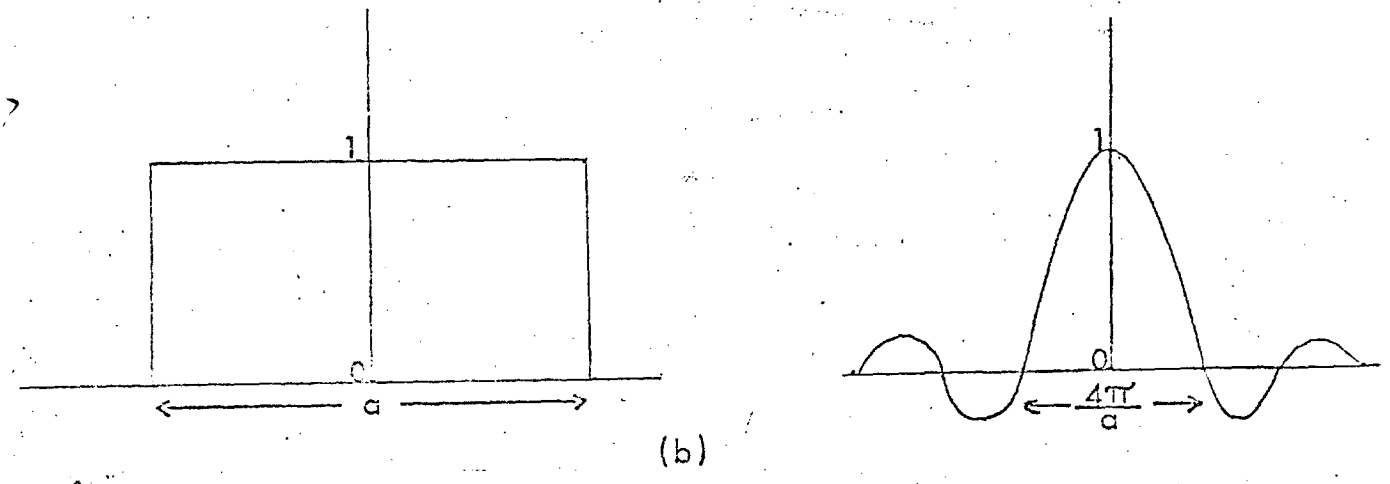
FIG. 5.4

Lengths of data, in days, required to separate particular constituents.



(a)

HAMMING WINDOW



(b)

BOXCAR WINDOW

FIG. 5.5

Hamming and Boxcar windows and their Fourier transforms

significant so far as they relate to this study, and the particular one chosen is the Hamming window Fig. 5.5b. This has much reduced sidelobes compared with the boxcar window and so there is less contamination of adjacent frequencies.

A good working estimate of the confidence limits that can be placed upon a spectral estimate can be obtained using a modified X^2 test (Båth, 1975). Fig 5.6. shows the confidence limits against degrees of freedom for a 95% significance level. The number of degrees of freedom, k, is given by; $k = 2T/\Delta$ where T is the length of the data sample and Δ is the sampling interval. For example for one months record sampled every three hours, $k = 480$ and a power estimate P' compared with a true power P would have a ratio $0.7 < P/P' < 1.55$. This obviously presents a severe limitation on the interpretation that can be placed on the results particularly in regard to tidal estimates.

To check the program and also to observe the effects of certain types of noise signal a series of tests on SPECANL were performed; in all these tests the data was subject to the same filtering procedure as all the real data.

In the power spectra shown subsequently in this chapter the tidal signal has been separated into ten components, the ten chosen being the most important of the semi-diurnal and diurnal terms, and their amplitudes and periods are given in table 5.1 below. As none of the

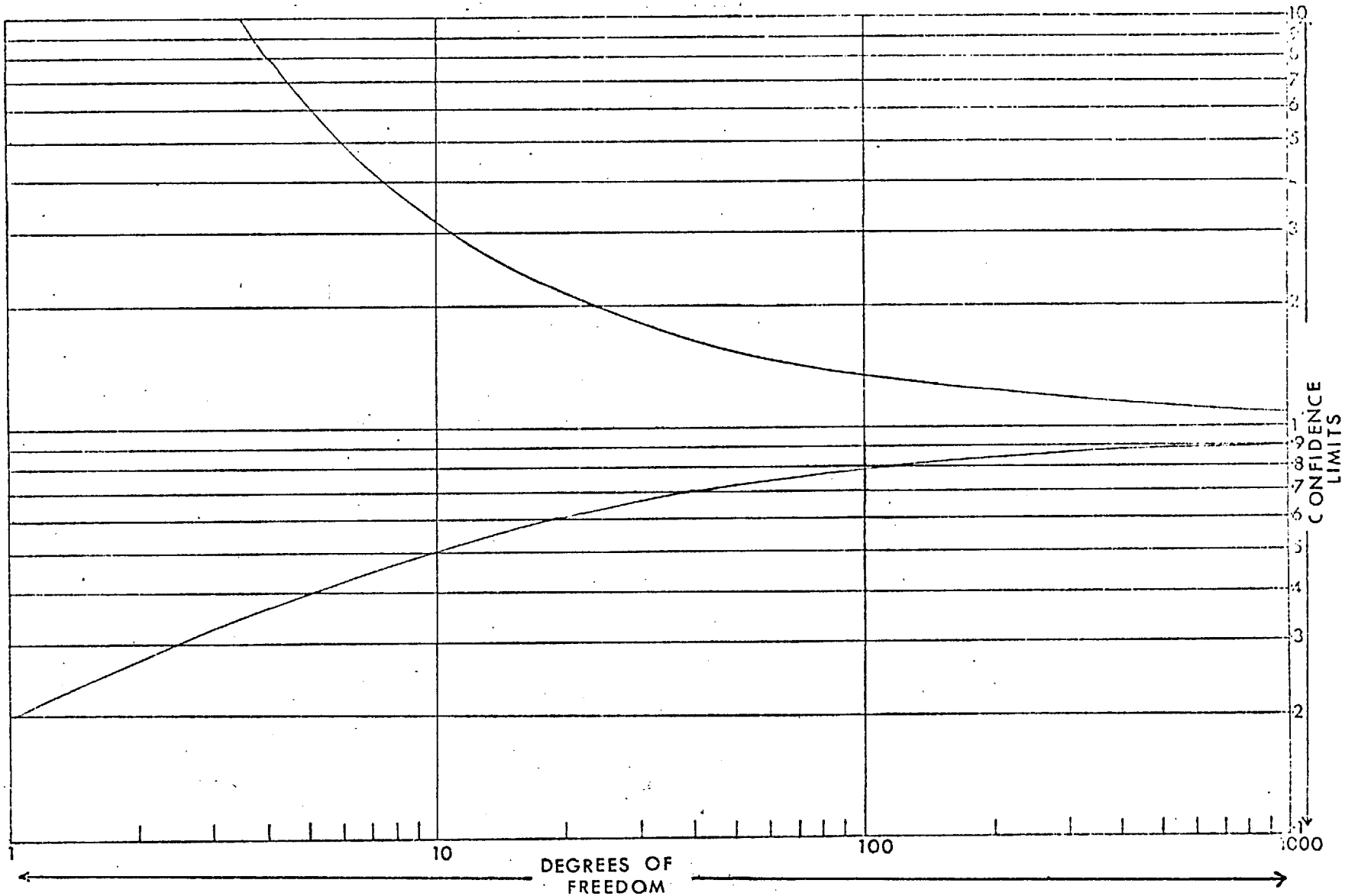

10
9
8
7
6
5
4
3
2
1
9
8
7
6
5
4
3
2
1
CONFIDENCE LIMITS
1
10
100
1000
DEGREES OF FREEDOM
χ²-TEST (α=95%)

FIG. 5.6

available records was longer than three months, it can be seen, from figure 5.4, that the S2 and K2 constituents cannot be separated. This also applies to the P1 and K1 constituents. They have been shown separately in the figures merely for the sake of convenience, and this is also the reason for equally spacing the components. In addition the power estimates have been normalized with respect to M2 = 1.0. This is common practice in tidal analysis.

Component	Period (Hrs.)	Amplitude
Q1	26.87	.079
O1	25.82	.415
P1	24.07	.193
K1	23.93	.584
J1	23.10	- .033
N2	12.66	.191
M2	12.63	1.0
L2	12.19	- .028
S2	12.00	.465
K2	11.97	.127

Table 5.1

Tidal Components Used in Analysis.

a) 12 HOUR SINE WAVE

A straightforward sine wave with a period of 12 hours was digitized hourly for 14 days. This test checks the power loss between adjacent components. As can be seen in figure 5.4, 14 days is just below the minimum resolution time for S2 - M2 resolution. The result of this is that the amplitude of the M2 signal is 48% of that of the S2 signal. The transference to the diurnal range is insignificant however, being less than 0.3%. The resultant spectrum is shown in figure 5.7 a.

b) 24 HOUR DISTURBANCE

This test is similar to the previous one, a 24 hours signal of 1μrad range being added to a normal tidal signal for 29 days. This signal is much larger than the tidal signal by a factor in excess of three. The resultant spectra is shown in Figure 5.7b Fig. 5.8 gives the normalised amplitudes of a prediced tide and the disturbed signal. Apart from the P1 K1 signal only the J1 amplitude is noticeably different; other differences can be readily accounted for by differences in sampling time. We can thus be confident that any perturbation will manifest itself at its true frequency with a smaller influence at adjacent frequencies, the magnitude of this influence being dependent upon the length of the record.

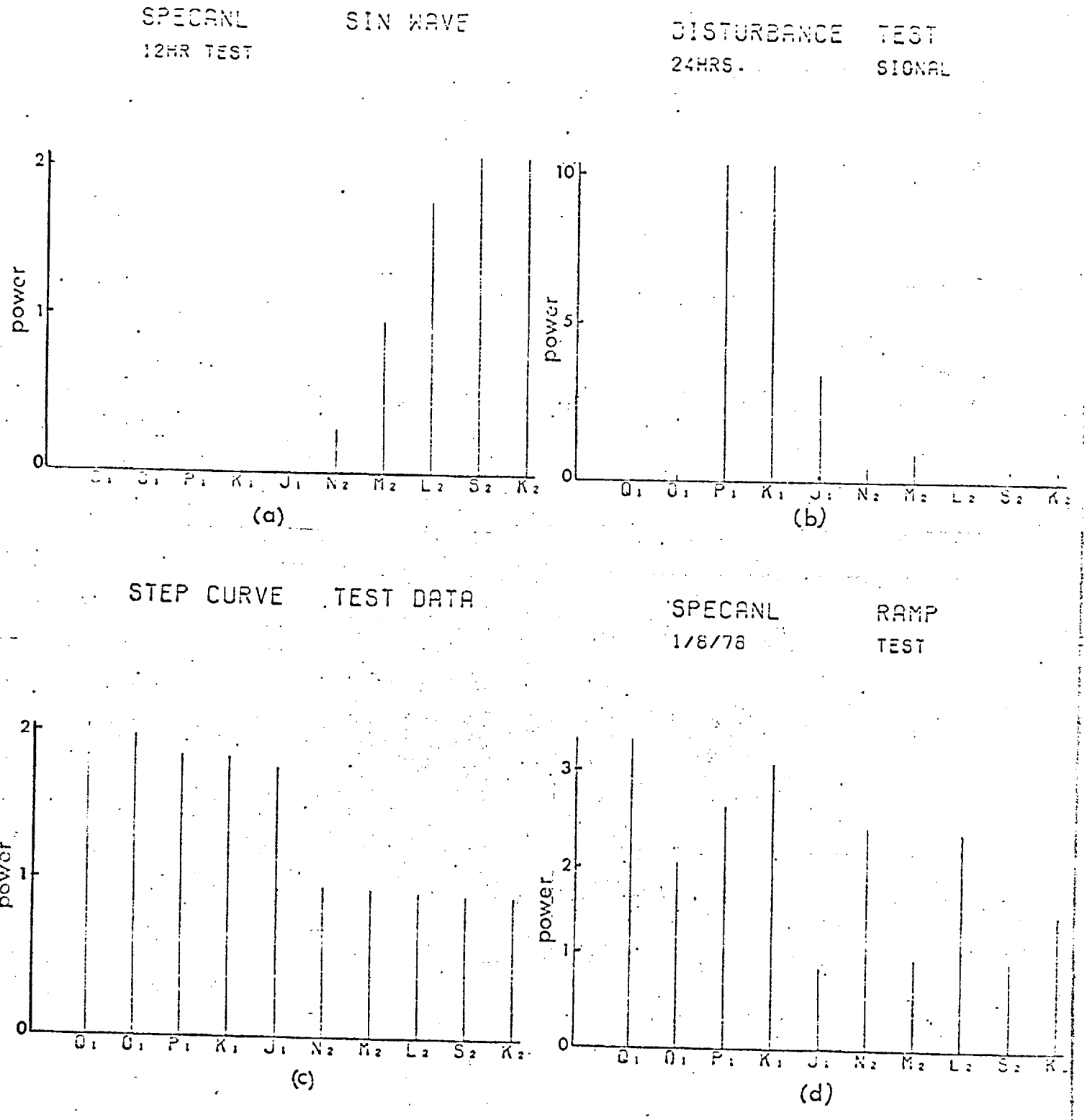


FIG. 5.7

Power spectra obtained for various SPECANL tests.

The powers are normalised with respect to M_2=1.

	K_2	S_2	L_2	M_2	N_2	J_1	K_1	P_1	O_1	Q_1
PRED.	·447	·510	·025	1·000	·177	·017	·228	·172	·191	·030
DIST.	·449	·451	·132	1·000	·498	3·527	10·650	10·651	·188	·084

FIG. 5.8

Normalised values of amplitudes for Predicted tidal data and a predicted signal plus a large (1μrad) 24 hour period disturbance.

c) STEP FUNCTION

This test and the following one were designed to examine the response of the program to the sort of tilt signal encountered on Etna. In this case a step is applied to a straight line. The resultant power spectrum is important, though it is that predicted by theory, since sudden changes of tilt are common and even after filtering their effects remain, as shown in Fig. 5.7c, the power being concentrated at the longer periods and decreasing steadily with increasing frequency.

d) RAMP TEST

This is designed to test the effect of uniform drift. Theoretically all this should be filtered out and no spectrum result. However, the Doodson filter is a 19 point filter, and so the first and last 19 points are not filtered out, only modified in amplitude. It is these 38 points that account for the spectrum of Fig. 5.7d. This effect is reduced with increased record length and would be dwarfed by any other periodic signals within the data.

5.4 ETNEAN TIDAL POWER SPECTRA

In the ensuing discussion the terms 'radial' and 'tangential' will be used then referring to a tiltmeter's alignment. As explained earlier, each tiltmeter was oriented so that one axis responded to tilt in the radial direction with respect to the summit of Etna and the other in the tangential direction. Figure 4.6 illustrates the use of these terms and also those regions where volcanic activity occurred during the course of this research. The arrows indicate the directions of uplift for a positive change in tilt, that is, a positive change in the radial tilt indicates summit inflation whilst a positive tangential tilt indicates inflation to the east. The azimuths of the radial axes are:

$13.5^{\circ} \pm 1^{\circ}$ - Observatory

$-19.0^{\circ} \pm 1^{\circ}$ - Borehole

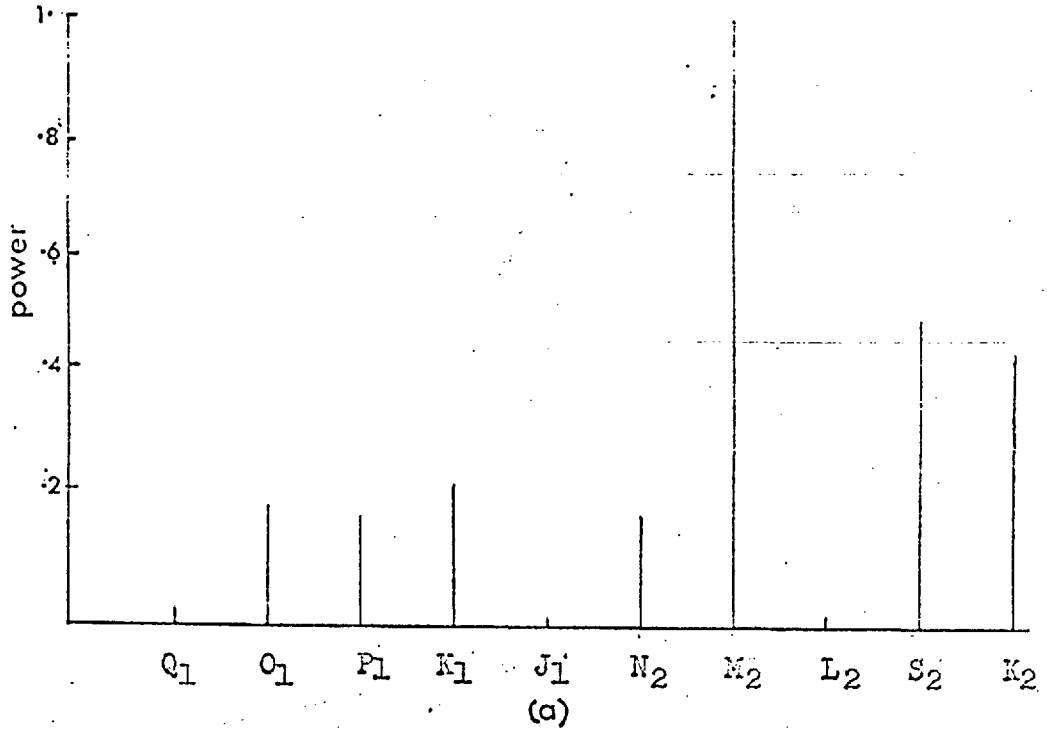
The map also illustrates the considerable advantage that would result from having at least one tiltmeter sited on the northern slopes, for example, in the direction of the Rifugio Linguaglossa (rif.ling.) especially as most of the activity of recent years has occured on these northern flanks.

The graph of theoretical tidal tilt amplitudes against latitude (figures 3.7a and b) shows that for 35°N the tide is predominately

composed of the M2 component in both N-S and E-W directions. The power spectra for azimuths 13.6° and 103.6° on Etna are shown in figures 5.9 a and b respectively and here the domination of the M2 component can be seen clearly. The S2 and K2 components each possess about half the power of M2 and the diurnalcomponents O2, P2, and K2 about 20% each. The spectra are remarkably similar and it follows that the spectra for any azimuth on Etna will be similar to these. It is not very surprising that these spectra resemble each other so closely, since, from fig. 3.8, it can be seen that the tilt vector at the Etnean latitude ($\sim 35^{\circ}$N) is very nearly circular.

The inference that can be drawn from these spectra is that, if the tides are the major influence on tilt, then spectra due to tilt data from the volcano should exhibit a similar power distribution. However, due to the factors discussed in Chapter 3, in particular the solar heating effect, there will be an increase in the power at 24 hours and 12 hours, thus affecting the P1 and S2 components respectively. Additionally, since we are not able to separate the S2 and K2 or P1 and K1 components with the lengths of data available, there will be contamination of the K2 and K1 power estimates. To a lesser extent there will be contamination of the J1 and L2 terms.

It is convenient to divide the data into separate periods to allow for ease of interpretation. These periods will be designated as a) Winter '73-'74, covering the period 1st December 1973 until



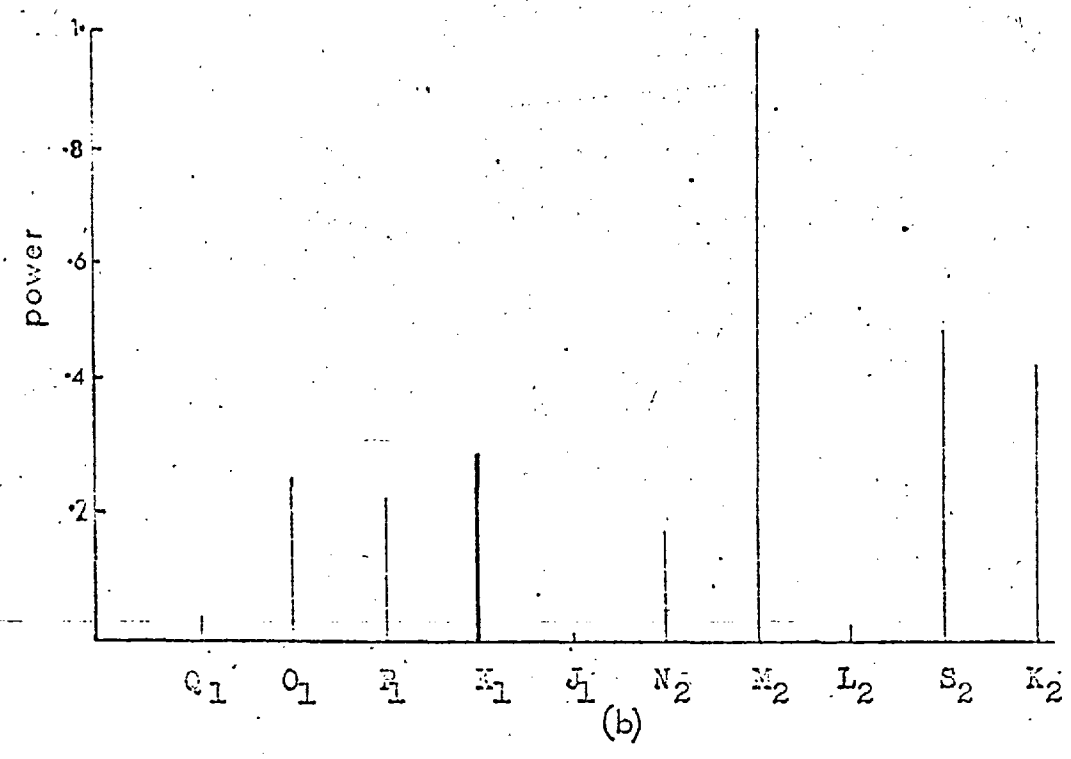


FIG. 5,9

Tidal tilt power spectra for theoretically predicted tides at Etna for the period 21/7/76 - 14/10/76.
(a) - Azimuth 13.6
(b) - " 103,6

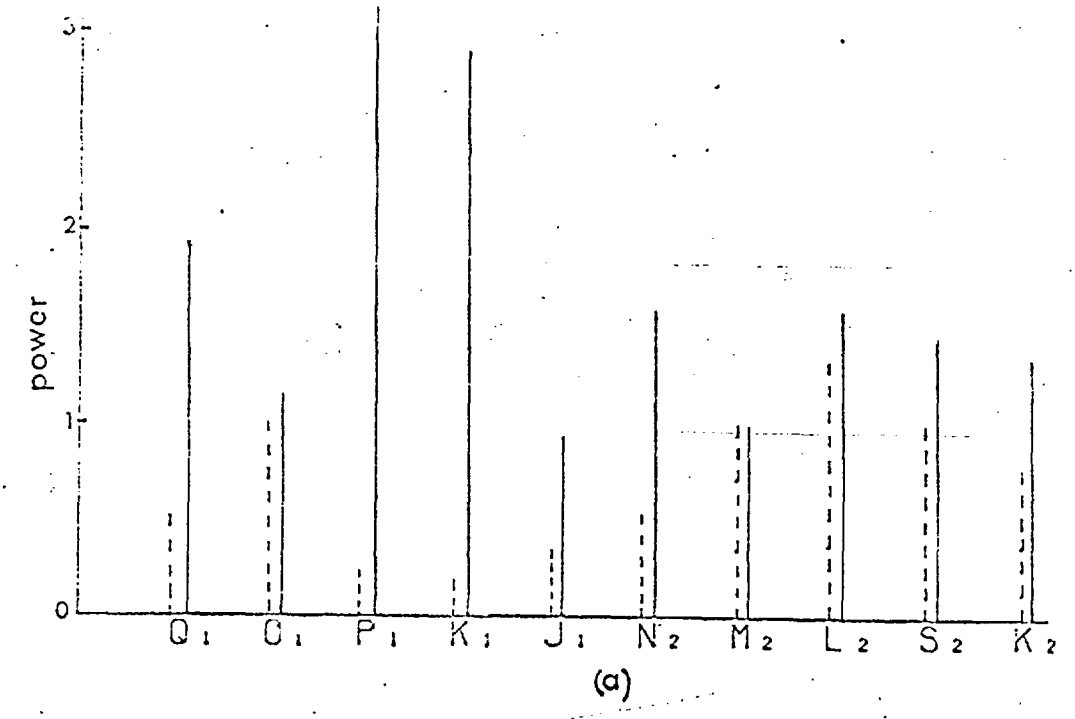
the 19th February, 1974, b) Winter '75-'76, covering the period 15th October 1975 until the 1st February 1976, c) Autumn 1976, covering the period 28th August 1976 until the 19th November 1976, d) Winter '76-'77, covering the period 10th December 1976 until the 16th February 1977, and c) Summer '77, covering the period 7th to 18th May 1977.

In the following figures, 5.10 to 5.11 , depicting power spectra, where both radial and tangential components have been simultaneously recorded, the radial component has been indicated by a solid line and the tangential by a dashed line. Where only one component has been recorded it is indicated by a solid line.

a) Winter '73-'74

During the period only the borehole tiltmeter was in operation, and the record was remarkable for the occurrence, during the period 1st January until 19th February '74, of an apparently diurnal signal well in excess of the predicted tidal signal. This large signal was recorded prior to and during the eruption beginning on January 30th (Wadge et al., 1975).

The data was split into two portions, one covering the comparatively quiet period before 1st January and the other covering the rest of the data. Figure 5.10a is the computed tidal power spectra for the radial and tangential components for the period 1/12/73 - 29/12/73. These clearly differ from a normal tidal signal (figure



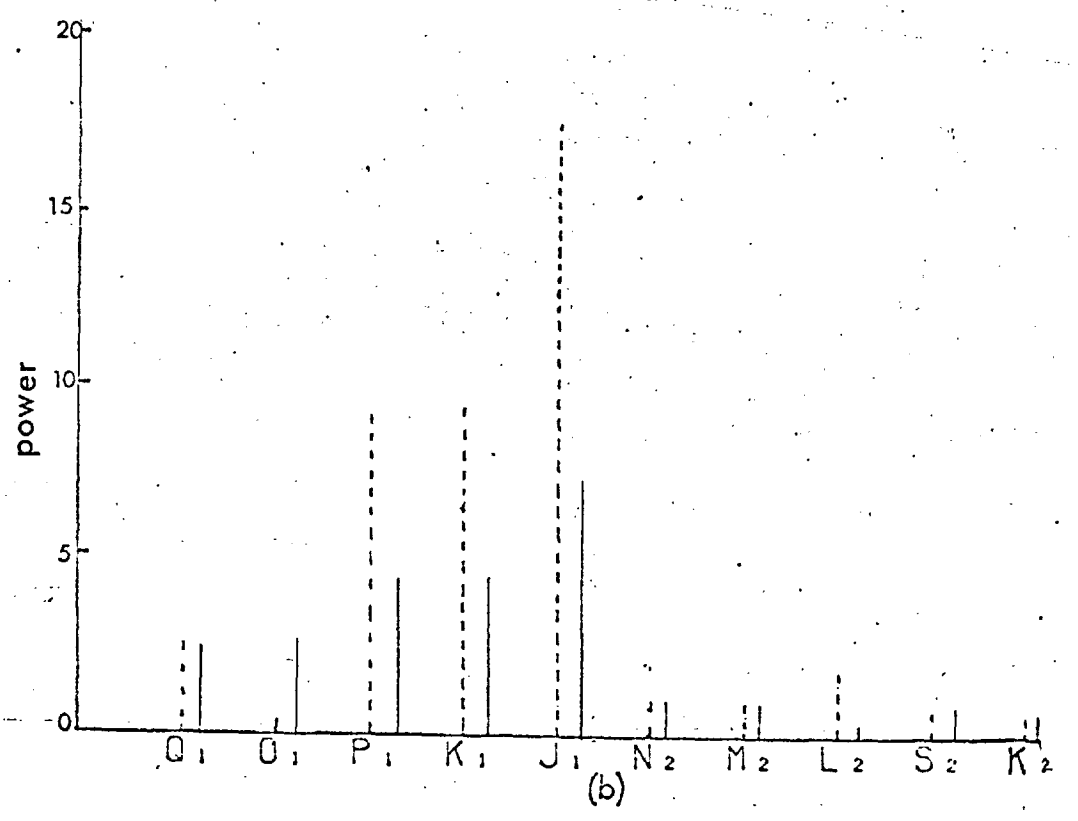


FIG. 5.10

Tidal power spectra obtained from data collected at the borehole site:
(a) for the period 1/12/73 - 29/12/73
(b) " 29/12/73 - 19/2/74

Straight lines: Radial tilt Dashed lines: Tangential tilt

5.8). These differences may be accounted for by reference to the long-period signal (figure 5.13a) where the rapid tilt changes cause an effect similar to that generated by the step function (figure 5. 7c). The differences between the radial and tangential axes may be similarly accounted for by reference to the differing long-period signals.

When the spectra for the period 29/12/73 - 19/2/74 are considered (figure 5.10 b), the large quasi-diurnal signal can be immediately seen. However, instead of occurring at the P2 K2 frequency (i.e. 24 hours) it is, in fact, the J1 component which is foremost. There does not seem any adequate reason for invoking a tidal explanation since the magnitude of J1 is small compared to the other components. Similarly no climatic argument would satisfactorily explain this. A possible explanation is inaccurate instrumental timing but this is belied by the good correspondence obtained between volcanic and tilt activity, described in section 5.6. The condusion, at present, is that this quasi-diurnal signal cannot satisfactorily be explained.

b) Winter '75-'76

An anomalous quasi-diurnal signal was again observed during January 1976 though, on this occasion, not associated with any volcanic activity. As with the '73-'74 data the data was split into two parts,

15/10/75 - 21/12/75 and 21/12/75 - 1/2/76. At this time only the tangential axis was operating, so no comparisons can be made between the radial and tangential components.

For the first period, the spectrum (figure 5.11a) is similar to that of the '73-'74 data (figure 5.11a). Figure 5. 11b for the period 21/12/75 - 1/2/76 shows heavy contamination at both 12 and 24 hours, the P1 K1 signal being particularly large. This contamination strongly implies that climatic factors are operating. Although this quasi-diurnal signal occurred at the same time of the year as the corresponding signal in 1974 there does not seem any similar cause, basically because of differences in the frequency of the signal, and also in the activity of the volcano.

c) Autumn '76

Although there was a good deal of data gathered during this period, it yields few results of volcanological interest from the point of view of spectral analysis. This is unfortunate because it includes the only record simultaneously recorded on both borehole and observatory instruments 28/9/76 to 7/10/76. The long-period signals, however, are interesting, ~~however,~~ and these will be discussed later, in section 5.6. Before leaving this period it may be remarked that all the signals exhibited large diurnalsignals. These can most

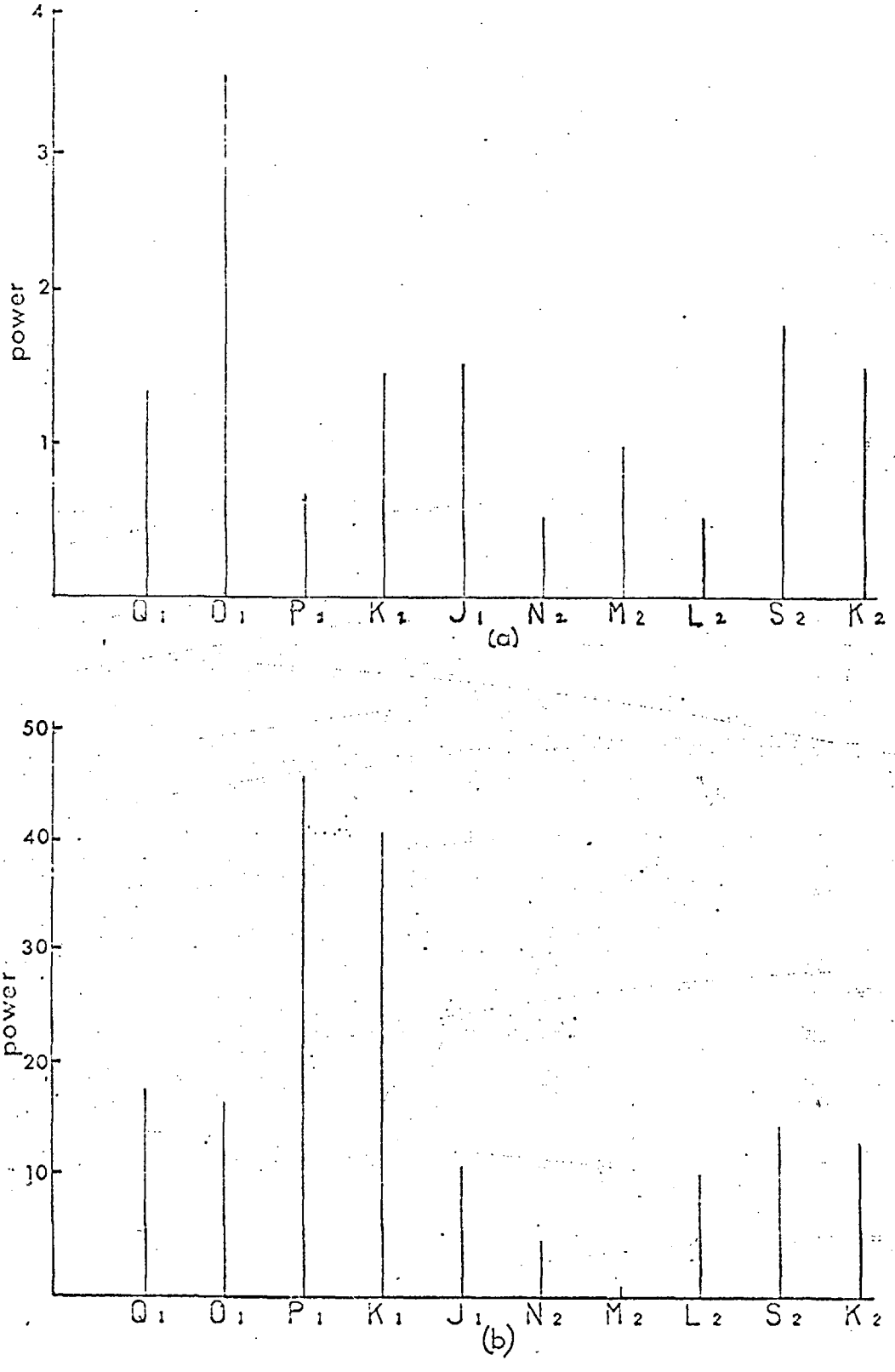


FIG.5.11

Tidal power spectra for the periods: (a) 15/10/75 - 21/12/75, and (b) 21/12/75 - 1/2/76 at the borehole site (tangential axis only).

probably, be explained by climatic effects, in the absence of any other explanation.

Similarly the data for periods d) Winter '76-'77 and e) Summer '77 provide little of interest in terms of power spectra. In fact, these two periods only provided three short sections of data and so the lack of any reasonable spectra is not surprising.

For the interested reader, the spectra not illustrated here have been included in a separate appendix (B).

ETNEAN TIDAL POWER SPECTRA - CONCLUSIONS

The tidal tilt spectra then generally demonstrate one or other of two forms. In the first the normalized amplitudes are similar for all components, with the P1 K1 term generally the largest but with 3 times the M2 amplitude. The other form of the spectrum is characterized by enormous diurnal amplitudes ≥ 7 times M2. Although the first occasion on which these large diurnal amplitudes were recorded coincided with a Etnean eruption (January 1973) the later examples bore no particular relation to any such activity. The most likely explanation for this effect is that ~~this~~ it is occasioned by large scale temperature changes in the vicinity of the tiltmeter. Harrison and Herbst (1978) have shown that in hilly areas local tilts due to diurnal temperature changes can be very large, in some cases up to 50 μrads. This is well in excess of the diurnal variations observed on Etna, where temperature changes can amount to 30°C over the course of a day.

The effect of rainfall is more difficult to assess. Wood and King (1977) found that rainfall caused anomalous tilts of around 1 μrad at a tilt monitoring site in Central California and such tilts could be even larger on Etna due to the terrain. It is extremely unlikely, however, that rain could have caused the regular quasi-diurnal signal since it would require the rain to fall at a specific time each day

for a number of days. The large diurnal tilts in fact continued for thirteen days.

A more likely cause is melting snow. The anomalous signals were observed during the winter months and there is snow on the upper slopes from October until May. Snow itself is a good thermal insulator (G.C.P. King personal communication) and its depth above the borehole tiltmeter is likely to have been at least ten feet, which would have maintained the ground temperature at a very stable value. If then a warm spell caused the surface snow to melt and run off this will induce anomalous tilts due to differential loading, the lower slopes possessing less snow and it melting faster than the upper slopes. Since the temperature actually measured at the sensor during 1973-74 was stable to within 2°C over the year and less than 1°C over the period of the large amplitude signals, the possibility of the tilts being caused by rain or melted snow percolating past the tilt sensor (Wood and King, 1977) can be rejected in this case. The results obtained made the calculation of the Love Numbers h and k impracticable even though a simultaneous tidal gravity survey was conducted (I. Mohamed, 1978). The observed M2 amplitude varied between 100 nrad. and 700 nrad. compared with the predicted value of 346 nrad. That the measured amplitude can be smaller than the theoretical tide is due to

the power being spread over a range of frequencies in the Fourier analysis when only short lengths of data are available.

The attempt to measure tilt tides on Etna must therefore be considered not to have been a success. Although the instruments are capable of resolving the tidal signal it is very close to the limit of resolution and an accurate determination of tidal tilts using these tiltmeters requires very low noise levels which cannot be attained on Etna.

There has been one previous attempt to measure tidal tilts on Etna (Jones L., 1965). This attempt involved the installation of two Verbaandert - Melchior horizontal pendula in an observatory built in a cave 1 km. north of Nicolosi. Although these instruments are standard tidal tiltmeters the results obtained from the first year's operation were extraordinarily erratic. The diminishing factor, γ, for M2 varied between 1.136 and 0.88 compared with the accepted worldwide value of around 0.7; the variations for S2 and N2 were even more widely spread as were the values of phase. This installation was intended to be the first of four tilt stations on Etna but there is no published record of any of these others, if they were operative, and it is believed that no further tilt observatories were ever built (A. Rittmann, personal communication).

5.5. ETNEAN ACTIVITY 1973-1977

Since one of the main intentions behind this research is the prediction of activity on the volcano it is important now to examine the data for correlations with such activity. A general summary of activity over the period November 1973 to May 1977 is given in the following pages. This summary has been garnered from reports by Guest et al. (1974), Booth (1975), Kieffer et al. (1975), Murray (1977), Guest and Murray (1977) as well as personal observations and personal communications from J. Murray, I. Mohamed and N. Henbest. Reports during the winter months are limited because of the heavy snowfall, which may last from October until May. It is likely that events which may be important precursors of activity would be unnoticed.

In the following summary the periods when the tiltmeters were in operation have been indicated.

1973

November - Strombolian activity at NE Crater.

1974

January 30th - Small fissure opened at 1680m. on Western slope. Eruption initially characterized by strong, almost continuous Strombolian activity.

Borehole tiltmeter in operation

February 9th - Small scoria cone of 30-40m. height had been built up at side of the eruption and activity became intermittent.

February 17th - Cessation of activity.

Between February 9 - 15 lava was extruded at an average rate of 1.7 m^3 sec^{-1}.

March 11 - Renewal of activity in the same area as the previous eruption.

Continuous until:

March 23 when all activity ceased.

During the two eruptions approximately 6.10^6 m^3 of lava was produced.

September 29th - N E Crater resumes Strombolian activity.

October 10th - Lava overflowed lip of NE Crater

1975

Intermittent Lava flows until February 24.

February 23/24 - NE Crater activity ceases. Effusive activity starts 1 km. to the north at 2600m. from vents on the north-east rift. Activity from this site continued throughout the summer and was generally quietly effusive, rates varying from less than 0.1 m^3 $sec.^1$ to 1.6 m^3 sec^1.

July-August - Variable activity at the North flank vent.

September 12 - Cessation of activity at north flank vent. NE crater exudes lava on Western edge.

Throughout 1975 explosive activity occurred in both the Bocca Nuova and the Chasm.

Borehole tiltmeter in operation

November 28 - Activity at NE Crater stops and a new vent opened north-east of Punta Lucia. Initially explosive activity.

Winter 75/76 - Pit opened on the western side of the NE Crater engulfing the new cone formed during September/October.

1976

May 16 - June 4 (Period of Observation) - Bocca Nuova exploding at a rate of 20 to 180 explosions per hour. Estimated depth of Chasm of several hundred metres. Effusive activity near Punta Lucia.

May 25 - Violent explosions start at Chasm at a rate of 20 to 25 explosions per minute. Activity reduced over the next few days. NE Crater inactive.

June 17 - New vent opened in region of NE Crater with Strombolian activity.

August 20 - Eruption stopped. During this period there was no lava eruption from this site and the NE Crater itself was inactive.

Observatory tiltmeter in operation 28/8/76 - 19/11/

September 8th - Activity stops at Punta Lucia and a large flow starts 2 km. north and 1 km. west of the Due Pizzi at an altitude between 2300 - 2400 m.

Borehole tiltmeter in operation 28/9/76 - 7/10

September 15 - October 4 - little activity in summit region.

September 27 - Flow from near the Due Pizzi ceased emerging and on:-

September 28 - New boccas opened east of Monte i Deserti.

October 1 - New boccas opened west of the Due Pizzi.

Activity continues from near Punta Lucia until the end of the year.

1977

Obsrevatory tiltmeter in operation

May - No effusive activity in summit region. Heavy snow cover precludes knowledge of activity elsewhere.

November 21/22 - Eruption commences at the NE Crater having been preceded by increases in microseismic activity. Explosive activity.

November 25 - Renewal of activity at NE Crater.

5.6 LONG-TERM TILT ACTIVITY

Figures 5.12 to 5.18 are plots of the long-term tilt activity, after filtering. As with the spectra, where radial and tangential data have been recorded simultaneously the radial signal is given by a solid line and the tangential by a dashed one. In the one example where there was simultaneous recording at the observatory and borehole sites the three axes have been marked on the same figure (5.16).

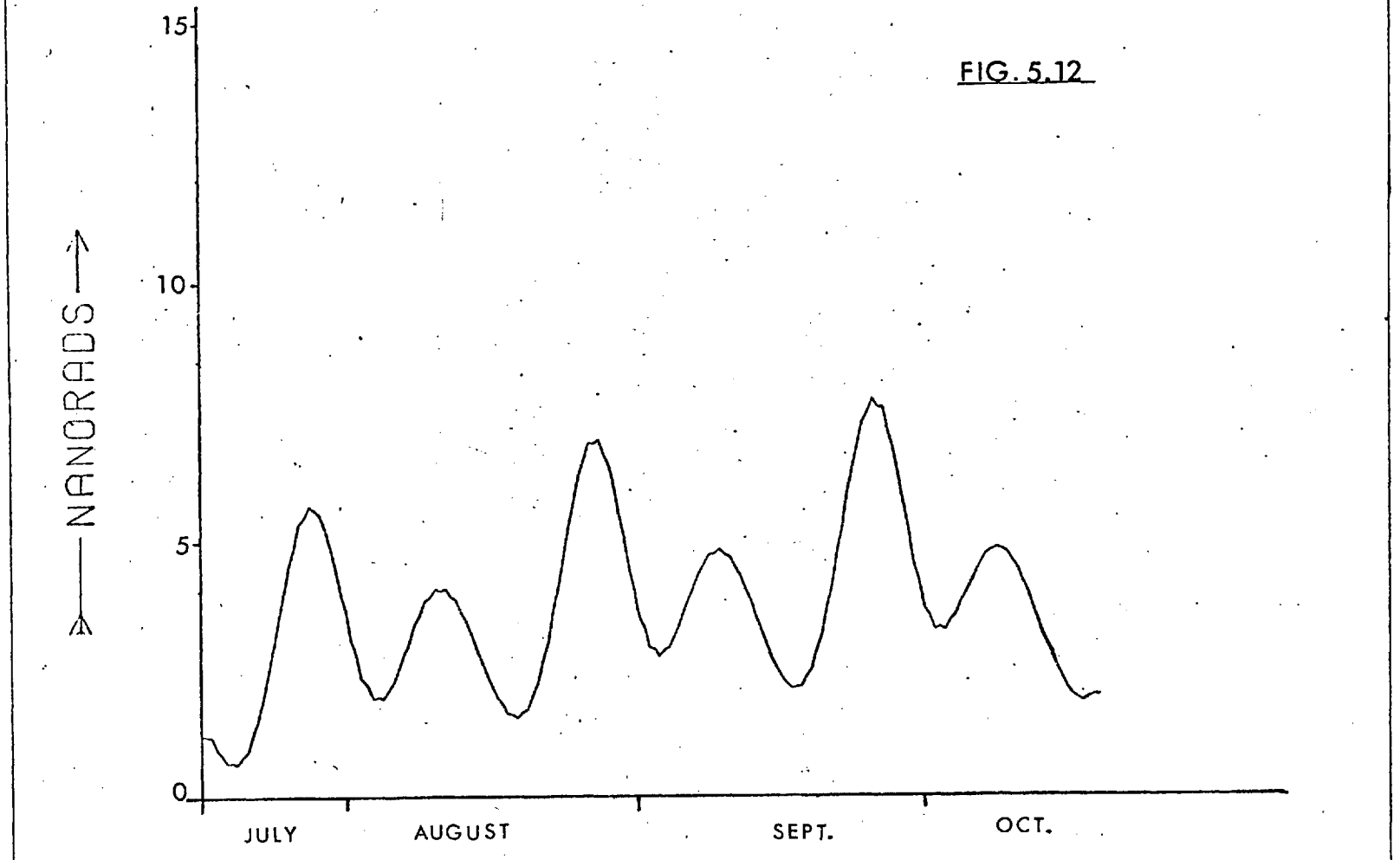
Figure 5.12 is a test curve using about three months predicted data. The fortnightly and monthly components are clearly visible, while the semi-annual and annual effects are manifested by the slight trend in the curve. It is important to note that the magnitude of the tilt has a range of about8nrads. This is considerably smaller than any of the long-period tilts observed, which are generally in the order of tens of μrads. There is, thus, very little likelihood of any tidal effects being observed.

Again, for convenience, the available data has been subdivided into five periods, being the same as used in the spectral analysis.

a) Winter '73-'74

Figure 5.13 a & b covers the period 1/12/73 to 19/2/74, which included the first eruptive period of the 1974 eruption. This data

FIG. 5.12



PREDICTED, LONG-PERIOD TIDAL TILT ETNA
21/7/76 – 14/10/76 (AZIMUTH 103·6)

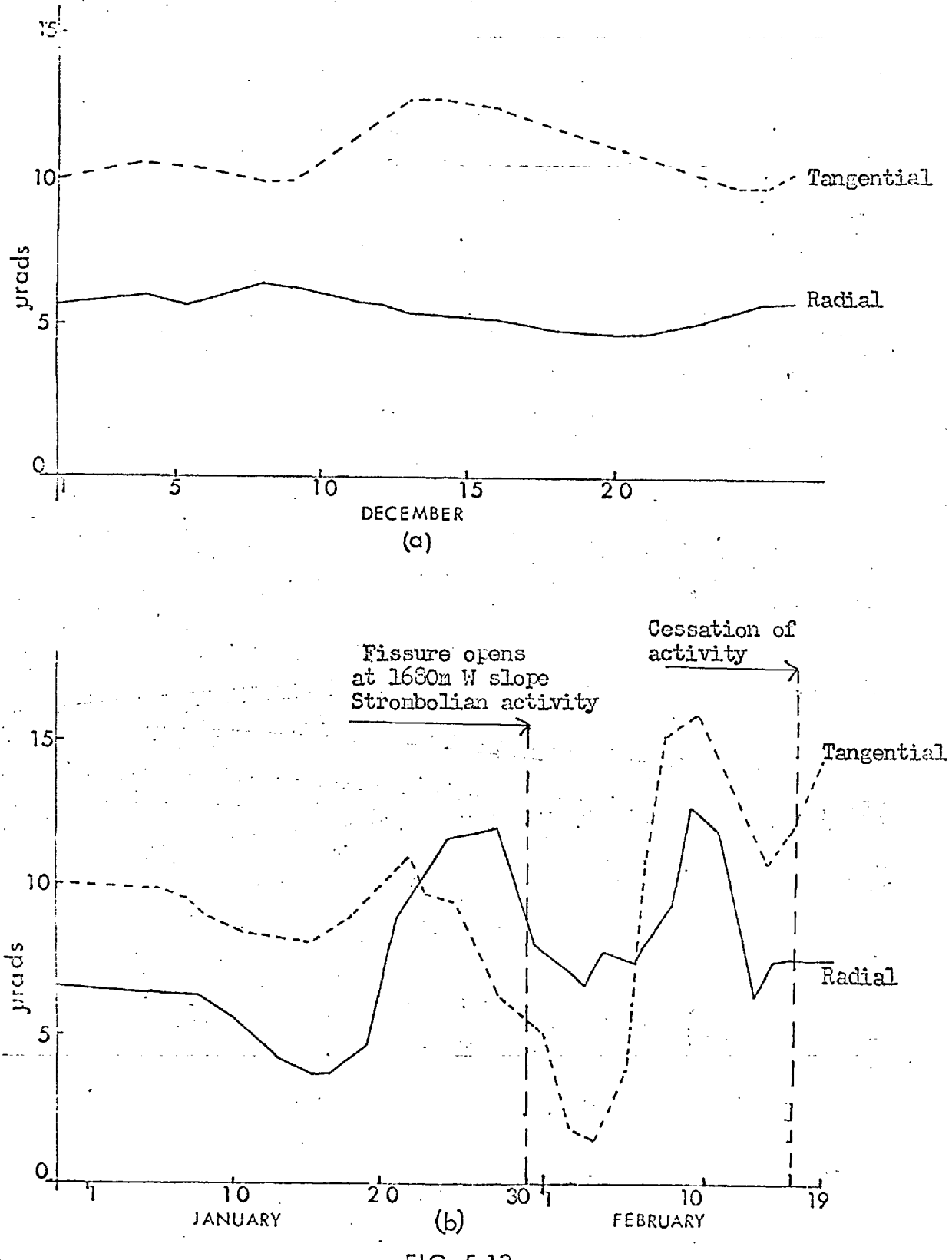


FIG. 5.13

Long-period tilts recorded at the borehole site for the periods (a) 1/12/73 - 29/12/73 , (b) 29/12/73 - 19/2/74

Major volcanological events are indicated.

has been analysed previously (Wadge et al., 1975) but without separation of the long and short period effects, or removal of the large amplitude (4 rads), short period (quasi-diurnal) effects, discussed earlier. Prior to the eruption (Fig. 5.13a), the changes in tilt are small, amounting to less than two μrads. Immediately before, and during the eruption, the magnitude of the tilts increase to about 10 μrads, although in the light of later data, these changes are not particularly large, although the rapidness and the subsequent equally rapid change (Jan. 21st for the tangential, and Jan. 27th for the radial axis) could indicate the movement of magma, the Radial axis indicating summit deflation followed by inflation. The ensuing period until 19th Feb. is marked by a gradual summit inflation of 8 μrads. between January 21st and January 30th. The tangential record indicates WSW inflation, i.e., dipping towards the Valle del Bove at the same time. This inflation ends with a sudden deflation of 4 μrads and a large tangential tilt change of 13 μrads. This tilt activity corresponds very closely with the observed eruptive activity which comprised the opening of a fissure at 1680 m. on the Western slopes. The tangential change at this time, indicating a deflation in the west, amply reflects this activity. A change in activity on February 9th from continuous to intermittent activity is also promptly recorded in the tilt record as is the cessation of activity (19th February). The clear correspondence between

volcanic activity and tilt activity for this eruption provides a strong justification for the use of tilt monitoring on Etna and the accuracy of recording magma movements. The changes in eruptive state are very quickly observed on the tilt record, a point which will be returned to when the rest of the records have been considered.

b) Winter '75-'76

As mentioned earlier, only the tangential axis of the borehole instrument was operating over this period (fig.5.14a & b).

It is a period of excessive tilt marked particularly by a western flank inflation of nearly 90 μrads. between 2nd November '75 and January 8th '76. This corresponds to a vertical change of 10 cm. over a distance of a kilometre in the tangential direction. Unfortunately, without the benefit of a corresponding radial axis it is impossible to pinpoint the location of this inflation or to say whether there was any summit inflation or deflation. As this record is over the middle of winter, reports of volcanic activity are sparse, though there is a change in activity on November 28th from the NE Crater to Punta Lucia, and this is mirrored by the small tilt change at 23rd November. The winter report merely states that there was renewed activity around the NE Crater but from the tilt observations alone it appears that there was definitely activity during the first and second weeks of January

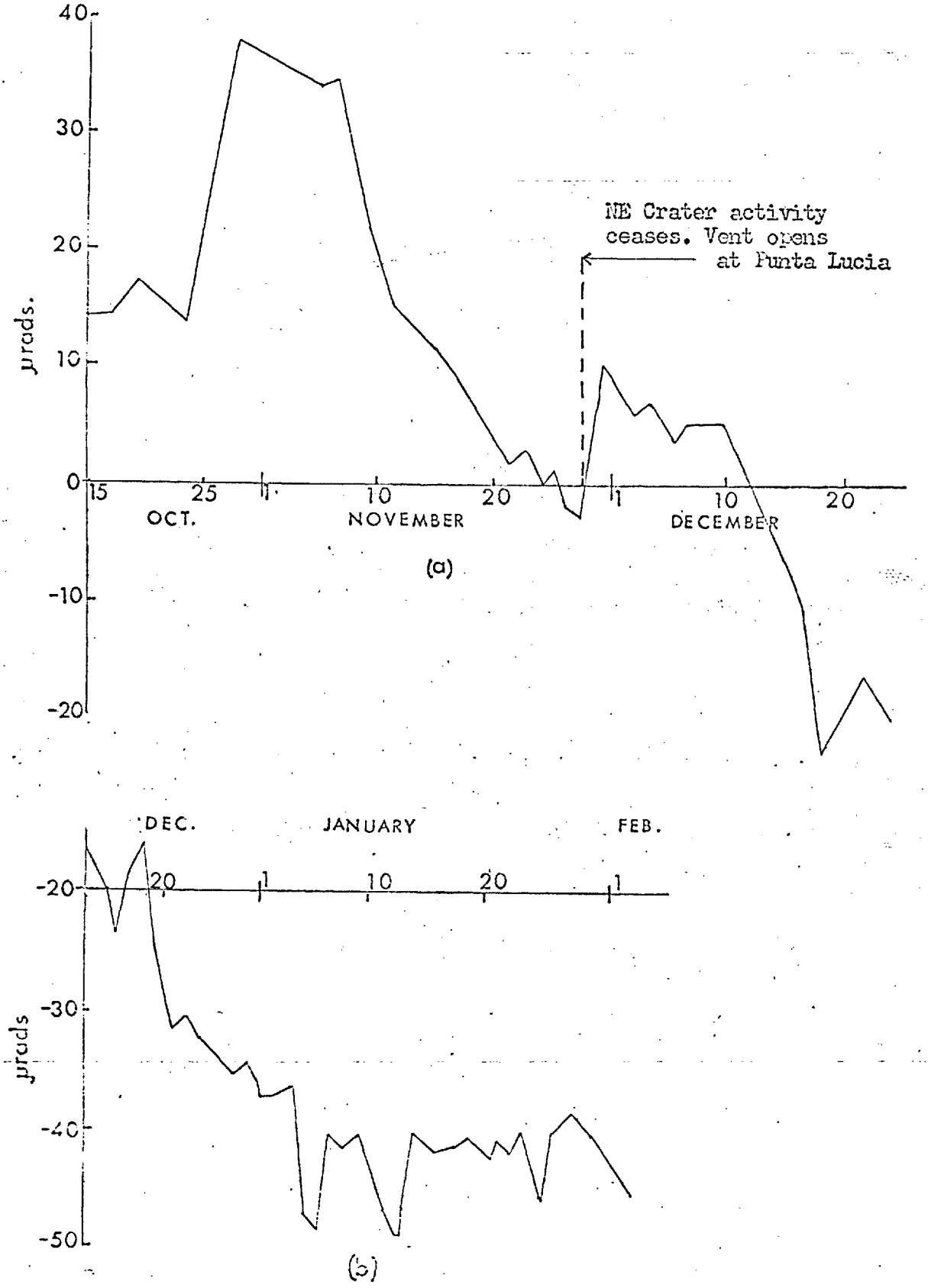


FIG. 5.14

Long-period tilts recorded by the tangential axis of the borehole tiltmeter for the periods:
(a) 15/10/75 - 21/12/75 , (b) 21/12/75 - 1/2/76

The major volcanological event during this period is marked

1976, though as to its nature or location little can be said.

c) Autumn '76

In contrast to the spectral data, the period from August '76 until February '77 was the most fruitful. As, for a period of ten days (28/9 - 7/10), not only was the Observatory Tiltmeter operating but also the Borehole tiltmeter, albeit the radial axis only. Because of excessive initial drift, the borehole tiltmeter was allowed to settle down for the first sixteen days following its installation on August 12th.

The first usable record covered the period from August 28th until 16 September Fig. 5. 15. The first tilt activity occurs around the 1st of September with a summit inflation amounting to 7μrads. continuing until September 5th. The activity north-west of the Due Pizzi begins on September 8th and the radial axis indicates this by a small summit inflation followed by a larger deflation continuing from the 12th until the 15th. of September. The tangential axis, however, records a continuing inflation in an easterly direction. As all the activity at this time occurs close to the radial axis it is difficult to distinguish between activity at the different centres since they would have no noticeable effect upon the tangential axis.

Figure 5.16 shows tilt activity for late September through October.

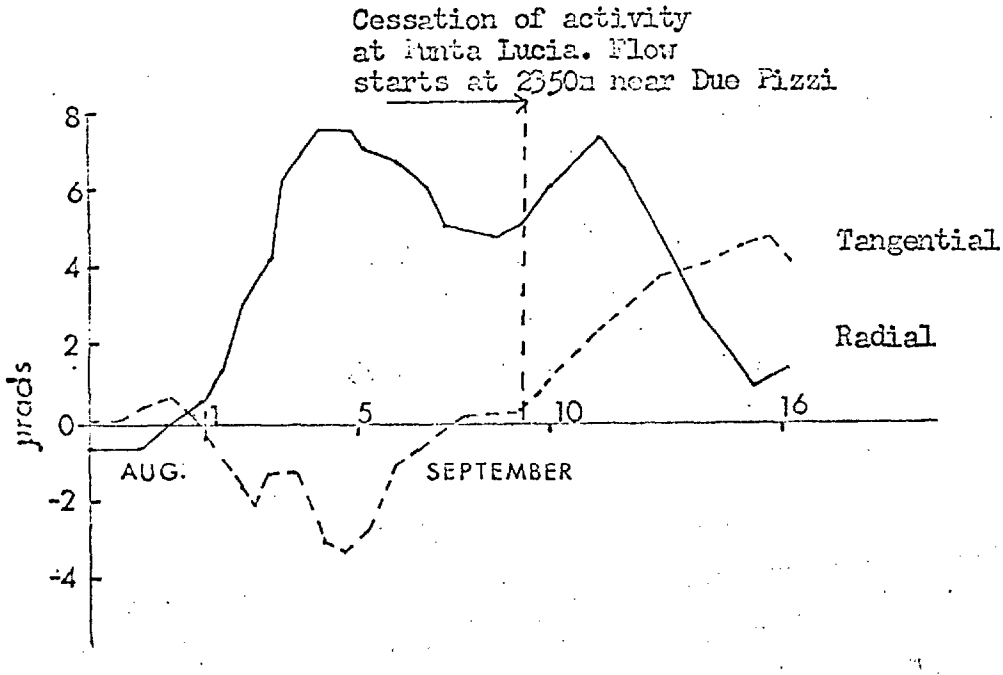


FIG. 5. 15

Tilts recorded at the observatory during the period 28/8/76 - 16/9/76

This is the only time, unfortunately, for which there is any simultaneous recording at both Observatory and Borehole sites and though it is only for a short time (10 days) it is quite interesting. On October 4 there is a rapid, large(33 μrads.) radial tilt at the borehole site, spread over two days, indicating a summit inflation. Although the summit inflation is also shown by the Observatory tiltmeter (fig5.16b)it is smaller (12 μrads) and not so rapid, starting two days earlier and spread over five days. One possible explanation of this is that as the borehole site had recently been visited and the tiltmeter electronics re-installed there was some short term electronically induced tilt acting in a contrary direction to that of the volcano.

The record from the Observatory indicates that the onset of a large radial tilt coincides with the onset of eruptive activity (September 29th) at the Due Pizzi. Confirmation of the tiltmeter recording is provided by the simultaneous measurements made by a team from Leicester University (Henbest et al. 1978) where both rates and magnitudes of tilt changes correspond very closely with those observed in this study (fig. 5.19). The fluctuations in summit inflation and deflation during the middle of October accompanied by a steady inflation towards the east most probably indicates cycles of activity from the different eruption centres, small accumulations of magma being

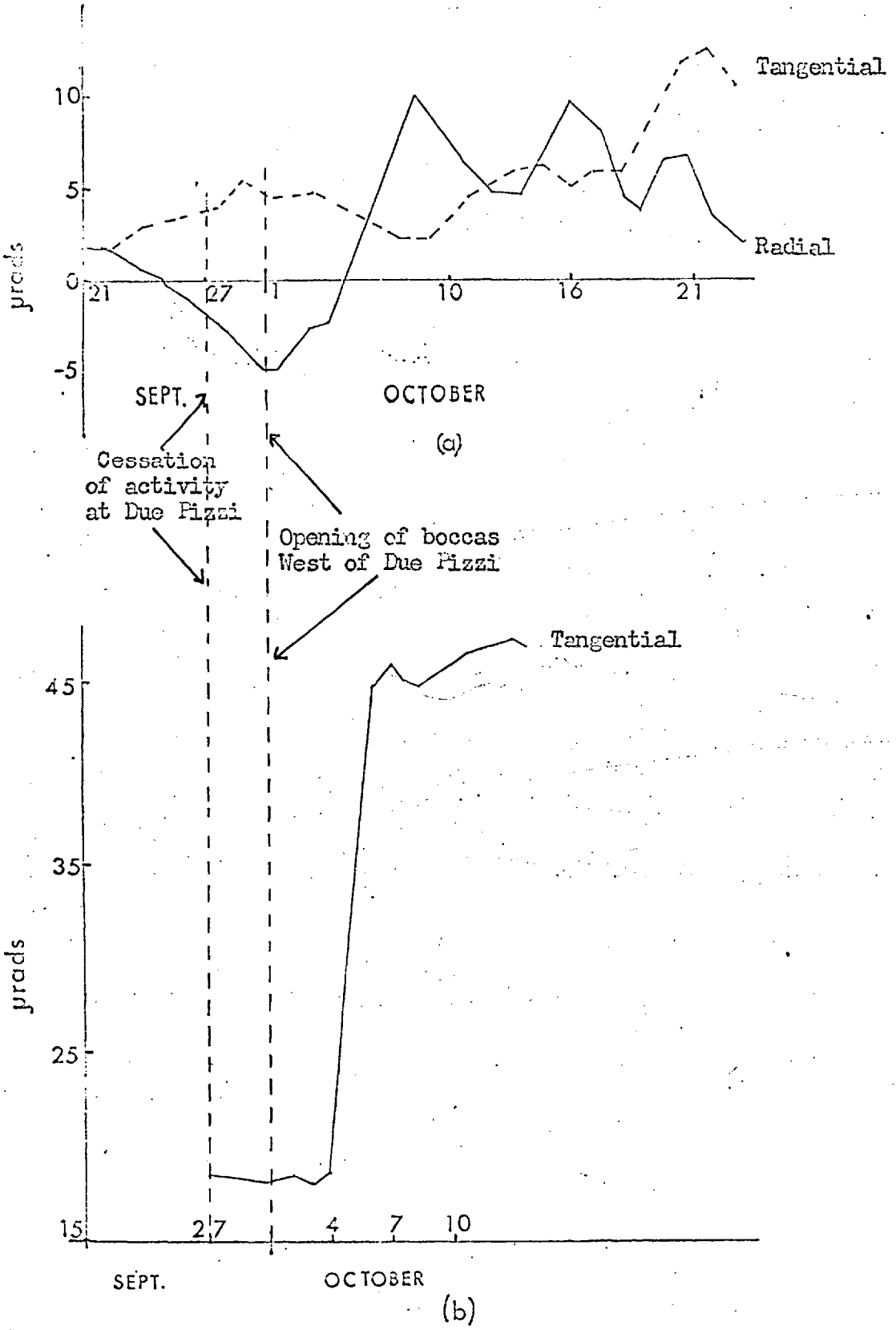


FIG. 5.16

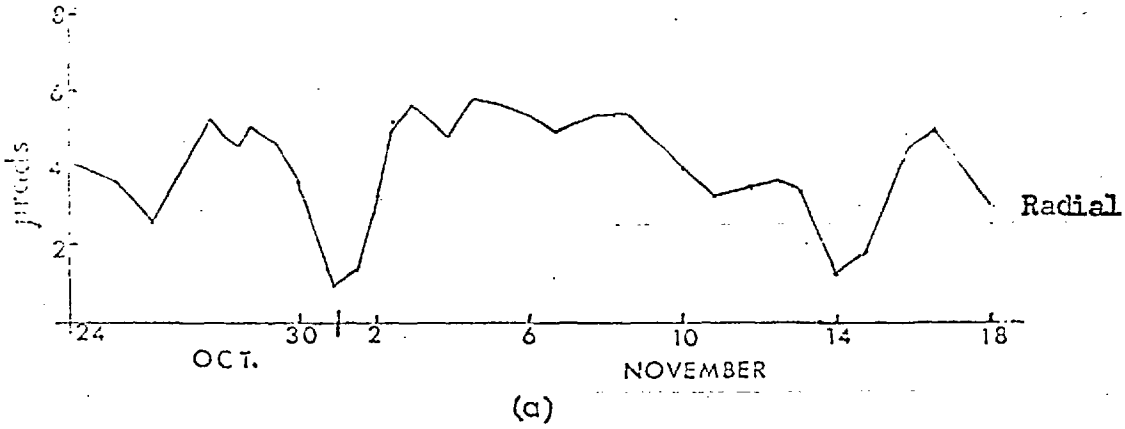
Tilts recorded at the observatory site (a) , and the borehole site (b) over the period 21/9/76 - 24/10/76

followed by effusions with the westward deflation being partially effected by lava loading. At this point issue must be taken with Henbest et al. (1978) who distinguish between the Punta Lucia and the Summit directions on the basis of the radial and tangential tilts. As was stated previously it is a practicable impossibility to do this since the accuracy of alignment is unlikely to be better than $\pm 1^{\circ}$ and the angle subtended at the Observatory by the Summit and Punta Lucia is only 7.5°.

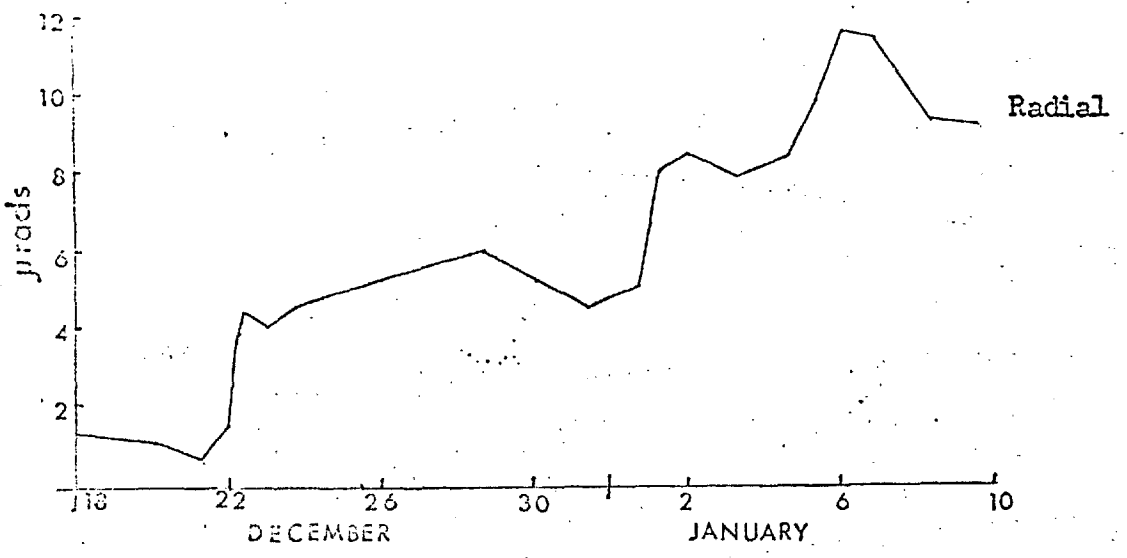
d) Winter '76-'77

The winter of '76-'77 was recorded, somewhat intermittently, by the radial axis from the Observatory (Fig. 5.17 a, b, & c). Again reports of volcanic activity over the winter are sparse and it appears from Fig. 5.17 that there was little near summit activity. Tilt changes are irregular and, at a maximum of 4 μrads, small compared with those recorded during periods of known activity. It is thus believed that the sort of activity shown in Fig. 5.17a is typical for the volcano during a semi-quiescent phase when the effects of the climate, particularly snow and the associated variable loading effects are taken into account.

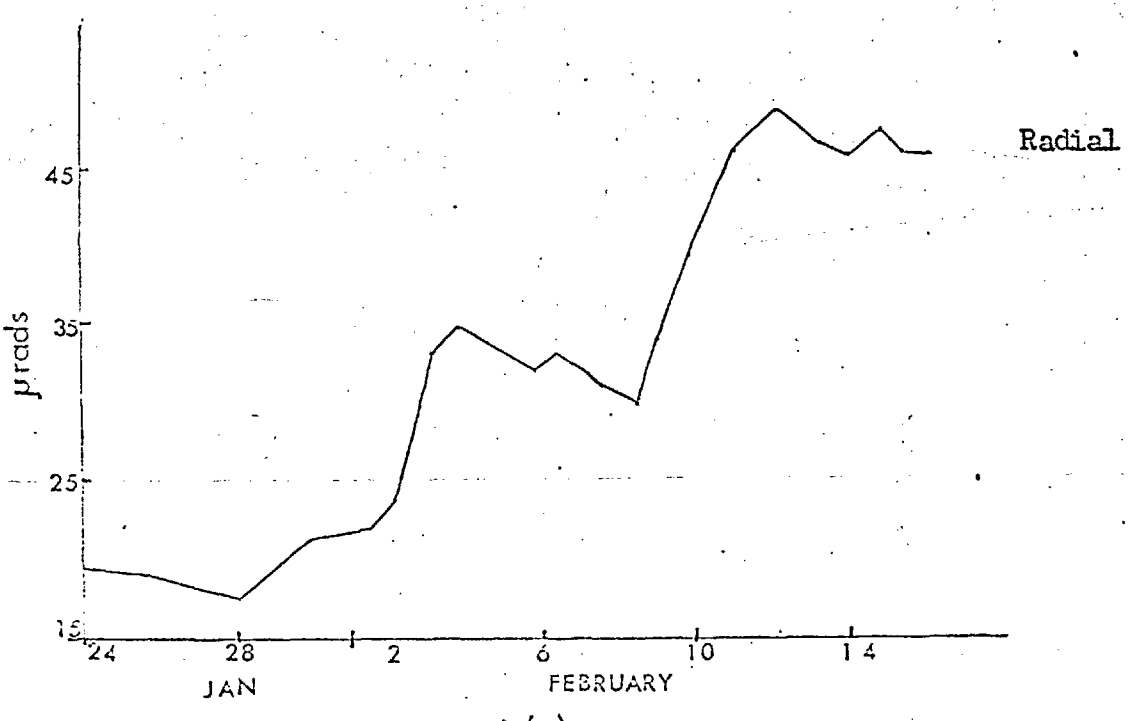
January and February of 1977 (Fig. 5.17b and 5.17 c) show a marked summit increase amounting to 45 μrads. There is no recorded



(a)



(b)



(c)

FIG. 5.17

Tilts recorded at the observatory over the periods: (a) 24/10/76 - 19/11/76 , (b) 18/12/76 - 10/1/77 , and (c) 24/1/77 - 16/2/77.

activity at this time and indeed the volcano appears to have been comparatively quiet with no effusive activity until November 1977. This inflation may then result from one or more of the following three causes:-

1) Long term meteorological effects - This is the least likely considering the magnitude of the changes, though localised snow falls and underground water movements could produce this sort of tilt. Its duration and consistency of rate militate against this solution.

2) Recovery from previous eruption - This effect really leads on to the third possible cause which is:-

3) Inflation leading to Further Eruptions - as the two are in many respects similar depending upon whether the status quo is eruptive activity or not. However, the next eruption was some ten months away and the short recording taken during May (fig . 5.18) shows only a very slight degree of inflation ($< 1 \mu$rad) and it cannot reasonably be regarded as such. The January - February inflation may be best regarded, then, as a recovery from the previous years eruptions and could indicate magma storage of some sort at high elevations.

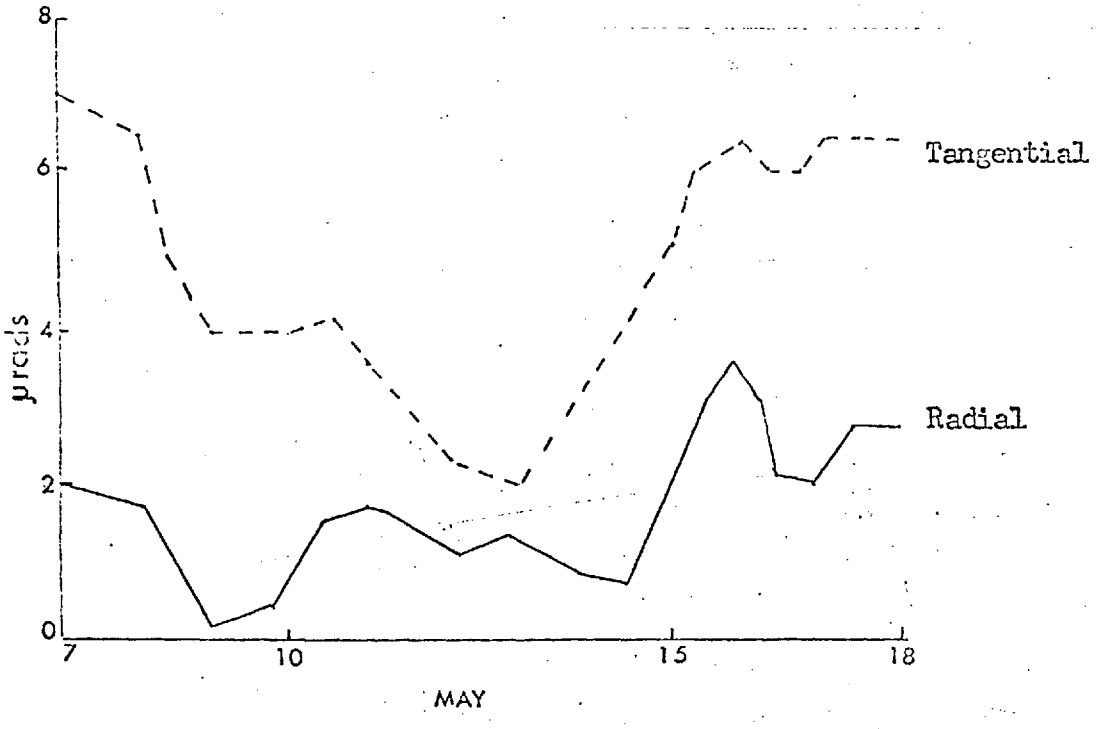


FIG. 5.18

Tilts recorded at the observatory over the period

7/5/77 - 18/5/77

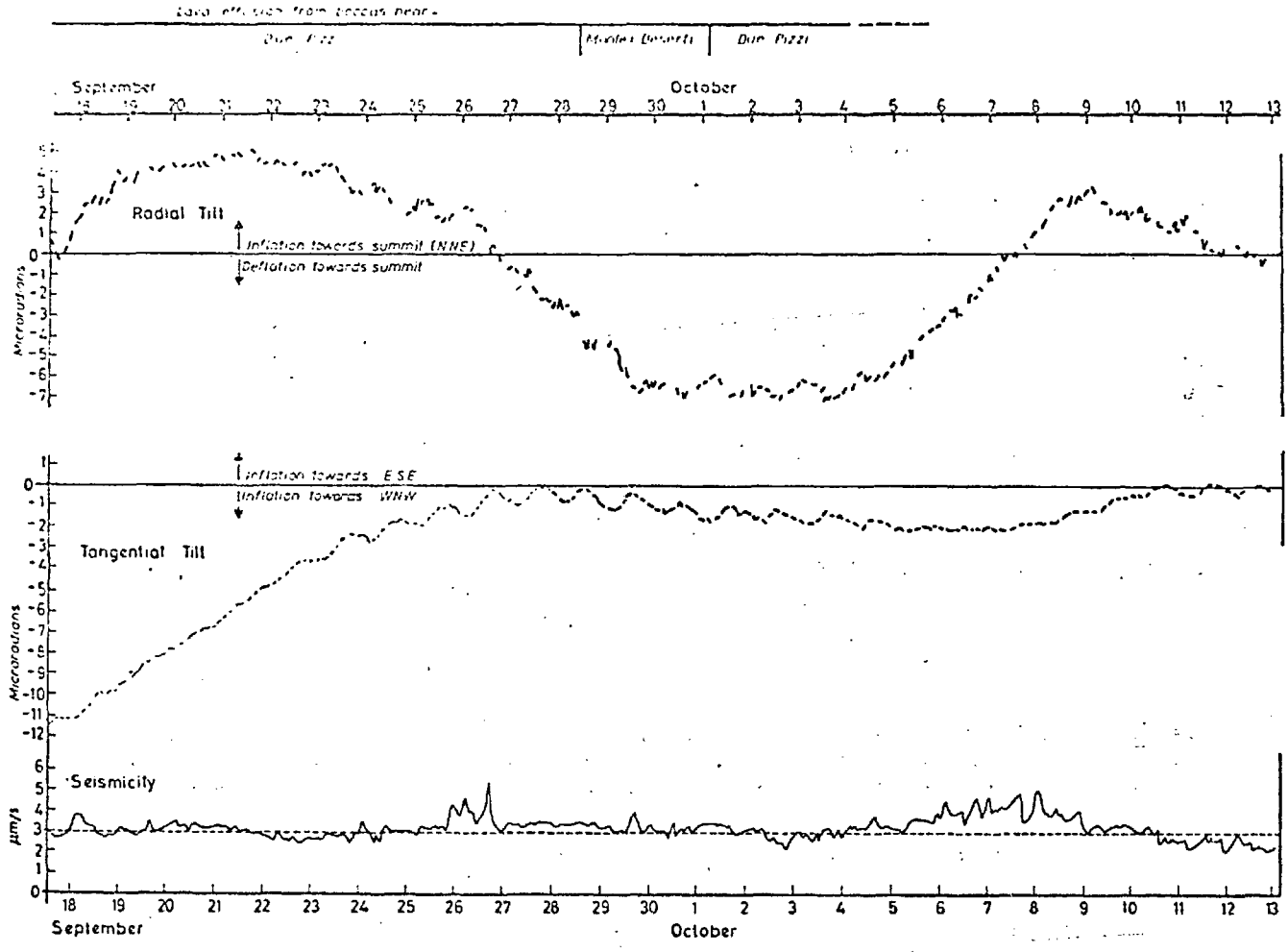


FIG. 5.19

Tilt and seismicity records for the period 18 September to 13 October 1976 (from Henbest et al., 1978)

Long-Term Tilt Activity - Conclusions.

There is no doubt that a clear correlation can be obtained between eruptive activity and tilt deformation. The value of this correlation as a tool for prediction is uncertain. There are two major problems; firstly there is no evidence of any pattern of tilt prior to an eruption. This is perhaps not surprising, considering the complexity of Etna and the variability of its eruptions. It is highly likely, though, that each eruption has distinctive tilt precursors or 'fingerprint', by which it can be recognized, and that eruptions from a particular centre would have similar 'fingerprints'. A knowledge of these 'fingerprints' would then enable an observer to predict the region of activity. At present, however, far too little information has been gained and too few eruptions monitored to attempt a prediction on this basis. For greater accuracy three tiltmeters would be required, as are three seismometers in detecting an earthquake location. The second problem is the lack of a consistent time delay between the observation of an anomolous tilt and the occurrence of an eruption. Long term inflation and deflation is seen but it is often easier to notice such changes in retrospect than when they are occurring. An associated difficulty is that these inflations or deflations can often be of the same order or smaller than the diurnal noise (i.e. $< 10\mu$rad) and it is only on the day of the eruptions or one or two days prior

to it that noticeably large tilts occur. Predicting eruptions more than one or two days in advance, on the basis of tilt observations, may become a job for a skilled interpreter with a thorough knowledge of the tilt precursors to previous eruptions. Fortunately, from the viewpoint of saving life, precise eruption prediction is not required. Whilst there is always the possibility of a vent opening near to a village or any of the other inhabited areas of the volcano this has, happily, never yet happened. There is, of course, always the potential danger to tourists, who annually deluge the volcano, when sightseeing near the summit; although the volcano guides are careful to prevent tourists endangering their own lives, small boccas may open suddenly as with the Bocca Nuova in 1955.

The greatest danger to life comes not from any sudden cataclysm but from the more insidious effects of the lava destroying sheep grazing land, vineyards and orchards. It was this overwhelming damage to the land and the ensuing starvation that was the main cause of death in the 1669 eruption.

The main use of the tilt data is then to provide greater information on the actual movements of magma within the volcano and to contribute to prediction via a knowledge of the internal structure of Etna. A major oversight with all theoretical models of volcano deformations is that they are not concerned with the problem of lava

loading. That this is a problem with Etna is illustrated in the paper by Murray et al. 1977 who reported a subsidence of one metre over a two km. area on the northern slopes, an effect which was eventually considered to be due to surface movements of lava (IAVCEI, Durham 1977). The rapid tilts immediately prior to effusive activity indicate that this is not a simple case of a magma chamber or column inflating or deflating but is more likely due to the thrust exerted upon the ground by the lava or other effusive material: From the data available it is impossible to test in detail any of the magma chamber theories conclusively and considerably more data will have to be collected before such an assessment is possible.

CHAPTER 6

PREDICTION OF ERUPTIONS

6.1 INTRODUCTION

In the previous chapter the monitoring of crustal deformation in real time was discussed and the possibility of utilising such information for short range prediction of eruptions. A second approach, to eruption prediction can be made by considering the eruptive history of the volcano to detect such phenomena as related periods between eruptions or the correlation of eruptions with possible triggering phenomena. Etna is particularly amenable to this sort of analysis because of its regular and high eruption rate and because its location has enabled it to be observed and recorded for far longer than most volcanoes.

Before proceeding to discussion of Etna's eruptions its eruptive mechanisms will be described, in so far as they are, at present, understood.

6.2. ERUPTIVE MECHANISMS OF MOUNT ETNA

Rittmann in 1963 published the, now generally accepted, theory of eruption types for Etna. He defines three types of eruption in addition to 'terminal' eruptions which are lava overflows of the central crater; these are, subterminal, lateral and eccentric.

a) SUBTERMINAL ERUPTIONS

Subterminal eruptions differ from terminal eruptions in that the magma, having been largely degassed in the main vent, flows into the main body of the volcano before emerging a short distance down the flanks in the form of a bocca.

b) LATERAL ERUPTIONS

Lateral eruptions originate by fracturing of the central magma conduit due to hydrostatic pressure. The fracture travels radially away from the summit and small pyroclastic cones are formed where the fracture breaches the surface, lava flowing from the lower extremity of this cone or cones. The resultant disturbance in the central conduit usually causes a violent ash eruption at the summit.

c) ECCENTRIC ERUPTIONS

The third type of eruption, eccentric eruptions, give rise to no

central activity at all and the eruption is completely independent of the central conduit system. These eruptions generally occur on the lower slopes of the volcano and are dictated by the local fault structure with no accompanying radial fracturing. Very often eccentric eruptions are manifested by violent explosive activity rapidly building up cones and producing a gas-rich lava. Rittmann regards them as independent minor volcanoes and for this reason it is quite possible that their eruptive behaviour is governed by influences unconnected with those governing subterminal and lateral eruptions. The three types of eruption are illustrated in Fig. 6.1.

This classification whilst possessing the undoubted virtue of simplicity has been found wanting in recent years particularly in its inability to adequately describe the notoriously complex eruption of 1971. Rittmann et al. (1971) attempting to describe this eruption evolved a scheme almost equally notable for its complexity. Many authors especially Carapezza (1962) stress the importance of the regional tectonic factors and these are undoubtedly influential. It is probably safe to say that Rittmann's classification provides an adequate but simple description of Etnean eruptions.

Wadge (1974) examined historical eruptions on Etna, principally from a tectonic viewpoint. He showed that rather than being randomly

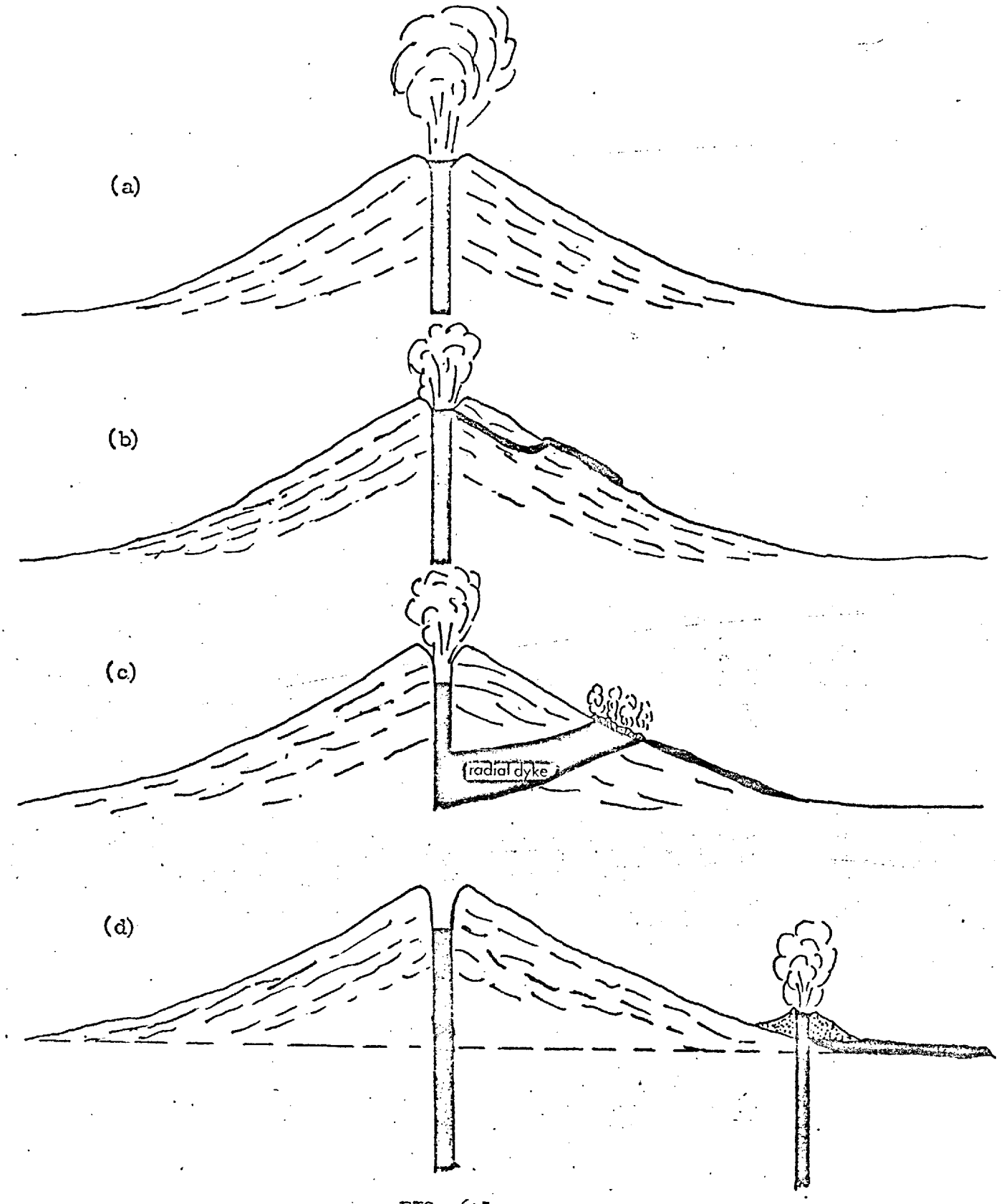


FIG. 6.1

Diagrammatic representation of Rittmann's types of Etnean eruption

(a) Terminal, (b) Sub-terminal, (c) Lateral, (d) Eccentric

distributed over the volcano, flank eruptions are more likely to occur round the 1800m. level and the azimuthal orientations of fissure eruptions fit into three main directions, though he does not assess the statistical significance of these results. It would appear to indicate, however, certain specific fault trends within the volcano rather than random fracturing. Wadge's conclusions about a magma reservoir essentially indicates a central, vertical, cylindrical body acting as the main magma reservoir coupled with a 'plexus' reservoir extending into the sedimentary basement about 2,000 metres below the summit. The interactions between the two reservoirs are complicated and not fully understood. Fig. 6.2 illustrates this theory of magma storage, and it will be reassessed later with reference to the results of Chapter 5 and in the light of the statistical investigations of this Chapter.

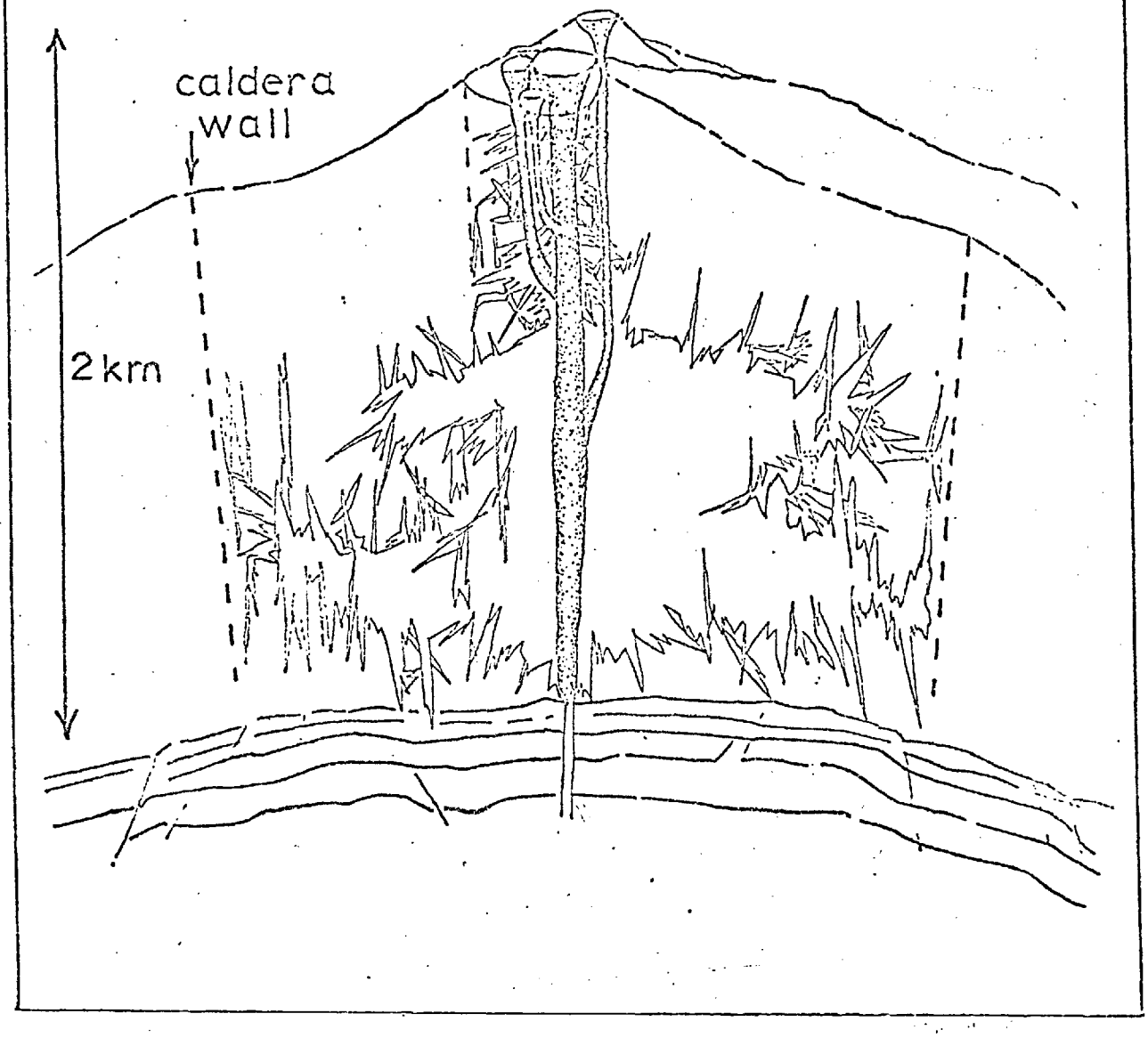


FIG. 6.2

Possible arrangement of magma conduits and plexus beneath Etna (after Wadge, 1974)

6.3. REPOSE PERIOD STATISTICS FOR ETNA

a) Theoretical Considerations

The first method of examining the eruptive history of Etna is concerned with repose periods, that is, the lengths of time separating eruptions, and is due to Wickman (1965 a, b, c, d, e). The fundamental assumption is that eruptions may be regarded as random events in time and the sequence of eruptions is a stochastic process. The theory is similar to that of renewal theory (Cox, 1962) and to comply with this certain secondary assumptions must be made. These are:-

1) Eruptions and repose periods are well defined in time. Whilst it is generally straightforward enough to determine the onset of an eruption it is often difficult to be sure when an eruption has ended. This is particularly so far Etna where an eruption at one part of the volcano may be followed by another elsewhere. This leads to inaccuracies when considering short reposes but there are enough eruptions available to counteract this problem. A related problem is that of persistent activity from the Central Crater - this is included under the repose period and it is probable that historical reports of eruptions lasting tens of years are, in fact, a series of separate eruptions with persistent activity in between.

2) The eruption time is a non-negative random variable, continuously distributed over the range $(0, \infty)$, its distribution being determined by a probability density function (p.d.f) $f(x) = 0$ for negative x. This assumption is enticed for the particular mathematical approach.

The following assumptions are based on the premise that a volcano can occur in different states and the probability of a given kind of eruption varies from state to state. In view of what has been said about Etna's eruptions this would seem a very reasonable premise.

3) During a repose period the activity of a volcano can be described by one of n states, E_1, E_2...En, each state 'i' occurring with a probability $\Pi_i(x)$ and $\sum_{i=1}^{n} \Pi_i(x) = 1$

4) During a particular state only a limited number of kinds of eruption, k, occur; and

5) The eruption - times belonging to each type of eruption within a state have the same p.d.f. , finally,

6) The different states are mutually independent.

Two specific functions are now defined:

a) The survivor function $F(x)$ defined as the probability that a repose period has not ended up to time x. That is

$$F(x) = \text{prob. } (X > x)$$

$$= \int_x^\infty f(u)\,du$$

and $F(0) = 1$ and $F(\infty) = 0$

where $f(x)$ is the probability density function of a random variable X (in this example, time) and

$$f(x) = \lim_{\Delta x \to 0} \frac{\text{prob } (x < X \leq x + \Delta x)}{\Delta x}$$

with $$\int_0^\infty f(x)\,dx = 1$$

thus $$f(x) = -F'(x)$$

b) The Age-Specific Eruption Rate, $\varphi(x)$. This is defined as follows:-

Consider a repose period known not to have ended at time x then

$$f(x) = \lim_{\Delta x \to 0} \frac{\text{prob } (x < X \leq x + \Delta x \mid x < X)}{\Delta x}$$

thus $\varphi(x)$ gives the probability of an immediate eruption for the volcano at a time x. Now for any two events A and B. the conditional probability is given by

$$\text{prob. } (A/B) = \frac{\text{prob } (A \text{ and } B)}{\text{prob } B}$$

but the event "$x<X\leqslant x+\Delta x$" and "$x<X$" is the same as the event

"$x<X\leqslant x+\Delta x$" Thus

$$\varphi(x) = \lim_{\Delta x\to 0} \frac{\text{prob.}(x<X\leqslant x+\Delta x)}{\Delta x} \cdot \frac{1}{\text{prob}(X>x)}$$

$$= \frac{f(x)}{F(x)}$$

Then since $f(x) = -F'(x)$

$$\varphi(x) = -\frac{F'(x)}{F(x)} = -\frac{d}{dx}(\ln F(x))$$

In analysing data using this approach, two graphs are plotted. The first is a plot of the loganthm of the survivor number, N, against time. N is defined as:-

$$N = No\ F(t)$$

Where No is the total number of repose periods. Thus N is the number of reposes that have not ended at a given time, t.

The second graph is a plot of the eruption rate, φ, against time where:-

$$\varphi(t) = \frac{-d}{dt}(\ln N(t))$$

Thus φ is given by the gradient of the first graph (N/t), and

gives the probability of an eruption at a time, t.

To illustrate the theory two graphs were constructed using artificial data (figure 6.3). Ten thousand random numbers, between 0 and 100, were generated and the occurrence of a particular digit (e.g. 9) was assumed to denote an eruption. The number of random numbers separating any two occurrences of the digit is then regarded as being the repose period in months.

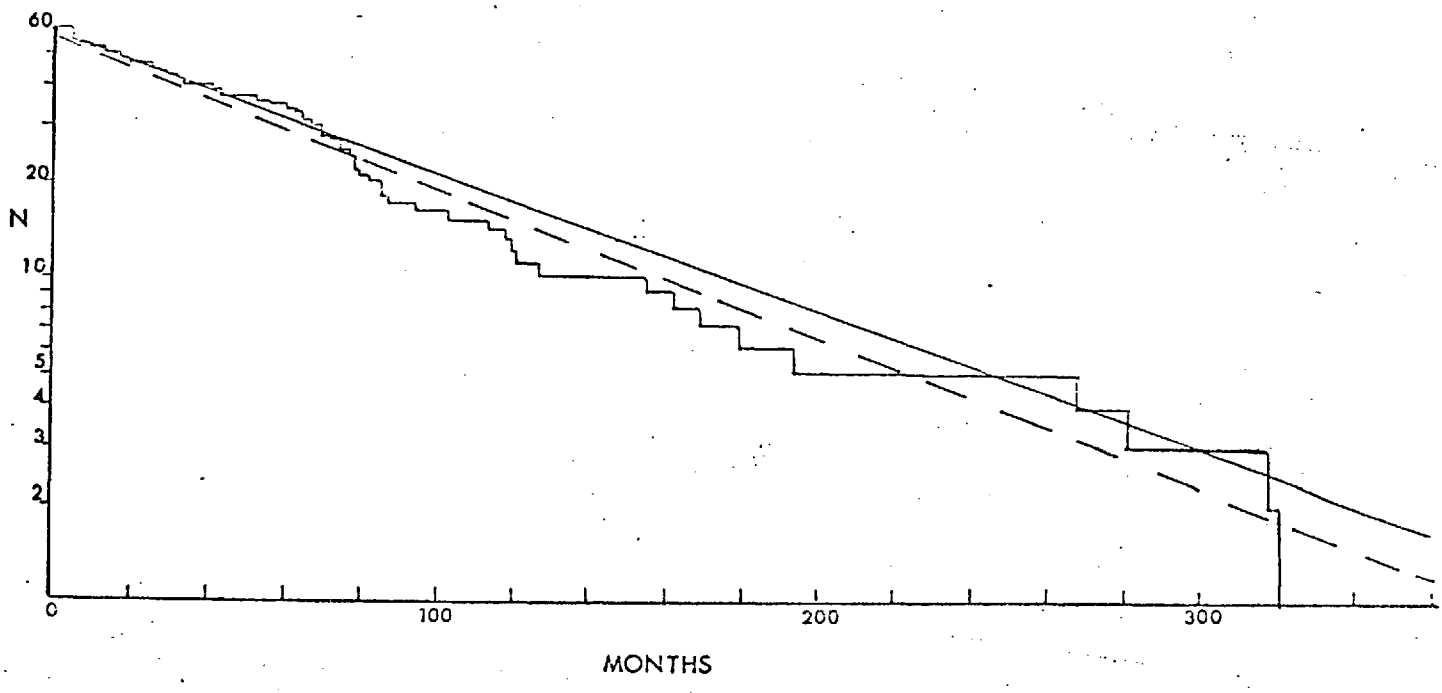
Since the numbers were generated with a uniform distribution, the probability of occurrence of a particular number is 1%, that is, $\varphi = 10^{-2}$ months $^{-1}$. Figure 6.3a shows a distribution with sixty random reposes, and 6.3b a distribution for one hundred random reposes. On both graphs two straight lines have been constructed, the solid line representing a value of $\varphi = .01$, that is, the value predicted by theory, and the dashed line is the least - squares fitted line:

These results and also for N = 50 (not graphed) are given in Table 6.1.

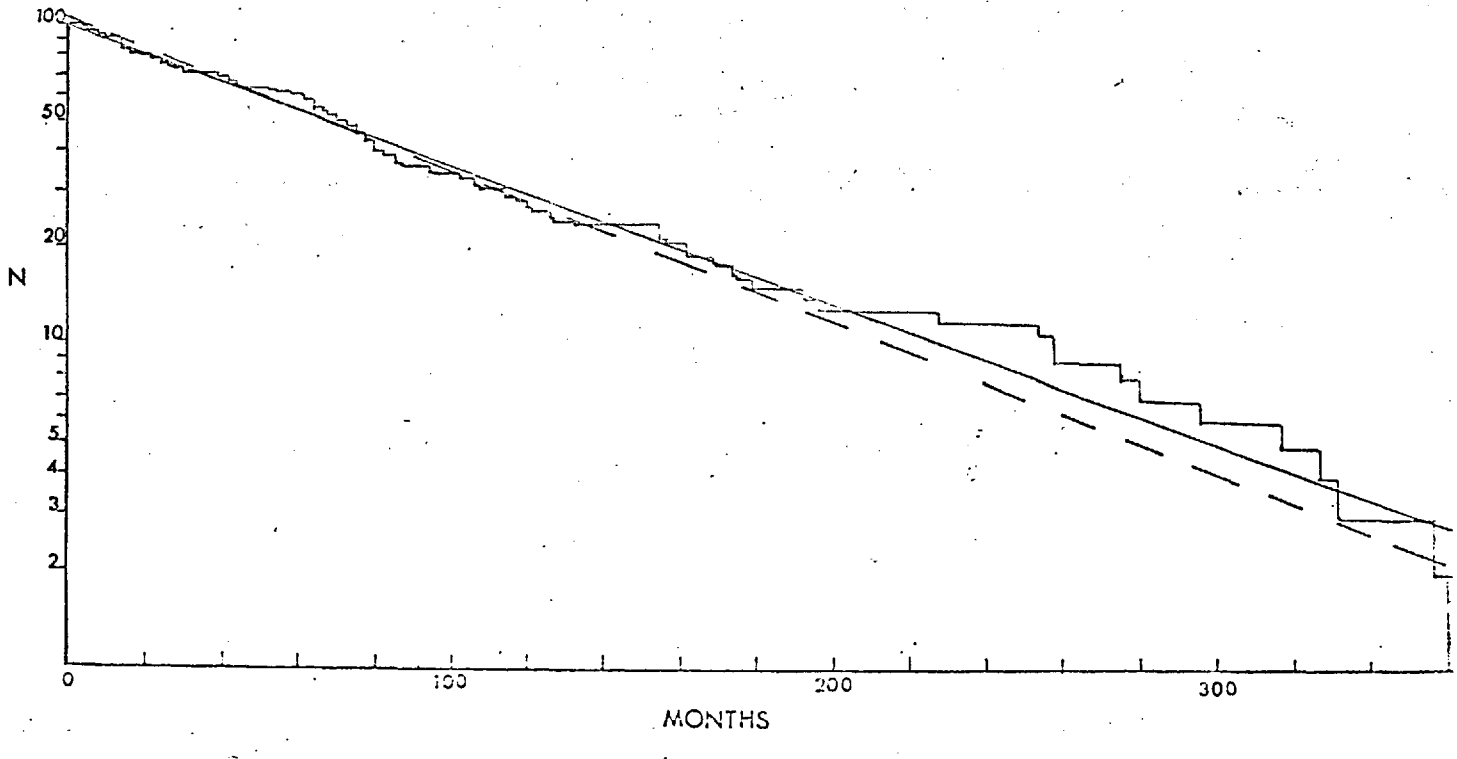
N	φ	Correlation r%
100	$.0108 \pm .0013$	99%
60	$.0108 \pm .0016$	97.5%
50	$.01061 \pm .0017$	98%

Table 6.1

Random Number Repose Statistics



(a)



(b)

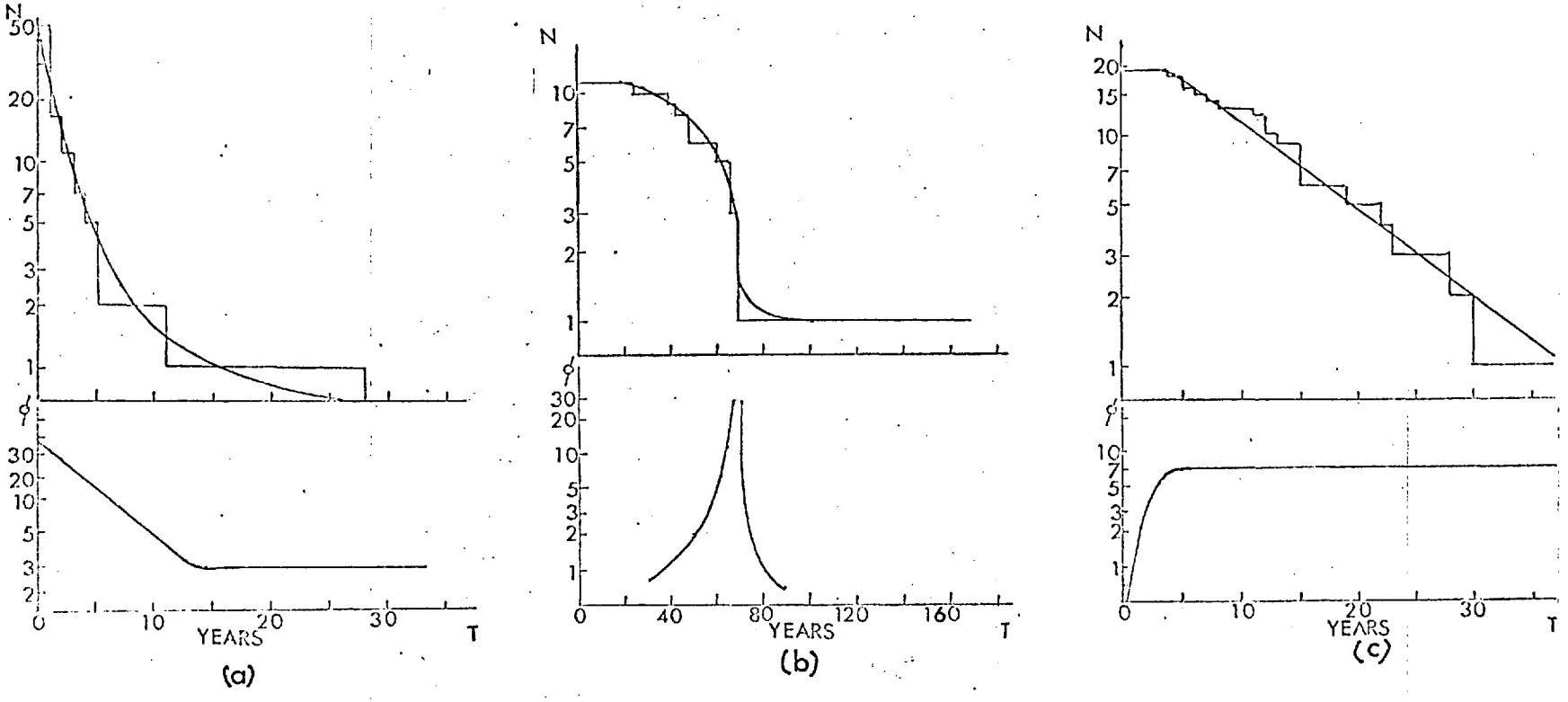
FIG. 6.3
Random number tests, Wickman's analysis.
N is the survivor function as defined in the text

Both graphs thus give values of φ very close to the theoretical value. They ~~are~~ approximate much more to $\varphi = .01$ for shorter repose periods. Fig. 6.3a shows large deviations from the theoretical line for longer repose periods especially those in excess of 80 months. The respective eruption-rate graphs have ~~ben~~ not been drawn since the gradient of the N/t graph is a constant, and so the φ/t graph would simply be a horizontal line at the particular value of the gradient.

b) Repose Period Statistics for Selected Volcanoes

Wickman (1965 a, b, c and d) evalu~~e~~ated at φ for a number of different world wide volcanoes. Three of the volcanoes considered have been selected here to show some of the different forms the eruption rate can take. Fig. 6.4 shows the survivor function and eruption rate graphs for Semeru, Miyake-Zima and Vesuvius volcanoes.

Semeru is a large strato-volcano on an island off the coast of Java. There have been 51 recorded eruptions between 1818 and 1947, the period used by Wickman (1965, b). The volcano is reported (Junguhn, 1854) to be in a state of persistent activity and as with Etnean summit eruptions it is difficult to distinguish between persistent activity and new eruptions. The initial high eruption rate arises because there has been no attempt to correct for persistent activity.



SEMERU MIYAKE-ZIMA VESUVIUS

Fig. 6.4

Repose Periods and eruption rates for Selected Volcanoes

For Miyake-Zima, a strato-volcano in the Izu Marianas Arc, a completely different state of affairs exists. There have been only eleven eruptions recorded over nine hundred years (1085-1940) and inevitably this reduces the level of confidence that can be placed in the result. Nonetheless the time dependence of φ is obvious. The implication of this graph is that the probability of occurrence of an eruption depends upon the time lapsed from the previous eruption. It is a reasonable assumption in the light of this result to say that Miyake-Zima possesses a magma chamber which is substantially emptied for each eruption.

The eruption rate for Vesuvius is different from both Miyake-Zima and Semeru. The aspect of most interest from the Etnean viewpoint is that it exhibits the phenomenon of a 'loading time', in the initial portion of the curve. Usually this loading is indicative of a magma chamber, as it arises because the volcano has a minimum repose period, the loading time, which is directly related to the time taken for the chamber to fill to an eruptive level. Unlike Miyake-Zima, however, Vesuvius does not erupt when a physically predetermined level is reached nor do its eruptions follow on after each other at regular intervals. What is probably indicated here is that a minimum quantity of magma is required to initiate an eruption and that a volume of lava and associated eruptive products in excess of this is expelled during an eruption but that the occurrence of this eruption is triggered by causes other than

merely the quantity of magma available. After the initial loading period, ρ is independent of time and the probability of an eruption is independent of the time lapsed from the previous eruption; this is an example of a Markov process.

In a later paper Wickman (1976) proposes different Markov models to explain the various types of eruption rate characteristics.

c) Previous Repose Period Statistics for Etna

Wickman's analysis of Etna, (1965c) is not as thorough as some of his other work and serves to illustrate the problems encountered when handling Etna data. He did not have access to Imbo's I.V.A. Catalogue (1965) and instead relied upon the list prepared by von Waltershausen (1880). In itself this limited the number of available eruptions (45 as against 83) but also there was no distinction made between flank and summit eruptions, a point stressed by Wadge (1976). When a comparison was made between Imbo/Wadge eruption times and the Wickman/von Waltershausen times a number of discrepancies were found. Another point raised by Wickman arises over reports of long eruptions, for instance 1614 - 24, 1669 - 82. It is considered that these long eruptions may, in fact, consist of a number of short eruptions, separated by short reposes, thus reducing the number of observed short reposes. This assumption appears to be justified in view of the fact that these lengthy eruptions are not recorded in more recent times.

The same consideration, however, does not apply to summit eruptions where numerous lengthy eruptions have been observed in the twentieth century, e.g. 1901-06, 1913-17, 1919-23 and 1935-40.

d) Results for Etna

The eruptions used in the following analyses are listed in Table 6.2. 1600 was selected as the starting date, since the records of eruptions, prior to this date, are very meagre (Imbo, 1965), in many instances no more than the year of the eruption being given. This is still a problem after 1600 and, rather than ignore an eruption completely, the time has been approximated to the middle of the year in which the eruption either began or ended, whichever the case may be.

It will also be noticed that on some occasions flank and summit eruptions occur simultaneously and this explains why the total number of reposes, 83, is not the same as the sum of the flank (50) and summit (47) reposes.

From the information given in Table 6.2 the following repose period data sets were computed.

1) Between separate flank eruptions, 2) between summit eruptions 3) between any two consecutive eruptions irrespective of whether they are flank or summit eruptions. Fig. 6.5 shows graphs of the survivor functions for these cases. As with the random number data

ERUPTIONS OF ETNA 1600 - 1974

FLANK		SUMMIT	
1603	15/7/ - ?		
1607	28/6/ - ?		
1609	/7/ - ?		
1610	6/2/ - ?		
1616 - 24	/7/ - ?		
		1633	21/2/ - ?
1634 - 38	19/12/ - 27/4/		
1646 - 47	20/11/ - 15/1/		
1651 - 53	16/1/ - 15/6/		
1669	11/3/ - 15/7/		
		1669 - 82	?
1682	1/9/ - ?		
		1688	?
1689	14/3/ - ?		
		1693	?
1702	8/3/ - 13/3/		
		1723 - 24	22/11/ - /4/
		1732 - 33	9/12/ - 30/1/
		1735 - 36	4/10/ - 15/7/
		1736	25/7/ - /9/
		1744 - 45	/7/ - /9/
1747 - 49	/9/ - /3/		
		1752 - 54	?
1755	9/3/ - 15/3/		
		1755 - 58	?
		1758 - 59	/11/ - /2/

TABLE 6.2

ERUPTIONS OF ETNA 1600 - 1974

PLAIN		SUMMIT	
		1759	14/4/ - 15/4/
1759	19/4/ - 1/8/		
		1759 - 63	?
1763	5/2/ - 10/3/		
1763	20/6/ - 10/9/		
1764 - 65	?		
1766	27/4/ - 6/11/		
1780	20/4/ - 1/6/		
		1781	/5/ - 10/5/
		1787	10/7/ - 22/7/
1792	11/5/ - 12/5/	1792	/5/ - ?
1792 -93	1/6/ - 29/3/		
		1798 - 99	?
		1802	?
1802	15/11/ - 18/11/		
		1805 - 07	/7/ - ?
		1805	11/7/ - 3/8/
		1805 - 09	3/8/ - 27/5/
1809	27/3/ - 9/4/		
1811 - 12	27/10/ - 24/4/		
1819	27/5/ - 1/8/		
		1831	4/3/ - 3/4/
1832	1/11/ - 22/11/		
		1838 - 39	2/8/ - /2/
		1842	27/11/ - 29/12/
1843	17/11/ - 23/11		

TABLE 6.2 (cont.)

ERUPTIONS OF ETNA: 1669 - 1974

FLANK		SUMMIT	
1852 - 53	20/8/ - 27/5/		
		1863	7/7/ - 25/7/
		1864	/8/ - 8/9/
1865	30/5/ - 30/6/		
		1868	/11/ - /12/
1869	26/9/ - ?		
1874	29/8/ - 31/8/	1874	/5/ - 29/8/
1879	26/5/ - 5/6/		
		1882 -83	22/3/ - ?
1883	22/3/ - 24/3/		
1886	18/5/ - 7/6/		
		1892	20/6/ - 21/6/
1892	8/7/ - 29/12/		
		1893 - 99	26/4/ - ?
		1899	19/7/ - ?
		1901 - 06	?
		1907	/5/
1908	29/4/ - 30/4/		
1910	23/3/ - 28/4/		
		1910 - 11	27/12/ - /2/
		1911	27/5/ - ?
1911	9/9/ - 22/9/		
		1913 - 17	13/11/ - /6/
		1917	24/6/ - ?
		1918	/3/ - /7/

TABLE 6.2 (cont.)

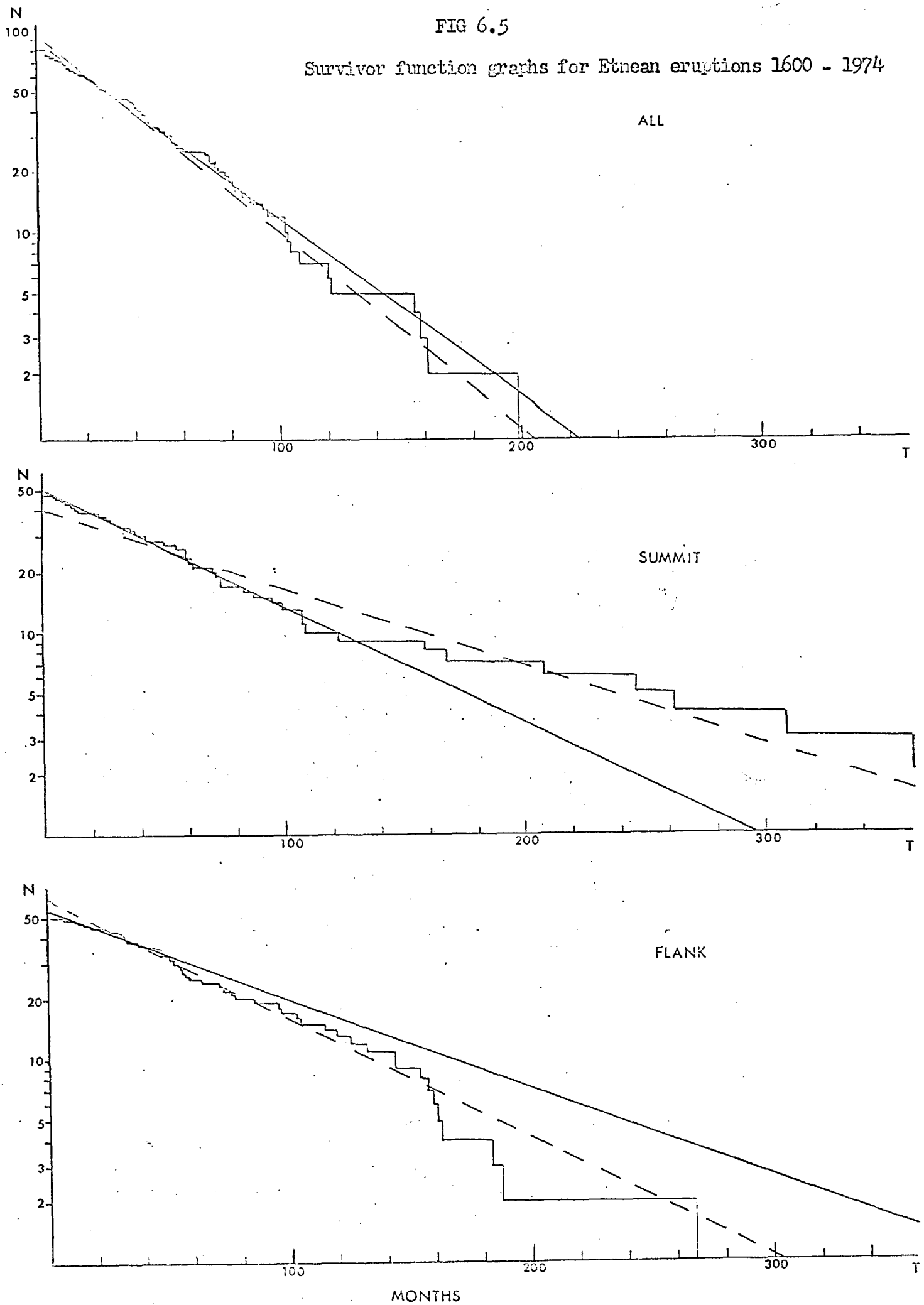
ERUPTIONS OF ETNA 1600 - 1974

FLANK		SUMMIT	
1913	29/11/ - ?		
		1919 - 23	/3/ - 16/6/
1923	16/6/ - 16/7/		
		1924 - 25	?
1928	2/11/ - 20/11/		
		1929	2/8/ - ?
		1931 - 32	/7/ - /3/
		1934	5/1/ - 7/1/
		1935 - 40	/3/ - ?
		1940	10/3/ - ?
		1940 - 42	/8/ - /6/
1942	21/2/ - 10/3/		
1949	2/12/ - 5/12/		
1950	25/11/ - /12/		
		1955 - 56	29/6/ - /4/
		1964	7/4/ - 5/7/
1971	7/5/ - 16/5/		
1971	11/5/ - 12/6/		
1974	30/1/ - 17/2/		
1974	11/3/ - 29/3/		

TABLE 6.2 (cont.)

FIG 6.5

Survivor function graphs for Etnean eruptions 1600 - 1974



computed previously two different straight lines have been fitted to the data. The dashed line is the least-squares straight line and the solid line is the one that most accurately follows the shorter repose periods. The second line has been constructed in view of the results obtained with the N = 60 random number test. The results are summarized in Table 6.3. The Max. repose, column 7, is the longest repose when considering the short reposes.

Eruption Type	N	All Reposes $\times 10^{-3}$	Correlation(%)	Short Reposes $\times 10^{-3}$	Correlation	Max. Repose
All	83	$22.11 \pm .04$	99.3	$20.0 \pm .30$	99.6	103
Summit	47	$8.96 \pm .15$	98.2	$13.2 \pm .26$	99.5	100
Flank	50	$13.48 \pm .20$	98.88	$10.1 \pm .25$	98.0	54

Table 6.3

Results for Etnean Reposes

a) All Eruptions

Considering 'All' eruptions, the values of obtained by the two approaches are very similar and the difference between then is negligible. This is not unexpected since only nine eruptions are excluded using the short repose approach. The conclusion from this data set is that the probability of an eruption of Etna in a given month is approximately

2% and independent of the time of the previous eruption.

b) Summit Eruptions

This is not the case for summit eruptions where the values of β for all and short reposes differ considerably, and the data can best be interpreted by assuming that it is time dependent. The change in gradient occurs for t = 120 months and a value of 7.0 for long reposes was calculated. The results given in Table 6.4 include a similar analysis for flank eruptions.

Eruption Type	Min. Repose	$\times 10^{-3}$	Correlation (%)
Summit	120	$7.0 \pm .36$	98.7
Flank	125	$23.0 \pm .43$	96.4

Table 6.4

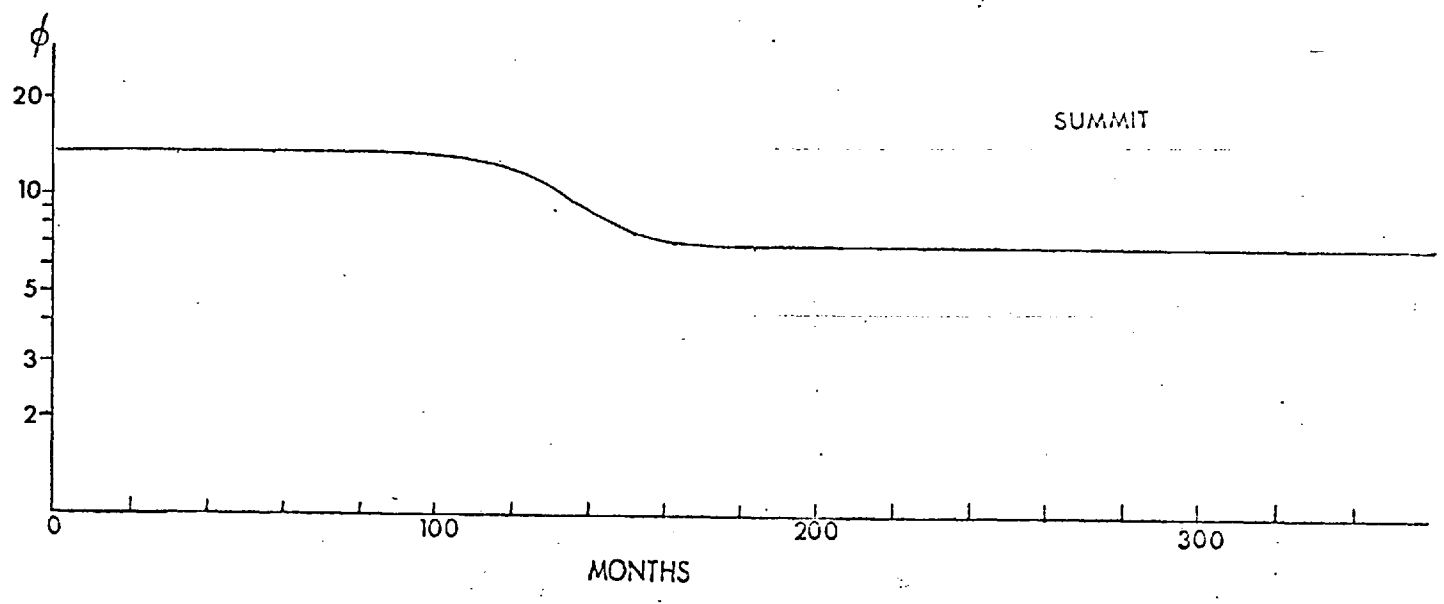
Results for Summit and Flank Reposes

c) Flank Eruptions

The flank eruptions are more complicated again than the summit eruptions. The 'all reposes' best line fits the data well for reposes

between 20 and 150 months but is inadequate for the longer reposes and is also wrong for reposes of less than 15 months. Eruption rate curves based on the values calculated above were constructed and are given in Fig. 6.6. The first aspect of these curves demanding attention lies within the region 100 to 180 months. During this period there is a decline in the rate of summit eruptions while it increases for flank eruptions. Although these changes are not commensurate there clearly appears to be a common factor between them. The higher eruption rate for flank eruptions should be signalled by a similar increase for 'all' eruptions. That this is not the case is due in the main to the greater weight given by short reposes, although as can be seen in Fig. 6.5. the longer reposes do indicate a higher eruption rate.

Certain tentative hypotheses can now be made on the basis of the preceding analysis. These can best be approached by considering Etna from the point of view of the summit eruptions. No support at all can be derived for any theory proposing a magma chamber supplying the summit eruptions. A magma chamber, if it is to behave as such, would exhibit the effects of loading and discharging in the repose pattern and these are not observed at all. If a magma chamber does exist then it behaves purely as an extension of a sub-crustal region and would be detectable either directly through seismic profiling or indirectly through petrological considerations.



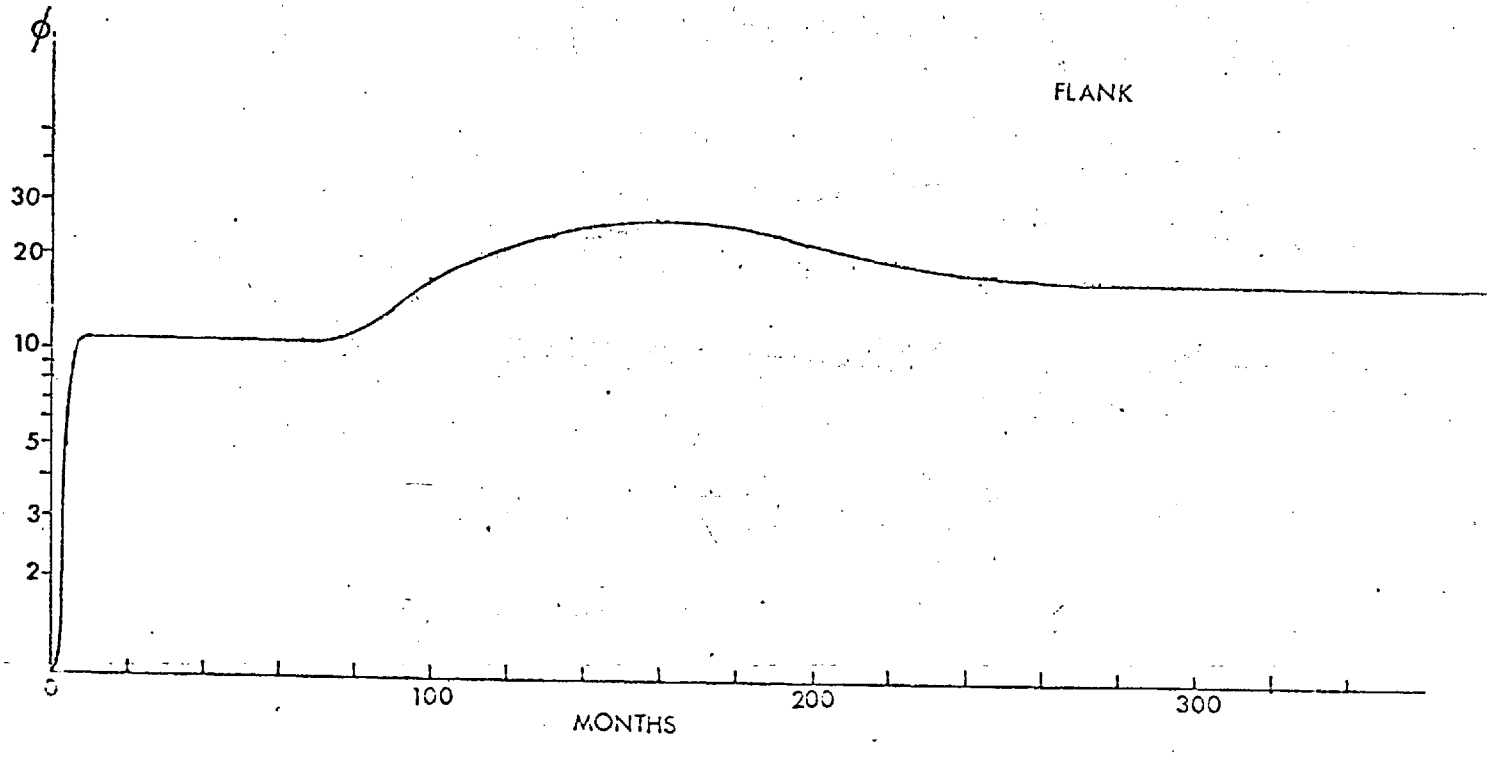


FIG. 6.6

Eruption rate curves for Etnean eruptions 1600 - 1974

If the evidence does not support a magma chamber then it does support, indeed necessarily implies, a two-state system (Wickman, 1976). The change in eruption rate for reposes in excess of 120 months signifies that some different mechanism has come into operation reducing the probability of an eruption. The accompanying increased rate for flank eruptions suggests that magma is diverted from feeding summit eruptions into supplying flank eruptions.

A possible mechanism to effect this would be a straightforward solidification of magma in the central conduit obstructing the normal flow of magma. This would further imply that those summit eruptions following reposes in excess of say, twelve years should be more violent than normal, a greater volume and rate of flow of magma being required to remove the obstruction. Unfortunately this is more difficult to test than might be anticipated. Information regarding summit eruptions is less detailed than for flank eruptions. With the information available Table 6.5 has been constructed for those summit eruptions occurring after a protracted repose.

Date of Eruption	Repose length	Description
7/7/1863	20 years	Very strong, explosive. No recorded lava effusion.
4/3/1831	21½ years	Very strong, explosive. Lava effusion.
May 1781	18 years	Lava effusion; lack of sufficient information.
22/11/1723	30 years	Lava Effusion.
11/3/1669	36 years	Very strong, explosive, lava effusion. A violent terminal explosion on March 25 resulted in the collapse of the Gran Cono caldera.
21/2/1633	79 years	Very strong, explosive. Insufficient Information.

Table 6.5 (Adapted from Imbo (1965))

Data for Eruptions Following Long Reposes.

It is probable that any earlier records are increasingly inaccurate as regards both eruption description and repose length.

The 79 years prior to 1633 may have produced some summit acitivity which was unrecorded but is important for this hypothesis. The available evidence, however inadequate it may be does lend support to this hypothesis.

The flank eruptions present greater interpretational difficulties. Here the possibility of a magma chamber cannot be entirely disregarded, because of the loading effect exhibited at the beginning of the curve. This is a more speculative part of the curve than the rest and must be treated accordingly. Indeed, the form of a magma chamber needed to supply such a wide area would be extremely complex particularly as it does not interfere with the central conduit. The large rise in the eruption rate for reposes around 160 months also indicates the possibility of a storage/discharging mechanism at work, but this could perhaps be explained by invoking Rittmann's (1963) view of eccentric eruptions as separate volcanoes controlled by separate, though related, mechanisms. Obviously if an eccentric eruptive centre were under different control then grouping it along with flank eruptions would in general lead to spurious results. The same result would follow if a particular flank cone were sub-controlled by additional local conditions.

6.4. TIDAL CONTROL OF ERUPTIONS

Over the centuries man has sought to explain apparently random events by attempting to correlate them with heavenly phenomena. Most of these attempts either proved fruitless or were based on specious data or argument and did not stand up to a more rigorous scientific investigation. Over recent years two particular phenomena have been subject to considerable investigation re the triggering of earthquakes and volcanic eruptions; tides and sunspots.

Tidal triggering of earthquakes has been a contentious subject for many years and contradictory evidence is produced seemingly with each new paper published on the subject. The most reasonable theoretical justification is given by Heaton (1975). He reasons that since almost all long period strain measurements of the Earth are dominated by the Earth tide then the tidal stress rates may be comparable with tectonic stress rates even though the actual tidal stresses may be three orders of magnitude smaller than the tectonic stresses. For instance suppose that an earthquake resulted from stress accumulations of the order of 150 bars and that an earthquake occurred in such a fault zone once a century then the average stress rate is .001 bars/6hr. compared with a tidal stress rate of 0.1 bars/6hr. This argument is dangerous, however, in

that earthquakes are more likely to occur when the tectonic stress rate increases to a large value than when it is constant.

It can be shown that for tidal stresses the minimum absolute principal stress axis is vertical for an observer near the earth's surface since the boundary condition imposed by the earth is one of no traction at its surface. Thus the remaining principal stress axes are in the horizontal plane.

Theoretical considerations or not, the problem is still unresolved. Knopoff (1964) examined over 9000 earthquakes of magnitude 2 or greater in the Pasadena network of Southern California and found no significant correlation with tides. Studies of world-wide earthquakes have been made by Shlien (1971) and Dix (1964) amongst others and here the results are inconclusive, e.g., in Shlien's case some significant (5% level) correlations were obtained, but the effect was not consistent or temporally stable. On the other hand, there are many who support tidal triggering. Allen (1936) and Tamrazyan (1964) find the effect more likely with large than small earthquakes whereas Ryall et al. (1968) and Willis and Taylor (1974) observed correlations with microseismic activity. In Ryall et al's (1968) case the results were based on a study of 7,800 aftershocks in the California - Nevada border region and showed a 99% level of confidence for a correlation between earthquake activity and earth tide gravity

highs. Knopoff and Gardner (1972) indicate, however, that man made noise has a diurnal period and this interferes with seismic noise levels and hence the measurement of microearthquakes.

Heaton (1975) is more detailed in his study of the particular types of earthquakes affected and concludes that for earthquakes of magnitude $\geq$ 5, shallow ($<$ 30km) larger magnitude oblique-slip and dip-slip earthquakes are triggered by tidal stresses but there is no corresponding triggering for shallow strike-slip earthquakes or for any type of intermediate or deep focus earthquakes.

The well-known association of earthquakes and volcanoes has prompted workers to consider tidal triggering of volcanic eruptions and also of volcanic microseismicity. For Mt. Etna, microseismicity during 1974 and 75 was tested for tidal correlations but the results were inconclusive (M. Zaman personal communication).

Attempts to correlate volcanic activity with Earth tides have only been attempted in recent years, although early workers noticed that certain types of volcanic activity appeared to possess semi-diurnal or diurnal periods e.g. Jaggar (1924). These observations were not subject to any rigorous analyses. However, in the past ten or so years there have been an increasing number of statistical investigations into

this phenomenon. Machado (1960 and 1967) and Mendoça Dias (1962) observed the effect with the long-period fortnightly tides for Azorean volcanoes. Johnston&Mauk (1972) also detected a significant fortnightly effect for the eruptions of Stromboli this century and in a later study Mauk & Johnston (1973) extended the survey to volcanoes throughout the world. This work seemed to indicate that andesitic and basaltic volcanoes behaved differently with respect to tidal effects and that different volcanic regions were triggered at different tidal phases. Michael & Christoffel (1975) found that over the period January 1972 - June 1974, Mt. Ngauruhoe in New Zealand has eruptive periods strongly correlated with the fortnightly tide. In a lengthy paper Hamilton (1973) examined world volcanic activity and obtained correlations with earth-tide cycles from fortnightly to nineteen yearly periods. Recently Golombek & Carr (1978) proposed tidal triggering for seismic and volcanic activity during the 1879-1880 eruption of Islas Quemadas in El Salvador; once again the fortnightly tide was responsible. Almost all the observed correlations have been with the fortnightly tides, though Eggers and Decker (1969) demonstrated some connection between volcanic activity and the semi-annual and annual tides.

From a physical point of view the justification for tidal

triggering is not readily apparent, and before proceeding to the results obtained for Etna is is pertinent to examine the physical background to the whole problem.

A common approach has been to consider the volcano magma chamber analagously with well-aquifer systems. Tidal effects in wells have been observed back to the time of Pliny (Melchior(1964)) and observations of lava levels in volcanoes have shown similar tidal cycles Jaggar (1920), Shimozuru and Nakagawa (1970). It has also been shown that the simple well-aquifer model Fig. 6.7 does not explain the results.

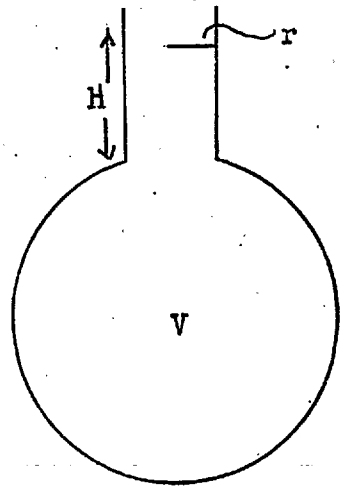


Fig. 6.7.

E - bulk modulus of water V - volume of cavity

r - radius of the well ρ - density of water dH - height change in well.

Melchior (1964), following on an earlier analysis by Blanchard and Byerly (1935) showed that, for a change in volume, dV, due to tidal forces:-

$$dH = \frac{dV}{\pi r^2 + (\rho g V/E)} = \frac{dV/V}{\pi r^2/V + \rho g/E} \qquad 6.1$$

then since $V \gg r^2$

$$dH = \Delta E/\rho g \qquad 6.2$$

where $\Delta = dV/V$ is the dilatation.

For the Earth tide $\Delta = 6. 10^{-8}$, that is approximately three times the linear strain and thus. for water:

$$dH \simeq 1.0 \text{ cm} \qquad 6.3$$

However, the generally observed value for dH is 2 cm. The important point arising from equation 6.1 is that provided $V \gg \pi r^2$ then the actual values of V and r are irrelevant to dH.

Bredehoeft (1967) sought to explain the discrepancy between predicted and observed fluctuations in terms of the porosity and specific storage of the aquifer. The specific storage is defined as the quantity of water that is released or taken into storage from a unit

aquifer volume per unit change in head. This analysis can obviously be extended to include volcano magma chambers. However, magma chambers contain magma and not water. Returning to equation 6.2, for basalt $\rho = 3.10^3$, $\Delta = 6.10^{-8}$ and $E = 7.5.10^{10}$

$$\text{then } dH \simeq 10^{-1} m$$

These values apply to the solid and not molten rock but this value is not likely to radically change. It is much less by factors of two and more than many magma column changes accorded to tidal effects, and would seem inadequate to trigger an eruption, even allowing for the pressure release on the magma promoting degassing, as suggested by Michael and Christoffel (1975).

A popular alternative to a spherical magma chamber is a cylinder and this is much less responsive to tidal influences than the spherical model. (Fig. 6.8).

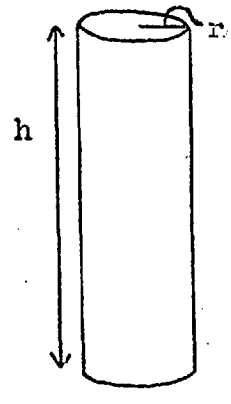


Fig. 6.8

Under compressive forces the mass in the cylinder will remain constant

$$\therefore M = \rho V$$

$$\text{and} \quad dM = \rho dV + V d\rho = 0$$

Now $d\rho/\rho = dp/E$ where dp is the resultant pressure change

$$\text{and} \quad dp = \rho g dh$$

$$\therefore \pi\rho(r^2 dh + 2rh dr) = -\pi r^2 h \rho g \, dh/E$$

$$\text{giving} \qquad \frac{dh}{h}\left(1 + \frac{h\rho g}{E}\right) = -\frac{2dr}{r}$$

Vertical strains are small, and have been ignored. Then unless the height is of the order of 10^5m. the bracketed term can be ignored and:-

$$\frac{dh}{h} = -2\frac{dr}{r}$$

and for the Earth tide $\frac{dr}{r} \simeq 2 \cdot 10^{-8}$

$$dh \simeq 10^{-7} h$$

In general then dh can be ignored for all physically feasible systems.

An additional factor influencing aquifers and volcanoes is the ocean tide and its loading. For Mt. Etna the influence of porosity and specific storage can only be hazarded at (Bredehoeft, in fact, estimates the porosity and specific storage of aquifers by measuring their tidal variation) but as shown in Chapter 3, the ocean load for the Mediterranean is very small and may be neglected.

Having established that there are valid reasons for the simple well-aquifer (magma chamber) model to be inadequate, even more advanced models still fall some way short of explaining the observed volcanological effects where variations of 2-3 metres were measured by Shimozuru and Nakagawa (1970) and tens of feet by Jaggar (1920).

It is important to now consider in detail the specific Earth tidal theory dealing with this problem since this highlights many faults in the previous analyses. The aforementioned problems of eruption timing reduce the triggering to a consideration of only those tides of fortnightly or longer periods. The periods and amplitudes of the principal long period components are given in table 6.6. The argument notation is the same as that used in Chapter 3.

As shown in Table 6.6. the principal tidal contribution for the fortnightly period comes from the wave MF and the closely related

WAVE		AMPLITUDE	ARGUMENT	FREQUENCY °/hour	PERIOD DAYS
Solar Annual	Sa	.01156	$h - p_s$	.041067	365.26
Solar Semi-Annual	Ssa	.07266	2h	.082137	182.62
Lunar Monthly	Mm	.08255	s - p	.544375	27.56
Variational Fortnightly	Msf	.01366	2(s - h)	1.015896	14.77
Principal Fortnightly	Mf	.15645	2s	1.098033	13.66
Nodal Varied Fortnightly	Mfm	.06482	2s - n	1.100240	13.63

TABLE 6.6

Amplitude, argument, frequency and period of the tidal components used in the study of tidal triggering of Etnean eruptions. See chapter 3 for explanation of the notation.

component MSF. Now the MF component has a period of 13.66 days so it is peculiar why at least three of these studies (Johnston & Mauk 1972; Mauk & Johnston 1973; Michael & Christoffel 1975) should select the comparatively unimportant MSF component as the principal tidal triggering component. In none of these papers is any justification given for this selection. Another problem overlooked in these studies is that, with the exception of Hamilton (1973), all consider the total tide and abstract a fortnightly component from it merely by taking the period between successive maxima or minima. This totally ignores the fact that since there are three principal fortnightly components with different arguments their combined period will vary. For the MF and MSF components the compound tide will be one of 14-22 days but will have a beat frequency of 1.1 days. This combined period variation is quite considerable and any attempt to correlate the times of eruptions with tidal phases is meaningless without taking this into account. This apparent lack of understanding of Earth-tidal theory is also illustrated by Mendoça Dias (1962) who correctly points out that the long period components have a node at latitudes $\pm 35^{\circ}/6'$ but appears to believe that the Mm (lunar monthly) component is exempt from this.

As a rider to this it may be pointed out how many of the volcanoes investigated for tidal influences lie very close to the 35°/ 6' nodal line - apart from the Azores (38°N) and Stromboli (38°N) there is also Nganihoe (38°S) and of course Etna (37.5°N). This grouping at least implies that the long period tides should exert similar influences on all the volcanoes. Interestingly the Japanese volcances also lie close to this nodal line with only the Hawaiian volcanoes, amongst well studied volcanoes, ~~lieing~~ lying appreciably distant from it.

The final problem is connected with the statistical approach. Many of the analyses treat an eruption as falling into a category designated as either a success or a failure depending upon its location in the tidal cycle. This is a very dangerous and unrealistic approach, however. Whilst it is quite in order to regard the toss of a coin or a die as possessing an unequivocal result and stable probability the same cannot be said for a volcanic eruption. Apart from the problems referred to earlier about the precise timing of the inception of an eruption, regarding an eruption as a point event must be done with caution. This problem was alleviated in the repose period study because the reposes themselves were considerably greater than the error inherent in the estimation of the time of an eruption. However,

when it comes to determining the time of an eruption within a period of 14 days (approx.) this problem cannot be ignored. Consider, for example, Michael and Christoffel's result (1975). Assuming a 14.7day tide they consider a success to be an eruption within 1.5 days of a tidal maximum. They found 7 successes in 12 eruptions and the probability of this, assuming a random distribution of eruption in time is given by:-

$$\frac{12!}{7!\,5!}\left(\frac{3}{14.7}\right)^{7}\left(\frac{11.7}{14.7}\right)^{5} \simeq 0.4\%$$

which is highly significant at the 5% significance level. However, if one eruption is wrongly placed in time the probability reduces to:-

$$\frac{12!}{6!\,6!}\left(\frac{3}{14.7}\right)^{6}\left(\frac{11.7}{14.7}\right)^{6} \simeq 1.7\%$$

which is still significant, though much less so. If two eruptions are out then the probability reduces to 5.7% which is not significant.

Following on the previous discussion where it was shown that the compound fortnightly cycle can vary by two days amply illustrates the need for extreme caution in treating all such data, especially when volcanological data is sparse.

The statistical test used in the following analysis is similar to that used by Mauk and Johnston (1973) and was extended by Shlien (1971) from an initial method by Rayleigh. The method consists in determining the phase of the tide at which an eruption occurred and plotting the results in a rose diagram. If the magnitude of the vector sum of n unit 2-dimensional vectors $(1, \phi_i)$ is denoted by R where ϕ_i are the erupti phases, then the probability Pr that a random set of n phases will produce a sum vector whose magnitude exceeds R is given by:-

$$Pr \simeq e^{-R^2/n}$$

This is only approximate but is sufficiently accurate when $n > 10$. For the standard rose diagram:-

$$R_1^2 = A_1^2 + B_1^2$$

where $A_1 = \sum_{i=1}^{n} \cos(2\pi \phi_i / 360)$; $B_1 = \sum_{i=1}^{n} \sin(2\pi \phi_i / 360)$

Shlien (1971) extended the test to include the possibility of triggering at opposite phases and a second parameter R2 is calculated thus:-

$$R_2^2 = A_2^2 + B_2^2$$

where $A_2 = \sum_{i=1}^{n} \cos(2\pi \phi_i / 180)$; $B_2 = \sum_{i=1}^{n} \sin(2\pi \phi_i / 180)$

Sixty-eight eruptions whose day of eruption was known were used. For each eruption tidal components were computed using the program TIDECOM specially written for this purpose for a 30 day period encompassing the eruption. The phase of the eruption was then calculated with the preceding maximum chosen as the point of zero phase. As with the repose period analysis the eruptions were distinguished as 'flank', 'summit' or 'all'. For each tidal component a rose-diagram was constructed and the data subject to the Rayleigh/ Shlien test. The tidal components selected were the three fortnightly components MF, MFM and MSF, the monthly component Mm and the annual component. For the annual component it is sufficient to consider the month of an eruption, since the phase of the yearly tide varies little with the calendar year ($p_S \simeq 20{,}000$ years), a semi-annual effect being shown up in a calculation of P2. Additionally the total tide was calculated for each eruption in the same way and a phase evaluated by measuring the time between the maxima before and after the eruption for each eruption individually. This procedure must be followed as it is insufficient merely to measure the time from the preceding maximum since there is no way of knowing what part of the cycle, if any, may be responsible for the triggering.

A control was provided by a random number test. Sixty-five random numbers were generated, in columns of 12, and the occurrence of a particular number (09) was assigned to a phase within a postulated 12 day tide. The results are displayed in Table 6.7 and the complementary rose-diagrams shown in Figs. 6.9-6.27.

In Table 6.7

$$P_1 = e^{-R_1^{2}/n} \qquad P_2 = e^{-R_2^{2}/n}$$

$$\psi_1 = \tan^{-1}\left(\frac{B_1}{A_1}\right) \qquad \psi_2 = \tan^{-1}\left(\frac{B_2}{A_2}\right)$$

In only one case, the MFM tide triggering flank eruptions, does the probability approach a level of significance of 5% and in all other cases it is considerably outside this level, especially when compared with P2 for random numbers.

The only reasonable conclusion that can be drawn from this survey is that there is no significant correlation between any Earth tide component and the eruptions of Mt. Etna. The MFM/Flank eruption case can probably be disregarded as it is close to the significance level and it is highly unlikely that a tide of 13.633 days would have

Tidal Component	P_1	P_2	ψ_1	ψ_2
All Eruptions				
Mf	.525	.626	82.83	269.27
Mfm	.106	.254	55.81	79.81
Msf	.912	.165	327.78	216.94
Mm	.515	.668	60.44	320.38
Annual	.124	.757	127.98	240.00
Total	.651	.748	237.35	306.43
Flank Eruptions				
Mf	.714	.477	35.41	358.59
Mfm	.046	.442	45.93	82.83
Msf	.764	.955	163.07	318.06
Mm	.835	.826	116.29	48.06
Annual	.267	.375	101.36	201.79
Total	.994	.453	284.00	348.85
Summit Eruptions				
Mf	.792	.577	322.84	65.72
Mfm	.672	.567	157.04	82.06
Msf	.393	.397	260.75	205.57
Mm	.509	.772	80.23	287.52
Annual	.255	.622	280.25	46.23
Total	.859	.821	157.49	156.59
Random Number Test				
	.824	.107	13.44	152.21

TABLE 6.7

Probalities of eruption triggering for specific tidal components.

a significant effect on a volcano whereas a larger amplitude tide of 13.661 days would not. The empirical conclusions support the theoretical considerations which also are opposed to tidal triggering.

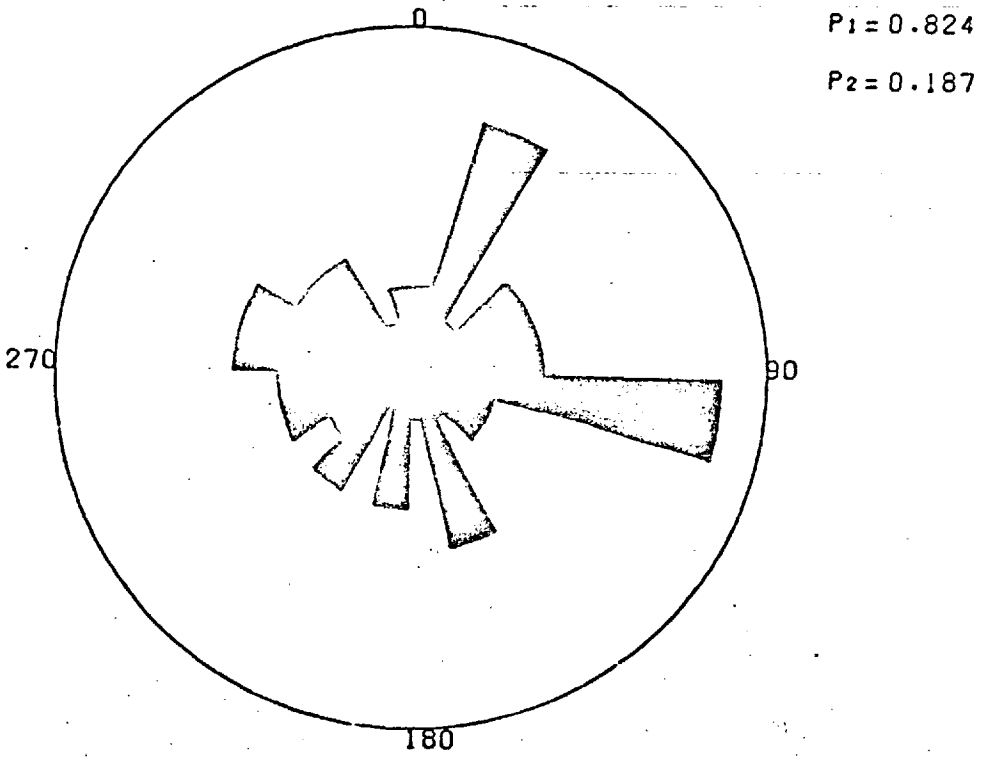

RANDOM NUMBER TEST
12 DAY TIDE
AT 15 DEGREE INTERVALS
P1 = 0.824
P2 = 0.187
0
90
180
270

FIG. 6.9

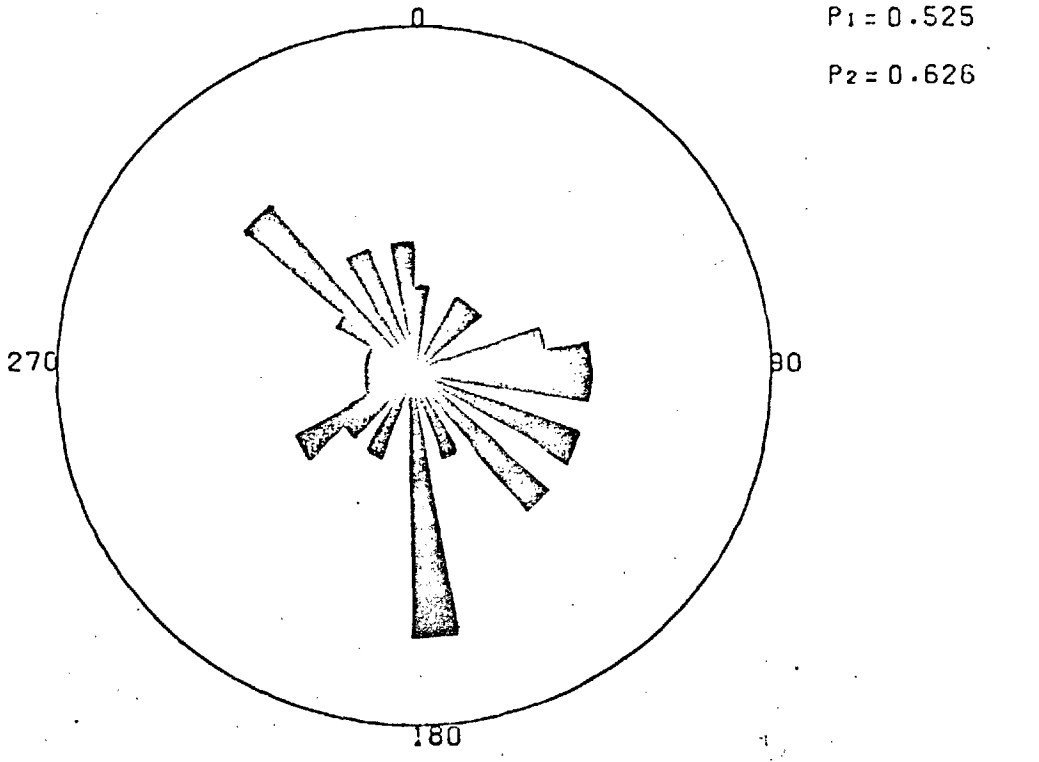

TIDAL TRIGGERING OF ETNA
MF COMPONENT
FLANK AND SUMMIT ERUPTIONS
P1 = 0.525
P2 = 0.626
0
90
180
270

FIG. 6.10

TIDAL TRIGGERING OF ETNA

MFM COMPONENT FLANK AND SUMMIT ERUPTIONS

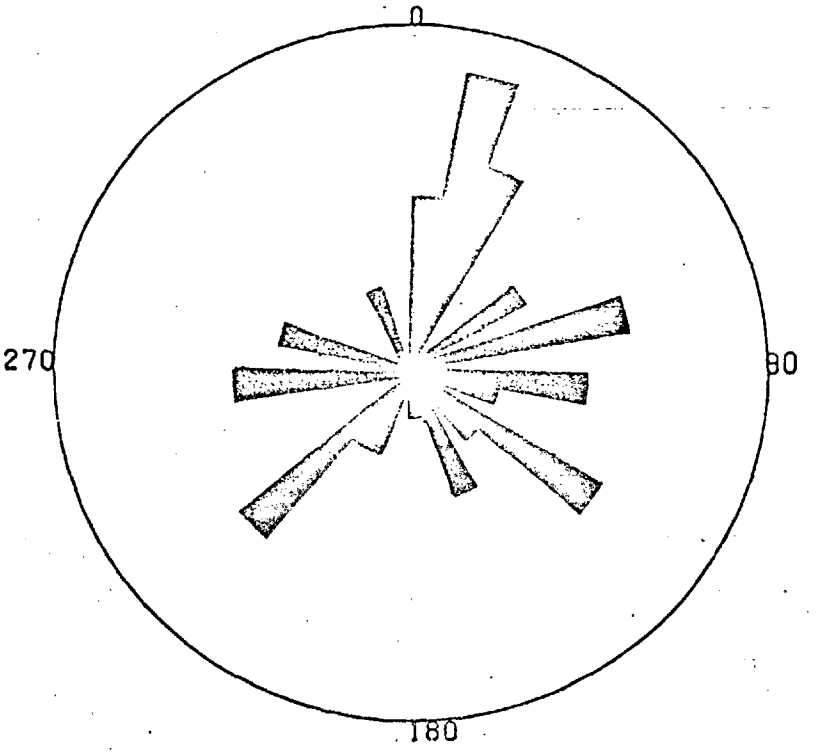


FIG. 6.11

TIDAL TRIGGERING OF ETNA

MSF COMPONENT FLANK AND SUMMIT ERUPTIONS

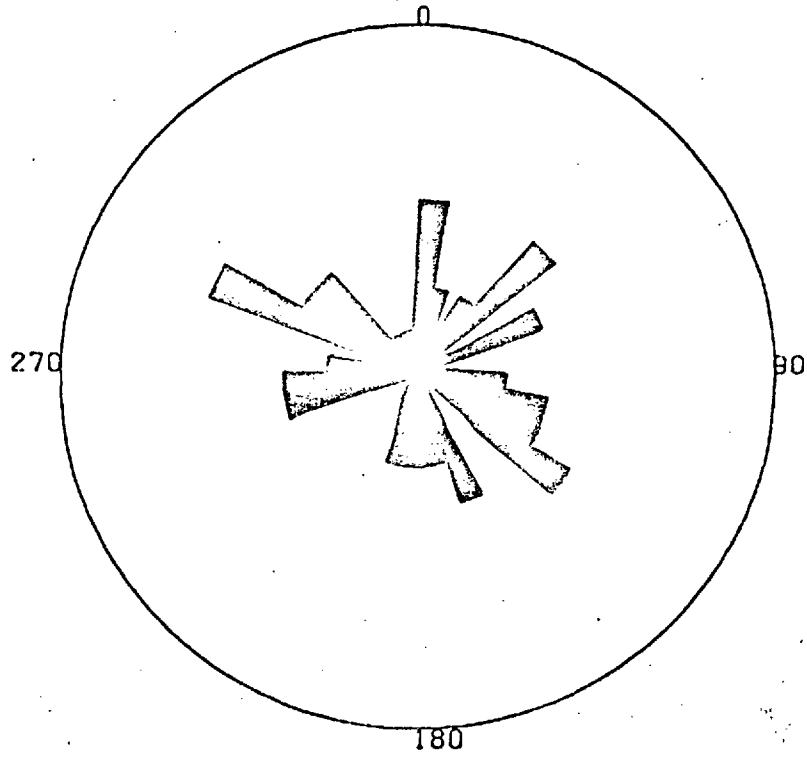


FIG. 6.12

TIDAL TRIGGERING OF ETNA

MM COMPONENT FLANK AND SUMMIT ERUPTIONS

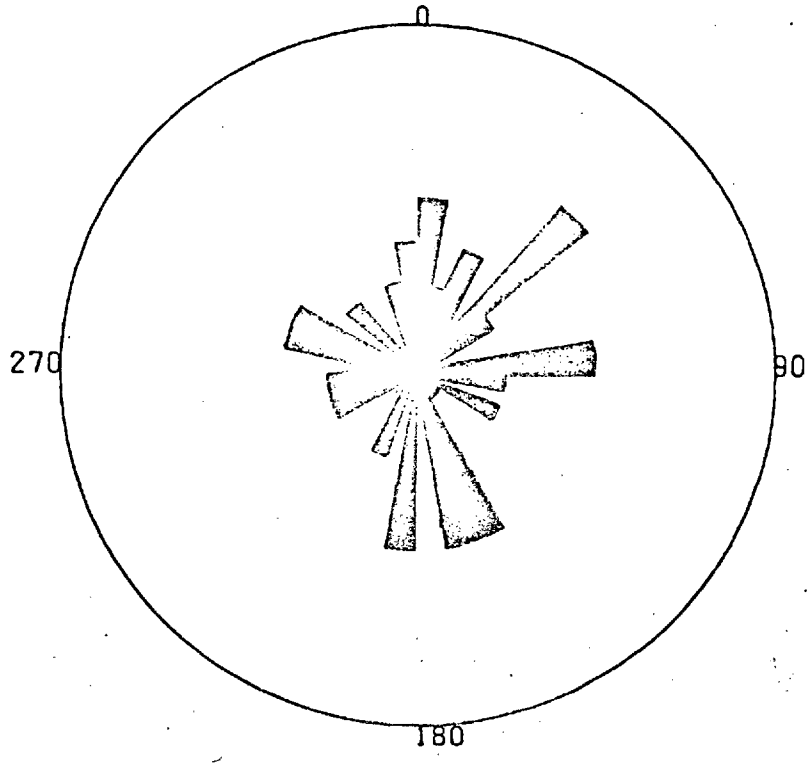


FIG. 6.13

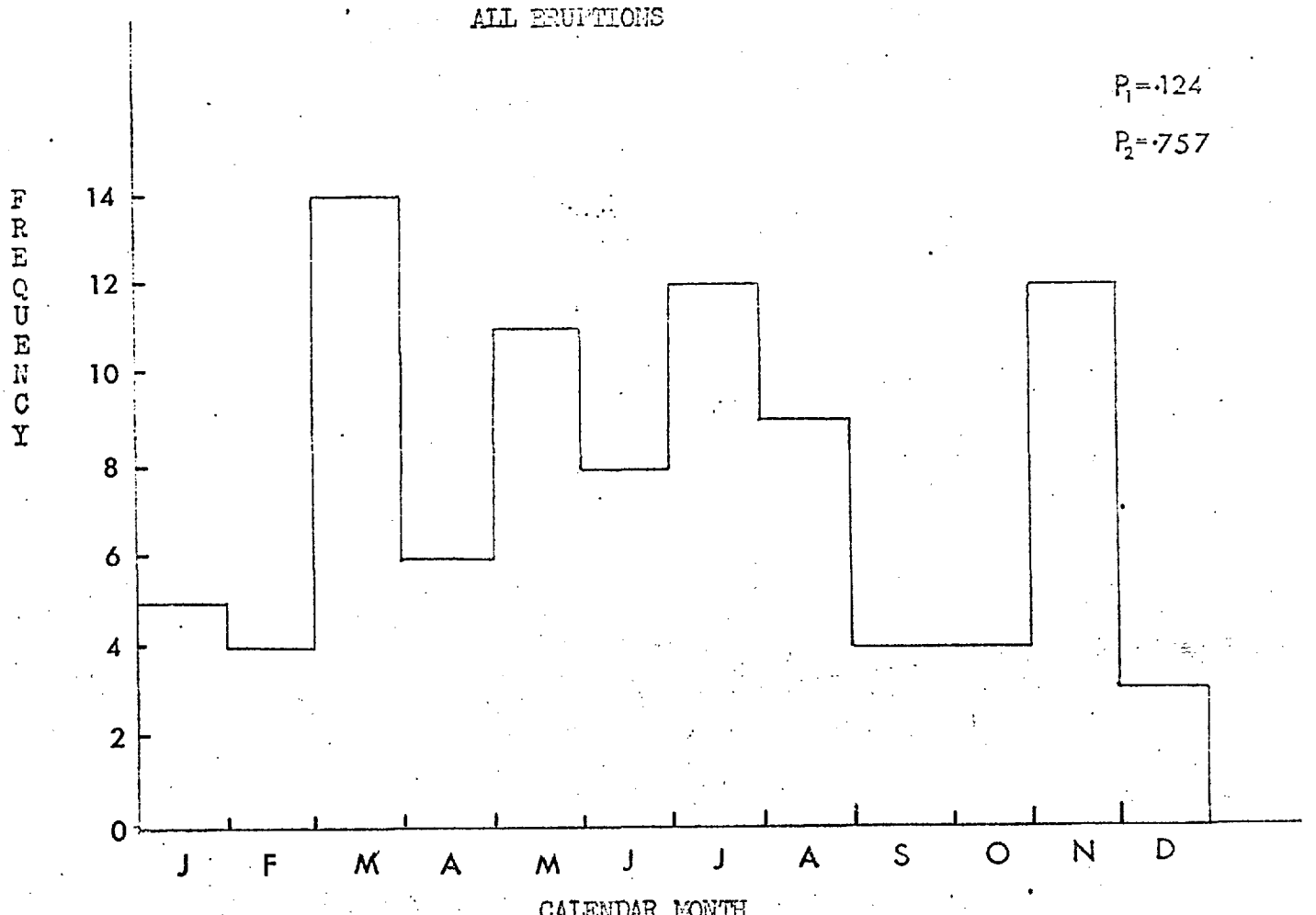


FIG. 6.14

Histogram of the frequency of onset of an eruption per calendar month Since the period of the annual earth tide is very close to the length of the civil year, this data can be used to evaluate the probability of tidal triggering due to annual and semi-annual tides. The terms P_1 and P_2 are as defined in the text.

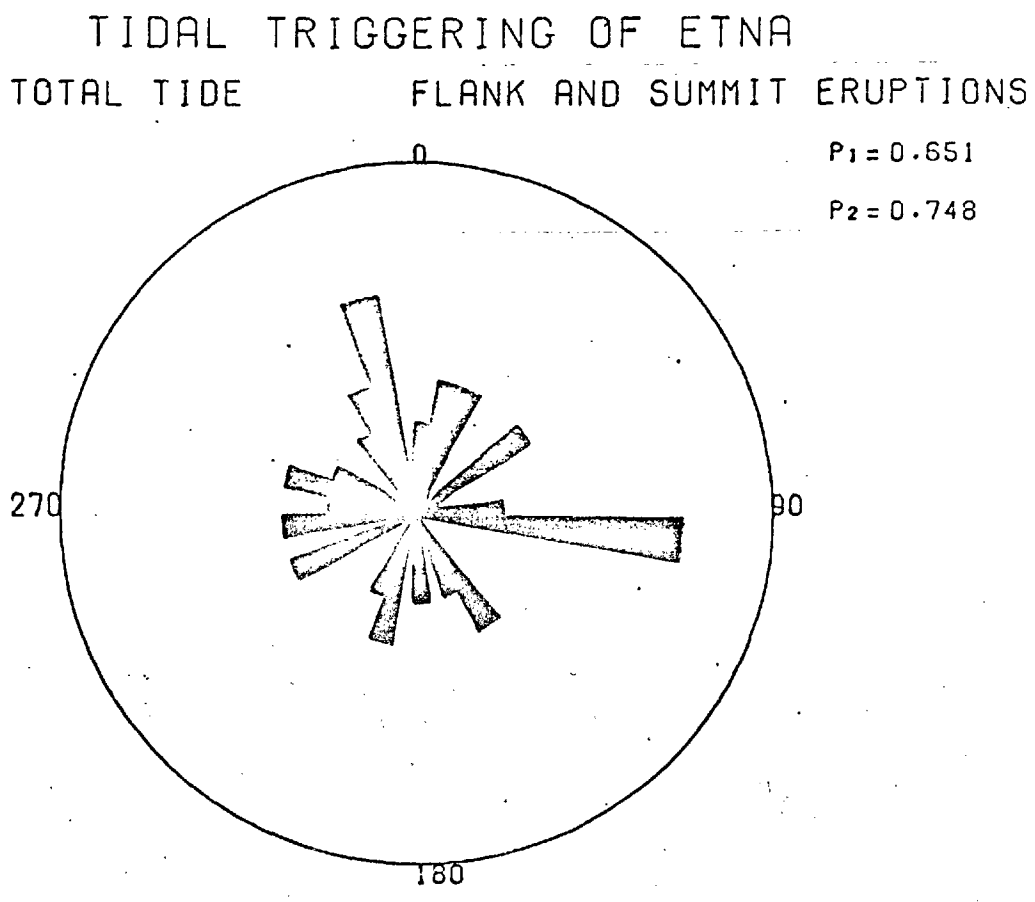

TIDAL TRIGGERING OF ETNA
TOTAL TIDE
FLANK AND SUMMIT ERUPTIONS
P1 = 0.651
P2 = 0.748
0
90
180
270

FIG. 6.15

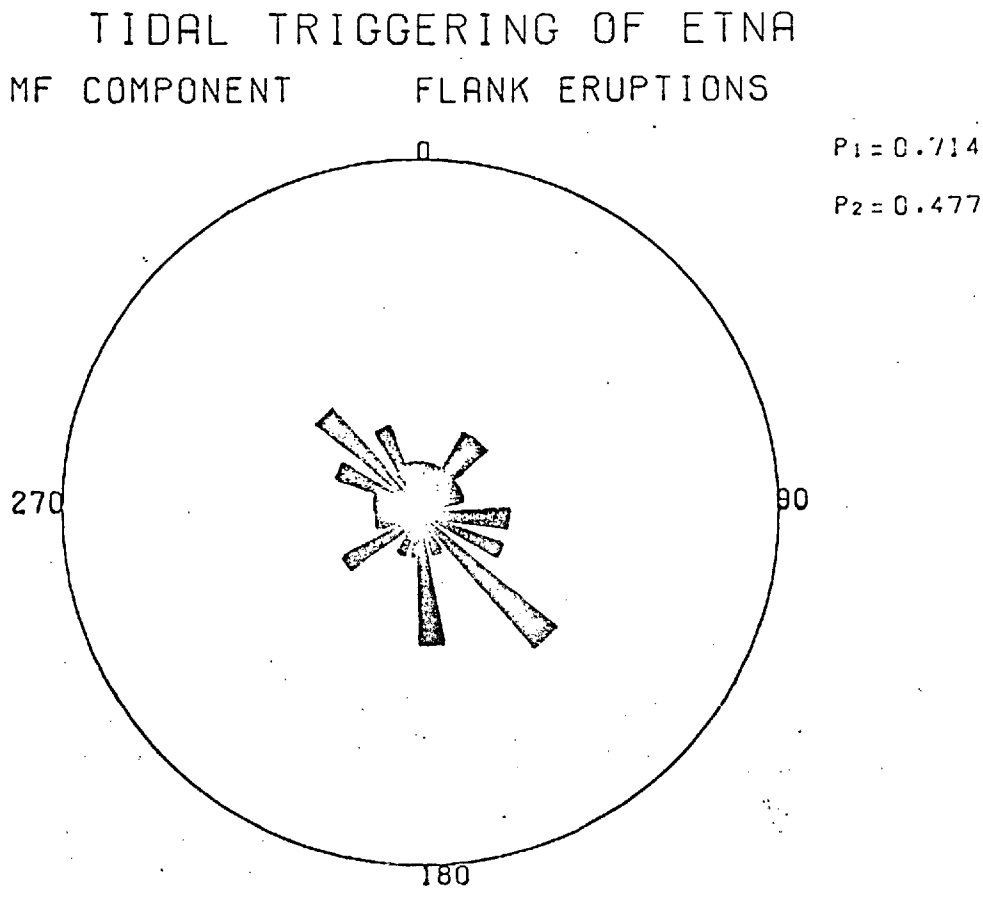

TIDAL TRIGGERING OF ETNA
MF COMPONENT FLANK ERUPTIONS
P1 = 0.714
P2 = 0.477
0
90
180
270

FIG. 6.16

TIDAL TRIGGERING OF ETNA

MFM COMPONENT FLANK ERUPTIONS

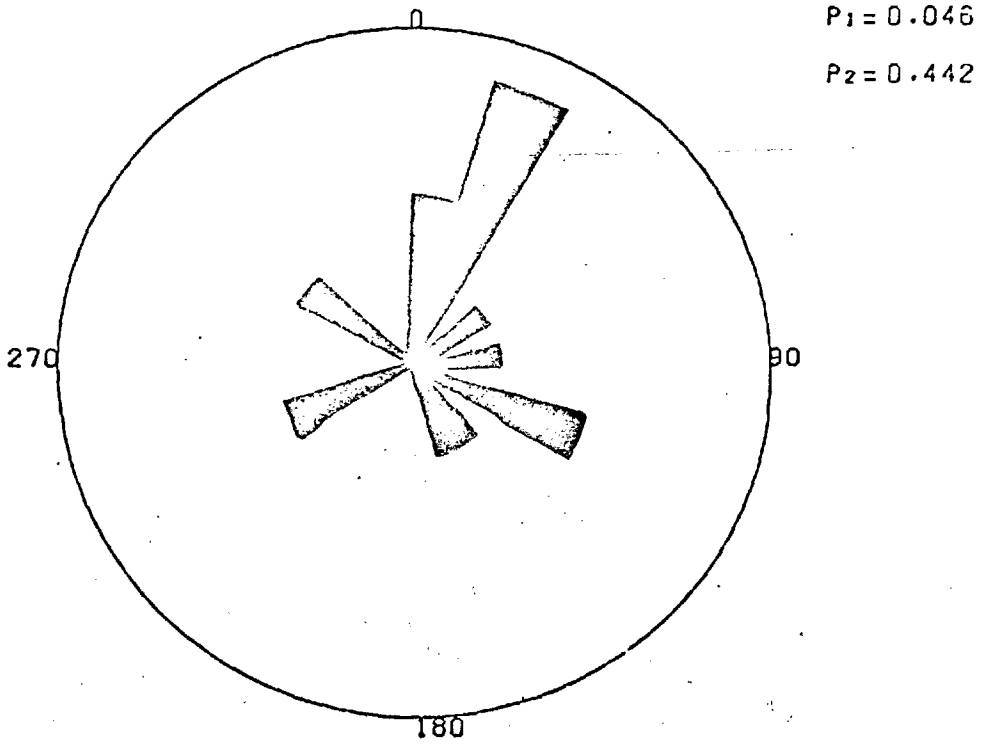


FIG. 6.17

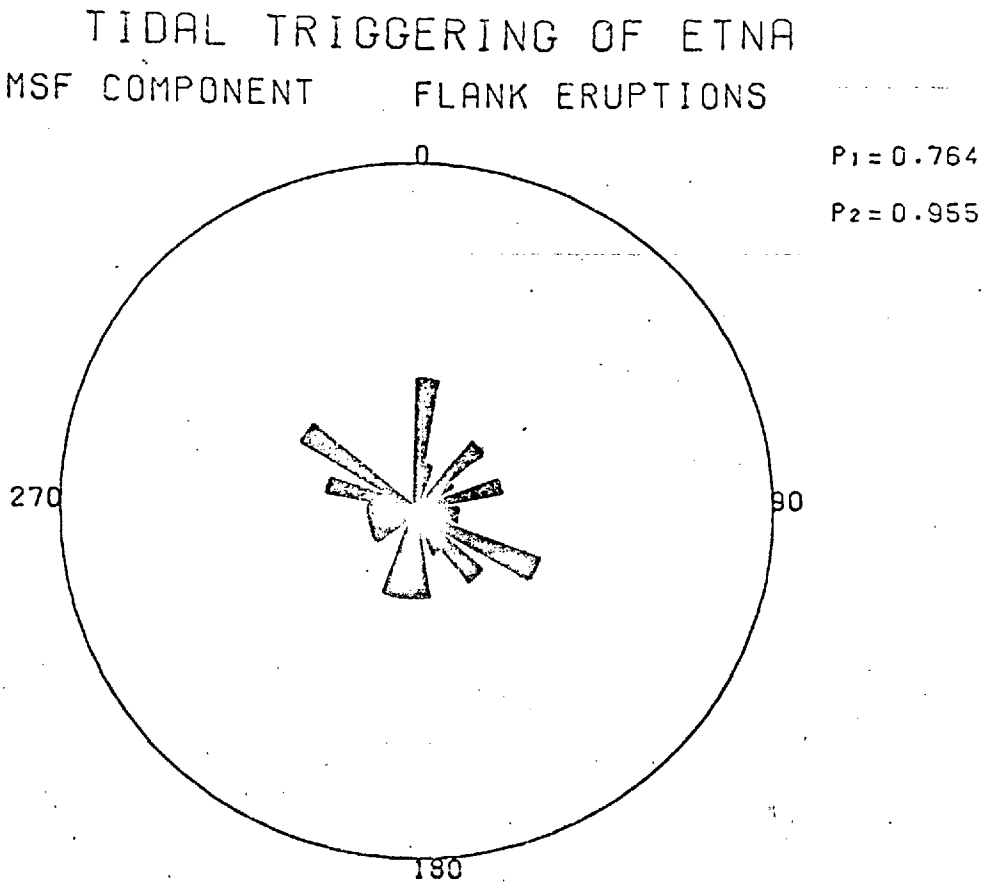

TIDAL TRIGGERING OF ETNA
MSF COMPONENT FLANK ERUPTIONS
P1 = 0.764
P2 = 0.955
0
90
180
270

FIG. 6.18

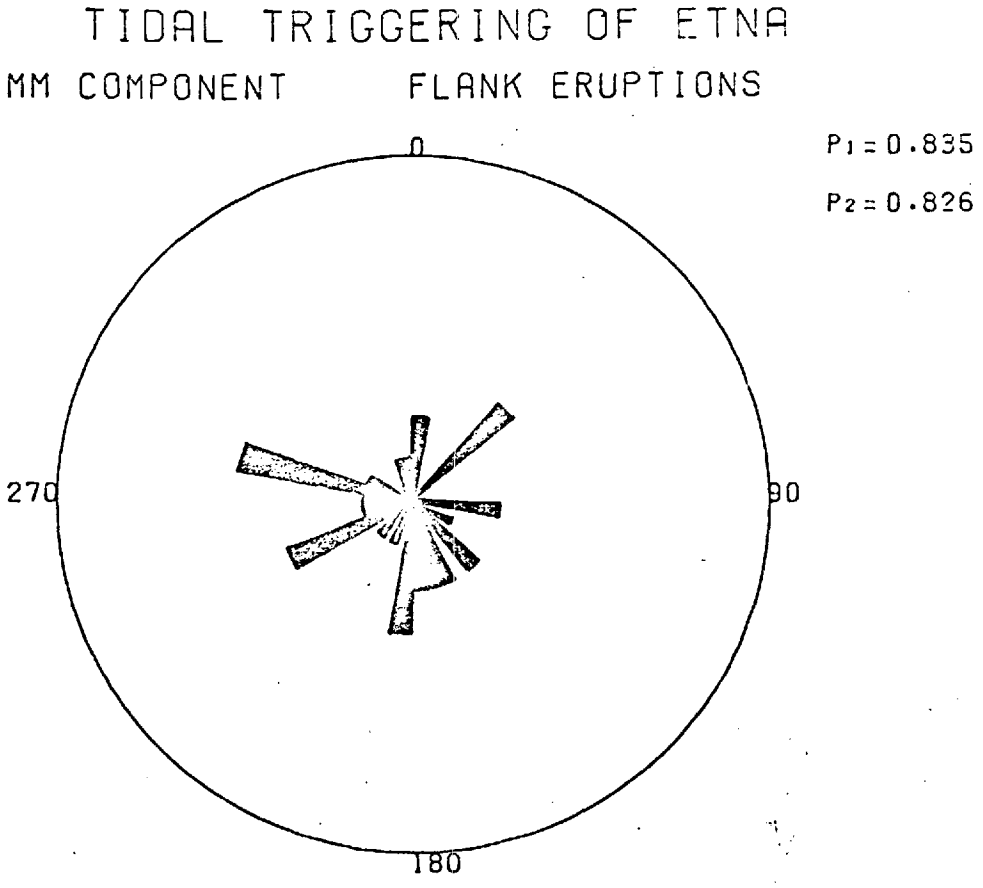

TIDAL TRIGGERING OF ETNA
MM COMPONENT FLANK ERUPTIONS
P1 = 0.835
P2 = 0.826
0
90
180
270

FIG. 6.19

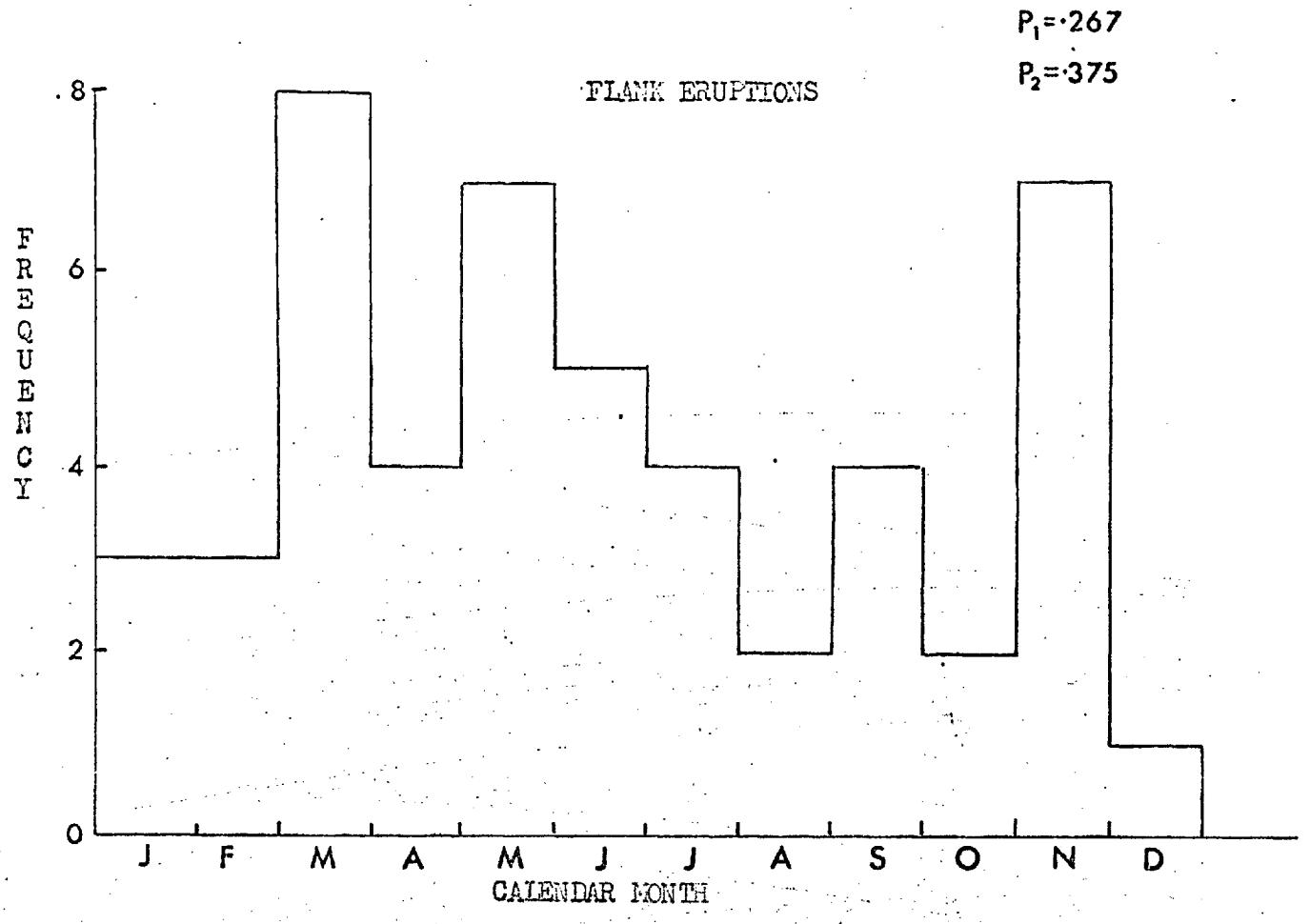


FIG. 6.20

Histogram of the frequency of the onset of a flank eruption per calendar month.

For explanation of use see figure 6.14

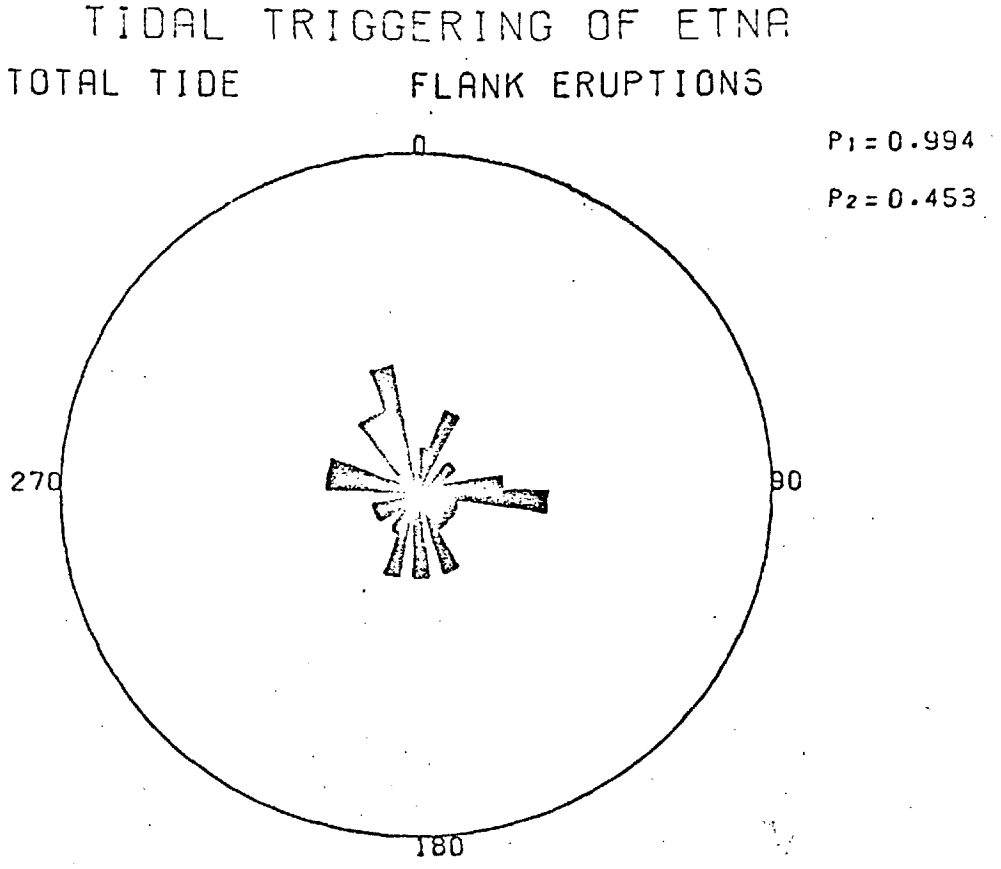

TIDAL TRIGGERING OF ETNA
TOTAL TIDE
FLANK ERUPTIONS
P1 = 0.994
P2 = 0.453
0
90
180
270

FIG. 6.21

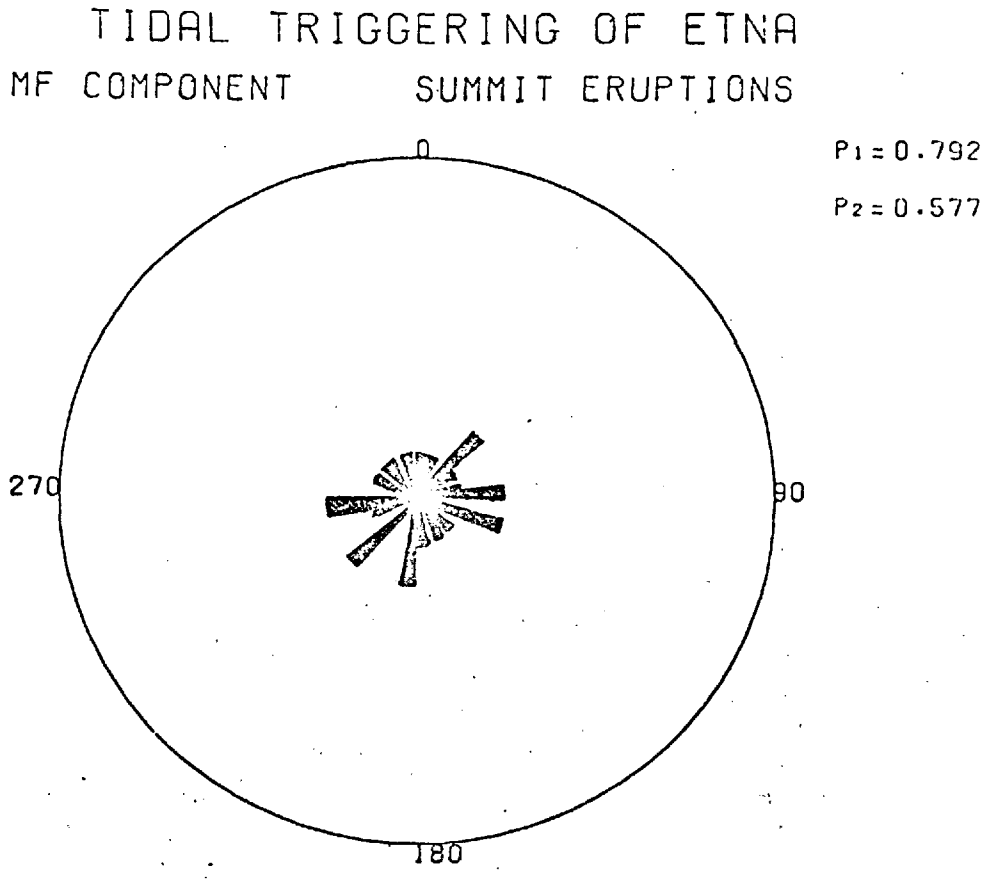

TIDAL TRIGGERING OF ETNA
MF COMPONENT SUMMIT ERUPTIONS
0
90
180
270
P1 = 0.792
P2 = 0.577

FIG.6.22

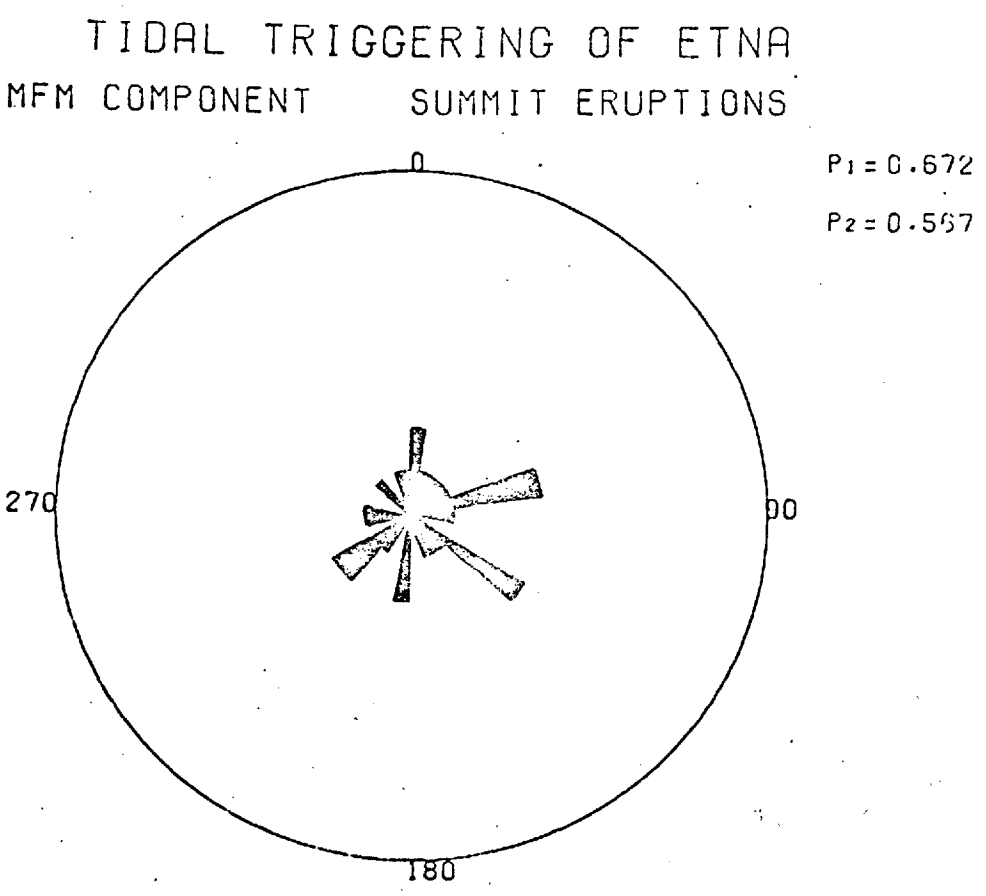

TIDAL TRIGGERING OF ETNA
MFM COMPONENT SUMMIT ERUPTIONS
P1 = 0.672
P2 = 0.567
0
270
180

FIG. 6.23

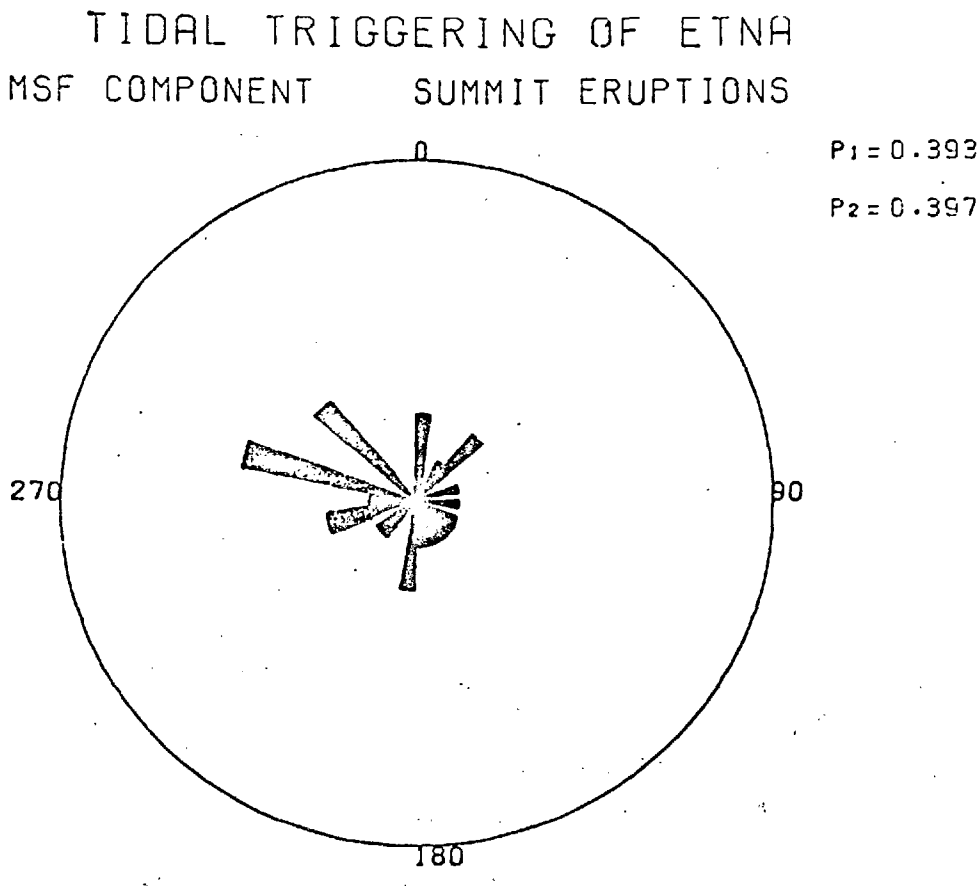

TIDAL TRIGGERING OF ETNA
MSF COMPONENT SUMMIT ERUPTIONS
0
90
180
270
P1 = 0.393
P2 = 0.397

FIG. 6.24

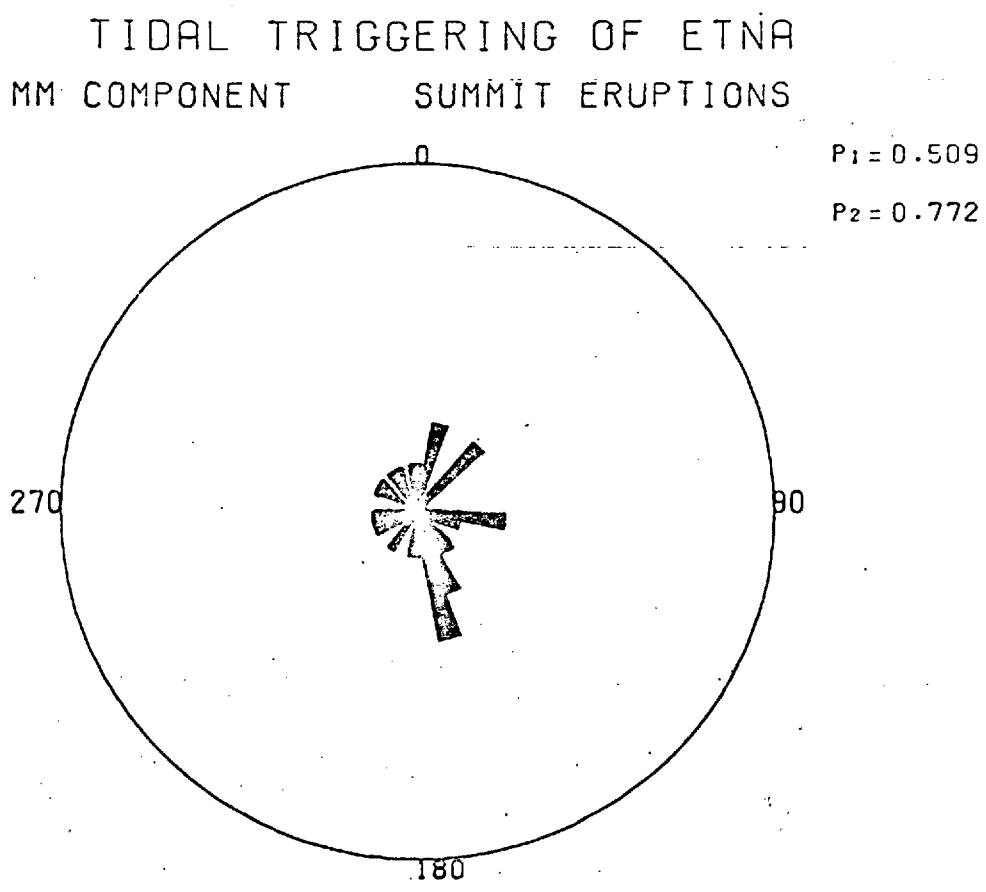

TIDAL TRIGGERING OF ETNA
MM COMPONENT SUMMIT ERUPTIONS
0
90
180
270
P1 = 0.509
P2 = 0.772

FIG. 6.25

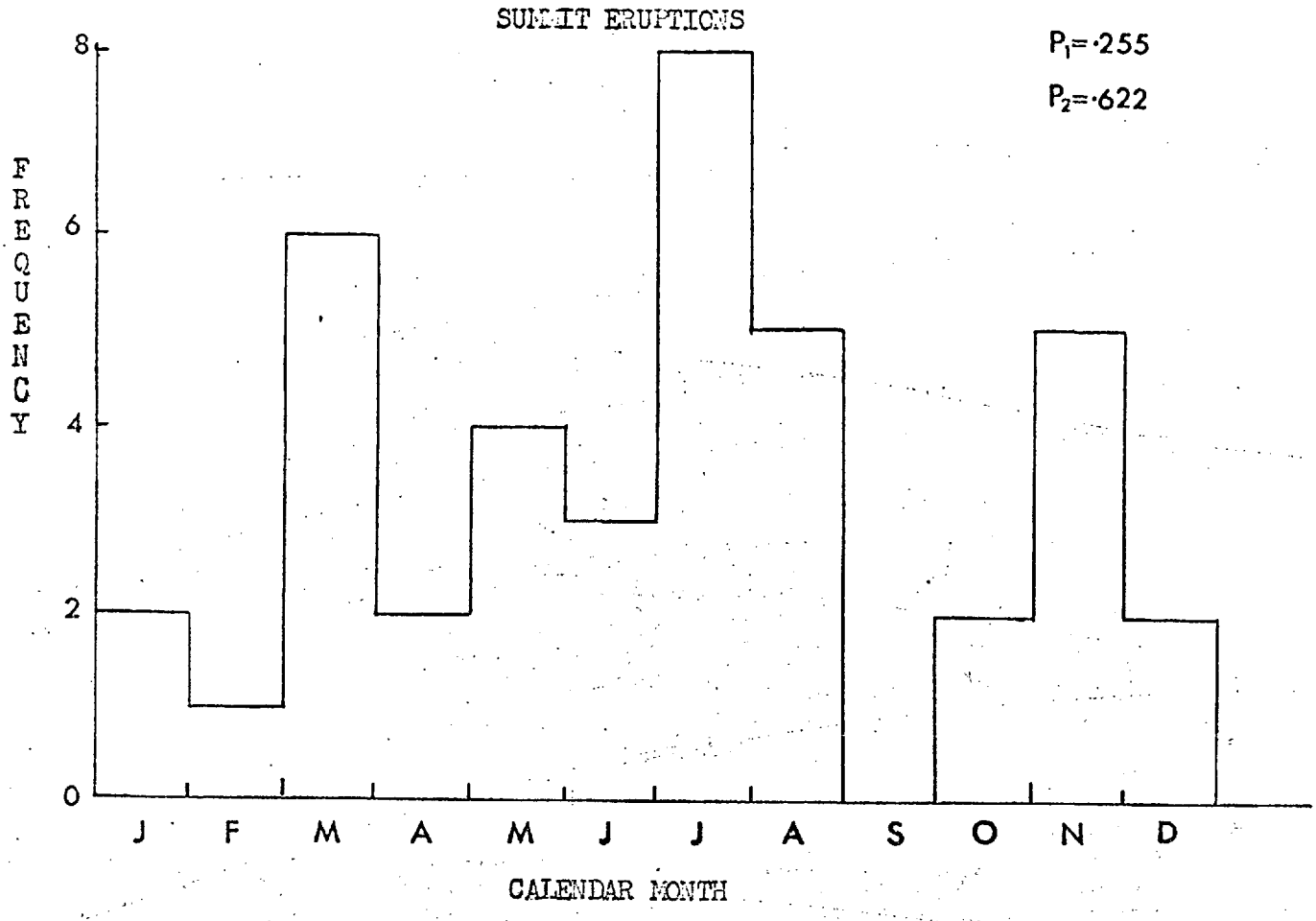


FIG. 6.26

Histogram of the frequency of the onset of summit eruptions per calendar month.

See figure 6.14 for explanation of use.

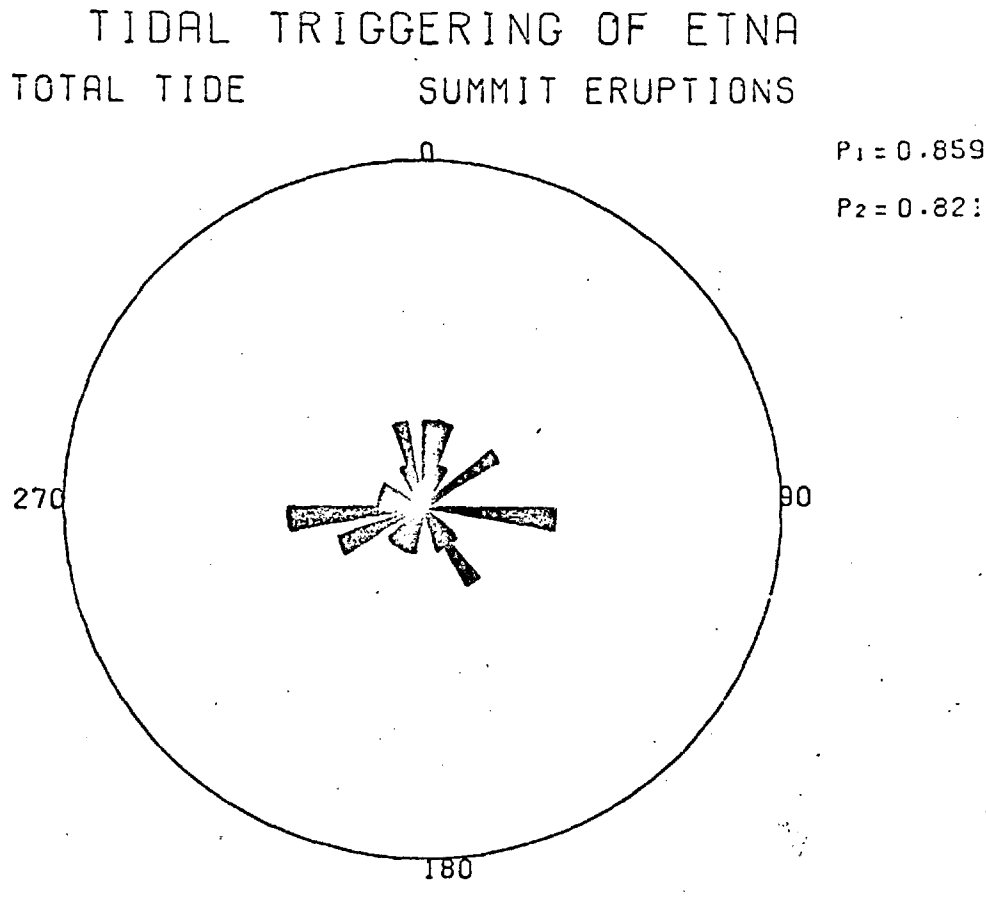

TIDAL TRIGGERING OF ETNA
TOTAL TIDE
SUMMIT ERUPTIONS
P1 = 0.859
P2 = 0.821
0
90
180
270

FIG. 6.27

6.5. SUNSPOT TRIGGERING OF ERUPTIONS

A second phenomenon which has over recent years increasingly attracted attention as a possible earthquake - volcanic eruption trigger is solar activity. Correlations between sunspot activity and volcanic activity have been noticed by Machado (1960) and Mendoça Dias (1962) and a detailed survey by Simpson (1967) resulted in his conclusion that

> solar activity, as indicated by sunspots ..... plays a significant but by no means exclusive role in the triggering of earthquakes.

He found an 87.5% correlation between world-wide seismic activity and sunspot number. He also observed that seismic activity was greatest during periods of moderately high and fluctuating solar activity when solar flares were at their greatest. He postulates two possible mechanisms for the interaction. The first involves abrupt changes in the angular velocity of the earth's rotation which might arise from magnetohydrodynamic coupling between the solar and terrestrial magnetic fields. The second possible mechanism is through surges of electrical current through the crust of the earth. Gribbin (1971, 1973) also suggests a connection between sunspot and seismic activity involving a change in the rotation rate referencing evidence presented

by Challiner (1971) and Mansinha and Smylie (1968). As a point of interest there have been hypotheses correlating sunspot activity with Earth tides (Bigg (1967). Wood and Wood (1965), Wood (1972),) Okal and Anderson (1973) believe all these apparent agreements arise due to the method of calculation used. If an agreement does exist it will lead back into the previous discussion.

Both of these mechanisms could conceivably be triggers for volcanic activity as well as earthquakes as it has been shown (Davis et al., 1974) that there is a pronounced magnetic effect associated with volcanic activity.

To determine the possible effect of sunspot activity on Etnean eruptions the monthly sunspot numbers for the period 1971-1974 were assigned to one of twenty-one groups, ranging from 1-10 to 201-210, where the numbers indicate the number of sunsports in a given month. The normalised probabilities for each group were then calculated. This was necessary since the sunspot numbers are not randomly distributed over the range 0-210 but some groups of values occur more commonly. Forty-one eruptions occurred during this period and it was decided that this number was not great enough to allow a separate analysis of flank and summit eruptions as previously. It

was then assumed that if the eruptions occurring during this period were randomly distributed with sunspot number then the forty-one eruptions should have associated sunspot numbers distributed with the same probability as the 1254 sunspot numbers.

The results of this analysis are given in Table 6.8. The first two columns are self explanatory; column 3 is the normalized probability obtained as shown; column 4 is the predicted distribution of 41 eruptions on a random basis; it is obtained by multiplying 41 by the equivalent probability of column 3. Column 5 is the observed distribution and column 6 is the binomial probability of obtaining the observed value for the probability of column 3.

$$\text{e.g. Category (51-60)} \quad P_{obs} = \frac{41!}{3!\,38!} (.103)^3 (.897)^{38} = 0.19$$

From an inspection of the table it is seen that only once (category 71-80) does the observed probability drop below the 5% significance threshold and that overall the observed data very adequately satisfies a random distribution hypothesis. Thus, as with the earth tide case, the conclusion is that there is no measured correlation between sunspot activity and Etnean volcanic activity.

	SUNSPOTS		ERUPTIONS		
GROUP	NUMBER/GROUP N	N/1254	E_{pred}	E_{obs}	PROB(Obs.)
1-10	196	.156	6.4	8	.12
11-20	167	.133	5.5	4	.16
21-30	126	.100	4.1	6	.11
31-40	89	.071	2.9	0	.05
41-50	92	.073	3.0	4	.17
51-60	129	.103	4.2	3	.19
61-70	112	.089	3.6	4	.17
71-80	82	.065	2.7	6	.03
81-90	47	.037	1.5	2	.26
91-100	38	.030	1.2	0	.29
101-110	58	.046	1.9	1	.29
111-120	32	.026	1.1	1	.37
121-130	10	.008	0.3	0	.72
131-140	18	.014	0.6	1	.33
141-150	18	.014	0.6	1	.33
151-160	10	.008	0.3	0	.72
161-170	5	.004	0.2	0	.85
171-180	5	.004	0.2	0	.85
181-190	10	.008	0.3	0	.78
191-200	8	.006	0.3	0	.78
201-210	2	.002	0.1	0	.92

TABLE 6.8

Results of the correlation of sunspot number with Etnean eruptions. See text for explanation

CHAPTER 7

CONCLUSIONS

In the introduction to this thesis the aims of the research were expressed as:-

1) Attempts to obtain long term crustal deformation measurements as an aid to both eruption forecasting and increased knowledge of the internal processes of the volcano.

2) Attempts to measure tidal parameters with a view to clarifying the position as regards tidal effects on Etna.

3) A statistical assessment of previous eruptions of Etna and based on these results the possibility of predicting eruptions and determining the internal mechanics of the volcano.

4) An investigation of the possibility of triggering eruptions by external forces due to Earth tides and sunspots.

The following is a summary of the conclusions arrived at in the course of this research:-

1) Etna is a little understood and as yet comparatively uninvestigated

volcano. The plate tectonic setting of Sicily appears to be contrary to that which would be expected for Etna to be situated where it is.

2) Previous geological and geophysical research give little or no support to the existence of a central magma chamber controlling Etnean eruptions but the complexity of Etna is such that there appears to be numerous magma conduits from separate sources, the whole volcano in certain respects behaving more like a conglomeration of separate volcanoes than a single one.

3) Previous gravity surveys indicated unusual tidal effects on the volcano, but attempts to measure tidal tilts were hindered by excessive noise and faulty instrumentation. No concrete conclusions could be arrived at in the investigation of tidal effects except that the measurement of tidal tilts on volcanoes is unlikely to be successful with present instrumentation.

4) Long term tilt measurement clearly indicate eruptive events and there is a very close temporal relationship between the tilts and the associated eruptions. This is more likely due to surface effects due to extrusion of lava than internal magma movements. Internal motion of magma is also observed as rather smaller but long period drifts. The possibility of

determining the actual movements of magma is limited by the number of instruments available and also by their inadequate operation.

5) The statistical analysis of previous eruptions provides considerable information on the internal mechanisms of the volcano and corroborates the results of previous geophysical research. Its value in predicting eruptions is limited since the probability of an eruption is found to be substantially independent of time.

6) There is no evidence that eruptions are triggered by Earth tides or sunspot activity. This is in accordance with theoretical considerations, but at variance with conclusions reached on other volcanoes. However, many of the latter are based on an incomplete understanding of tidal theory which considerably reduces their validity.

Overall then, no progress has been made, or was even attempted, in understanding the tectonic setting of Etna. This would require a different geophysical approach, which will be considered in the suggestions for future research below.

As regards the prediction of eruptions the situation is unclear. The monitoring of crustal deformation definitely provides indications of

incipient volcanic activity but is insufficient by itself to indicate anything more than the possibility of activity until an eruption actually begins. There is insufficient data at present to enable an estimate to be made of where the eruption will occur.

Valuable information about the internal structure of the volcano can be obtained by monitoring crustal deformation and such information can also be obtained from a statistical analysis of the intervals between eruptions.

In the light of the result of this research and with its aims in mind certain suggestions for future Etnean research can be made.

The measurement of tidal tilt on volcanoes is incompatible with the measurements of secular crustal deformation with the instruments available during this research project, and since there has been no successful attempt to measure tides on volcanoes attention should be aimed entirely at the monitoring of secular changes. The secular changes also provide more information. However, the monitoring of the secular changes can be best effected by disposing an array of borehole tiltmeters (at least three) around the volcano in the

vicinity of the summit. The summit is generally the site of most activity and most information would be gained by siting the tiltmeters as near as possible to the centre of activity. There is, of course, always the danger that the instruments would be lost under a lava flow.

The gathering of data from such instruments presents a problem since access to the upper slopes is limited by the heavy winter snow and it is a severe disadvantage not to be able to observe tilt changes actually during an eruption: The problems of telemetering the information have been referred to in the text, one of the most important being lightning strikes, but this does appear to be the only possible solution, backed up with slow recording, low power digital recorders at the instrument site. There should also be at least one tiltmeter fully accessible at all times. The 'Observatory' site at Serra La Nave would be very suitable for such an instrument.

Returning to the measurement of tidal tilt. This is at present out of the question with the present instrumentation. The recent development of long baseline tiltmeters (Horsfall and King, 1978) may enable this to be achieved in the future. Such tiltmeters would obviate the effects of local disturbances but are extremely cumbersome

and have not, as yet, been tested under the rigorous conditions that would be faced on Etna.

If these suggestions were adopted, the increased instrumentation on Etna would require more, and more continuous, supervision. The maintenance of continuously recording instruments has presented difficulties in the past, and the only satisfactory solution would appear to be to employ personnel full-time for the purpose. Greater collaboration with the Institute of Volcanology, Catania and the University of Catania might be helpful.

On a broader basis a biannual precise gravity profile for at least the upper half of the volcano should be initiated. This would be useful in itself but especially when combined with the current levelling profiles of Guest and Murray.

A renewal of the precise distance measuring that was done in 1972 (Wadge, 1974) though over a wider area would also tie in with a tilt monitoring programme. Knowledge of Etna would also be enlarged by precise distance measurements to determine the local plate boundary. A preliminary attempt was made by Caputo et al. (1974) but the results were inconclusive, as discussed in Chapter 2. These measurements should ideally be repeated using a more

accurate instrument such as the Mekometer. However, it may be that both sides of the Messina Straits are on the same side of the plate boundary and the results would be inconclusive. If, however, Georan becomes available measurements to distant sites could be taken from the summit of Etna and in due course the local plate boundary with respect to Etna could be determined.

REFERENCES

Allen, M.W., (1936) The Lunar Triggering of Earthquakes in Southern California. Bull. Seism. Soc. Am., 26, 146-157

Allen, R.V., (1972) A Borehole tiltmeter for measurements at tidal sensitivity. Bull. Seis. Soc. Am., 62, 3, 815-821

Allen, R.V., Wood, D.M. and Mortensen, C.E., (1973) Instruments and techniques for tilt (tidal) measurement. Phil, Trans. R. Soc. Lond., 274A, 219-222

Alsop, L.E. and Kuo, J.T., (1964) Characteristic numbers of semi-diurnal earth tidal components for earth models. Annales de Geoph., 20(3), 286-300

Anokhina, K.M. and Ostrovsky, A.E., (1970) On the effect of temperature on tidal tilts of the earth's surface. Obs. Roy. de Belgique Comm. Ser. A, 9, 97-100.

Baker, T.F. and Lennon, G.W., (1973a) Calibration: Confidence in the performance of tiltmeters and gravimeters. 7th Int. Sym. Earth Tides, Sopron Hungary.

Baker, T.F., and Lennon, G.W., (1973b) Tidal Tilt Anomalies. Nature, 243, 75-76

Barberi, F., Gasparini, P., Innocenti, F. and Villeeri, L., (1973) Volcanism of Southern Tynhenian Sea and its geodynamic implications. J Geophys. Res., 78, 5221-5232.

Barberi, F., Civetta, A., Gasparini, P., Innocenti, F., Scandone, R. and Villari, L., (1974a) Evolution of a section of the Africa-Eruope plate boundary: Palaeomagnetic and volcanological evidence from Sicily. Earth and Plant. Sei. Letters, 22, 123-132

Barberi, F., Innocenti, F., Ferrara, G., Keller, J. and Villari, L., (1974b) Evolution of Eolian Arc volcanism (Southern Tyrrhenian Sea). Eart and Plan. Sei. letters, 21, 269-276.

Barford, N.C., (1967) Experimental Measurements: Precision, Error and Truth. Addison-Wesley.

Bartels, J., (1957) Gezeitenkrafte, Encyclopaedia of Physics Vol. 48 Geoph II, 734-774, Springer-Verlag

Båth, M., (1975) Spectral Analysis in Geophysics. Elsevier

Beavan, R.G., (1975) Earth Strain: Ocean Landing and analysis, Ph.D, Thesis Cambridge University.

Belderson, R.H., Kenyon, N.H. and Stride, A.H., (1974) Calabrian ridge, a newly discovered branch of the Mediterranean ridge. Nature, 247, 453-454.

Berger, J., (1975) A note on thermoelastic strains and tilts. J. Geophys. Res., 80, 2, 274-277

Bigg, E.K., (1967) Astron. J., 72, 463

Blanchard, F.B. and Byerly, P., (1935) A study of a well-gauge as a seismograph Bull. Seis. Soc. Am., 25, 4, 313-321

Booth, B., (1975) Some observations on the 1974 Mount Etna eruption (9-15 February). United Kingdom Research on Mount Etna, 1973 London, Royal Society

Bottari, A. and Riuscetti, M., (1967) La stazione Simica di Serra La Nave sull'Etna. Ann. di. Geofis., 20, 243-264

Bredehoeft, J.D., (1967) Response of well-aquifer systems to earth tides. J. Geophys. Res., 72, 12, 3075-3087

Caire, A., (1970) Sicily in its Mediterranean setting. in: Geology and History of Sicily Pet. Expl. Soc. Libya, Tripoli

Caputo, M., Panza, G.F. and Postpischl, D., (1970) Deep structure of the Mediterraniean basin. J. Geophys. Res., 75, 26, 4919-4923

Caputo, M., Folloni, G., Pieri, L. and Unquendal, M., (1974) Geodimetric control across the Straits of Messinu. Geophys. J.R. astr. Soc., 38, 1-8

Carapezza, M., (1962) Un essernpio di enizione Caterale da Faglia rell' aparto eniltiur Etneo. Acta. Geol. Alpina, 8, 249-276

Carter, S.R. and Bell, J.D., (1975) Geological studies of the Bronte and Randazzo areas. United Kingdom Research on Mount Etna 1974. London, Royal Society

Cartwright, D.E. and Tayler, R.J., (1971) New computations of the tide-generating potential. Geophys. J.R. astr. Soc., 23, 45-74

Challinor, R.A., (1971) Science, 172, 1022

Cooper, G.L., (1970) Development and use of a two-axis electrolytic bubble level as a precision vertical reference and tilt indicator. Guidance, Control and Flight Mechanics Conference of AIAA Scenta Barbara, California 1970

Cox , D.R., (1962) Renewal Theory. Methuen and Co., London.

Cristofolini, R., (1973) Recent trends in the study of Etna. Phil. Trans. R. Soc. Lond., 274A, 17-35

Darwin, G., (1882) The Lunar disturbance of gravity. Scient. Papers, 1, 14, 430-443

Darwin, G., (1907) On variations in the vertical due to elasticity of the earth's surface. Scientific Papers Vol.I Cambridge University Press.

Davis, P.M., Hastie, L.M. and Stacey, F.D., (1974) Stresses within an active volcano - with particular reference to Kilanea. Tectorophys. 22, 355-362

Decker, R.W. and Kinoshita, W.T., (1972) Geocletic Measurements. in The Surveillance and Prediction of Volcanic Activity, UNESCO.

Decker, R.W., (1973) State-of-the-Art in volcano forecasting. Bull. Volc., 37, 3, 372-393

Dietrich, J.H. and Decker, R.W., (1975) Finite element modeling of surface deformation associated with volcanism. J. Geophys. Res., 80, 29, 4094-4102

Dix, C.H., (1964) Earthquakes and earth tides, Unpublished Report, Caltech.

Doodson, A.T., (1922) The harmonic development of the tide-generating potention. Proc. R. Soc. Lond., 100A, 305-329

Ducarme, B. and Melchior, P., (1978) A trans-world gravity profile. Phys. Earth and Plan. Int., 16, 257-276

Eaton, G.P. and Lipman, P.W. (1977) Changes in deformation mode of Kilanea volcano. IAVCEI Durham (Abs.)

Eaton, J.P., (1959) A portable water-tube tiltmeter. Bull. Seis. Soc. Am., 49, 4, 301-316

Eaton, J.P., (1962) Crustal structure and volcanism in Hawaii. in: The Crust of the Pacific Basin, Geophys. Monog. 6, Eds. Smith, W., MacDonald, G.A. and Kuno, H.

Eggers, A.A. and Decker, R.W., (1969) Frequency of historic volcanic eruptions. EOS, Trans. Am. Geoph. Union, 50 : 343(Abs)

Endo, E.T., Ward, P.L., Harlow, D.H., Allen, R.V. and Eaton, J.P., (1974) A prototype global volcano surveillance system monitoring seismic activity and tilt. Bull. Volc., 38, 2, 3-5-344

Explanatory Supplement to the Astronomical Ephemeris (1961) HMSO, London

Fedotov, S.A., Enman, V.B., Nikitenko, Yu. P., Shulman, V.A., Magustin, M.A., levin, V.E., Zhaninov, N.A. and Enman, S.V., (1977) Crustal deformations near new Tolbachik volcanies. IAVCEI, Durham (Abs)

Fiske, R.S. and Kinoshita, W.T., (1969) Inflation of Kilanea volcano prior to its 1967-1968 eruption. Science, 165, 3891, 341-349

Fiske, R.S., Jezouin, G., Kinoshita, W.T., Rowley, K., Shepherd, J.B., Siebert, L., Tomblin, J.F. and Viode, J.P., (1977) Tilt monitoring stations established on Lesser Antillean volcanoes. IAVCEI, Durham (Abs).

Francaviglia, A., (1959) L'Imbasamento sedimentario dell'Etna e il golfo pre-Etneo. Boll. Serv. Geol. Ital., 81, 4-5, 583-684

Giese, P., Morelli, C. and Steinmetz, L., (1973) Main features of crustal structure in western and southern Europe based on data of explosion seismology. Tectorophys., 20, 367-379

Golombek, M.P. and Carr, M.J., (1978) Tidal triggering of seismic and volcanic phenomena during the 1879-1880 eruption of Islas Quemadas volcano in El Salvador, Central America. J. Volcanol. Geotherm. Res., 3, 299-307

Gorshkov, G.S., (1960) Some results of seismometric investigations at the Kamchatka volcanological station. Bull. Volc., 23, 121-128

Gribbin, J., (1971) Relation of sunspot and earthquake activity. Science, 173, 3996, 558

Gribbin, J., (1973) Planets, Sunspots and Earthquakes. The Observatory, 93, 994, 121

Grindley, G.W., (1973) Structural control of volcanism at Mount Etna Phil. Trans. R.Soc. Lond., 274A, 165-175

Guest, J.E., (1973) The summit of Mount Etna prior to the 1971 eruptions. Phil. Trans. R. Soc. Lond., 274A, 63-78

Guest, J.E., Huntingdon, A.T., Wadge, G., Brander, J.L., Booth, B., Carter, S. and Duncan, A. (1974) Recent eruption of Mount Etna. Nature, 250, 385-387

Guest, J.E. and Murray, J.B., (1977) Summary of volcanic activity during 1975/76. United Kingdom Research on Mount Etna 1976-76. London, The Royal Society.

Hagiwara, T., (1947) Observation of changes in the inclination of earth's surface at Mount Tsukuba (Third Report). Bull. Earth. Res. Inst., 25, 27-32

Hagiwara, T., Rikitake, T. and Yamada, J., (1948) Observations of the deformation of the earth's surface at Aburatsubo, Miura Peninsula. Part 2. Bull. Earth. Res. Inst., 26, 23-26.

Hagiwara, T., Rikitake, T., Kasahara, K., and Yamada, J., (1949a) Observations of the deformations of the earth's surface at Aburatsubo, Miura Peninsula. Part II. Bull. Earth. Res. Inst., 27, 35-38

Hagiwara, T., Rikitake, T., Kasahara, K. and Yamada, J., (1949b) Observations of the deformations of the earth's surface at Aburatsubo, Miura Peninsula. Part III. Bull. Earth. Res. Inst., 27, 39-44

Hagiwara, T., Kasahara, K., Yamada, J. and Saitu, S., (1951) Observations of the deformations of the earth's surface at Aburatsubo, Miura Peninsula. Part IV. Bull. Earth. Res. Inst., 29, 455-468.

Hagiwara, T. and Kasahara K., (1951) Observations of the deformations of the earth's surface at Aburatsubo, Miura Peninsula. Part V. Bull. Earth. Res. Inst., 29, 558-561

Hamilton, W.L., (1973) Tidal cycles of volcanic eruptions. Fortnightly to 19 yearly periods. J. Geophys. Res., 78, 17, 3363-3375

Harrison,J.C., (1976a) Cavity and topographic effects in tilt and strain measurements. J. Geophys. Res., 81, 2, 319-328

Harrison, J.C., (1976b) Tilt observations in the Poorman mine near Boulder, Colorado. J. Geophys. Res., 21, 2, 329-336

Harrison, J.C. and Herbst, K., (1977) Thermoelastic strains and tilts revisited

Heaton, T.H., (1975) Tidal triggering of earthquakes. Geophys. J.R. astr. Soc., 43, 307-326

Henbest, S.N., Mills, A.A. and Ottey, P., (1978) Tilt and seismicity measurements on Mount Etna, September to December 1976. J. Volcanol. and Geotherm. Res., 4, 1/2,133-149

Homma, S., (1952) Some problems on the thermo-elastic deformations of the earth's crust. The Geophysical Magazine, 23, 2, 125-144

Horsfall, J.A.C. and King, G.C.P., (1978) A new geophysical tiltmeter. Nature, 274, 5672, 675-676

Imbo, G., (1965) Catalogue of the active volcanoes and solfatara fields of Italy. Catalogue of the active volcanoes of the world Part XVIII. Ed. International Association of Volcanology.

Jaggar, T.A., (1920) Seismometric investigation of Hawaiian lava column. Bull. Seis. Soc. Am., 10, 4, 120-275

Jaggar, T.S. and Finch, R.H., (1929) Tilt records for thirteen years at the Hawaiian volcano observatory. Bull. Seis. Soc. Am., 19, 30-51

Jenkins, G.M. and Watts, D.G., (1969) Spectral Analysis and its applications. Holden - Day.

Jobert G., (1960) Perturbations des Marees Terrestres. Ann. Geoph., 16, 1-55

Johnston, M.J.S. and Mauk, F.J., (1972) Earth tides and the triggering of Mount Stromboli, Italy. Nature, 239, 266-267

Jones, A.E., (1937) Ground-surface displacements and earthquakes at Kilanea, Hawaii, First half-year 1935. Bull. Seis. Soc. Am., 27, 113-138

Jones, L., (1964) La station clinometrique souterraine de Nicolosi au volcan Etna. Comm. Obs. Roy. de Belgique, 10, 236, 280-288

Kelvin, Lord (1863) Dynamical problems regarding elastic speroidal shells and spheroids of incompressible liquid. Oscillations of a liquid Sphere. Phil. Trans. R. Soc. Lond., 153

Keffer, G., (1969) Origine explosive de la Oalle del Bove (Etna, Sicile). C.R. Acad. Sei. Paris, 269, 1938-1941

Keffer, G., (1975) Sur l'existence d'une "rift zone" a l'Etna (Sicile). C.R. Acad. Sei. Paris, Ser. D, 280, 263-266

King, G.C.P., (1971) The siting of strainmeters for teleseismic and tidal studies. in: Recent Crustal Movements, Royal Soc. New Zealand Bull, 9, 239-247

King, G.C.P. and Bilham, R.G., (1973) Tidal tilt measurement in Europe. Nature, 243, 74-75

Klerkx, J., (1970) La caldera de la Valle del Bove: sa signification dans l'evolution de l'Etna. Bull. Volc., 34, 726-737

Knopoff, L., (1964) Earth tides as a triggering mechanism for earthquakes. Bull. Seis. Soc. Am., 54, 6, 1865-1870

Knopoff, L. and Garner, J.K., (1972) Higher seismic activity during local right on the raw world-wide earthquake catalogue., Geophys. J.R. astr. Soc., 28, 311-313

Kubotera, A. and Yoshikawa, K., (1963) Prediction of volcanic eruption ASO and Sukurazima and some related geophysical problems. Bull. Volc., 26, 297-317

Lennon, G.W. and Baker, T.F., (1973) Earth tides and their place in geophysics (summary). Phil. Trans. R. Soc. Lond., 274A, 199-202

Love, A.E.H., (1909) The yielding of the earth to disturbing forces. Proc. Roy. Soc. Lond., 82, 73-88

Love, A.E.H., (1911) General Theory of Earth Tides. in: Some problems of geodynamics. Cambridge University Press

Machado, F., (1960) Secular variation of seismo-volcanic activity in the Azores. Bull. Volc., 23, 101-107

Machado, F., (1965) The Messina earthquake of 1908 and the magma chamber of Etna. Bull. Volc., 28, 375-380

Machado, F., (1967) Activity of the Atlantic volcanoes 1947-1965. Bull. Volc., 30, 29-34

Machado, F., (1974) The search for magmatic reservoirs. in: Physical Volcanology Eds. Caretta, A., Casparine, P., Luongo, G. and Rapolla, A.

Mansinha, L. and Smylie, D., (1968) Earthquakes and the Earth's Wobble Science, 161, 1127

Mason, R.G., (1975) Distance and tilt measurement. United Kingdom Research on Mount Etna 1974. London, Royal Society

Mason, R.G., Bill, M.G. and Muniruzzaman M, (1975) Microgravity and Microearthquake studies. United Kingdom Research on Mount Etna 1974. London, Royal Society

Mauk, F.J. and Johnston, M.J.S., (1973) On the triggering of volcanic eruptions by earth tides. J. Geophys. Res., 78, 17 3356-3362

McDonald, G.A., (1972) Volcanoes, Prentice-Hall, New Jersey.

McKenzie, D.P., (1970) Plate tectonics of the Mediterranean region. Nature, 226, 239-243

Melchior, P., (1966) The Earth Tides., Pergamon Press, London

Melchior, P., Kuo, J.T. and Ducarme, B., (1976) Earth tide gravity maps for western Europe. Phys. Earth and Plan. Int., 13, 184-196

Mendoza Dias, A.A. de, (1962) The volcano of Capelinhos (Azores), the solar activity and the earth tide. Bull. Volc., 24, 212-221

Michael, M.D. and Christoffel, D.A., (1975) Triggering of eruptions of Mt. Ngaurguhoe by fortnightly earth tide maxima, January 1972 - June 1974. N.Z. Journ. Geol. and Geophys., 8, 2, 273-277

Minakami ., T., (1942) On volcanic activities and tilting of the earth's surface. Bull. Earth. Res. Inst., 20, 432-464

Minakami ., T., (1947) Recent activities of volcano Usu (II) Bull. Earth. Res. Inst., 25 65-70

Minakami ., T., (1950) Recent activities of volcano Usu (V). Bull. Earth. Res. Inst., 28, 143-152

Minakami ., T., (1960) Fundamental Research for predicing volcanic eruptions (I). Earthquakes and crustal deformations originating from volcanic activities. Bull. Earth. Res. Inst., 38, 497-544

Minakami., T., (1964) On the possibility of impossibility of standardizing the observations in volcanological observations. Bull. Volc., 27, 413-414

Minakami., T., (1974) Prediction of Volcanic Eruptions. in: Physical Volcanology Eds., Civetta, L., Gaspanini, P., Luongo, G. and Rapolla, A., Elserier

Mogi, K., (1956) Relations between the eruptions of various volcanoes and the deformations of the ground surfaces around them. Bull. Earth. Res. Inst., 36, 99-134

Mohamed, I., (1978) Earth tide studies on Mount Etna, Sicily. Ph.D. Thesis. London University.

Morrissey, S.T., (1976) Special study of the adaptation of commercial tiltmeters for monitoring geophysical phenomena in harsh environments. U.S.G.S. Technical Report.

Muniruzzaman, M., (1977) Micro-earthquake and background seismic noise studies on Mount Etna, Sicily. Ph.D Thesis University of London

Murray, J.B., (1977) Changes at the summit of Mount Etna 1973-1975. United Kingdom Research on Mount Etna 1975-76. London, Royal Society

Murray, J.B., Guest, J.E. and Butterworth, P.S., (1977) A large ground deformation on Mount Etna volcano. Nature, 226, 338-340

Ogniben, L., (1966) Lineamenti idrogeological dell' Etna. Rev. Min. Sicil., 24, 100-102

Okal, E. and Anderson, D.L., (1975) On the planetary theory of sunspots. Nature, 253, 5492, 511-513

Omori, F., (1911) The Usu-San eruptions and earthquakes and elevation phenomena Bill. Earth. Invest. Comm., Japan 5 and 9

Phillips, I.M. (1978) Crustal deformation of Mount Etna. Geophys. J.P. Astr. Soc., 53, 168 (Abs.)

Popov, V.V., (1960) Thermal deformations of the earth's surface. Bull (IEV) Acad. Sci, USSR. Geoph. 7, 611-615

Rayleigh, Lord, (1919) On the problem of random vibrations and of random flights in one, two or three dimensions. Phil. Mag. J. of Sci., 37

Ritsema, A.R., (1969) Seismic data of the western Mediterranean and the problem of oceanization. Verhand. Kon. Ned. Geol. Myn. XXVI, 105-120. (Symposium on the problem of oceanization in the western Mediterranean).

Rittmann, A., (1962) Volcanoes and their Activity. J. Wiley and Sons, London.

Rittmann, A., (1963) Volcanismus and Tektonik der Aetna. Geol. Rand., 53, 788-800

Rittmann, A., (1973) Structure and evolution of Mount Etna. Phil. Trans. R. Sec. Lond., 274A, 5-16.

Rittmann, A., Romano, R, and Stariale, C., (1971) L'erizione Etnea dell' Aprile - Guigno. Atti. Accad. Gioenia Sci. Nat. Catania, Ser. 3,

Ryall, A., Van Wormer, J.D. and Jones, A.E., (1968) Triggering of microearthquakes by earth tides and other features of the Truckee, California, earthquake sequence of September, 1966. Bull. Seis. Soc. Am., 58, 1, 215-248

Shida, T., (1912) Horizontal pendulum observations of the change of plumb line at Karnigamo, Kyoto. Memoirs of the Coll. of Science and Engineering, Kyoto Imperial Univ., 4, 23-174

Shimozuru, D. and Kakagawa, I., (1970) Tidal oscillation of Halemaumau lava lake, Kilanea, Hawaii and its implication for existence of a magma reservoir. Obs. Roy. de Belgique Comm. Ser. A., 9, 163-166

Shirokov, I.A. and Anokhina, K.M., (1976) Local temperature tilts of the earth's surface Proc. VII INT. SYM. Earth Tides, Sopron (Hungary).

Schlien, S., (1972) Earthquake-tide correlation. Geophys. J.R. Astr. Soc. 28, 27-34

Simpson, J.F., (1967) Solar activity as a triggering mechanism for earthquakes. Earth and Plan. Sci. Letters, 3, 417-425

Sturiale, C., (1967) Su alaine piroclastiti del passo versante meridionale dell' Etna Rend. Soc. Min. Ital., 23, 427-452

Takeuchi, H., (1950) On the earth tide of the compressible earth of variable density and elasticity, Trans. Am. Geoph. Union, 31, 651-689

Tamrazyan, G.P., (1968) Principal regularities in the distribution of major earthquakes relative to solar and lunar tides and other cosmic sources. Icarus, 9, 574-592

Tanaka, T., (1969) Study on meteorological and tidal influences upon ground deformations, Spec. Contrib. Geoph. Inst. Kyoto Univ, 9, 29-90

Tokarev, P.I., (1971) Forecasting volcanic eruptions from seismic data. Bull. Volc., 35, 243-250

Tomaschek, R., (1957) Tides of the solid earth. in: Encyclopaedia of Physics Vol. 48. Geoph. II, Springer-Verlag 1957

Wadge, G., (1974) Volcanic deformation and the eruptive mechanism of Mount Etna, Ph.D. Thesis. London University.

Wadge, G., (1976) The deformation of Mount Etna 1971-1974, J. Volcanol. Geotherm. Res., 1, 237-263

Wadge, G., (1977) The storage and release of magma on Mount Etna, J. Volcanol. Geotherm. Res., 2, 361-384

Wadge, G., Horsfall, J.A.C. and Brander, J.L., (1975) Tilt and strain monitoring of the 1974 eruption of Mount Etna. Nature, 254, 21-23

Waltershausen, W.S. von, (1880) Der Atna, Vol. I, II, W. Engelman, Leipzig

Wickman, F.E., (1966) Repose-period patterns of volcanoes. I. Volcanic eruptions regarded as random phenomena. Arkiv.Miner. Geol., 4, 291-301

Wickman, F.E., (1966b) Repose-period patterns of volcanoes. II. Eruption histories of some East-Indian volcanoes. Arkiv. Miner. Geol., 4, 303-317

Wickman, F.E., (1966c) Repose-period patterns of volcanoes. III. Eruption histories of some Japanese volcanoes. Arkiv. Miner. Geol., 4, 319-335

Wickman, F.E., (1966d) Repose-period patterns of volcanoes. IV. Eruption histories of some selected volcanoes. Arkiv. Miner. Geol., 4, 337-350

Wickman, F.E., (1966e) Repose-period patterns of volcanoes. V. General discussion and a tentative stochastic model. Arkiv. Miner. Geol., 4, 5, 351-367

Wickman, F.E., (1976) Markov models of repose-period patterns of volcanoes. in: Random Processes in Geology ed. Mernam, D.F., Springer-Verlag.

Willis, D.E. and Taylor, R.W., (1974) Investigation of multiple seismic events and first zone discriminants, ARPA semi-annual technical report, April 1974, Caltech.

Wood, K.D., (1972) Sunspots and planets. Nature, 240, 5376, 91-93

Wood, R.M. and Wood, K.D., (1965) Nature, 208, 129

Yamakawa, N., (1955) Zisin (Jour. Seis. Soc. Japan) (ii) 8, 84

Yokoyama, I., (1971) A model for the crustal deformations around volcanoes. J. Phys. Earth. 19, 3, 199-207

Yokoyama, I., (1972) Gravimetric, magnetic and electrical methods in: The Surveillance and Prediction of Volcanic Activity. UNESCO 197

Yokoyama, I., (1974) Crustal deformations associated with volcanic activities. Tectonophys., 23, 349-360

Zadro, M.B. and Chiaruttini, C., (1973) Loading effects of the Mediterranean tides. Proc. VII. Int. Sym. Earth Tides. Sopron (Hungary).

APPENDIX A

COMPUTER PROGRAMS

A.1 INTRODUCTION

Three computer programs have been used in the course of this study. Two of these, SPECANL and TIDE are modified versions of programs supplied by the Co-operative Institute for Research in Environmental Sciences, and were written by J.C.Harrison (1971). The third program TIDECOM was written specially for this research.

SPECANL is the program that was used in the data processing and is predominately a spectral analysis program, as its name implies. TIDE and TIDECOM are the two programs that were used to predict the tides.

The modifications that have been made to the programs have been, mainly, to allow them to be implemented on the particular computer installation at Imperial College. In a few cases there have been some changes in the coding and provision has been for graphical output.

A.2 SPECANL

SPECANL is the program that has been used for all the data processing. It comprises five subroutines four of which can been called through the main program and the other called by another subroutine.

The subroutines are:

1. REMOVO

REMOVO amends the data to allow for any offsets. These may have arisen as a result of a calibration signal being applied to the record, or when the trace has been re-centralised to keep it on the chart paper.

2. DOODSON

As its name implies, this subroutine applies a Doodson filter to the offset corrected (if necessary) data. This filter can be written using Labrouste's notation as:

$$X_0 = \frac{1}{30}(2Y_1 + Y_2 + Y_3 + 2Y_4 + Y_6 + Y_7 + 2Y_9 + Y_{11} + Y_{12} + Y_{14} + Y_{17} + Y_{19})$$

where $Y_n = y_n + y_{-n}$

and the y's are the values of the various data points. The drift corrected value is given by:

$$y'_0 = y_0 - X_0$$

3. FOSCAN

FOSCAN controls the Fourier analysis of the processing and in turn calls subroutine FRQ which then computes the Fourier spectrum. Initially the Doodson filtered data, from which the long period components have been removed as descibed above, is smoothed by the application of a Hamming filter:

$$Y''_n = Y'_n\ (.54+.46\cos(-\pi+2n\pi/(N-1)))$$

where Y''_n is the nth. smoothed point

and Y'_n " " " unsmoothed, drift corrected, data point.

The Hamming filter is a low pass filter.

FRQ performs a standard Fourier analysis as has been described in Chapter 5. The computed spectrum is calculated between limits specified in the input data. The output spectrum is then smoothed by the application of a Parzen filter.

4. ALIN

This subroutine calculates a least-squares straight line to fit the data, and removes it from the data. This is effectively removing any long period components from the data. It is, however, not as discriminatory as a Doodson filter and is also inappropriate for those cases where there are changes in the direction of the drift, particularly important in this study.

In practice, therefore, all the data was first filtered by a Doodson filter and then its spectrum calculated by Fourier analysis.

A block diagram of SPECANL is given in figure A.1.

A.3 TIDE

Of the two programs used in tidal prediction, TIDE is used to predict the total tide. It is accurate to 0.1% (Harrison, 1971).

The main program first calls a subroutine NOMAN1 which, when supplied with the required starting time for the tidal prediction, the number of computations of the tide and the interval between computations, calculates the polar angles of the sun and moon and their longitude east of Greenwich.

A second subroutine TIDE67 is then called. This subroutine utilizes the data calculated in NOMAN1 and then computes the tide for a specific location. The tide may be either the gravity tide normal to the Earth ellipsoid, or the tilt tide in a tangent plane to the Earth ellipsoid.

The mathematics involved is quite complicated and is given in detail in Harrison (1971).

A block diagram of the program is given in figure A.2.

A.3 TIDECOM

TIDECOM calculates separate tidal components by evaluating, in each case, the argument, as described in Chapter 3, and multiplying by a factor dependent upon the location at which the tides are computed.

A subroutine ASTRO computes the various orbital parameters s,h,p etc. from initial values provided by the Astronomical Epheneris, and also the latitude dependent terms:

$$\text{LNGPFAC} = 1/2(1 - 3\sin^2(2\pi\theta/360)).C$$

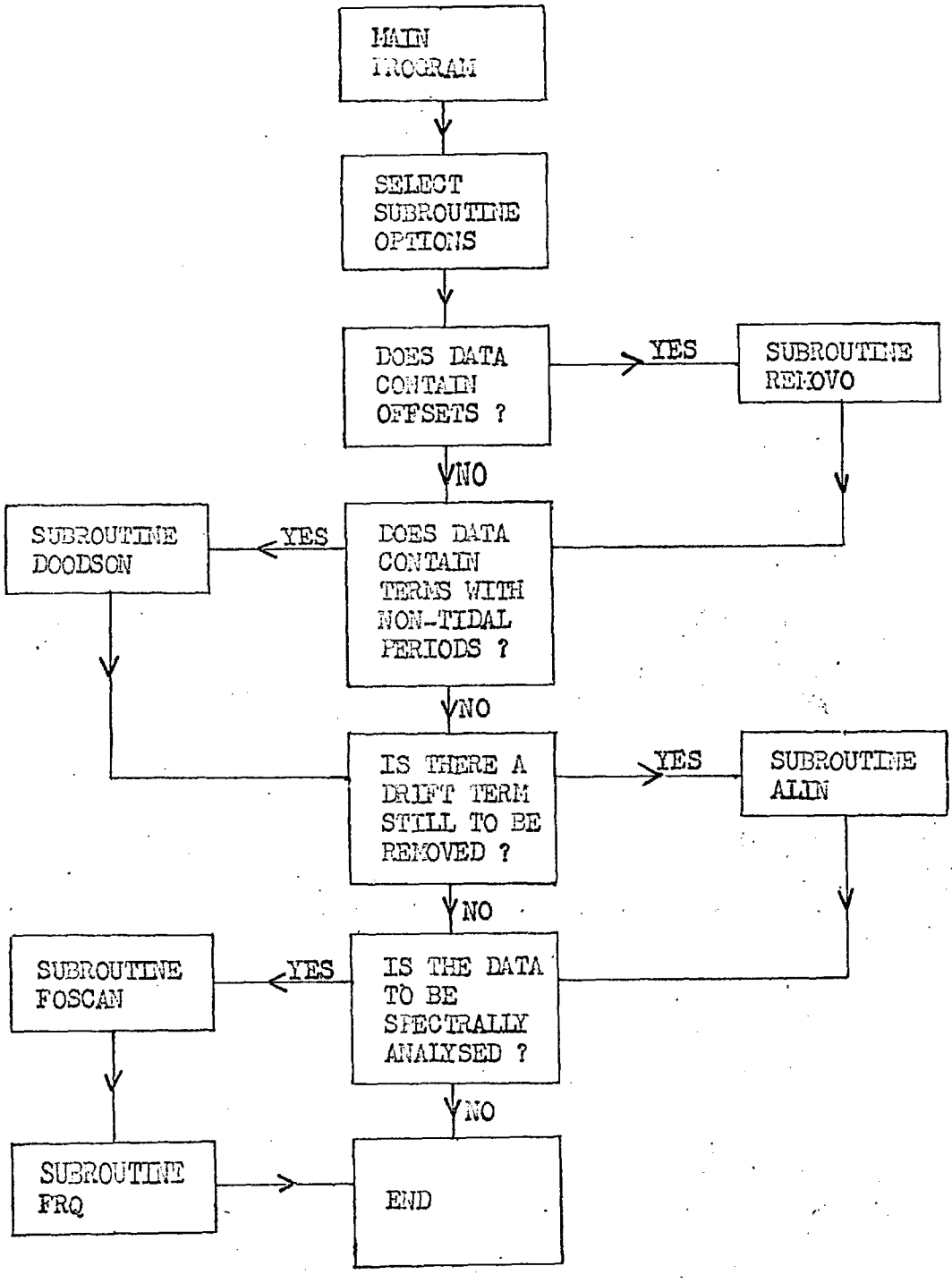
$$\text{DIURFAC} = \sin(4\pi\theta/360).C$$

$$\text{SEMIFAC} = \cos^2(2\pi\theta/360).C$$

where LNGPFAC, DIURFAC, and SEMIFAC are the factors for the long period, diurnal and semi-diurnal terms respectively, and C is a multiplying constant.

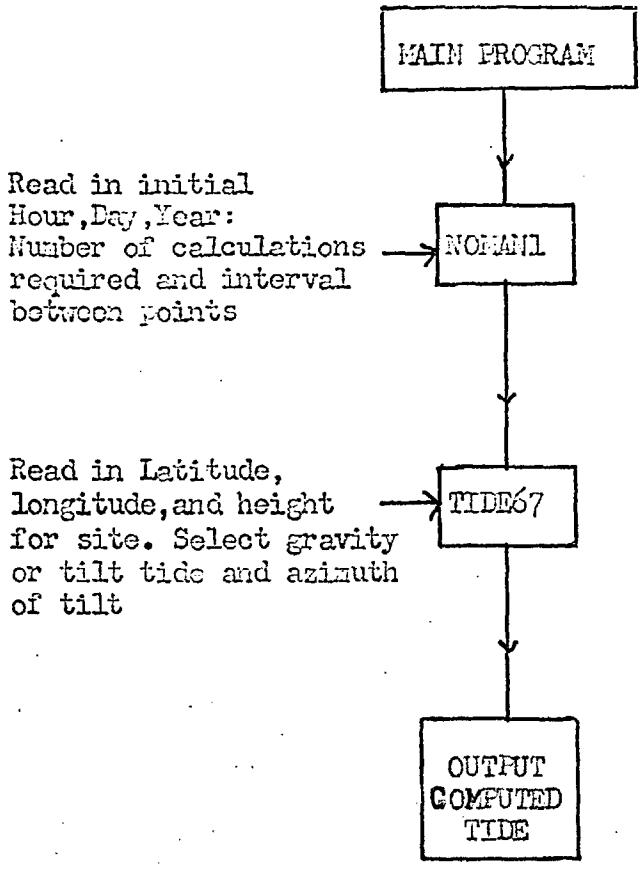
Separate subroutines for each tidal component can then be called as required. These calculate the arguments for the components and then compute the gravity tide only.

A block diagram of the program is given in figure A.3



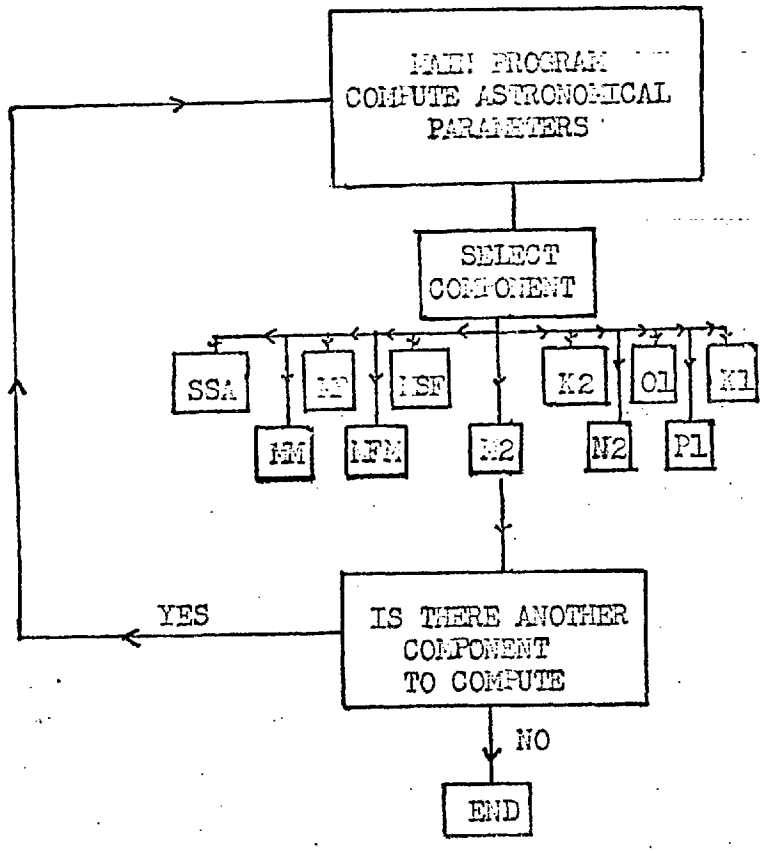
SPECANL

FIG.A.1


MAIN PROGRAM
Read in initial Hour, Day, Year: Number of calculations required and interval between points
NOMAN1
Read in Latitude, longitude, and height for site. Select gravity or tilt tide and azimuth of tilt
TIDE67
OUTPUT COMPUTED TIDE

TIDE

FIG. A.2



TIDECOM

FIG. A.3

APPENDIX B

The following six figures are the tidal power spectra which were not included in Chapter 5. In general, heavy contamination of the tilt signals due to atmospheric effects, or rapid tilt changes have rendered the resultant power spectra of little value as regards tidal signals.

As with the similar figures in Chapter 5 all the power spectra have been normalised with respect to M2=1.

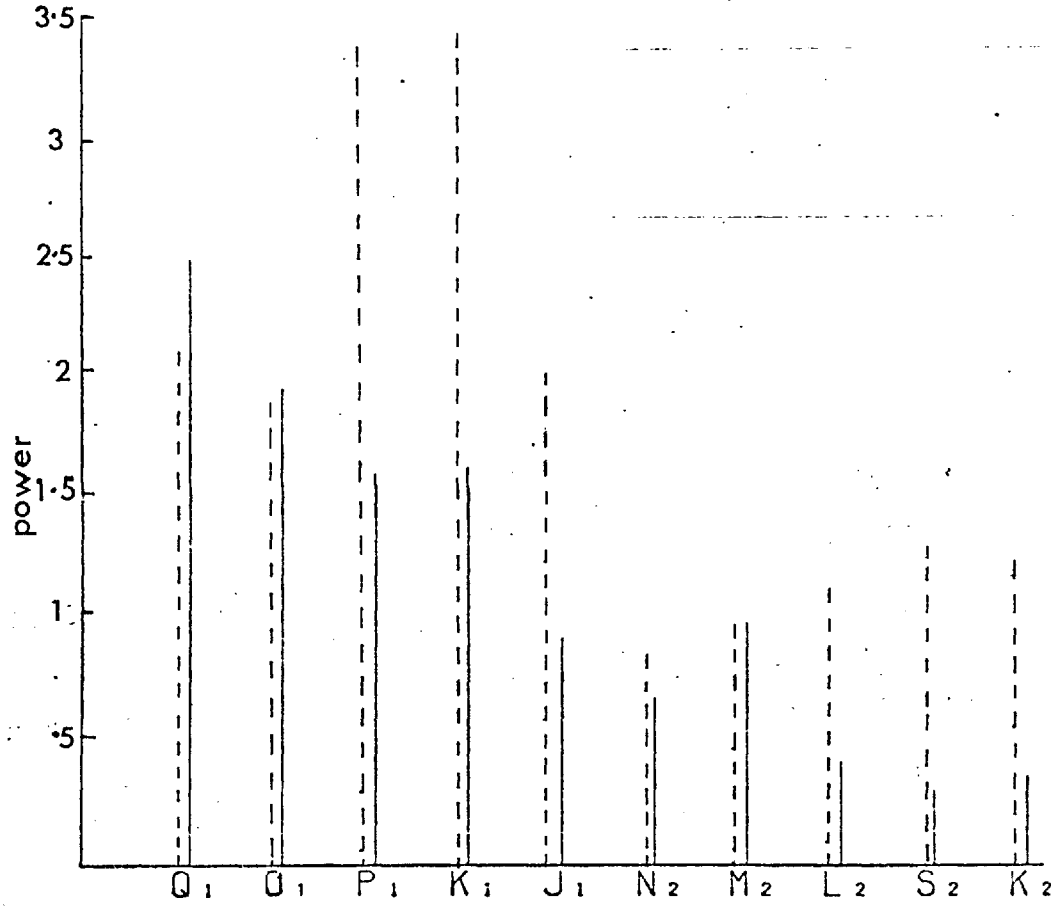
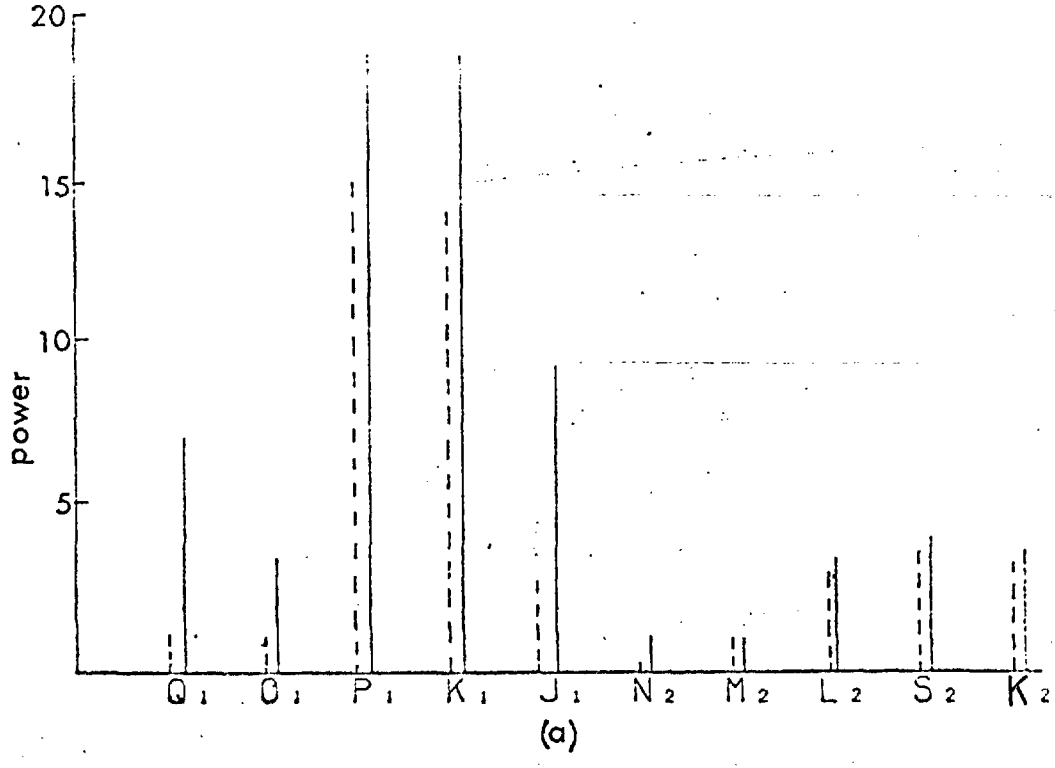


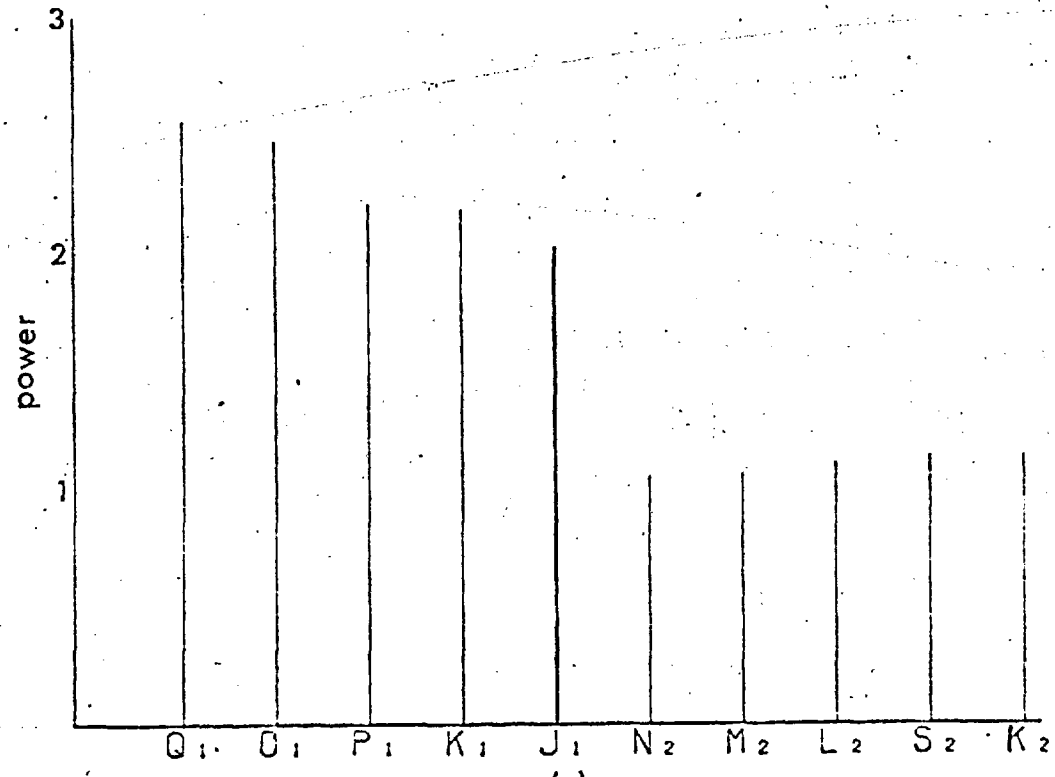
FIG. B.1

Tidal power spectra obtained from data collected at the observatory site over the period 28/8/76 - 16/9/76.

Straight lines - radial axis ; Dashed lines - Tangential axis



(a)



(b)

FIG. 3.2

Tidal power spectra obtained from data collected at

(a) the observatory over the period 21/9/76 - 24/10/76
(b) the borehole " " " 28/9/76 - 7/10/76

Straight lines - radial axis ; Dashed lines - tangential axis

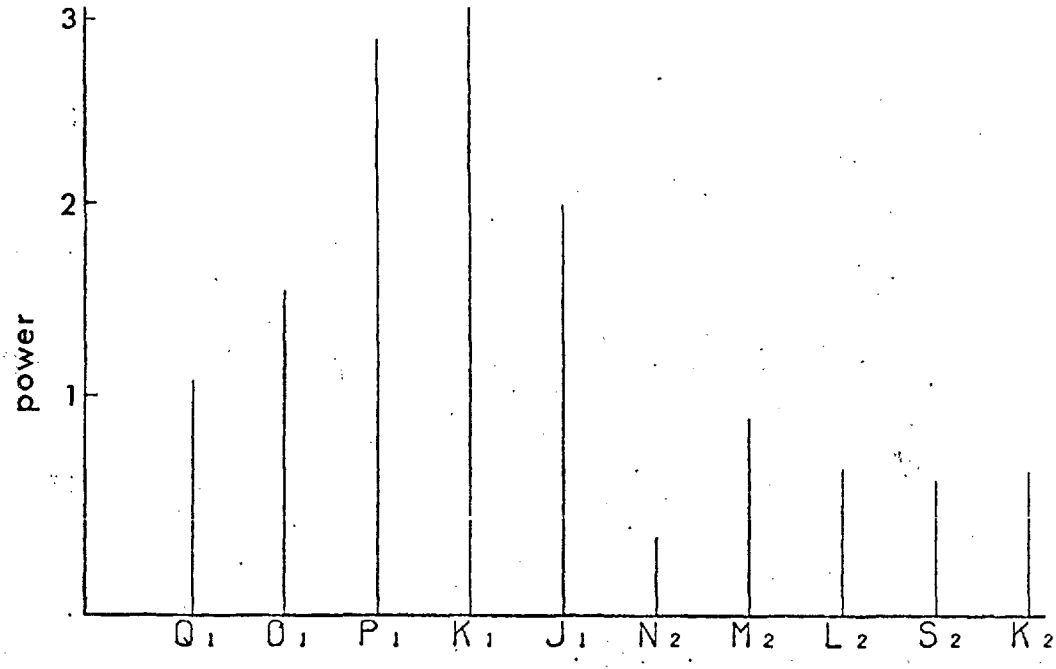


FIG. B.3

Tidal power spectra for the observatory tiltmeter radial axis over the period 24/10/76 - 19/11/76

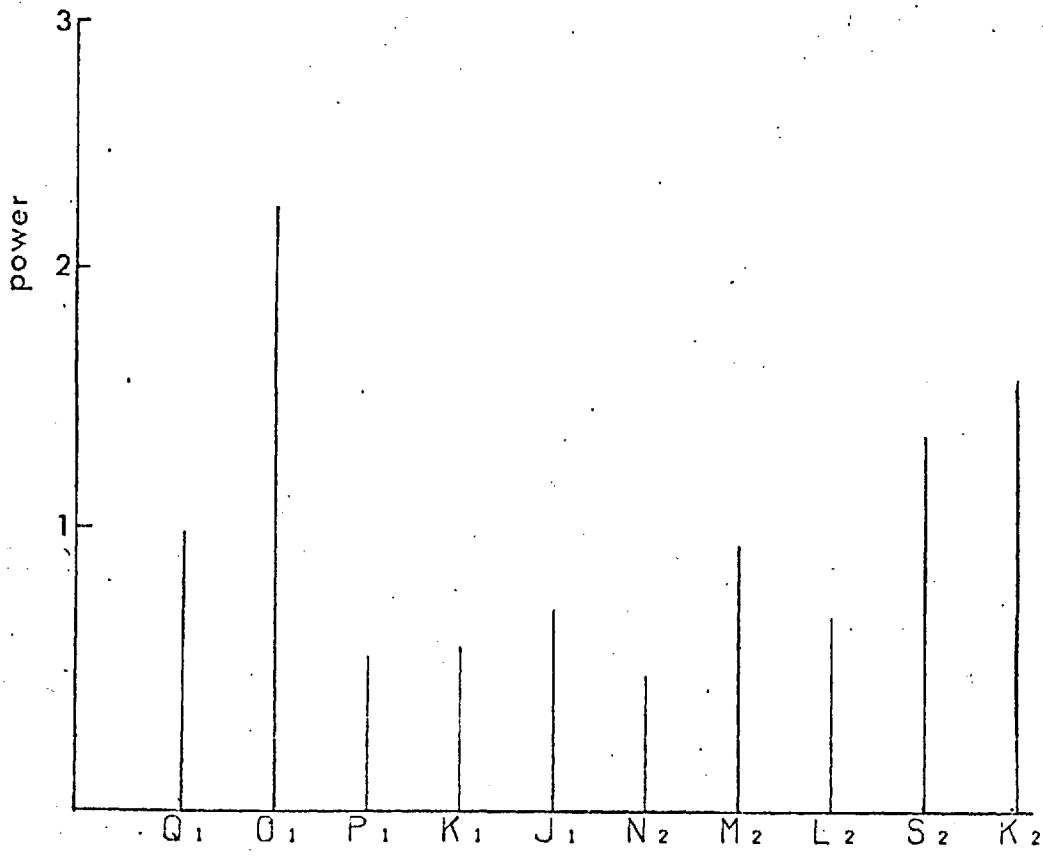


FIG. B.4

Tidal power spectrum for the observatory tiltmeter, radial axis for the period 13/12/76 - 10/1/77

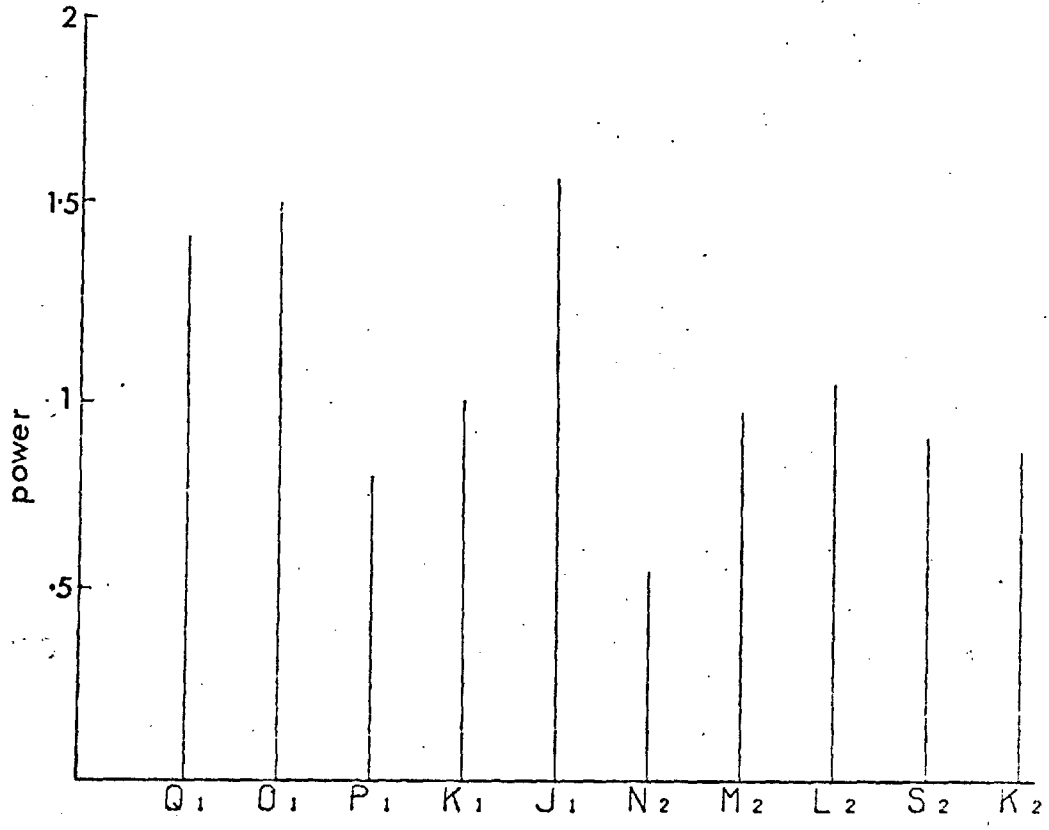


FIG. B.5

Tidal power spectrum for the observatory tiltmeter radial axis for the period 24/1/77 - 16/2/77

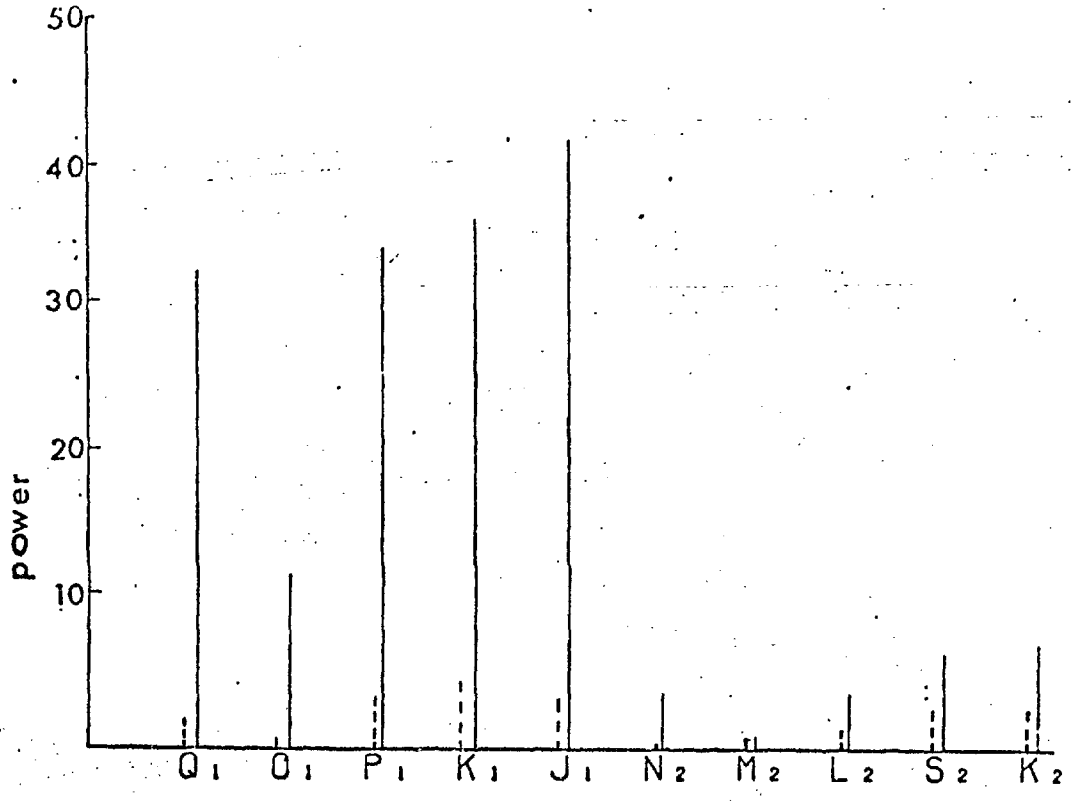


FIG. B.6

Tidal power spectra for the observatory tiltmeter over the period 7/5/77 - 18/5/77

Straight lines - radial axis ; Dashed lines - tangential axis